AD_____

Award Number: DAMD17–03–2-0001

TITLE: Advanced Technologies in Safe and Efficient Operating Rooms

PRINCIPAL INVESTIGATOR: Adrian E. Park, M.D.

CONTRACTING ORGANIZATION: University of Maryland Medical Center
Baltimore, Maryland

REPORT DATE: February 2009

TYPE OF REPORT: Final

PREPARED FOR: U.S. Army Medical Research and Materiel Command
Fort Detrick, Maryland 21702-5012

DISTRIBUTION STATEMENT: Approved for Public Release;
Distribution Unlimited

REPORT DOCUMENTATION PAGE

Form Approved
OMB No. 0704-0188

1. REPORT DATE *(DD-MM-YYYY)*	**2. REPORT TYPE**	**3. DATES COVERED** *(From - To)*
01-02-2009	Final	1 Nov 2002 - 31 Jan 2009

4. TITLE AND SUBTITLE

Advanced Technologies in Safe and Efficient Operating Rooms

5a. CONTRACT NUMBER

5b. GRANT NUMBER
DAMD17–03–2-0001

5c. PROGRAM ELEMENT NUMBER

6. AUTHOR(S)
Adrian E. Park, M.D.

E-Mail: gmoses@smail.umaryland.edu

5d. PROJECT NUMBER

5e. TASK NUMBER

5f. WORK UNIT NUMBER

7. PERFORMING ORGANIZATION NAME(S) AND ADDRESS(ES)

University of Maryland Medical Center
Baltimore, Maryland

8. PERFORMING ORGANIZATION REPORT NUMBER

9. SPONSORING / MONITORING AGENCY NAME(S) AND ADDRESS(ES)
U.S. Army Medical Research and Materiel Command
Fort Detrick, Maryland 21702-5012

10. SPONSOR/MONITOR'S ACRONYM(S)

11. SPONSOR/MONITOR'S REPORT NUMBER(S)

12. DISTRIBUTION / AVAILABILITY STATEMENT
Approved for Public Release; Distribution Unlimited

13. SUPPLEMENTARY NOTES

14. ABSTRACT The current research project was initially based upon three pillars of research, OR Informatics, Simulation for Training and Smart Image. A fourth pillar, cognitive ergonomics/human factors, was added during the past year. At the beginning of this period of performance, there were five projects that comprised the Informatics pillar and two for Smart Image. The Simulation pillar has been comprised of a single project, The Maryland Virtual Patient. Going forward, this pillar will be expanded to include research conducted in and for the larger Simulation Training Program in the MASTRI Center. This research effort has proceeded under the mantle of "Operating Room of the Future" research. We have replaced that theme with the more appropriate "Innovations in the Surgical Environment." The original contract was extended twice to permit the conclusion of verifiably innovative research related to the surgical environment. We believe that this research initiative has opened the door to refinements in the use of informatics to support safe and efficient operating room procedures, the use of simulation to improve and accelerate the training of competent surgeons, and the blending of imaging capabilities to provide clearer and safer interactions between patient and surgeon.

15. SUBJECT TERMS
No subject terms were provided.

16. SECURITY CLASSIFICATION OF:			**17. LIMITATION OF ABSTRACT**	**18. NUMBER OF PAGES**	**19a. NAME OF RESPONSIBLE PERSON**
a. REPORT	**b. ABSTRACT**	**c. THIS PAGE**			USAMRMC
U	U	U	UU	126	**19b. TELEPHONE NUMBER** *(include area code)*

Table of Contents

Introduction

During the past decade, we witnessed an extraordinary evolution in surgical care based upon rapid advances in technology and creative approaches to medicine. The increased speed and power of computer applications, the rise of visualization technologies related to imaging and image guidance, improvement in simulation-based technologies (tissue properties, tool-tissue interaction, graphics, haptics, etc) has caused an explosion in surgical advances. That said, we remain far behind scientists in applying information systems to patient care. This research effort has proceeded under the mantle of "Operating Room of the Future" research. We have replaced that theme with the more appropriate "Innovations in the Surgical Environment."

The content of this final report contains information pertinent to continued activities in relation to the contract DAMD-17-03-2-0001, "Advanced Technologies in Safe and Efficient Operating Rooms" work. This initial research endeavor underpinned and was scoped to fit seamlessly into a continuing project, W81XWH-06-2-005, "Advanced Technologies in Safe and Efficient Operating Rooms".

The current research project was initially based upon three pillars of research, OR Informatics, Simulation for Training and Smart Image. A fourth pillar, cognitive ergonomics/human factors, was added during the past year. At the beginning of this period of performance, there were five projects that comprised the Informatics pillar and two for Smart Image. The Simulation pillar has been comprised of a single project, The Maryland Virtual Patient. Going forward, this pillar will be expanded to include research conducted in and for the larger Simulation Training Program in the MASTRI Center.

Last summer, we convened our annual conference, Innovations in the Surgical Environment, a meeting that serves as a deep recapitulation of research performed under the contract. Additionally, the conference presents an opportunity to explore innovative approaches to surgical research with government, academic and industry partners, and expands our capability to develop collaborative relationships. This year, the conference theme was lessons learned from the high-stakes environments of aviation and astronautics applied to the high-stakes environment of the operating room.

Body

A. OR Informatics

Informatics subgroup 1. The Perioperative Scheduling Study (WORQ)

The Perioperative Scheduling Study examined how using post-operative destination information during the process of surgery scheduling can influence congestion in postoperative units such as ICUs and IMCs, which lead to overnight boarders in the PACU. The research team is composed of Jeffrey W. Herrmann, Ph.D., and Greg Brown, a graduate student, both with the University of Maryland, College Park. The team is working closely with Michael Harrington, Ramon Konewko, R.N., and Paul Nagy, Ph.D., for guidance and assistance.

The surgery scheduling process has been carefully studied to understand the different organizations and persons who participate in the process, including the schedulers in the surgical services, the perioperative services office, the PACU manager, and the OR charge nurse. Interviews with many of these groups and observations of their scheduling process were conducted on January 17, 2008. These groups also provided copies of their scheduling policies and typical schedules.

We are currently developing a mathematical model for evaluating congestion in postoperative units, including ICUs, IMCs, and floor units. This model will require data about post-operative destinations and length-of-stay distributions for different types of surgeries. Data about cardiac surgeries from two years were analyzed to develop a methodology for computing the needed information. This methodology was applied to a larger set of historical data to generate a complete set of information to execute the congestion evaluation model.

Informatics subgroup 2. Operating Room Glitch Analysis (OGA)

The OGA project, focusing on institutional learning, examined the workflow around performance indicators in the peri-operative environment and building a graphical dashboard to allow data mining and trend analysis of operating indicators. The dashboard platform was built in a tiered architecture consisting of information extraction, data warehousing and manipulation, and user interface layers. The system has clearly segmented application components and a modular programming code base. Combined with web and programming standards, the tiered architecture has kept the software extensible despite its complexity.

To combat the complexity introduced by the disparate clinical information systems (surgery, anesthesia, patient tracking, facilities, quality) used throughout the peri-operative environment the information extraction layer uses an abstracted interface based on RESTful web services to receive information provided by any number of systems. Initial extraction, transformation, and loading (ETL) work have been done for the surgical case data. Case information is pulled from the clinical database once per day and loaded into the data warehouse. Though the current information feed is poling the clinical system once per day, the data warehouse itself will allow for clinical integration with the data warehouse at transactional speed, as real time information is made available.

The data warehousing and manipulation layer contains a relational database (MySQL) in which information from the receiver layer is stored. A business intelligence rules engine, written in erlang, provides the means to aggregate low-level information into key performance indicators (KPI). The semantic linking between the data is also stored to provide access to each level of information that powers the aggregated KPI. The KPIs are generated by a data analyst through a web interface. When a new KPI is defined by the analyst the data is immediately aggregated and kept up to date in real time without the need for user interaction.

The user interface contains three major components.

1. A data manipulation layer that allows interaction with the data warehouse and provides analysts with means to create and track new metrics.
2. A visualization toolkit to create graphs and web pages to display information effectively. This includes the means to create clickable and animated graphs.

3. Semantic services which generate data drilling functionality for graphs and data tables without the need for extra programming or user configuration. These semantic services also enable filtering of information and the ability to view related metrics in the same filtered context simultaneously.

Completed stages of the project:

- A pipeline for case information from *Surginet*
- Business intelligence engine and data warehouse to handle aggregation, manipulation, and storage of data
- Web interface to interact with and aggregate data into KPI's
- Web interface to build data visualizations
- Web Interface to build dashboard pages
- Semantic services

Areas of future improvement:

- Observation engine to evoke actions on specified events within the data pipeline
- Web interface to add/edit/delete actions and events in the observation engine
- Formalized evaluation of the scalability of the warehouse
- Improved usability for the web interface
- More advanced visualizations for user creation
- Forms management of quality metrics

Informatics subgroup 3. Context Aware Surgical Training (CAST)

We proposed to design and implement a prototype context aware surgical training environment (CAST) as part of the University of Maryland Medical System's SimCenter. This system would be used to explore the role that an intelligent pervasive computing environment can play to enhance the training of surgical students, residents and specialists. The research built on prior work on context aware "smart spaces" done at UMBC; leveraging our experience in working with RFID in the DARPA Trauma Pod program as well as in incorporating Web-based infrastructure and software applications in academic and professional development programs. The project resulted in a pilot system integrating one or two training resources available in the SimCenter into a context aware training environment that could recognize the presence of a trainee and or mentor and take appropriate action based on known training goals and parameters. The project will advance the knowledge of context aware training environments in a highly technical medical field and provide a basis for incorporating more advanced technology assisted learning experiences in medicine. This "smart environment" may then, if successful, be scaled to meet the needs of an operative environment where the technological demands may be the similar or analogous to those seen in the training environment. A goal of this project was to advance interactive information, resource, and content management via a seamless process. Ultimately, the advanced training and potential for use in perioperative environments have a long-term end goal of improving patient safety and adding to the body of knowledge in surgical training. Initially, we saw a situation were clinicians in training can receive a tailored curriculum. Additionally, we envision a system that offers real-time feedback and decision support and education metrics to faculty.

A key goal this year was to prototype the CAST system. Initially, we met with the MASTRI team responsible for the training efforts to iron out the requirements for the

system and came up with the following set of tasks to be accomplished; Student Tracking, Enforcing Prerequisites, Video Capture and Instructor Feedback.

Also, we defined a typical use case for our system.
A student enters the simulation center. The system identifies the student (for instance, using their Bluetooth phone or their badge), and does a prerequisite check based on the simulator the student wants to perform the procedure. Only if the student is done with the prerequisites, is he/she allowed to proceed. When the student indicates that they are ready to begin, the system starts capturing the external and internal view until the student indicates that they have completed the task. The captured video is then transferred to the video server for review by the instructor. The instructor interface allows the instructor to see the entry logs of students in terms of when they entered and exited the centre along with the corresponding external view.

We employed the spiral prototyping approach as an experimental test bed; we designed and implemented an initial system prototype that would meet the above functional requirements. The prototype integrates two machines with each simulator -- a small Nokia 800 device for resident interaction, and a larger PC for video capture. Note that this is for the proof of concept. A single small form factor but computationally powerful machine could be used instead. In fact, for simulators such as the VR, we expect that eventually manufacturers could integrate our system directly into the computer that drives the simulation.

Our prototype used Bluetooth for localization of residents in the simulation centre. It was designed to be modular, so that any other technology (such as resident ID cards) could be integrated easily. We also hosted training materials including videos for FLS, Kentucky and Rosser tasks in our system, and tracked student progress through the chapters checked out. This was used for enforcing prerequisites when students entered the simulation centre to perform procedures. In addition to enforcing prerequisites, there was a need for the instructors to visually see what the residents were doing during their simulation procedures. We use N800's built in camera to capture the residents' external views. These video feeds are then fed into a central server for review by the instructor. For location detection, we also experimented with using the Awarepoint tags. Awarepoint uses a zigbee based mesh network for localization and exposes the location information through a web service. Our experiments indicated that Awarepoint could provide us room level information, but not anything finer. While this would help identify if the residents were in the simulation center, it would not help determine which machine they were using, which was needed for CAST. We demonstrated our first system prototype at the ORF workshop by going through a typical student workflow.

Based on feedback on individual components of the first prototype, we started the secondversion of the prototype to be deployed at the MASTRI center. The key changes in thesecond prototype from the first one are described below.

- We no longer use awarepoint for locationing since it could provide us only room level accuracy.
- On the student identification front, we are using a standard username and password method for now. Also, since we have external camera views from the N800, students identified can be verified during the review process by the instructor. Bluetooth based identification exists, but is not used since we were told that most residents may not have phones with Bluetooth. Multiple candidate

technologies for identification such as Bluetooth, RFID, nearfield RF badges etc. have emerged and been discussed with MASTRI staff. No single choice has been made yet – the idea is to first make the system robust from a use perspective, and then integrate identification technologies based on further discussion with MASTRI staff. Our system is capable and flexible enough to handle a variety of lower level locationing technologies and therefore we would choose the one that is most practical in MASTRI scenario.

• Due to hospital network firewall policies, we had to move away from using a wireless network for transferring videos from the N800 to the MASTRI video server. We currently achieve this by tunneling through the internal view capturing machine which is hooked to the N800 by a USB cable.

• Prerequisite checks are temporarily suspended since the initial classes being taught in MASTRI are not following FLS.

We also focused on moving the system from UMBC machines to the MASTRI infrastructure where they will be housed. We purchased a small factor Dell machine to be used for capturing internal views from simulators. Storage was purchased and added to the mastri-internal server for archiving both internal and external video feeds with help from a computer scientist. Also, we have

• Integrated the student database from the hospital
• Hosted FLS and other training videos on the hospital infrastructure
• Hacked internal views of the simulators

We have now developed the system to capture internal video feeds and metrics from the following simulators

• Promis
• Stryker
• Laproscopic VR simulator

We use external s-video frame grabbers to capture the simulator internal video feeds. These feeds are synchronized with the external view from the N800 and stored on the video server. Thus, the instructor now has access to both the internal and external feeds during review, and consequently they can provide better feedback. Currently our system uses email to send back feedback.

Web Interface:

We have integrated the student database into our web-based curriculum management system. The student database contains all the current residents and one guest account that can be used for testing. If a student wants to view the training videos, he or she will first need to log in using their SMail Userid. When they pass the authentication, a categorized web structure will be displayed, and they can choose to sort the tasks by category, by difficulty (FLS integrated), or by each (Basic, Instrument, Procedural Skills, and FLS), which is shown in the following screenshot. This structure was developed in consultation with the MASTRI team, particularly Ivan George and Ethan Hagan.

Then the student can pick any training video they want to view. Suppose the student wanted to view the bagging skill, and then it will display the following screen. As for the instructor interface, the instructor first needs to pass authentication to access the student training records. Then, they can pick the student name that they want to view from a drag-down list that contains all the residents. The appropriate student record will pop up in the next page, which contains the following information: the chapters that the

student has checked out, the student training history (simulator type, start time, end time, internal video record, external video record), and the instructor can provide their feedback for every training record of this student via email.

At the end of this period of performance, research on the CAST system was judged to have reached its maximum potential. Advances in related technology and off-the-shelf equipment facilitated the accomplishment of the broad goals of the project. Going forward, the team of computer scientists, faculty and students of the University of Maryland - Baltimore, were redirected into a project of vital importance to the surgical environment, that of enhancing video summarization of surgical cases.

Informatics subgroup 3 (revised) Video Summarization
Background

The research endeavor is a recent inclusion to the Innovations in the Surgical Environment program. Thus, the initial description of our work will include a meta-analysis of sorts, acquainting the reader with the technology and technical developments in the arena of video summarization. Within this section of the report, references to the literature are inserted apart from the overall bibliography of work conducted under the auspices of the Innovations in the Surgical Environment research program.

Laparoscopic surgery is a minimally invasive technique. It was first performed in 1987, and is now the method of choice for a number of surgical procedures. The laparoscopic approach involves the user of narrow tubes, called trocars, which are inserted into the abdomen through small incisions. A camera is passed through one of the trocars to visualize the surgical field. Instruments are passed through the other trocars to cut, manipulate, and sew.

Compared with an open procedure, patients who undergo laparoscopic surgery have smaller scars, reduced pain, and a quicker recover. There are, however, a number of technical challenges with the laparoscopic approach. Access is limited to small incisions through which long instruments are passed. Tactile feedback is reduced. Visualization is restricted to two-dimensional video [1].

Because of these technical challenges, the traditional apprenticeship model is not sufficient for trainees to develop laparoscopic skills. Additional methods are used to develop competency, such as box trainers, virtual reality simulators, and video-based assessment [2].

Our overall goal is to develop a software tool to assist with video-based assessment. Such a tool would automatically divide each video into the eleven basic steps of the cholecystectomy (360-degree surveillance, trocar placement, preliminary dissection, and so on) and provide a set of tools to efficiently review each video segment. It would allow an evaluator to navigate to any section of the surgical procedure, skip to a particular section, alter the viewing order, spend more time on critical sections, or view the same section of a procedure from multiple trainees. See Figure 1.

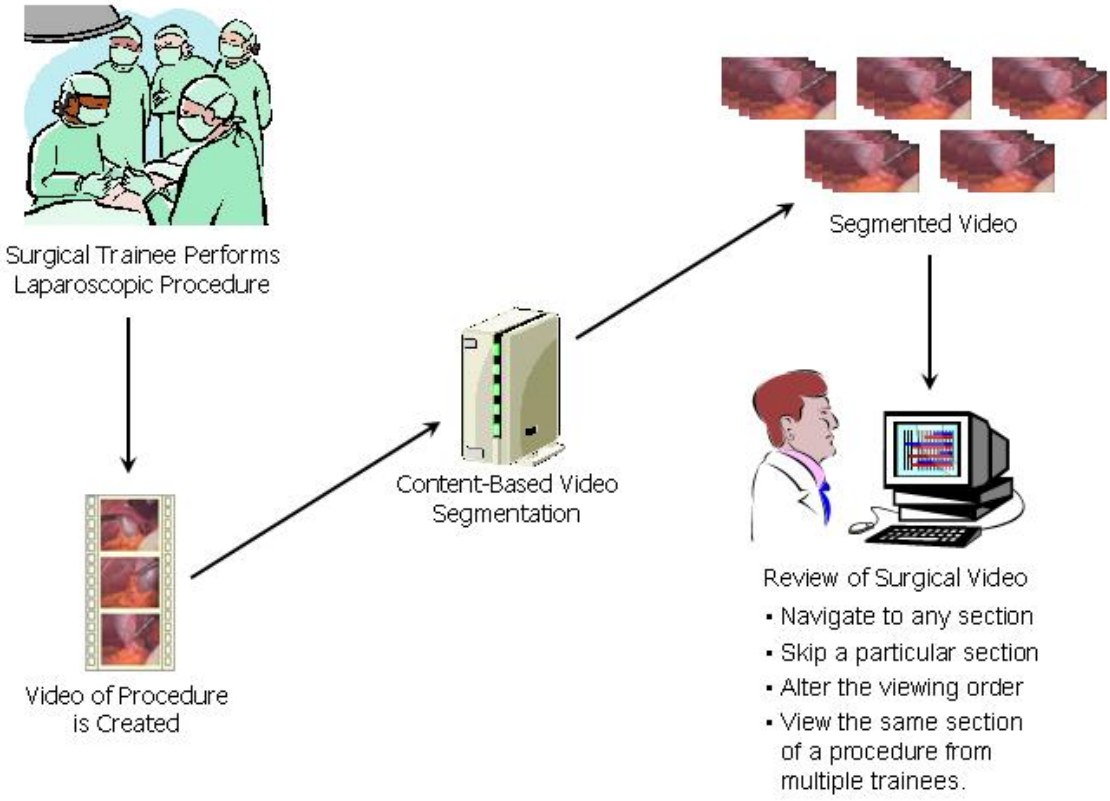

Figure 1. Proposed laparoscopic video segmentation and review scheme

This report presents an initial feasibility study. We used image classification techniques and distance metrics to identify the critical view of a laparoscopic cholecystectomy (surgical procedures to remove the gall bladder). The critical view is the point in the surgery when the essential anatomy has been identified, and is an important validation step before clipping the cystic duct and artery. See Figure 2.

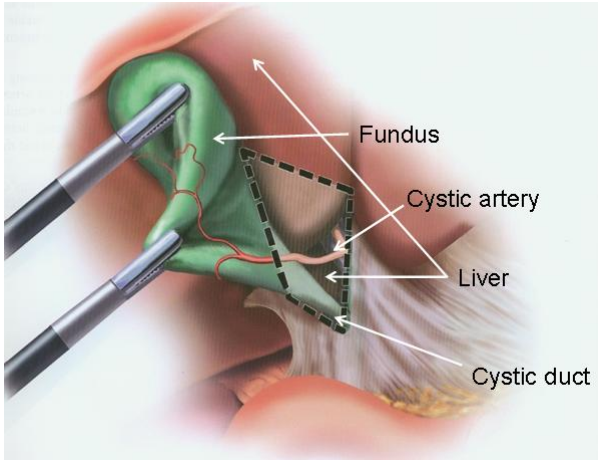

Figure 2. Critical view image.

Spectral and textural features can both be used for image analysis. Spectral features describe the tonal or color variations in an image. Histograms are used to represent the distribution of tones in an image. Textural features describe the spatial distribution of tonal variations, and are often represented as a gray-level co-occurrence matrix (GLCM) [3]. Related efforts include the use of color histograms to segment hysteroscopy video [4], color histograms and state information to segment echocardiogram video [5], and the use of texture feature to analyze images from and breast tissue histopathology [6], prostate cancer [7], and capsule endoscopy [8].

Methods

Our objective was to compare image features using distance metrics, in an attempt to identify the critical view of a laparoscopic cholecystectomy. This was to determine feasibility of recognizing other steps in a laparoscopic cholecystectomy for the purpose of surgical video segmentation.

Five laparoscopic cholecystectomy videos were provided to us by the University of Maryland School of Medicine, which contained 24-bit color video at 29 frames per second. The videos were reviewed by a surgeon to determine the timing of the critical view. We used FFmpeg to convert the video to a sequence of 24-bit color JPEG images (http://ffmpeg.mplayerhq.hu/). We used ImageJ for to extract image features features (http://rsbweb.nih.gov/ij/). The distance metric we used to compare these results was the Jeffrey Divergence [9]. See Figure 3.

We applied the Jeffrey Divergence to the data 5 times, each time using a critical view image from a different case as our basis for comparison. If a comparison using the Jeffrey Divergence was below a given threshold, it was assume to be a critical view image. We chose threshold values empirically to maximize both sensitivity and specificity.

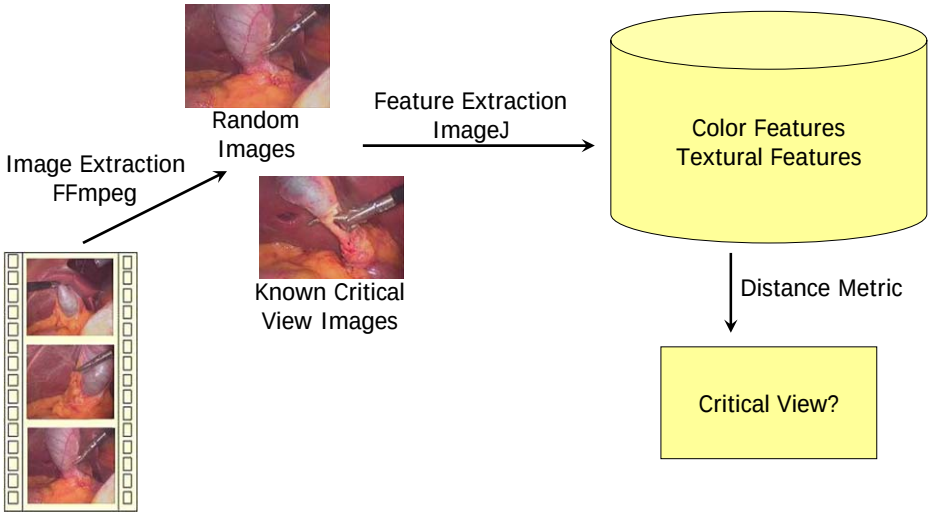

Figure 3. Methodology.

Results

A summary of the images use are shown in Table 1. The data included 378 representative images taken randomly throughout the 5 laparoscopic cholecystectomies,

with 104 of the images collected near the critical view. We analyzed 49 separate spectral and textural features, the most promising of which are shown below. They included 4 textural features: energy (uniformity), entropy (complexity), contrast (local variation), and correlation (linear patterns). They also included 4 spectral features: 3D histogram (color distribution in the 3 dimensional space), color histogram (distribution of each color individually), and binary versions of the 3D and color histograms.

Feature	Sensitivity	Specificity
Energy	66.4%	67.2%
Entropy	60.9%	62.5%
Contrast	62.4%	62.6%
Correlation	62.2%	60.0%
3D Histogram	64.0%	64.8%
Color Histogram	71.5%	72.2%
Binary 3D Histogram	61.2%	59.5%
Binary Color Histogram	66.0%	66.1%

Table 1. Sensitivity and specificity.

Discussion

Our initial results show promise with a sensitivity and specificity up to 72%. Energy, which is a textural measure of pixel similarity, and color histogram, which is a measure of color distribution performed the best. Accuracy, however, must improve before there can by any practical application of this approach.

The image analysis process was very data intensive. At 29 frames per second, roughly 100,000 images were produced from every hour of video. Each 3D histogram generated about 17,000,000 pieces of data per image. Because of this, we quantized this color distribution into a more manageable size, which is probably why it did not perform as well.

When interpreting our results it is important to consider several limitations. The study was small in size. The cases were restricted to a single academic medical center. Finally, our comparisons were limited to one feature from one image at a time.

We are currently working on a more robust image classifier, based on the lessons learned from this research. We are using particle analysis and edge analysis [10] to identify the characteristics of the major objects in an image. We are also experimenting with support vector machines, which are supervised learning methods that use multiple image features to classify images using and n-dimensional hyperplane [11]. Other features being considered are the use of temporal information, logical workflow, and relevant clinical data to increase the accuracy of our image classifier.

In summary, we compared image features with a distance metric to identify the critical view of a laparoscopic cholecystectomy. Our initial results were promising, but more work needs to be done to increase accuracy. We are currently experimenting with particle analysis, edge analysis, and support vector machines as ways to create a more robust image classifier.

1. Aggarwal R, Moorthy K, Darzi A. Laparoscopic skills training and assessment. Br J Surg. 2004 Dec;91(12):1549-58.
2. Dent TL. Training, credentialling, and granting of clinical privileges for laparoscopic general surgery. : Am J Surg. 1991 Mar;161(3):399-403.
3. Haralick RM, Shanmugam K, Dinstein I. Textural features for image classification. IEEE Transaction on Systems, Man, and Cybernetics. 1973 Nov; 3(6):610-621.
4. Scharcanski JN, Neto WG, Cunha-Filho JS. Diagnostic hysteroscopy video summarization and browsing. Proceedings 27th IEEE-EMBS. 2005;:5680-5683.
5. Roy A, Sural S, Mukherjee J, Majumdar AK. State-based modeling and object extraction from echocardiogram video. IEEE Transaction on Information Technology in Biomedicine. 2008 May;12(3):366-376.
6. Doyle S, Agner S, Madabhushi A, Feldman M, Tomaszewski J. Automated grading of breast cancer histopathology using spectral clustering with textural and architectural image features. Biomedical Imaging: From Nano to Macro (ISBI 2008), May 2008;: 496-499.
7. Doyle S, Hwang M, Shah K, Madabhushi A, Feldman M, Tomaszewski J. Automated grading of prostate cancer using architectural and textural image features.
8. Barbosa DJ, Ramos J, Lima CS. Detection of small bowel tumors in capsule endoscopy frames using texture analysis based on the discrete wavelet transform. Conf Proc IEEE Eng Med Biol Soc. 2008;1:3012-5.
9. Bugatti PH, Traina AJ, Traina C. Assessing the best integration between distance-function and image-feature to answer similarity queries. Proceedings ACM SAC. 2008;:1225-1230.
10. Gonzalez R, Woods R. Digital Image Processing, Addison Wesley, 1992, 414-428.
11. Burges, C. A tutorial on support vector machines for pattern recognition. Data Mining and Knowledge Discovery. 1998;2(2):121-167.

Informatics subgroup 4. Operating Room Clutter (ORC)

The project team has worked on the use of advanced video technology to support coordination in operating rooms. Our activities were in four areas indicated below, each of which contains a summary of publications. For this portfolio of the Informatics pillar of Innovations in the Surgical Environment, the measure of our success is depicted in the number and nature of professional publications. Like other pillars of innovation, there is a ground-breaking aspect to the work. We perceive a scientific responsibility to gather and disseminate information as quickly and widely as possible. Thus, our report refers the reader to specific publications of work conducted in each research activity. All publications referred to may be found in our website: http://hfrp.umaryland.edu. For full length journal articles, PDF files may be downloaded. For others, abstracts are available. In all, we published 8 full-length peer reviewed journal articles, 2 full-length peer reviewed proceeding articles, and 8 conference abstracts. The references below can provide further details.

A. Models of decision making for operating room management.

We reviewed literature and developed a synthesis report on the state of the art of decisions on the day of surgery. Furthermore, we developed models for decision support systems for operating room management. The activities in this area were reported in the following publication:

1. Dexter F, Xiao Y, Dow AJ, Strader MM, Ho D, Wachtel RE. Coordination of Appointments for Anesthesia Care Outside of Operating Rooms Using an Enterprise Wide Scheduling System. *Anesthesia and Analgesia. 105:1701-1710. 2007*

2. Xiao Y, Strader M, Hu P, Wasei M, Wieringa P. Visualization Techniques for Collaborative Trajectory Management . *ACM Conference on Human Factors in Computing Systems, pp.1547 - 1552. 2006*
3. Xiao Y, Wasei M, Hu P, Wieringa P, Dexter F. Dynamic Management in Perioperative Processes: A Modeling and Visualization Paradigm. *12th IFAC Symposium on Information Control Problems in Manufacturing. (3)647-52. 2006*
4. Dutton R, Ho D, Hu P, Mackenzie CF, Xiao Y. Decision Making by Operating Room Managers: The Burden of Changes. *Anesthesiology, 103:A1175. 2005*
5. Dexter F, Epstein RH, Traub RD, & Xiao Y. Making Management Decisions on the Day of Surgery Based on Operating Room Efficiency and Patient Waiting Times. *Anesthesiology, 101(6):1444-1453. 2004*

B. Operating room multimedia system design and methodology.

We developed technology, primarily based on algorithms of video processing and biosignal processing, to display status of operating rooms. The displays are to inccfrease situational awareness. The technological advances made by our group were reported in the following publications:

6. Xiao Y, Schimpff S, Mackenzie CF, Merrell R, Entin E, Voigt R, Jarrell B. Video Technology to Advance Safety in the Operating Room and Perioperative Environment. *Surgical Innovation. 14(1): 52-61. 2007*
7. Hu P, Xiao Y, Ho D, Mackenzie CF, Hu H, Voigt R, Martz D. Advanced Visualization Platform for Surgical Operating Room Coordination: Distributed Video Board System**.** *Surgical Innovation. 13(2):129-135. 2006*
8. Hu P, Seagull FJ, Mackenzie CF, Seebode S, Brooks T, XiaoY. Techniques for Ensuring Privacy in Real-Time and Retrospective Use of Video. *Telemedicine and e-Health, 12(2): 204, T1E1. 2006*
9. Xiao Y, Hu P, Hu H, Ho D, Dexter F, Mackenzie CF, Seagull FJ, Dutton D. An algorithm for processing vital sign monitoring data to remotely identify operating room occupancy in real-time. *Anesthesia & Analgesia,(101)3:823-829 . 2005*
10. Hu PF, Burlbaugh M, Xiao Y, Mackenzie CF, Voigt R, Brooks T, Fraser L, Connolly MR, Herring T. Video Infrastructure and Application Design Methods for an OR of the Future. *Telemedicine and e-Health. 11(2), 211, T3C2. 2005*
11. Hu PF, Hu H, Seagull JF, Mackenzie CF, Voigt R, Martz D, Dutton R, Xiao Y. Distributed Video Board: Advanced Telecommunication System for Opearation Room Coordination**.** *Telemedicine and e-Health. 11(2), 248, P28. 2005*
12. Hu PF, Xiao Y, Mackenzie CF, Seagull FJ, Brooks T, LaMonte MP, & Gagliano D. Many to One to Many Telemedicine Architecture and Applications. *Telemedicine Journal and e-Health. 10(Supplement 1), S-39. 2004*

C. Survey and descriptive studies of operating room management, with and without the support of advanced video technology.

In conjunction with technology development, we conducted observational and survey studies of operating room management. These studies and associated results were in the following publications:

13. Seagull FJ, Xiao Y, & Plasters C. Information Accuracy and Sampling Effort: A Field Study of Surgical Scheduling Coordination**.** *IEEE Transactions on Systems,*

Man, and Cybernetics, Part A:Systems and Humans. 24(6), 764-771. 2004
14. Dutton R, Hu PF, Mackenzie CF, Seebode S, Xiao Y. A Continuous Video Buffering System for Recording Unscheduled Medical Procedures. *Anesthesiology, 103:A1241. 2005*
15. Gilbert TB, Hu PF, Martz DG, Jacobs J, Xiao Y**.** Utilization of Status Monitoring Video for OR Management. *Anesthesiology, 103:A1263. 2005*
16. Dutton R, Hu P, Seagull FJ, Scalea T, Xiao Y, . Video for Operating Room Coordination: Will the Staff Accept It?. *Anesthesiology: 101: A1389. 2004*

D. Technology evaluation.

We conducted evaluation studies of the technology deployed. The primary focus was on user acceptance and usage patterns. The focus was chosen because the current science of operating room management has concluded that improvement of decision making on the day of surgery will lead to improvement in intangible outcomes, such as situation awareness, and will unlikely lead to improvement in operating room throughput (e.g., volumes and economic returns). Our work was reported in the following publication.

17. Xiao Y, Dexter F, Hu FP, Dutton R. Usage of Distributed Displays of Operating Room Video when Real-Time Occupancy Status was Available . Anesthesia and Analgesia 2008; 106(2):554-560. 2008
18. Kim Y-J, Xiao Y, Hu P, Dutton RP. Staff Acceptance of Video Monitoring for Coordination: A Video System to Support Perioperative Situation Awareness. *Journal of Clinical Nursing (accepted). 2007*

Informatics subgroup 5. Improving Perioperative Communications:

During the period of performance of this project, multiple versions of work teams were tried in an effort to get the right people to the task. A correct mix of expertise was determined including representatives of Perioperative scheduling, Administration, IT Support, as well as team members from surgery, anesthesiology, and other OR services.

Data Analysis

The team has actively performed a re-review/study of the performance metrics available from various Perioperative data stores. In particular, near past analysis has been benefited by work performed via the OGA team.

Background:

In the UMMS OR, the Cardiac Surgery Service utilizes a common communications point (a “cardiac phone line”) that in a sense is used to acquire information and provide that information to any team member who calls the line to acquire information. The cardiac phone line has been scripted and is actively in use through a voice mail system. It can only be altered by dedicated personnel with password capability. The script involves the following standardized information: Identification of individual providing information, the Date of surgery, the Total number of cases, and OR location, patient name, case order, medical record number, age, surgeon, anesthesiologist and procedure. Evening schedule updates have been made possible through a second phone line option.

Problem Statement:

After some effort, we can now move to track updates on the phone line and correlate these updates with OR start delays. Thus, we refined the IPC question to Does more accurate information as evidenced by updates on the phone line, ie improved communication, result in fewer problems in the morning with cardiac surgical cases starting on time- are instruments better prepared for the procedure, are operating rooms better equipped for the appropriate case, are the correct pick lists utilized for the correct surgeon, is there less of a transport delay because the patient's hospital location has been identified? The question contains reference to some of the delay codes that are currently utilized by the Operating room tracking system and reported for glitch analysis.
With the assistance of the communications personnel we will reconfigure the cardiac phone line so that we can actually track the phone calls made to the phone line. This will enable us to: Determine key personnel who are utilizing the phone line, Determine groups of personnel utilizing the phone line (i.e. nursing, anesthesia, perfusion), Determine which groups are not utilizing phone line information (i.e. anesthesia techs), Determine whether there is a time variable; is there a better time to call for updates? Should updates be made at predetermined times or should they be more dynamic?
We hypothesize that information gained from increased communication improves OR efficiency. If this is the case we can them move to see if more real-time enabling technologies might be deployed to other services within the UM ORs and perhaps other ORs "everywhere".

The IPC project progressed to identify and utilize new technologies (Cell, WiFi, IM, Web fusion technologies) being developed in the UM Radiology department. This simple phone line will establish a form of communication that is more mobile, accurate, up-to-date, and shares a common lexicon.

B. Simulation

This report introduces the basics of the Maryland Virtual Patient simulation approach, discusses its place on the map of intelligent systems in clinical medicine and describes the project's status and research and development activity presently under way. The work on the Maryland Virtual Patient project will continue after termination of the current contract. Additional funds from government agencies will be sought to sustain the effort on this important contribution to simulation training: that is, the only known cognitive simulation training system.

Simulation: The Maryland Virtual Patient

We present here a simplified description of the MVP simulation, interaction and tutoring system. A virtual patient instance is launched and starts its simulated life, with one or more diseases progressing. When the virtual patient develops a certain level of symptoms, it presents to the attending physician, the system's user.1 The user can carry out, in an order of his or her choice, a range of actions: interview the patient, order diagnostic tests, order treatments, and schedule the patient for follow-up visits. The patient can also automatically initiate follow-up visits if its symptoms reach a certain level before a scheduled follow-up. This patient-physician interaction can continue as long as the patient "lives."

As of the time of writing, the implemented MVP system includes a realization of all of the above functionalities, though a number of means of realization are temporary placeholders for more sophisticated solutions, currently under development. The most obvious of the temporary solutions is the use of menu-based patient-user interaction instead of natural language interaction. While this compromise is somewhat unnatural for our group, which has spent the past 20 years working on knowledge-based NLP, it has proved useful in permitting us to focus attention on the non-trivial core modeling and simulation issues that form the backbone of the MVP system.

MVP currently covers six esophageal diseases pertinent to clinical medicine: achalasia, gastroesophageal reflux disease (GERD), laryngopharyngeal extraesophageal reflux disease (LERD), LERD-GERD (a combination of LERD and GERD), scleroderma esophagus and Zenker's diverticulum. At the beginning of a simulation session, the system presents the user with a virtual patient about whose diagnosis he initially has no knowledge. The user then attempts to manage the patient by conducting office interviews, ordering diagnostic tests and prescribing treatments. Answers to user questions and results of tests are stored in the user's copy of the patient profile, represented as a patient chart. At the beginning of the session, the chart is empty and the user's cognitive model of the patient is generic – it is just a model of the generalized human. The process of diagnosis results in a gradual modification of the user's copy of the patient's profile so that in the case of successful diagnosis, it closely resembles the actual physiological model of the patient, at least, with respect to the properties relevant to the patient's complaint. A good analog to this process of gradual uncovering of the user profile is the game of Battleship, where the players gradually determine the positions of their opponent's ships on a grid.

At any point during the management of the patient, the user may prescribe treatments. In other words, the system allows the user not only to issue queries but also to intervene in the simulation, changing property values within the patient. Any single change can induce other changes – that is, the operation of an agent can at any time activate the operation of another agent.

Simulation: Utility

The MVP project can be viewed as just one of a number of applications in the area of intelligent clinical systems. The latter, in turn, can be viewed as one of the possible domains in which one can apply modeling teams of intelligent agents featuring a combination of physical system simulation and cognitive processing. So, in the most general terms, our work can be viewed as devoted to creating working models of societies of artificial intelligent agents that share a simulated "world" of an application domain with humans in order to jointly perform cognitive tasks that have until now been performed exclusively by humans. Sample applications of such models include:

- a team of medical professionals diagnosing and treating a patient (with humans playing the role of either a physician or a patient)
- a team of intelligence or business analysts collecting information, reasoning about it and generating analyses or recommendations (with humans playing the role of team leader)

- a team of engineers designing or operating a physical plant (with humans playing the role of team leader)
- a learning environment (where humans play the role of students).

As can be seen, this work is at the confluence of several lines of research – cognitive modeling, ontological engineering, reasoning systems, multi-agent systems, simulation and natural language processing.

Simulation: Accomplishments

In Year 4 of the project, our team has delivered two new versions of the Maryland Virtual Patient Environment. The realism of the simulation has been enhanced by including coverage of "unexpected" interventions; allowing discontinued treatments; allowing new diseases to develop due to side effects of treatments. The user interface has been redesigned. A new agent-based architecture has been developed to support enhanced cognitive capabilities of the virtual patient and the intelligent tutor, including language capabilities. In the area of language processing, a dialog processing model was developed. Work has continued on improving the language understanding capabilities, centrally including treatment of referring expressions. Enhancement of static knowledge resources, the ontology and the lexicon, has been ongoing. Work on extending the coverage of diseases has been ongoing: a further improvement of the model of GERD is under way, as is the modeling of cardiovascular diseases. A totally reworked system version, with dialog support, is planned for release in June 2008. Work has also been ongoing on improving and extending the set of development tools – the DEKADE demonstration, evaluation and knowledge acquisition environment supporting natural language work has been revamped; the interface for creating instances of virtual patients has also been enhanced; a web-based environment for supporting internal documentation has been installed. Finally, we have written, submitted, published or delivered 6 conference and journal papers.

C. Smart Image

Introduction

The overall objective of this "Smart Image" project has been to demonstrate the technical feasibility of live augmented reality (AR), which is the fusion of live volumetric computed tomography (CT)-generated views of the surgical field with laparoscopic views. The advantage of live AR is that internal structures absent in laparoscopic views can be visualized using CT. Being able to see internal structures, especially underlying vessels, before making a dissection has been a longstanding need of minimally invasive surgeons.

Although the proposed use of continuous volumetric CT is advantageous to creating renderings of the internal structures with their orientations refreshed at a rapid rate (appox. 1 Hz), it is also imperative that new technologies be created to reduce the radiation dose to the patient and the surgeon alike originating from the use of CT. Our first three objectives address the radiation dose problem while providing a means to visualize the vasculature throughout the surgery with a single administration of the CT contrast agent. The fourth objective is devoted to creating spatially and temporally synchronized AR views.

Objective 1: Dose reduction strategy: Registration between high dose-low dose CT

This objective has allowed us to track tissue motion through the use of continuous intra-operative volumetric CT scans acquired at ultralow doses. Because intra-operative ultralow dose CT scans are not contrast enhanced and have low image quality, we successfully tested the concept of first acquiring a diagnostic quality contrast-enhanced CT scan immediately prior to the surgery and then modifying (i.e., warping) it to spatially register with low-dose CT. The net result is that high-quality contrast-enhanced CT images of the surgical field are available throughout the surgery.

We earlier demonstrated this capability using simulated low-dose CT images (low-dose image simulated from a high-dose scan) [1]. In this last project year, we re-tested this capability with actual high- and low-dose CT scans of a pig liver. To test the accuracy of registration, we further placed 5-6 tiny markers (2-3 mm segments of a thin guidewire) in the liver parenchyma. The results of registration for a representative case are shown in Figure 1. A better structural alignment is seen after registration.

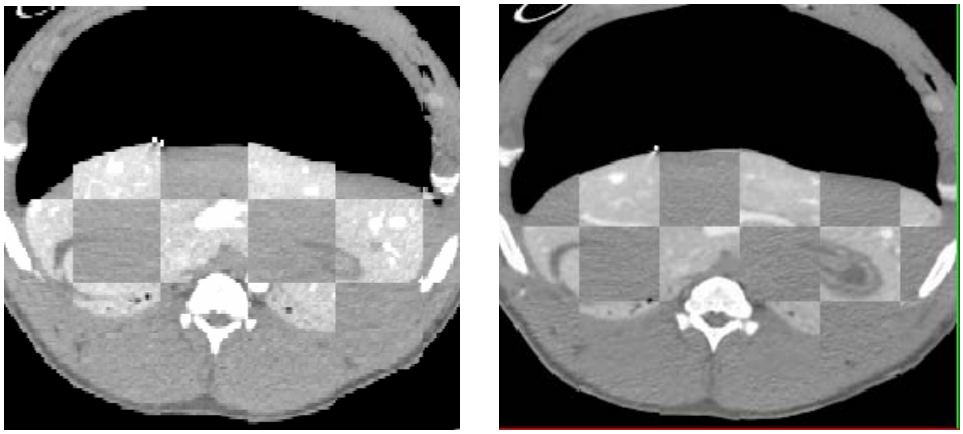

Figure 1. Superposition of initial CT and intra-operative CT (acquired at 200 mAs) before (left) and after (right) nonrigid registration. Note better structure alignment after registration.

We have further investigated the accuracy of registration quantitatively using implanted markers. The target registration error (or misalignment) before and after registration are shown in Table 1. Overall, the registration was able to reduce ~3.5 mm of initial misalignment to an acceptable approx. 1.5 mm for all dose levels. This also indicates that intra-operative CT can be conducted at 25 mAs, which is roughly 10 times smaller than the diagnostic dose. An abstract accepted for presentation at the June 2009 meeting of Computer Assisted Radiology and Surgery (CARS) conference on this topic is included with this report.

Table 1. Image misalignment before and after registration for helical scans.

Dose (mAs)	Initial Misalignment (mm)	Misalignment after Registration (mm)
200 (high)	3.12	1.47

75 (medium)	3.63	1.67
25 (low)	3.25	1.45

Note that the potential to further reduce the dose exists. First, the 25 mAs setting is the lowest setting that our current CT scanner allows. As confirmed by our earlier simulation study, registration is expected to work even at 10 mAs. We plan to explore this in the future. Replacing the standard reconstruction technique with an iterative technique, as explained below, offers the potential to further reduce the dose.

Objective 2: Dose reduction strategy: Iterative reconstruction

Iterative reconstruction techniques are known to give better quality image reconstructions in the presence of noise. Hence these techniques are better suited for reconstruction of low dose images. Over the past year, we implemented the iterative Paraboloidal Surrogate (PS) algorithm and compared the reconstruction performed with it with those from the standard filtered backprojection (FBP) algorithm that clinical CT scanners use. As iterative techniques are generally computationally intensive, we also accelerated the PS algorithm on a cluster of CPUs and also a graphics processing unit (GPU).

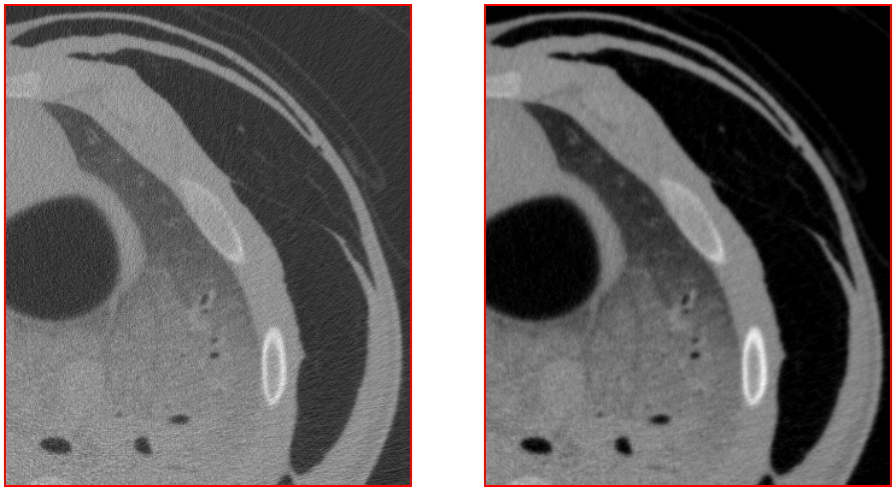

Figure 2. Reconstruction of low 25 mAs data using the standard FBP method (left) and iterative PS method (right). The right image is sharper and less noisy.

Using actual low-dose scanner data, we found PS algorithm provided improved image quality as seen in Figure 2. Figure 3 has a plot of image quality, measured as PSNR, versus CT dose for both the algorithms. Although an absolute comparison between the two techniques is difficult using PSNR, we observed that the image quality drops precipitously with the lowering of the dose with the standard FBP algorithm, whereas the image quality stays unchanged with dose for the iterative PS algorithm.

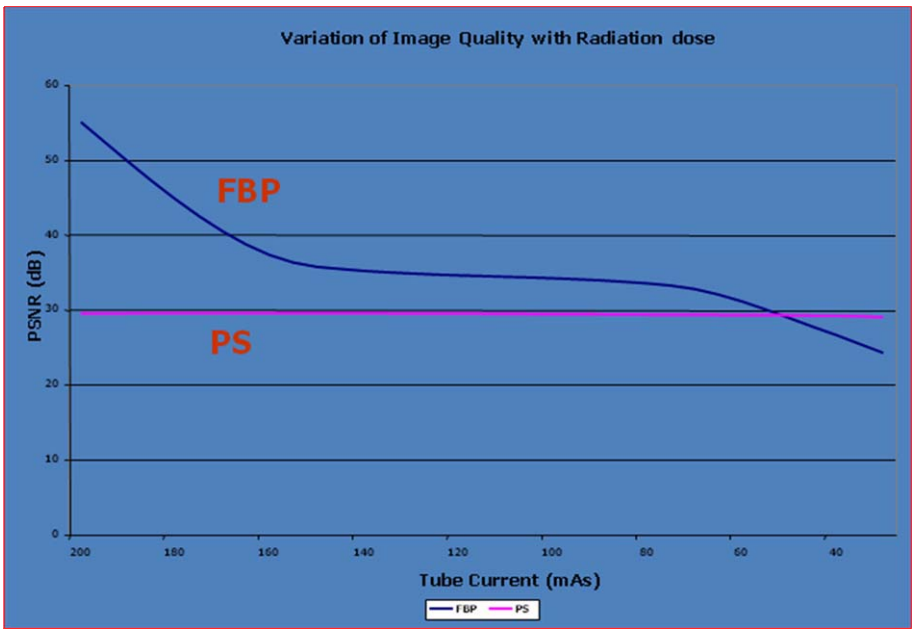

Figure 3. Image quality (in terms of PSNR) versus radiation dose (in terms of x-ray tube current) for the two reconstruction algorithms.

The time of reconstruction is variable with the image size. For 512 x 512 image matrix, which is the standard size of clinical CT images, the GPU is capable of performing 1 reconstruction per second. This speed is comparable to the reconstruction speed on most CT scanners. Two abstracts were presented on this work during the last project year. The IEEE Nuclear Science Symposium and Medical Imaging Conference abstract is attached with this report.

Objective 3: High-speed implementation of non-rigid registration

Non-rigid registration between intra-operative CT and initial CT images is a fundamental need for live AR. Computational complexity of non-rigid registration, however, is high and was addressed by this technical objective.

We earlier reported publishing of the initial architectural design for accelerated non-rigid image registration [2]. This architecture is capable of calculating mutual information, a compute intensive step in intensity-based image registration, approx. 40-times faster than a software-based implementation, and can reduce the execution time of non-rigid registration from hours to minutes. We also fully tested this implementation using high- and low-dose CT images.

In the last year, our efforts were directed at showing the optimality of our hardware implementation. A full-length paper on this work is in the press and is included with this report.

Objective 4: Tracking and visualization

We have presented in detail in prior reports our methods to link CT and laparoscope coordinate systems using optical tracking, which is a prerequisite for creating AR views. Working systematically with phantoms and ex-vivo specimens, we devoted considerable effort on identifying the sources of spatial misregistration in merging CT

and laparoscopic views and removing those. After perfecting spatial calibration, we conducted two additional animal (pig) experiments in which we collected the necessary CT and laparoscopic data for creating live AR visualization. All methods were finalized and all new data have been processed. Figures 4 and 5 show new, spatially well registered CT and laparoscopic views. Good spatial registration can also be verified by the co-location of two markers we had placed on the surface of the liver in the two modalities. An abstract summarizing our overall live AR concept and initial results has been accepted for presentation at the annual meeting of the Society of American Gastrointestinal and Endoscopic Surgeons in April 2009.

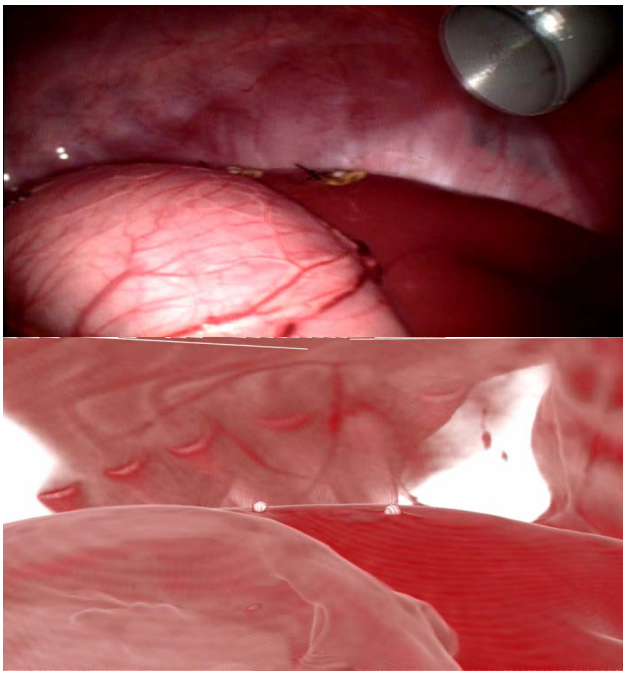

Figure 4. Side-by-side optical (laparoscopic) and CT views. A good overall alignment between anatomic structures and two fiducial markers can be observed, indicating high-accuracy augmented reality if the two views are superimposed.

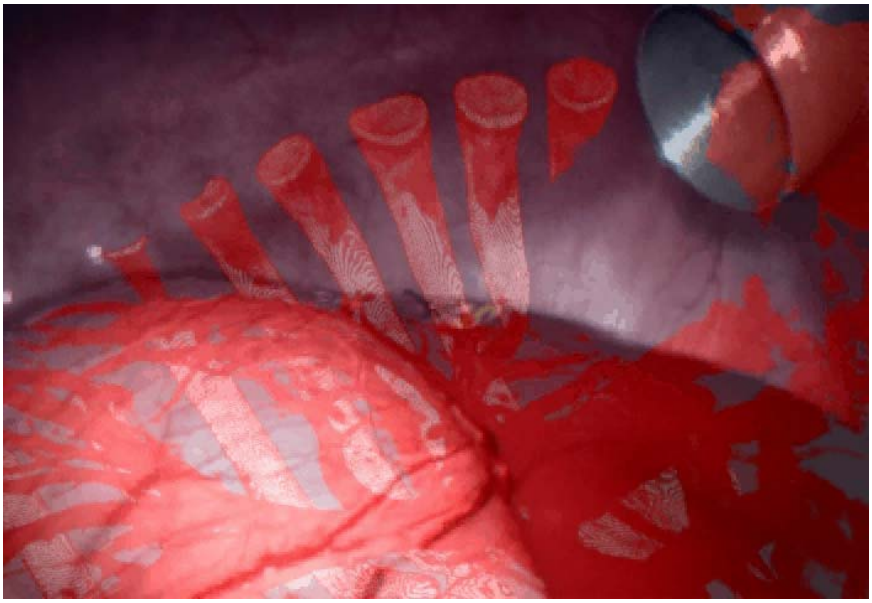

Figure 5. A snapshot of rendered CT showing internal structures overlaid on the laparoscopic image.

References

[1] O. Dandekar, K. Siddiqui, V. Walimbe, and R. Shekhar, "Image registration accuracy with low-dose CT: how low can we go?," in 3rd IEEE International Symposium on Biomedical Imaging: Nano to Macro, 2006, pp. 502-505.

[2] O. Dandekar and R. Shekhar, "FPGA-accelerated Deformable Registration for Improved Target-delineation During CT-guided Interventions," IEEE Transactions on Biomedical Circuits and Systems, vol. 1(2), pp. 116-127, 2007.

C.2. Smart Image: Image Pipeline

Smart Image: Image Pipeline

During the last phase of the contract, the following goals have guided the work of our group:

- Continued development and evaluation of registration techniques for integrating the view from the laparoscope (visual texture) onto a 3D surface model of target organs.(global 3D shape) without pose tracking.
- Exploration of techniques for integrating full volumetric models, surface models, and surface texture.
- Initiation of work on interpolation of missing or obscured image parts by use of statistical models, and on the incorporation of deformation models to pre- or itnra-operative volumetric data to allow better registration of intra-operative video sequences to these 3D data sources.

- ❖ Development and evaluation of a visualization test environment – the Dual Display Environment – to allow us to determine user preferences and to document usability enhancements likely to result from our "smart image" advances.

Texturing 3D Surface Models Without Pose Tracking

This research is driven by the need to increase the surgeon's field of view and to add depth cues to laparoscopic images. Our approach is to find software solutions that utilize data from the scope itself rather than by adding additional cameras or other sensors into the surgical environment. This assumes that 3D models will eventually be available from scope data, and we have in fact explored some possible ways of addressing this challenge (i.e., Light Falloff Stereo, see previous annual report). We have focused instead on determining how to match a series of views from the laparoscope to a 3D surface model of target anatomy, specifically using feature tracking to stitch together sequential, overlapping images. Although this task can be accomplished through the tracking of camera parameters, we have discussed a number of limitations with this approach, including accuracy concerns associated with the offset between the scope's end and the motion tracking sensors. However, in the long run, we anticipate that our method might be combined with other tracking schemes to enhance reliability of the texturing process over that achieved by any single method in isolation.

We presented a poster at the ACM SIGGRAPH International Symposium for Interactive 3D graphics (I3D), shown below, that detailed our procedures. This poster illustrated the application of our technique, which is presently semi-automated, requiring that surgeons match the first set of 2D and 3d features, to faces, teeth, and a liver.

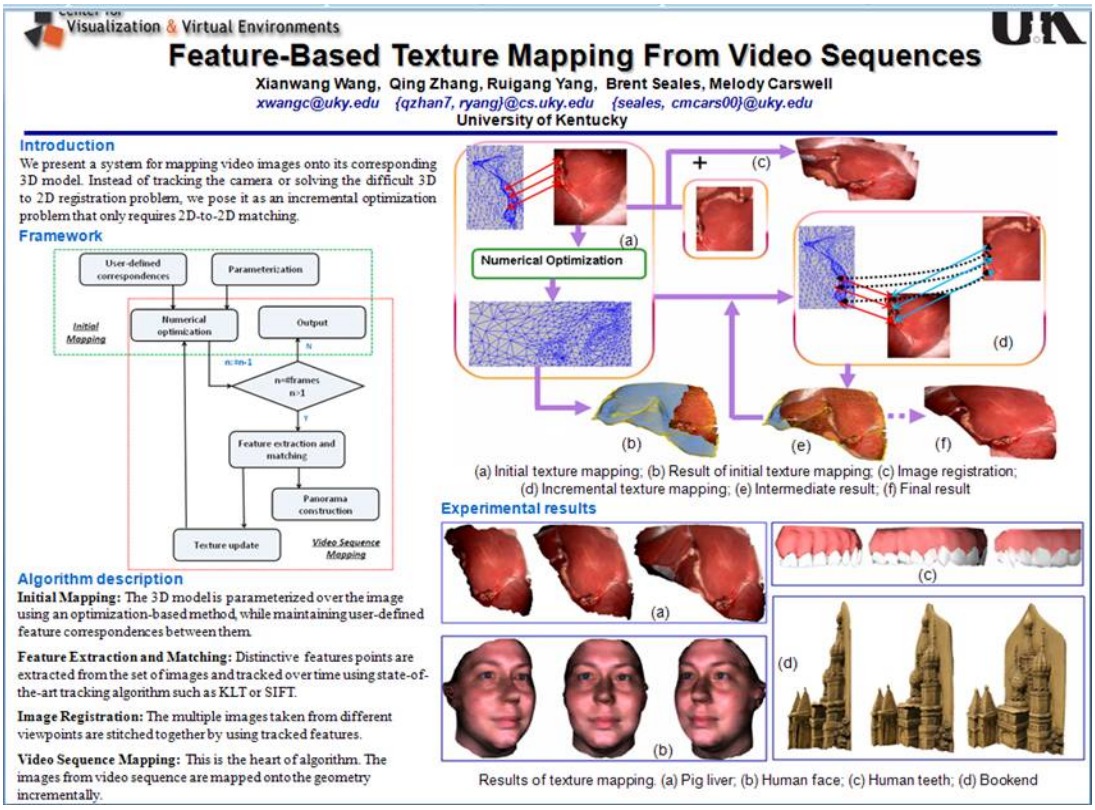

In order to better evaluate our technique against the traditional pose tracking method, we collected video segments from real anatomical training models during the first quarter of the year. However, we were faced with technical challenges when developing the baseline against which to compare our new technique. Specifically, the Faro Arm used for tracking camera pose was either broken or off site for extended periods, and we also had to develop a method of rigidly mounting our Stryker 1088 endoscope to the tracking arm. We resolved those issues during the second quarter and conducted our evaluations, finding that our method resulted in less registration error than the traditional method. These data were written up in a paper submitted to IEEE Trans.Medical Imaging which we are currently revising after the first round of largely positive reviews. The paper is appended, and the following are two views of our texture-mapping results applied to a training model of an intestine. The 3-d model is presented on the right, and the textured result is provided on the left.

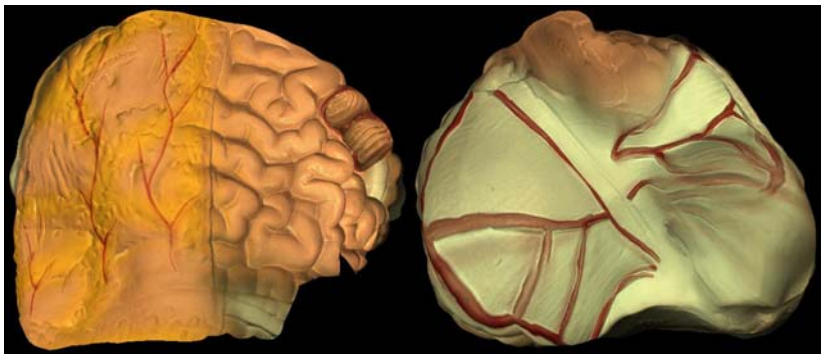

Extending Methods to Deformable Objects

Our current method assumes that a *rigid* 3D model is known a priori (e.g., from pre-op imaging). Our plan is to extend this method to handle deformable objects without requiring the knowledge of a 3D model as input. The basic idea is to use machine learning methods to find a mapping between the 2D appearance and its 3D structure of a 3D model. We will first collect a training data set of a deformable model with known 2D to 3D correspondences. This can be obtained via simulation data. Then non-linear dimension reduction techniques can be applied to automatically find the mapping. After the training is done, we will evaluate its effectiveness with real data. Ultimately the goal is to create complete 3D models from a monocular video sequence.

Based on this work, a paper was submitted to ISBQ 2009 (under review). It focuses on using a geometric deformation model to guide registration of a 3D model from pre-operative images to a small set of reconstructed 3D surface landmarks from a laparoscopic video sequence. Intra-operative tissue deformations of the target object are used to estimate deformations of important substructures, such as a tumor or a group of vessels, of the target object. Our method only requires a small number of reconstructed surface landmarks on the object, and it does not require modeling material properties. Evaluation of results of the registration and the deformation estimation show that our method performs well on the type of soft tissue deformations in our driving application – laparoscopic renal cryoablation.

The following are examples of deformation models, including bending (first two rows) and twisting (last row):

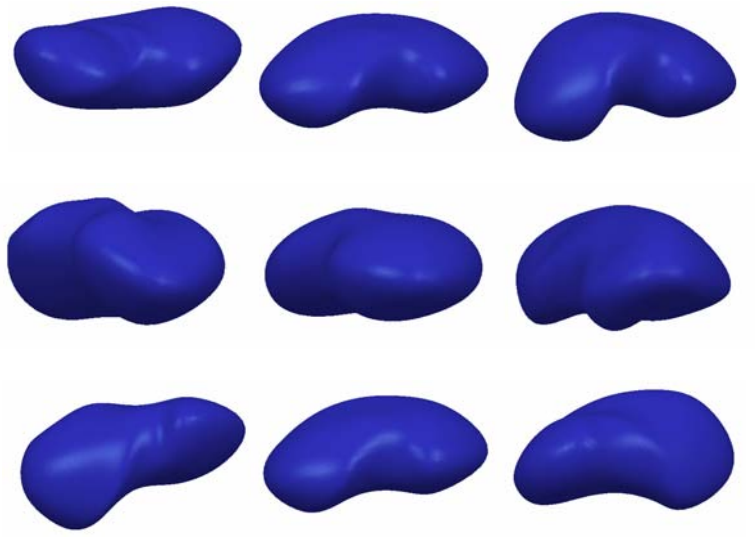

Visualization Methods and Cognitive Ergonomics

At the same time that we are developing better ways to create 3d models and integrate them with scope-acquired images, we are also trying to determine the most effective ways to view the information. We are giving special emphasis to integrating local information (scope view texture) and global information (3d panoramas) to optimize performance in a variety of surgical navigation tasks (e.g., navigation of the scope itself, navigation of instruments, searching for target "terrain"). To this end, we have proposed a dual display environment, in which the scope view and the global view are rendered side by side or, in some cases, with one superimposed on the other. In order to test the effectiveness of various configurations we have begun by getting feedback on early prototypes. This was done, first, during a visit of the team to UMMC in the first quarter of the year. We were able to get input from one fellow, 2 residents, and 4 surgeons/attending surgeons. We also introduced an early prototype of the visualization environment at the 2008 SAGES conference where surgeons viewing our demonstration provided additional feedback.

In the final phase of this project, we began developing a usability testing simulation for the visualization techniques. Our goal was to have a simulation that supports appropriate test tasks that can be used in future usability testing for a variety of variations on the basic dual display visualization scheme. The target objects in the simulation can vary from objects familiar to nonspecialists (e.g., human faces) to livers, kidneys, and other anatomical structures. A screen shot from the simulation of a human face is presented below. The left side shows the global, perspective view; the left side shows a simulation of what would be seen through the "scope." The small cone in the global view shows the location of the scope. A series of screen shots is also shown using a model of a kidney. These screen shots show other interactions that the surgeon can have with the simulation, including manipulating the global view, and varying the transparency of surface structures.

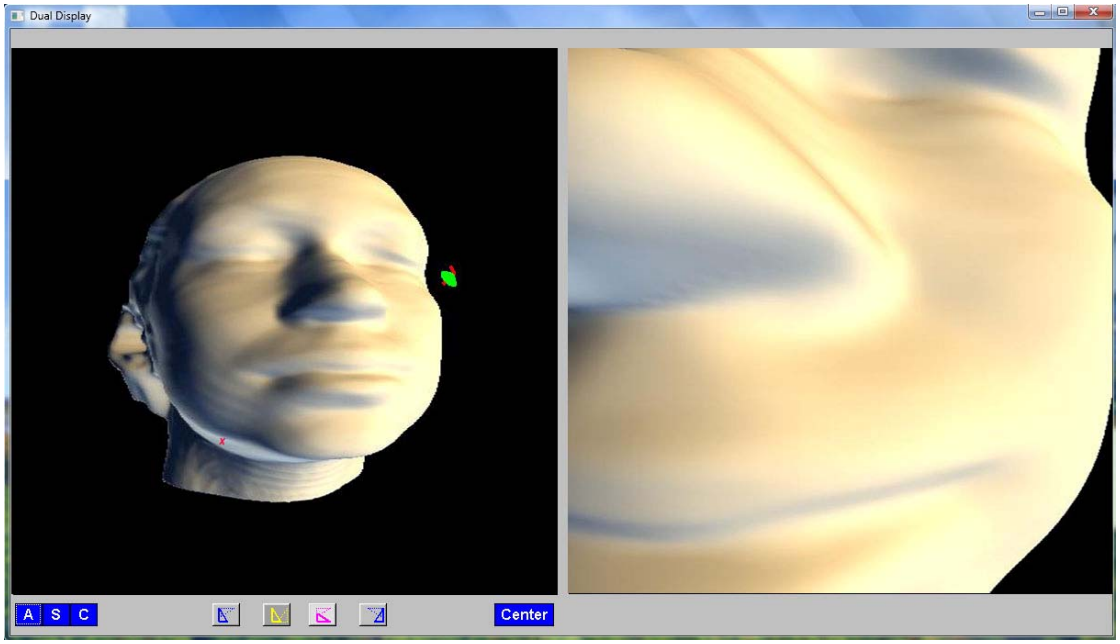

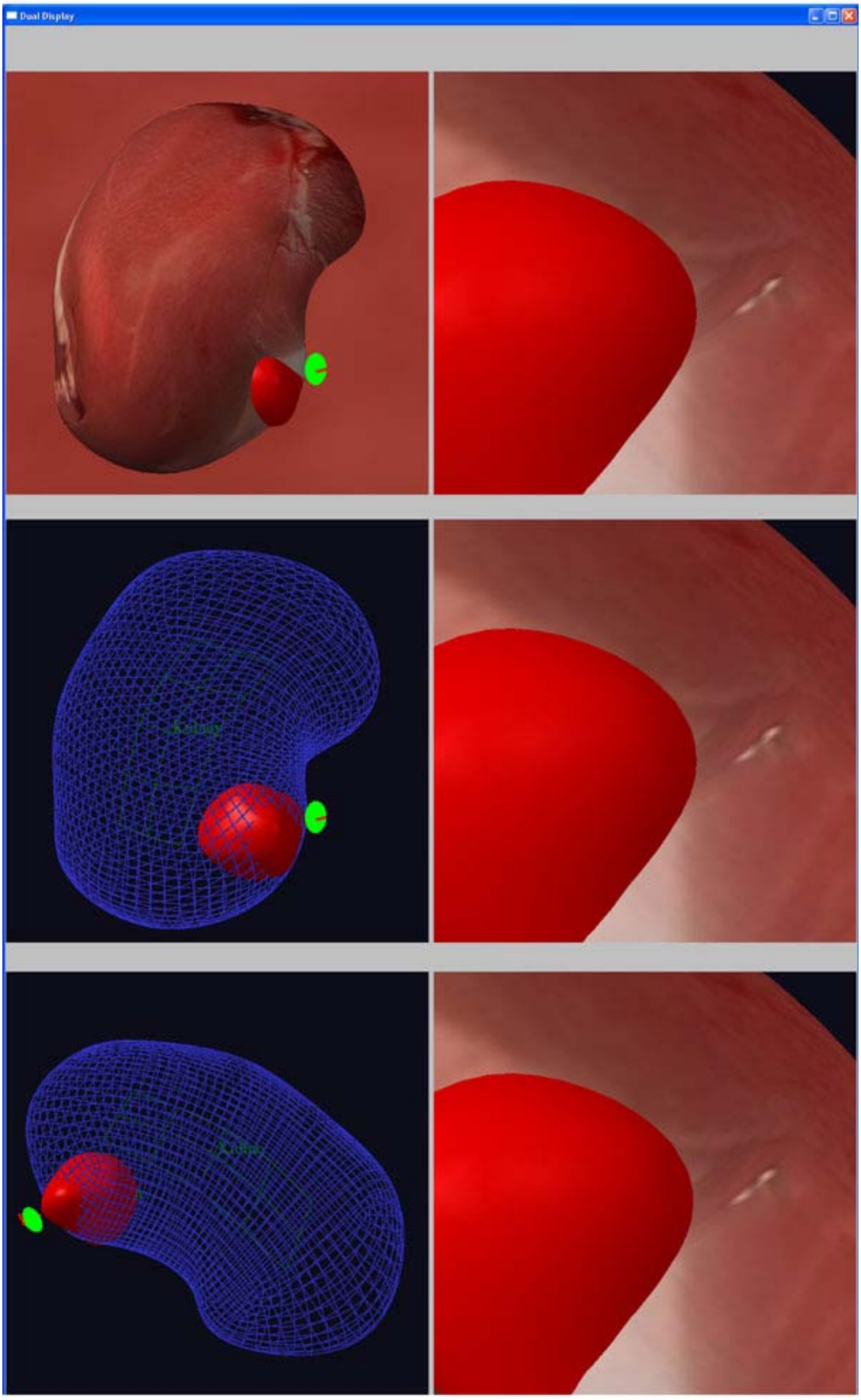
Dual Display

Experimental tasks are based on a variety of surgical navigation tasks that are likely to be aided by providing the surgeon with a global view in addition to detailed views. Some tasks are relatively simple, for example, finding a target symbol hidden amongst other structures. In this circumstance, the global view will provide a way for participants to keep track of where they have already searched. Other tasks involve finding the shortest path between landmarks and retracing one's path. The relative location of our component displays (global vs. local), color coding, and method of integration can all be tested to determine differences in search time, search efficiency, and perception of mental workload. The simulation uses a phantom desktop haptic display device to allow a research participant to manipulate the simulated "scope." The system allows for the acquisition of search times, search efficiency metrics, and search similarity metrics. Discussions of the proposed advantages of the dual display framework have been discussed at the 2008 ISE conference, and another paper is currently under review.

Papers and Presentations

Carswell, Melody, Han, Qiong, and Lio, Cindy (2008). Cognitive Ergonomics and Display Development for Minimally Invasive Surgery. Poster presented at SAGES 2008: Society of Gastrointestinal and Endoscopic Surgeons. April 2008, Philadelphia, PA.

Carswell, C.M. (2008). Surgical Navaids. Presented at Innovations in the Surgical Environment Conference, Baltimore, MD June.

Han, Q., Carswell, M., Seales, W., and Strup, S. (in submission to ISBI 09). Model-based Estimation and Visualization of global object deformations for laparoscopic renal cryoablation.

Yang, Ruigang, Carswell, Melody, Wang, Xianwang, Zhang, Qing, Han, Qiong, Seales, Brent, and Lio, Cindy. (in submission). A dual display framework for laparoscopy: Mapping the way. Surgical Innovations.

Wang, Xianwang, Zhang, Qing., Yang, Ruigang, Seales, Brent, and Carswell, Melody. (2008). Feature-based texture mapping from video sequence Presented at the 2008 symposium on Interactive 3D graphics and games, ACM SIGGRAPH.

Wang, Xianwang, Zhang, Qing, Han, Qiong, Yang, Ruigang, **Carswell, M**., and Seales, B. (in submission). Endoscopic video texture mapping on pre-built 3D anatomical objects without camera tracking. In revision for *IEEE Transactions on Medical Imaging*.

Key Research Accomplishments

A. Informatics

Informatics subgroup 1. Perioperative Scheduling Study

• A mathematical model was developed to evaluate congestion in the perioperative units. This model now drives medical center planning and patient movement activity.

Informatics subgroup 3. Operating Room Glitch Analysis

• A user interface (dashboard) was developed, containing a data manipulation layer that allows interaction with the data warehouse and provides analysts with means to create and track new metrics, a visualization toolkit to create graphs and web pages to display information effectively, and semantic services which generate data drilling functionality for graphs and data tables without the need for extra programming or user configuration. This resulted in a monitoring system of perioperative activity that is used daily in the medical center.

Informatics subgroup 3. Video Summarization

An effort evolved from the CAST system that led to the initiation of efforts to develop a summarization system for video events in the operating room. The research team compared image features with a distance metric to identify the critical view of a laparoscopic cholecystectomy. Initial results were promising, but more work needs to be done to increase accuracy. We are currently experimenting with particle analysis, edge analysis, and support vector machines as ways to create a more robust image classifier

B. Simulation (Virtual Patient)

Over the course of this project, the research team has delivered two new versions of the Maryland Virtual Patient Environment. This includes coverage of "unexpected" interventions, discontinued treatments, and new diseases to develop due to side effects of treatments. The user interface has been redesigned and a new agent-based architecture has been developed to support enhanced cognitive capabilities of the virtual patient and the intelligent tutor, including language capabilities. In the area of language processing, a dialog processing model was developed. A totally reworked system was completed in 2008 with significant enhancements in coverage of diseases.

C.1. Smart Image: CT guided imaging

The highlights of this research effort include the demonstration of the feasibility of deformable image registration with low-dose CT, demonstration of the potential for up to 20-fold reduction in radiation dose, the development of an iterative reconstruction algorithm for reconstruction of low-dose CT images. This implementation offers improved image quality at low-dose when compared with scanner-based reconstruction. Additionally, this project saw the development of an FPGA-based architecture for accelerated implementation of deformable registration algorithm. This architecture is capable of providing 40-fold speedup for image registration. The team achieved the capability of performing rigid registration (first step to deformable image registration) under 1 minute.

C.2. Smart Image: Image Pipeline

The highlights of this research program included the development of a new method of intra-operative registration that relies on feature-based texture mapping to spatially integrate video sequences into panoramas, the publishing of initial technical evaluations on the new registration technique, the development of "baseline" registration samples using more traditional (camera tracking) procedures against which to compare our new technique and the development of a new method of intra-operative depth acquisition dubbed "light fall-off stereo."

The team initiated collaboration with Stryker Endoscopy to integrate light fall-off stereo into a prototype endoscope and developed design concepts for visualization techniques based on principles of cognitive ergonomics.

Reportable Outcomes

Informatics subgroup 1. WORQ

We have now completed a mathematical model for evaluating congestion in the postoperative units, including ICUs, IMCs and floor units. This model is currently in use within the medical center to predict patient flow.

Informatics subgroup 2. OGA

The clinical information system developed by this project is in regular use by the hospital to monitor operating room delay and consequent patient flow. A live dashboard portraying OR timing is on the desk of the Heads of Surgery, Radiology and Anethesiology.

Simulation

The Maryland Virtual Patient has been developed into the only known cognitive simulation training system. Specific clinical aspects of LERD/GERD can be taught with realism and accuracy.

Programmatic

Overall, the research program, Innovations in the Surgical Environment, has produced a significant growth in the scientific knowledge pertaining to the surgery milieu. The annual research conference has matured from a local, PI-update type of meeting to an important and well-respected international scientific event. Attendees to this meeting include representatives of the highest national health agencies, the National Institutes of Health, major academic settings and military organizations. More than two hundred publications and presentations have been generated directly from research conducted under the auspices of this contract.

Conclusion

This report began with the recognition that an extraordinary evolution in surgical care has occurred caused by rapid advances in technology and creative approaches to medicine. The increased speed and power of computer applications, the rise of visualization technologies related to imaging and image guidance, improvement in simulation-based technologies (tissue properties, tool-tissue interaction, graphics, haptics, etc) have interacted to advance the practice of surgery. However, the medical profession lags behind other applications of information systems. The research program reported here has proceeded under the mantle of “Operating Room of the Future”. As a natural occurrence in the outcome of lessons learned in medicine, we replaced that theme with the more appropriate “Innovations in the Surgical Environment.”

There are three major portions of this study; OR informatics, simulation research, and smart image. Future research efforts here at Maryland will incorporate work related to cognitive ergonomics and human factors as these impact the surgical environment.

The purpose of the OR informatics program is to develop, test, and deploy technologies to collect real-time data about key tasks and process elements in clinical operating rooms. We have established testbeds of activities in both simulated and operational environments. We are currently performing tests of the hardware, refining software, and applying lessons learned to hospital operational functions. The objective of Simulation research is to create a system where a user can interact with a virtual human model in cognitive simulation and have the virtual human respond appropriately to user queries and interventions in clinical situations, with a focus on cognitive decision making and judgment. We have made significant strides toward realizing these goals. The MVP simulation functions well for esophageal disorders, and is continuing to expand the repertoire of diseases that are in the simulation model.

The objective of smart image was to use real-time 3D ultrasonography and 40-slice highframe-rate computed tomography (CT) for intraoperative imaging to volume rendered anatomy from the perspective of the endoscope. We are combining CT and Ultrasound to overlay image and data to enhance the performance of surgeons-intraining. We have carried out animate model testing of the image registration with great success. We continue to refine and expand our capability through hardware and software refinement.

In the future, OR workspace layout would be optimized through ergonomic data and human factors analysis, and this optimization would lead to the establishment of "best practices" for an array of surgical operations. Proper layout would reduce risks of infection, speed operations, and reduce fatigue of surgeons and staff, all elements that could contribute to a reduction in AEs and improved patient safety.

The year ahead is full of promise for refinements in the use of informatics to support safe and efficient operating room procedures, the use of simulation to improve and accelerate the training of competent surgeons, and the blending of imaging capabilities to provide clearer and safer interactions between patient and surgeon.

References

Year 1 (2004)

- Shekhar R, Zagrodsky V, Garcia M, Thomas JD: Registration of real-time 3D ultrasound images of the heart for novel 3D stress echocardiography. IEEE Transactions on Medical Imaging 23(9), p 1141-1149, 2004.
- Tang M, Shekhar R, Huang D: Mean curvature mapping for detection of corneal shape abnormality. IEEE Transactions on Medical Imaging 24(3), p 424-428, 2005.
- Castro-Pareja CR, Shekhar R: Hardware acceleration of mutual information-based 3D image registration. Journal of Imaging Science and Technology 49(2), p 105-113, 2005.

- Li J, Papachristou C, Shekhar R: An FPGA-based computing platform for real-time 3D medical imaging and its application to cone-beam CT reconstruction. Journal of Imaging Science and Technology 49(3), p 237-245, 2005.
- Zagrodsky V, Walimbe V, Castro-Pareja CR, Qin JX, Song J-M, Shekhar R: Registration-assisted segmentation of real-time 3-D echocardiographic data using deformable models. IEEE Transactions on Medical Imaging 24(9), 1089-1099, 2005.
- Shekhar R, Walimbe V, Raja S, Zagrodsky V, Kanvinde M, Wu G, Bybel B: Automated three-dimensional elastic registration of whole-body PET and CT from separate or combined Scanners. Journal of Nuclear Medicine 46(9), 1488-1496, 2005.
- Tang M, Shekhar R, Miranda D, Huang D: Characteristics of keratoconus and pellucid marginal degeneration in mean curvature maps. American Journal of Ophthalmology 140(6), 993-1001, 2005.
- Xiao Y, Seagull JF, Mackenzie CF, Klein K. Adaptive Leadership in Trauma Resuscitation Teams: A Grounded Theory Approach to Video Analysis. Cognition Technology & Work, 12:158-164, 2004 Anbari, KK, Garino JP, Mackenzie, CF. Hemoglobin substitutes. Eur Spine J. 13: Supp/1: S76-82,
- Xiao Y, Mackenzie CF. Introduction to the special issue on video-based research in high risk settings: Methodology and experiences. Editorial. Cognitive Technology and Work. 12:130, 2004.
- Hu PF, Xiao Y, Mackenzie CF, Seagull FJ, Brooks T, LaMonte MP, & Gagliano D. Many to One to Many Telemedicine Architecture and Applications . Telemedicine Journal and e-Health. 10 (Supplement 1), S-39. 2004
- Xiao Y, Gagliano D, Hu PF, LaMonte MP, & Mackenzie CF. Designing mobile telemedicine applications: A testbed and lessons learned. Telemedicine Journal and e-Health. 10 (Supplement1), S-119. 2004
- Mackenzie CF, Xiao Y, Horst RL. Video Task Analysis in High Performance Teams. Cognition Technology &Work, 12: 139-147, 2004.
- J. Caban and W. B. Seales, " Reconstruction and Enhancement in Monocular Laparoscopic Imagery ," in Proceedings of Medicine Meets Virtual Reality (MMVR) 2004, Newport Beach, California, January, 2004.
- W. B. Seales and Duncan Clarke, " Computing Support for Information-Rich Laparoscopy ," in Surgical Innovation, Volume 12, Number 4 (December), 2004.

Year 2 (2005)

- Segan R, Park A: Training Competent Minimal Access Surgeons: Review of Tools, Metrics, and Techniques Across the Spectrum of Technology. Surgical Technology International XIII. Universal Medical Press. 2005; pp 25-32.
- Jarrell BE, Mallott, DE, Raczek, J, Skinner, C, Jarrell, K, Shimko, M: Observations for Electronic Medical Simulation: The Heuristic Patient, Surgical Innovation, Volume 12, No 1, 43-49, March 2005
- Fullum TM, Kim S, Dan D, Turner PL. Laparoscopic "Dome-down" cholecystectomy with the LCS-5 Harmonic scalpel. JSLS. 2005 Mar; 9(1):51-7.

- Siegel EL, KM Siddiqui, JP Johnson, BI Reiner, A Musk, Nagy PG, Safdar N Compression of multislice CT: 2D vs 3D JPEG2000 and effects of slice thickness. SPIE :PACS and Imaging Informatics 2005
- Nagy PG, Siegel EL, Reiner BI, Siddiqui KM, Dal Molin J. Openrad: an open collaboratory for radiology informaticians. SPIE :PACS and Imaging Informatics 2005
- Siegel EL, Musk A, Siddiqui KM, Reiner BI, Nagy PG, Safdar N. Impact of the use of dual energy subtraction on the performance of a computer-assisted diagnosis system in the detection Proc. SPIE :PACS and Imaging Informatics 2005
- Nagy P, Schultz T. Chapter 16: Storage and Arching, In: PACS: A Guide to the Digital Revolution 2nd Edition, New York, New York: Springer, 2005
- Nagy P, George I, Bernstein W, Caban J, Klein R, Mezrich R, and Park A. Radio frequency identification systems technology in the surgical setting. Surg Innov 13(1): 61-67, 2006
- Dutton R, Ho D, Hu P, Mackenzie CF, Xiao Y. Decision Making by Operating Room Managers: The Burden of Changes. Anesthesiology, 103:A1175. 2005. Mackenzie CF (Editorial). Sacred Cows: Milking the controversies in resuscitation. Hosp. Med (London), 66:68-69, 2005.
- Dutton R, Hu PF, Mackenzie CF, Seebode S, Xiao Y. A Continuous Video Buffering System for Recording Unscheduled Medical Procedures. Anesthesiology, 103:A1241. 2005.
- Hu PF, Burlbaugh M, Xiao Y, Mackenzie CF, Voigt R, Brooks T, Fraser L, Connolly MR, Herring T. Video Infrastructure and Application Design Methods for an OR of the Future. Telemedicine and e-Health. 11(2), 211, T3C2. 2005.
- Hu PF, Hu H, Seagull JF, Mackenzie CF, Voigt R, Martz D, Dutton R, Xiao Y. Distributed Video Board: Advanced Telecommunication System for Operation Room Coordination. Telemedicine and e-Health. 11(2), 248, P28. 2005.
- Hu PF, Mackenzie CF, Xiao Y, Seagull JF, Lam D, Gagliano D. Mobile Video Transfer System for Homeland Security and Disaster Management. Telemedicine and e-Health. 11(2), 248,P29. 2005.
- Kavic SM, Segan RD, Turner PL, George IM, Park AE. Repair of a complex foregut hernia aided by three-dimensional surgical reconstruction (abstract). Surg Endosc Supplement 19 2005
- Segan RD, Kavic SM, George IM, Turner PL, Park AE. A novel conceptual model of the current classification of paraesophageal hernias using dynamic three-dimensional Reconstruction (abstract). Surgic Endosc (Supplement 19). 2005
- Jesus J. Caban, W. Brent Seales, Adrian Park, Heterogeneous Displays for Surgery and Surgical Simulation. Proceedings of Medicine Meets Virtual Reality 13, January 2005.
- Carswell, C, Clarke, D., Seales, W., "Assessing Mental Workload during Laparoscopic Surgery"
- Seales, W. and Clarke, D, "Computing Support for Information-Rich Laparoscopy"
- Lee G. et al, "Pilot study -- Correlation between postural stability and performance time during fundamentals of laparoscopic surgery"

- Lee G. et. al: " Jont Kinematics vary with performance skills during laparoscopic exercise"
- Lee G. et al: "Postural instability does not necessarily correlate to poor performance"
- Li Ding, Tim Finin, Anupam Joshi, Yun Peng, Rong Pan and Pavan Reddivari, Search on the Semantic Web, IEEE Computer, October 2005.
- Anand Patwardhan, Filip Perich, Anupam Joshi, Tim Finin and Yelena Yesha, Active Collaborations for Trustworthy Data Management in Ad Hoc Networks, 2nd IEEE Int. Conf. on Mobile Ad-Hoc and Sensor Systems, 7-10 November 2005, Washington DC.
- Mark Burstein, Christoph Bussler, Tim Finin, Michael Huhns, Massimo Paolucci, Amit Sheth, Stuart Williams and Michal Zaremba, A Semantic Web Services Architecture, IEEE Internet Computing, pp 52-61, v9, n5, September/October 2005.
- Li Ding, Rong Pan, Tim Finin, Anupam Joshi, Yun Peng and Pranam Kolari, Finding and Ranking Knowledge on the Semantic Web, Proc. 4th Int. Semantic Web Conf., Galway IE, Nov. 2005.
- Akshay Java, Tim Finin and Sergei Nirenburg, Integrating Language Understanding Agents Into the Semantic Web, First Int. Symposium on Agents and the Semantic Web, 2005 AAAI Fall Symposium Series, Arlington VA, 4-6 November, 2005.
- Harry Chen, Filip Perich, Tim Finin and Anupam Joshi, The SOUPA Ontology for Pervasive Computing, in Ontologies for Agents: Theory and Experiences, Valentina Tamma, Stephen Cranefield, Tim Finin and Steven Willmott (Eds), Springer Verlag, June 2005.
- Valentina Tamma, Stephen Cranefield, Tim Finin and Steven Willmott (Eds), Ontologies for Agents: Theory and Experiences, Springer Verlag, June 2005, ISBN: 3-7643-7237-0.
- Tim Finin, Li Ding, Rong Pan, Anupam Joshi, Pranam Kolari, Akshay Java and Yun Peng, "Swoogle: Searching for knowledge on the Semantic Web", Intelligent Systems Demonstration, Proc. 20th National Conf. on Artificial Intelligence, July 2005.
- Filip Perich, Anupam Joshi, Yelena Yesha and Tim Finin, "Collaborative Joins in a Pervasive Computing Environment", VLDB Journal, v14 n2, pp 182-196, April 2005.
- Li Ding, Tim Finin and Anupam Joshi, Analyzing Social Networks on the Semantic Web, IEEE Intelligent Systems (Trends and Controversies), v9, n1, Jan/Feb 2005.

Year 3 (2006)

- Agarwal, S., Joshi, A., Finin, T. and Yesha, Y. A Pervasive Computing System for the Operating Room of the Future, technical report TR-CS-06-xx, Computer Science and Electrical Engineering, University of Maryland, Baltimore County, September 2006. http://ebiquity.umbc.edu/paper/html/id/339/
- Agarwal, S., Context-Aware System to Create Electronic Medical Encounter Records, M.S. thesis, Computer Science and Electrical Engineering, University of

Maryland, Baltimore County, May 2006.
http://ebiquity.umbc.edu/paper/html/id/338/

- Agarwal, S., Joshi, A., Finin, T., Ganous, T. and Yesha, Y. Context-Aware System to Create Electronic Medical Records, technical report TR-CS-06-05, Computer Science and Electrical Engineering, University of Maryland, Baltimore County, July 2006. http://ebiquity.umbc.edu/paper/html/id/312/
- Akshay Java, Tim Finin and Sergei Nirenburg, Text understanding agents and the Semantic Web, 39th Hawaii Int. Conf. on System Sciences, Kauai HI, 4-6 January, 2006.
- Akshay Java, Tim Finin, and Sergei Nirenburg, SemNews: A Semantic News Framework, Proceedings of the 21st National Conf. on Artificial Intelligence, July 2006.
- Anand Patwardhan, Filip Perich, Anupam Joshi, Tim Finin and Yelena Yesha, Querying in packs: Trustworthy Data Management in Ad Hoc Networks, International Journal of Wireless Information Networks, 2006.
- Boanerges Aleman-Meza, Meenakshi Nagarajan, Cartic Ramakrishnan, Amit Sheth, Budak Arpinar, Li Ding, Pranam Kolari, Anupam Joshi, and Tim Finin, "Semantic Analytics on Social Networks: Experiences in Addressing the Problem of Conflict of Interest Detection", WWW2006, Edinburgh, May 2006.
- Cynthia Parr, Andriy Parafiynyk, Joel Sachs, Li Ding, Sandor Dornbush, Tim Finin, Taowei Wang, and Allan Hollander, Integrating Ecoinformatics Resources on the Semantic Web, poster paper, 15th International World Wide Web Conf., Edinburgh, May 2006.
- Dandekar O, Walimbe V, Siddiqui K, Shekhar R: Image registration accuracy with low-dose CT: How low can we go? In Proceedings of 2006 IEEE International Symposium on Biomedical Imaging, p 502-505.
- Dandekar O, Walimbe V, Shekhar R: Hardware implementation of hierarchical volume subdivision-based elastic registration. In Proceedings of the 28th Annual International Conference of the IEEE Engineering in Medicine and Biology Society (IEEE EMBC 2006), p 1425-1428.
- Dandekar O, Castro-Pareja CR, Shekhar R,"FPGA-based Reconfigurable 3D Image Pre-processing for Image Guided Interventions. Journal of Real-Time Image Processing. (Submitted)
- Goodman L, Gulsun M, Washington L, Nagy P, Piacsek K Inherent Variability of CT Lung Nodule Measurements In Vivo Using Semi automated Volumetric Measurements Am J Roentgenol, 186: 989-994, 2006
- Hu P, Xiao Y, Ho D, Mackenzie CF, Hu H, Voigt R, Martz D. Advanced Visualization Platform for Surgical Operating Room Coordination: Distributed Video Board System. Surgical Innovation. 13(2):129-135. 2006
- Jarrell B, Nirenburg S, McShane M, Fantry G, Beale S, Mallott, D, Raczek J: “Simulation for Teaching Decision Making in Medicine: The Next Step”, In Proceedings of Medicine Meets Virtual Reality : IGT-Registration & Navigation, 2007.
- Jim Parker, Anand Patwardhan, Filip Perich, Anupam Joshi and Tim Finin, Trust in Pervasive Computing, in The Handbook of Mobile Middleware, P. Bellavista and A. Corradi (eds.), pp. 473-496, CRC Press, May 2006.

- Kavic SM, Segan RD, George IM, Turner PL, Roth JS and Park A. Classification of hiatal hernias using dynamic three-dimensional reconstruction. Surg Innovation. 2006; 13: 21-25.
- Kavic SM, Segan RD, George IM, Turner PL, Roth JS, Park AE. Classification of hiatal hernias using dynamic three-dimensional reconstruction, Surg Innov 13(1): 49-52, 2006
- Kavic SM, Segan RD, George IM, Turner PL, Roth JS, Park AE. Classification of hiatal hernias using dynamic three-dimensional reconstruction, Surg Innov, March 2006.
- Lalana Kagal and Tim Finin, Modeling Conversation Policies using Permissions and Obligations, Journal of Autonomous Agents and Multi-Agent Systems, to appear, 2006.
- Nagy P, George I, Bernstein W, Caban J, Klein R, Mezrich R, and Park A. Radio frequency identification systems technology in the surgical setting. Surg Innov 13(1): 61-67, 2006
- Nagy P, George I, Bernstein W, Caban J, Klein R, Mezrich R, Park A. Radio frequency identification systems technology in the surgical setting. Surg Innov 13(1): 61-67, 2006
- Nirenburg, S., M. McShane, S. Beale, T. O'Hara, G. Fantry, J. Raczek, B. Jarrell, "Cognitive Simulation in Virtual Patients", accepted for presentation at the 19th International FLAIRS Conference, Melbourne Beach, Florida, May 11-13, 2006.
- Pranam Kolari and Tim Finin, A Framework for Multi-Relational Analytics on the Blogosphere, (abstract), Proceedings of the 21st National Conf. on Artificial Intelligence, July 2006.
- Pranam Kolari, Akshay Java and Tim Finin, "Characterizing the Splogosphere", Third Annual Workshop on Weblogging Ecosystem: Aggregation, Analysis and Dynamics, held in conjunction with WWW2006, Edinburgh, May 2006.
- Pranam Kolari, Akshay Java, Tim Finin, Tim Oates, and Anupam Joshi, Detecting Spam Blogs: A Machine Learning Approach, Proceedings of the 21st National Conf. on Artificial Intelligence, July 2006.
- Pranam Kolari, Tim Finin and Anupam Joshi, SVMs for the Blogosphere: Blog Identification and Spam Detection, AAAI Spring Symposium on Computational Approaches to Analyzing Weblogs, Stanford, March 2006.
- Pranam Kolari, Tim Finin, Yelena Yesha, Kelly Lyons, Jen Hawkins and Stephen Perelgut, Policy Management of Enterprise Systems: A Requirements Study, short paper, 2006 IEEE Workshop on Policy for Distributed Systems and Networks, 5-7 June 2006, London, Ontario CN.
- Ross, J.M., T.M. Bayles, C. Parker, S.L.Titus, B. Jarrell and J. Raczek, Engineering in Health Care Multimedia Curriculum for High School Technology Education, accepted for presentation in the K-12 Engineering Outreach Division of the 2006 American Society for Engineering Education Annual Conference & Exposition in Chicago, IL, June 2006
- Shekhar R, Dandekar O, Kavic S, George I, Mezrich R, Park A, "Development of continuous CT-guided minimally invasive surgery," In Proceedings of SPIE Medical Imaging 2007: Visualization and Image-Guided Procedures, vol. 6509, pp. 65090D, 2007

- Shekhar R, Dandekar O, Kavic S, George I, Mezrich R, Park A, "Development of 16 continuous CT-guided minimally invasive surgery," In Proceedings of Medicine Meets Virtual Reality: IGT-Registration & Navigation, 2007
- Tim Finin and Li Ding, Search Engines for Semantic Web Knowledge, Proceedings of XTech 2006: Building Web 2.0, 16-19 May 2006.
- Vartak, N., Protecting the privacy of RFID tags. (M.S. thesis) Computer Science and Electrical Engineering, University of Maryland, Baltimore County, May 2006.
- Walimbe V, Shekhar R: Automatic elastic image registration by interpolation of 3D rotations and translations from discrete rigid-body transformations, Medical Image Analysis of 3D rotations and translations from discrete rigid-body transformations, Medical Image Analysis
- Wasei M, Xiao Y, Wieringa P, Strader M , Hu P, Mackenzie C. Visualization of Uncertainty to Support Collaborative Trajectory Management in Hospital Care. 2006 Conference of International Ergonomics Association.3721-3726. 2006
- Xiao Y, Strader M, Hu P, Wasei M, Wieringa P. Visualization Techniques for Collaborative Trajectory Management . ACM Conference on Human Factors in Computing Systems, pp.1547 - 1552. 2006
- Xiao Y, Wasei M, Hu P, Wieringa P, Dexter F. Dynamic Management in Perioperative Processes: A Modeling and Visualization Paradigm. 12th IFAC Symposium on Information Control Problems in Manufacturing. (3)647-52. 2006

Year 4 (2007)

- Dexter F, Epstein RH, Traub RD, & Xiao Y. Making Management Decisions on the Day of Surgery Based on Operating Room Efficiency and Patient Waiting Times. Anesthesiology, 101(6):1444-1453. 2004
- Dexter F, Xiao Y, Dow AJ, Strader MM, Ho D, Wachtel RE. Coordination of Appointments for Anesthesia Care Outside of Operating Rooms Using an Enterprise Wide Scheduling System. Anesthesia and Analgesia. 105:1701-1710. 2007
- Dexter F, Xiao Y, Dow AJ, Strader MM, Ho D, Wachtel RE. Coordination of Appointments for Anesthesia Care Outside of Operating Rooms Using an Enterprise Wide Scheduling System. Anesthesia and Analgesia. 105:1701-1710. 2007
- Dutton R, Ho D, Hu P, Mackenzie CF, Xiao Y. Decision Making by Operating Room Managers: The Burden of Changes. Anesthesiology, 103:A1175. 2005
- Dutton R, Hu P, Seagull FJ, Scalea T, Xiao Y, . Video for Operating Room Coordination: Will the Staff Accept It?. Anesthesiology: 101: A1389. 2004
- Dutton R, Hu PF, Mackenzie CF, Seebode S, Xiao Y. A Continuous Video Buffering System for Recording Unscheduled Medical Procedures. Anesthesiology, 103:A1241. 2005
- Gilbert TB, Hu PF, Martz DG, Jacobs J, Xiao Y. Utilization of Status Monitoring Video for OR Management. Anesthesiology, 103:A1263. 2005
- Hu P, Seagull FJ, Mackenzie CF, Seebode S, Brooks T, XiaoY. Techniques for Ensuring Privacy in Real-Time and Retrospective Use of Video. Telemedicine and e-Health, 12(2): 204, T1E1. 2006

- Hu P, Xiao Y, Ho D, Mackenzie CF, Hu H, Voigt R, Martz D. Advanced Visualization Platform for Surgical Operating Room Coordination: Distributed Video Board System. Surgical Innovation. 13(2):129-135. 2006
- Hu PF, Burlbaugh M, Xiao Y, Mackenzie CF, Voigt R, Brooks T, Fraser L, Connolly MR, Herring T. Video Infrastructure and Application Design Methods for an OR of the Future. Telemedicine and e-Health. 11(2), 211, T3C2. 2005
- Hu PF, Hu H, Seagull JF, Mackenzie CF, Voigt R, Martz D, Dutton R, Xiao Y. Distributed Video Board: Advanced Telecommunication System for Opearation Room Coordination. Telemedicine and e-Health. 11(2), 248, P28. 2005
- Hu PF, Xiao Y, Mackenzie CF, Seagull FJ, Brooks T, LaMonte MP, & Gagliano D. Many to One to Many Telemedicine Architecture and Applications. Telemedicine Journal and e-Health. 10(Supplement 1), S-39. 2004
- Kim Y-J, Xiao Y, Hu P, Dutton RP. Staff Acceptance of Video Monitoring for Coordination: A Video System to Support Perioperative Situation Awareness. Journal of Clinical Nursing (accepted). 2007
- Kim Y-J, Xiao Y, Hu P, Dutton RP. Staff Acceptance of Video Monitoring for Coordination: A Video System to Support Perioperative Situation Awareness. Journal of Clinical Nursing (accepted). 2007
- Dandekar and R. Shekhar, "FPGA-accelerated Deformable Registration for Improved Target-delineation During CT-guided Interventions," IEEE Transactions on Biomedical Circuits and Systems, vol. 1(2), pp. 116-127, 2007.
- Dandekar, C. Castro-Pareja, and R. Shekhar, "FPGA-based real-time 3D image preprocessing for image-guided medical interventions," Journal of Real-Time Image Processing, vol. 1(4), pp. 285-301, 2007.
- Dandekar, K. Siddiqui, V. Walimbe, and R. Shekhar, "Image registration accuracy with low-dose CT: how low can we go?," in 3rd IEEE International Symposium on Biomedical Imaging: Nano to Macro, 2006, pp. 502-505.
- Dandekar, V. Walimbe, and R. Shekhar, "Hardware Implementation of Hierarchical Volume Subdivision-based Elastic Registration" in 28th Annual International Conference of the IEEE: Engineering in Medicine and Biology Society, 2006, pp. 1425-1428.
- O. Dandekar, W. Plishker, S. Bhattacharyya, and R. Shekahr, "Multiobjective Optimization of FPGA-Based Medical Image Registration" IEEE Symposium on Field-Programmable Custom Computing Machines, Under Review, 2008.
- R. Shekhar, O. Dandekar, S. Kavic, I. George, R. Mezrich, and A. Park, "Development of continuous CT-guided minimally invasive surgery," Multimedia Meets Virtual Reality (MMVR), 2007.
- R. Shekhar, O. Dandekar, S. Kavic, I. George, R. Mezrich, and A. Park, "Development of continuous CT-guided minimally invasive surgery," Proc SPIE, Medical Imaging 2007.
- Seagull FJ, Xiao Y, & Plasters C. Information Accuracy and Sampling Effort: A Field Study of Surgical Scheduling Coordination. IEEE Transactions on Systems, Man, and Cybernetics, Part A:Systems and Humans. 24(6), 764-771. 2004
- Xiao Y, Dexter F, Hu FP, Dutton R. Usage of Distributed Displays of Operating Room Video when Real-Time Occupancy Status was Available . Anesthesia and Analgesia 2008; 106(2):554-560. 2008

- Xiao Y, Hu P, Hu H, Ho D, Dexter F, Mackenzie CF, Seagull FJ, Dutton D. An algorithm for processing vital sign monitoring data to remotely identify operating room occupancy in real-time. Anesthesia & Analgesia,(101)3:823-829 . 2005
- Xiao Y, Hu P, Moss J, de Winter J, Venekamp D, Mackenzie CF, Seagull FJ, Perkins S. Opportunities and challenges in improving surgical work flow. Cognition, Technology & Work, accepted. 2007
- Xiao Y, Schimpff S, Mackenzie CF, Merrell R, Entin E, Voigt R, Jarrell B. Video Technology to Advance Safety in the Operating Room and Perioperative Environment. Surgical Innovation. 14(1): 52-61. 2007
- Xiao Y, Schimpff S, Mackenzie CF, Merrell R, Entin E, Voigt R, Jarrell B. Video Technology to Advance Safety in the Operating Room and Perioperative Environment. Surgical Innovation. 14(1): 52-61. 2007
- Xiao Y, Strader M, Hu P, Wasei M, Wieringa P. Visualization Techniques for Collaborative Trajectory Management . ACM Conference on Human Factors in Computing Systems, pp.1547 - 1552. 2006
- Xiao Y, Wasei M, Hu P, Wieringa P, Dexter F. Dynamic Management in Perioperative Processes: A Modeling and Visualization Paradigm. 12th IFAC Symposium on Information Control Problems in Manufacturing. (3)647-52. 2006

Appendices

A. An image registration-based approach for continuous volumetric CT-guided interventions. Accepted for presentation at the 2009 Computer Assisted Radiology and Surgery (CARS) Conference. R. Shekhar, A. Prithviraj. [Abstract]

B.. High-speed reconstruction of low-dose CT using GP-GPU. Accepted for presentation at the 2008 IEEE Nuclear Science Symposium and Medical Imaging Conference. V. Bhat, R. Shekhar [Extended Abstract]

C. Multiobjective optimization for reconfigurable implementation of medical image registration. Accepted by International Journal of Reconfigurable Computing. Dandekar O, Plishker W, Bhattacharyya SS, Shekhar R [Preprint]

D. Augmented Reality for Laparoscopic Surgery Using a Novel Imaging Method – Initial Results from a Porcine Animal Model. R Shekhar, C Godinez, S Kavic, E Sutton, V Bhat, O Dandekar, I George, A Park. To be presented at 2009 Society of American Gastrointestinal and Endoscopic Surgeons Conference. [Abstract]

E Novel, Web-Based, Information-Exploration Approach for Improving Operating Room Logistics and System Processes

F. A Research Portfolio for Innovation in the Surgical Environment

G. Methodological Infrastructure in Surgical Ergonomics: A Review of Tasks, Models, and Measurement Systems

H. Ergonomic risk associated with assisting in minimally invasive surgery

I. Endoscopic Video Texture Mapping on Pre-Built 3D Anatomical Objects with Camera Tracking

J. Model Based Estimation and Visualization of Global Object Deformations for laparoscopic Renal Cryoablation

K. The Maryland Virtual Patient

L. Surgical Ergonomics in Minimally Invasive Surgery

An image registration–based approach for continuous volumetric CT-guided interventions

Raj Shekhar, Ananthranga Prithviraj

Department of Diagnostic Radiology, University of Maryland School of Medicine

Purpose

Minimally invasive image-guided interventions (IGIs) that include biopsies, ablations, and surgeries are less than optimal because of the unavailability of continuous three-dimensional (3D) visualization of the anatomy. When continuous or real-time, intraoperative imaging remains two-dimensional as in conventional and computed tomography (CT) fluoroscopy, ultrasound, magnetic resonance (MR) imaging, and endoscopy. When three-dimensional (3D), as in volumetric CT and MR imaging, the imaging remains temporally discrete and the resulting image guidance is stop-and-go and inefficient.

Recent advances in multidetector CT (MDCT) are beginning to permit continuous 3D imaging during an IGI. With the latest MDCT scanners, it is now possible to scan up to 10–12-cm thick regions of the anatomy at an extremely high spatial resolution multiple times per second. But radiation exposure concerns and inability to visualize the vasculature (contrast agents cannot be administered continuously) limit clinical implementation of continuous 3D CT, despite being technically feasible.

We present here a novel concept based on high-speed 3D image registration that addresses both these problems. We acquire a single contrast-enhanced volumetric CT scan (called initial CT) at a diagnostic dose at the start of the IGI. Subsequently, CT is operated at a low dose without contrast. A diagnostic-quality contrast-enhanced image of the operative field is obtained by rapidly and nonrigidly registering the initial CT with intraoperative low-dose CT. We present here the feasibility of our concept in terms of registration time and accuracy, savings in radiation dose, and intraoperative vessel visualization.

Methods

Our imaging specimen was a swine prepared for a mock laparoscopic liver surgery under experimental CT guidance. All CT images were acquired using a 64-slice CT scanner (Philips Brilliance-64) following pneumoperitoneum. Before imaging, 4 markers (2-4 mm guidewire pieces) were implanted in the liver parenchyma and 2 2.3-mm calcium markers sutured onto the liver surface for objective validation of image registration. The initial CT was a helical CT scan of the liver (53-cm axial coverage) at normal breathing with arterial phase enhancement at a diagnostic dose (250 mAs tube current). The swine was then overventilated to accentuate liver motion and deformation from the time of initial CT. CT scanning, simulating intraoperative imaging, was then performed at high, medium, and low doses (200, 75, and 25 mAs, respectively) to determine the lower limit of low-dose CT. For all 3 doses, this CT was performed in 2 modes: helical and axial. The helical mode allowed complete coverage of the liver but provided only a snapshot of it. The axial mode could acquire repeated scans (we acquired 100) at 0.9 Hz, but the 4-cm axial coverage of the CT scanner used permitted only partial liver coverage. Using a previously reported, hardware-accelerated implementation of nonrigid image registration, we registered the initial CT with each of the 3 helical CT scans and each of the 100 scans in the 3 axial CT scan sequences. The initial relative position of image pairs was based on slice location data saved with images. Using the implanted markers, the initial and postregistration misalignments (reflective of registration accuracy) were computed. The time of registration was also recorded.

Results

For 3 helical scans, approximately 3-mm initial misalignment reduced to approximately 1.5 mm for all 3 doses after nonrigid registration of initial CT with intraoperative CT (Table 1). The results show that the dose had virtually no effect on registration accuracy, indicating that intraoperative CT could be performed at 25 mAs. Most structural mismatches before registration were removed after registration (Figure 1). In Figure 2, volume rendering of the original intraoperative CT and registered initial CT (representing intraoperative anatomy) is shown. Note that using our concept, the vasculature can be visualized throughout an IGI without having to administer CT contrast. A similar registration was performed between initial CT and axial scan sequences at the 3 doses. The mean initial and postregistration misalignments (averaged over 100 scans) are shown in Table 2. The nonrigid registration exhibited acceptable accuracy despite small coverage. These results, too, suggest that intraoperative CT at 25 mAs is acceptable. The mean registration time for larger helical data sets was 430 s and for smaller axial scans was 63 s.

Table 1. Image misalignment before and after registration for helical scans.

Dose (mAs)	Initial Misalignment (mm)	Misalignment after Registration (mm)
200 (high)	3.12	1.47
75 (medium)	3.63	1.67
25 (low)	3.25	1.45

Table 2. Average image misalignment before and after registration for axial scans.

Dose (mAs)	Mean Initial Misalignment (mm)	Mean Misalignment after Registration (mm)
200	4.40	1.05
75	4.51	1.12
25	4.69	1.21

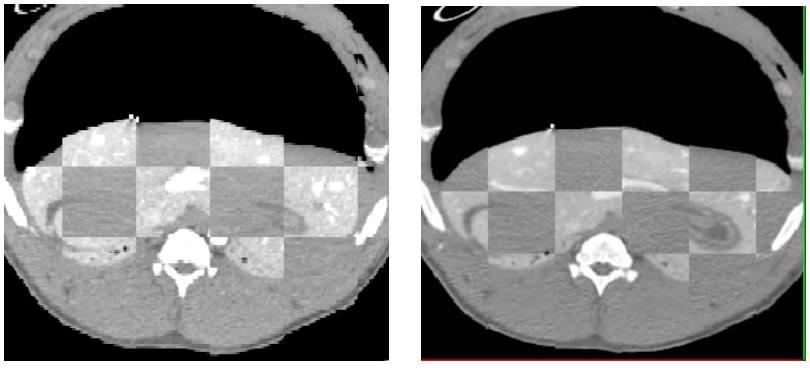

Figure 1. Superposition of initial CT and intraoperative CT (acquired at 200 mAs) before (left) and after (right) nonrigid registration. Note better structure alignment after registration.

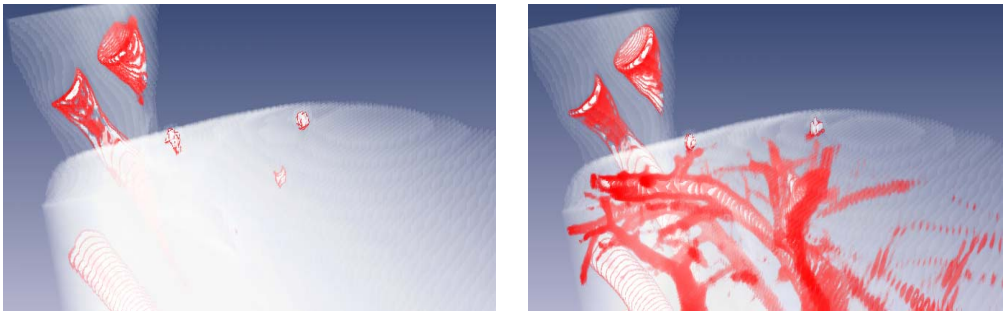

Figure 2. Volume rendering of original intraoperative CT and registered initial CT. Note that the latter shows the vasculature.

Conclusions

We have presented proof-of-concept results using high-speed image registration to substitute noncontrast low-dose intraoperative CT images with a modified contrast-enhanced diagnostic-quality initial CT image during an IGI. The latter contains contrast enhanced structures for which visualization may be critical during an IGI. Our strategy also led to a 10-fold savings in radiation dose (tube current reduced from 250 mAs to 25 mAs). 25 mAs was the lowest setting on the CT scanner used, suggesting that further dose savings are possible if the CT scanner could be operated at a lower dose. Finally, the residual misregistration on the order of 1 mm is acceptable, because the targeting uncertainty in most IGIs is currently much greater. It should also be noted that the concept extends to *any* preoperative image and is likely to vary depending on specific imaging needs of an IGI. Ours was an offline feasibility study. Its clinical implementation will require further speed improvement of CT reconstruction and image registration. Overall, we have presented a novel concept along with demonstration of its feasibility that promises to enable use of the latest MDCT for continuous 3D visualization at acceptably low doses during most IGIs.

HIGH-SPEED RECONSTRUCTION OF LOW-DOSE CT USING GP-GPU

Venkatesh Bhat, Raj Shekhar

ABSTRACT

Minimally invasive image-guided Interventions(IGIs) lead to improved treatment outcomes while significantly reducing patient trauma and recovery time. Ultrasound and fluoroscopy have been traditionally used for image guidance. But these modalities do not provide a comprehensive 3D view of the anatomy. Because of features such as fast scanning, high spatial resolution, 3D view and ease of operation, CT is increasingly being used to navigate IGIs. The risk of radiation exposure, however, limits its current and future use.

We perform ultralow-dose scanning to overcome this limitation. To address the image quality problem with ultralow-dose CT, we reconstruct images using iterative Paraboloidal Surrogate(PS) algorithm. As iterative techniques are generally compute intensive, we have accelerated the PS algorithm on a GPU. Here, we first compare the quality of the low-dose images reconstructed using the PS algorithm and the standard filtered-back projection(FBP) algorithm. Using actual scanner data, we achieved visually acceptable improvement in the quality of reconstructed images using the iterative algorithm.

We further demonstrate a fast implementation of the Ordered Subsets version of the PS algorithm for axial scans on an NVIDIA 8800 GTX GPU using CUDA(Compute Unified Device Architecture). Several studies in the recent past have reported computing forward and back projection on GPU using the rasterization framework. However the GP-GPU(General Purpose GPU) framework used in the implementation, being more generic, accommodated a wide variety of penalty functions on the GPU and thus obviated the need to transfer data between the GPU and CPU during reconstruction.

We have compared the GPU implementation using the ray-tracing method to a similar implementation on the CPU and the traditional CPU implementation using a weight matrix. We demonstrate two orders of improvement in speed while the image quality remains comparable to the traditional CPU implementation.

High-Speed Reconstruction of Low-Dose CT Using GP-GPU

I. OVERVIEW

As discussed in the abstract, optimal use of CT for IGIs mandates the acquisition of data at low radiation doses. Although it is widely acknowledged that iterative algorithms are better suited for reconstruction of noisy data, it has not been proven that these algorithms lead to better quality images from low-dose CT scans as compared to the more common FBP algorithm. In this study we acquire low radiation dose CT scans and compare the images reconstructed using the FBP and PS algorithms. These results are shown in section II.

It is a well known fact that iterative algorithms are computationally intensive as compared to the FBP algorithm. In Section III, we demonstrate a ray-tracing based method for fast implementation of the PS algorithm for axial scans. We implement this method on the CPU as well as the GPU and compare the speedups and the image reconstruction quality in section IV.

II. LOW-DOSE CT RECONSTRUCTION

In this study, we acquired axial scans using a 64-slice Philips Brilliance CT scanner at the minimum permissible tube current of 25 mA. We acquired the scanner preprocessed data after angular rebinning to obtain parallel beam sinograms. We then used the FBP and the PS algorithms [1] to reconstruct the data. Every slice was reconstructed to 1024 × 1024 voxels from 400 views with 1498 detectors each. The results are as shown in Fig. 1.

It is clear from the images that the PS algorithm provides higher quality reconstructed images in comparison to the FBP algorithm for the low radiation dose scans.

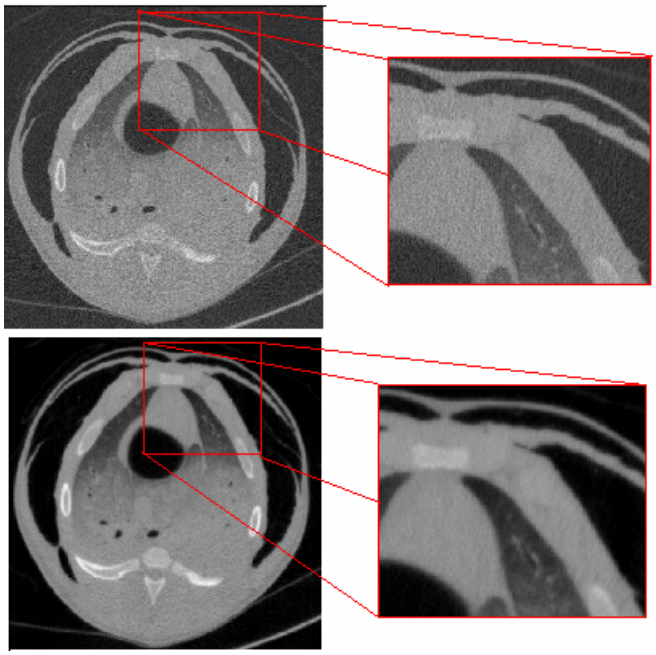

Fig 1. a)Image reconstructed using FBP algorithm(top). b) Image after 10 iterations of PS algorithm.

III. FAST IMPLEMENTATION OF PS ALGORITHM

In the past, results have been presented on the use of graphics processors for CT image reconstruction. In [2] a general framework for the use of GPU in reconstruction algorithms was presented. This was mainly based on the use of the graphics pipeline for acceleration of forward and back projection steps. In [3] the GPU was used to accelerate these steps of the convex algorithm using the framework suggested in [2]. Other algorithms such as SART and OSEM have also been accelerated using similar frameworks. All of these implementations relied on languages such as OpenGL and other shading languages that prevented direct programming of the GPU for various kinds of mathematical operations.

In [4], the FDK algorithm was accelerated for 3D cone beam geometry using CUDA. We accelerate the PS algorithm for parallel beam data from axial scans using CUDA. The generic PS algorithm [1] mainly consists of 3 steps: 1) forward projection 2) back projection 3) pixel update. For the GPU based implementation, we reconstruct 4 slices at a time to make optimal use of the 4 channels (RGBA) in the texture memory. We also make use of the hardware based bilinear interpolators in the texture memory for the interpolation purposes. For the CPU, a software implementation of the bilinear interpolator is used.

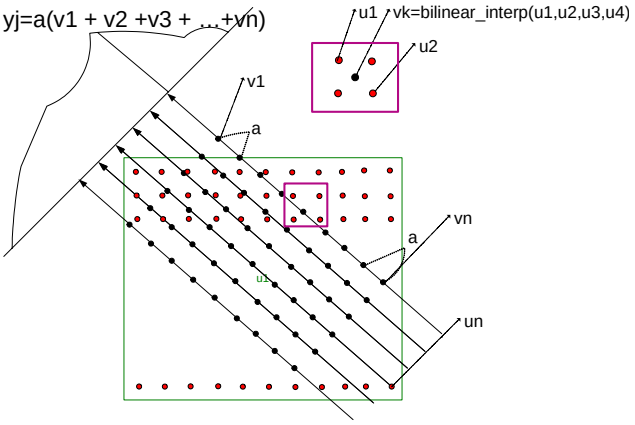

Fig 2. The forward projection mechanism based on ray tracing.

The CUDA forward projection kernel consists of a 2D grid of blocks of size 16 × 16, where each thread represents a ray. The image from the previous iteration is loaded into the texture memory. A single warp per block is used to calculate the sine and cosine values for the rotation matrix which is stored in the local shared memory. The incident rays are rotated according to the sine and cosine values and every thread sums up the bilinearly interpolated pixel values along the uniformly sampled points on the rays to obtain the new sinogram. Fig 2 demonstrates the forward projection idea.

For the back projection, the accumulated data for every view (i.e., each row of the sinogram) is duplicated, leading to the creation of an 'extended' sinogram. This 'extended sinogram' is loaded into the texture memory. The kernel consists of 16 × 16 blocks where each thread represents a

pixel on the resulting image. The image is rotated and the value of each pixel location is shifted vertically such that it lies between the 2 rows of the 'extended sinogram' for the corresponding view. Bilinear interpolation is then used to obtain the pixel value.

Thus each iteration consists of one call to the 'forward projection kernel' and one call to the 'back projection kernel' apart from one call to the 'pixel update kernel' that calculates the penalty function and updates the image. The forward and back projection kernels are preceded by a single transfer of data to the texture memory from the main GPU memory.

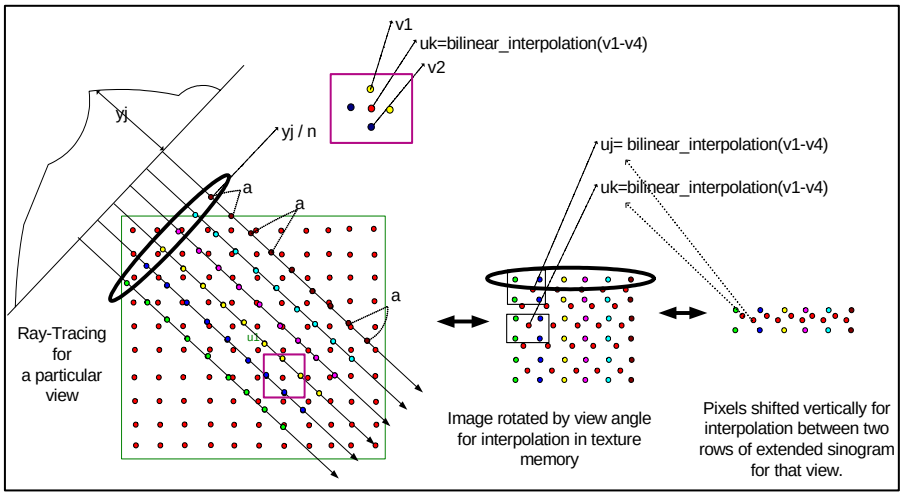

Fig 3. The back projection algorithm

IV. RESULTS

We created synthetic projections from a clinical phantom image. The projections were then used to reconstruct the phantom image using three methods:

a) An unmodified implementation of the PS algorithm on the CPU using pre-computed weights.
b) The ray-tracing version of the PS algorithm on the CPU.
c) The ray-tracing version of the PS algorithm on the GPU.

The reconstructed images were compared using PSNR as a measure of comparison and the original phantom image as the benchmark.

OSEM Subsets	CPU (sec) (Pre-Computed)	CPU (sec) (Ray Tracing)	GPU(s) (Ray Tracing)
5	242	6.66	0.03596
10	244	6.68	0.05418

Table 1: Comparison of time per iteration on CPU(using pre-computed weights and ray tracing algorithms) and GPU for a 256×256 image slice with 400 views. This includes all communication overhead except the one time latency for transfer of sinogram from the scanner. On the GPU, the time taken for reconstruction of 1,2,3 or 4 slices is the same.

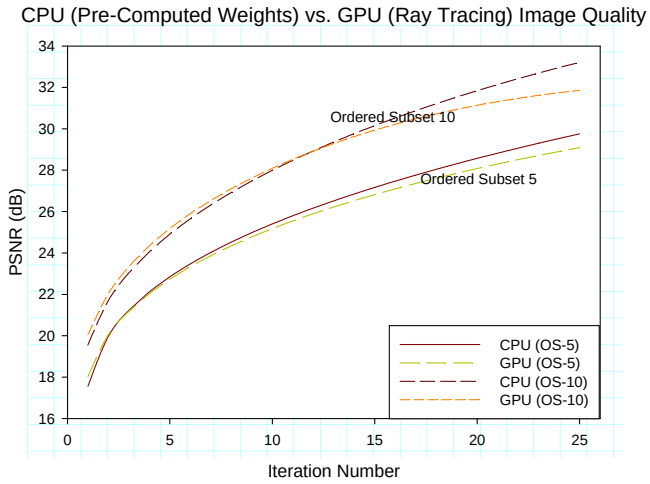

*Fig 4. Reconstruction quality for a 256*256 image slice with 400 views using CPU and GPU.*

V. CONCLUSION

From table 1, it is clear that a speedup of about 30X is obtained by the ray-tracing algorithm and related algorithmic improvements. A further acceleration of 150-200X is obtained by the parallel implementation using CUDA on the GPU. Fig. 4 compares the quality of the reconstructed images on the GPU using ray tracing method and the CPU using accurate Pre-computed weight matrix. The PSNR curves for the GPU closely follow the same for the CPU based implementation. It is clear that the use of the discrete ray tracing method and single precision computations on the GPU do not significantly impact the quality of the reconstructed images. The convergence rate improves with the use of suitable penalty functions as described in [1]. In this implementation no penalty function was used in order to compare the native algorithms.

REFERENCES

1) H. Erdogan, J. Fesslar, "Monotonic Algorithms for Transmission Tomography", IEEE Trans. Med. Imaging, Sept 1999, pp. 801-814.
2) F. Xu and K. Muller."A Unified framework for Rapid 3D Computed Tomography on Commodity GPUs", IEEE Medical Imaging Conference,2003.
3) J.S. Kole et al., "Evaluation of accelerated iterative X-ray CT image reconstruction using floating point graphics hardware", IEEE Nuclear Science Symp.,2004..
4) H. Scherl et al., "Fast GPU-Based CT Reconstruction using the Common Unified Device Architecture (CUDA)", IEEE Nuclear Science Symp., 2007

Hindawi Publishing Corporation
International Journal of Reconfigurable Computing
Volume 2008, Article ID 738174, 17 pages
doi:10.1155/2008/738174

Research Article

Multiobjective Optimization for Reconfigurable Implementation of Medical Image Registration

Omkar Dandekar,[1,2] William Plishker,[1,2] Shuvra S. Bhattacharyya,[1] and Raj Shekhar[1,2]

[1] *Department of Electrical and Computer Engineering, University of Maryland, College Park, MD 20742, USA*
[2] *Department of Diagnostic Radiology and Nuclear Medicine, University of Maryland School of Medicine, Baltimore, MD 21201, USA*

Correspondence should be addressed to Raj Shekhar, rshekhar@umm.edu

Received 6 March 2008; Revised 11 September 2008; Accepted 27 November 2008

Recommended by Juergen Becker

In the field of real-time signal processing, a single application often has multiple computationally intensive kernels that can benefit from acceleration from custom or reconfigurable hardware platforms, such as field-programmable gate arrays (FPGAs). For adaptive utilization of resources at run time, FPGAs with capabilities for dynamic reconfiguration are emerging. To exploit run-time reconfiguration, especially in the presence of unknown or dynamically varying resource availability, it is useful for designers to derive sets of efficient design configurations that trade off application performance with fabric resources. Such sets can then be maintained at run time so that the best available design tradeoff is used based on run-time operating conditions. However, finding a single-optimized configuration is known to be a difficult problem, and generating a family of optimized configurations suitable for different run-time scenarios is even more difficult and relatively understudied. Toward this end, this paper presents a novel multiobjective wordlength optimization strategy developed in the context of FPGA-based implementation of a representative computationally intensive image processing application, medical image registration. The tradeoff between FPGA resources (area and memory) and implementation accuracy is explored, and Pareto-optimized wordlength configurations are systematically identified. Within this framework, we also compare several search methods for finding Pareto-optimized design configurations and demonstrate the applicability of search based on evolutionary techniques for efficiently identifying superior multiobjective tradeoff curves in the context of the chosen problem. Furthermore, through postsynthesis validation, we demonstrate the feasibility of such a framework in the context of FPGA-based medical image registration. With additional work, this optimization strategy may also be adapted to a wide range of signal processing applications, including applications for processing various kinds of image and video signals.

1. Introduction

In the field of real-time signal processing systems, acceleration of computationally intensive algorithmic components is often achieved by mapping them to custom or reconfigurable hardware platforms, such as field-programmable gate arrays (FPGAs). Often, multiple kernels in a single application can benefit from this approach to acceleration, requiring them to share a single fabric. This is particularly necessary in applications where multiple kernels share data and feed results to each other. For example, in medical imaging it has been shown that both image preprocessing [1–3] and image registration [4–6] can achieve high levels of speedup through hardware acceleration. To maximize the performance of an application and to optimize the fabric resource utilization, the kernels must be designed to meet their application requirements while balancing their resource consumption on the fabric. Application requirements often change at run time and strategies based on static design must try to identify a reasonable "average case" design configuration that accommodates all possible scenarios. Because this approach can be highly suboptimal and can result in significant under- or overutilization of the fabric in many scenarios, modern FPGAs are emerging with run-time reconfiguration capabilities. Self-monitoring FPGA implementations are able to adapt to variable application requirements and reconfigure their processing structures to better-suited design configurations [7]. This not only improves

application performance but also results in more effective utilization of fabric resources. To exploit this technology, it is highly desirable that the designers provide quality design configurations that trade off application performance with fabric resources. Consequently, the primary focus of this work is to develop a framework that enables the designers to identify such optimized design configurations.

A common system parameter for trading off resource and performance is datapath wordlength. Typically, algorithms are first developed in software using floating-point representation and later migrated to hardware using finite precision (e.g., fixed-point representation) for achieving improved computational speed and reduced hardware cost. These implementations are often parameterized, so that a wide range of finite precision representations can be supported [8] by choosing an appropriate wordlength for each internal variable. As a consequence, the accuracy and hardware resource requirements of such a system are functions of the wordlengths used to represent the internal variables. Determining an optimal wordlength configuration that minimizes the hardware implementation cost while satisfying a design criterion such as maximum output error has been shown to be nondeterministic polynomial-time (NP)-hard [9] and can take up to 50% of the design time for complex systems [10]. In addition, a single optimal solution may not exist, especially in the presence of multiple conflicting objectives. Moreover, a new configuration generally must be derived when the design constraints are altered.

An optimum wordlength configuration can be identified by analytically solving the quantization error equation as described previously by several authors [11–15]. This analytical representation, however, can be difficult to obtain for complex systems. Techniques based on local search or gradient-based search [16] have also been employed, but these methods are limited to finding a single feasible solution as opposed to an optimized tradeoff curve. An exhaustive search of the entire design space is guaranteed to find Pareto-optimal configurations. Execution time for such exhaustive search, however, increases exponentially with the number of design parameters, making it unfeasible for most practical systems. Methods that transform this problem into a linear programing problem have also been reported [11], but these techniques are limited to cases in which the objectives can be modeled as linear functions of the design parameters. Other approaches based on linear aggregation of objectives may not find proper Pareto-optimal solutions when the search space is nonconvex [17]. Techniques based on evolutionary methods have been shown to be effective in searching large search spaces in an efficient manner [18, 19]. Furthermore, these techniques are inherently capable of performing multipoint searches. As a result, techniques based on evolutionary algorithms (EAs) have been employed in the context of multiobjective optimization (SPEA2 [20], NSGA-II [21]). However, their application to solving wordlength optimization problems has been limited.

We formulate this problem of finding optimal wordlength configurations as a multiobjective optimization, where different objectives—for example, accuracy and area—generally conflict with one another. Although this approach increases the complexity of the search, it can find a set of Pareto-optimized configurations representing strategically chosen tradeoffs among the various objectives. This allows a designer to choose an efficient configuration that satisfies given design constraints and provides ease and flexibility in modifying the design configuration as the constraints change. In this work, we present this novel multiobjective optimization strategy and demonstrate its feasibility in the context of FPGA-based implementation of medical image registration. The tradeoff between FPGA resources (area and memory) and implementation accuracy is systematically explored, and Pareto-optimized solutions are identified. This analysis is performed by treating the wordlengths of the internal variables as design variables. We also compare several search methods for finding Pareto-optimized solutions and demonstrate, in the context of the chosen problem, the applicability of search based on evolutionary techniques for efficiently identifying superior multiobjective tradeoff curves. In comparison with the earlier reported techniques, our work captures more comprehensively the complexity of the underlying multiobjective optimization problem and demonstrates the applicability of our framework in finding superior Pareto-optimized solutions in an efficient manner, even in the presence of a nonlinear objective function.

This paper is organized as follows. Section 2 provides background on image registration and outlines an architecture for its FPGA-based implementation. We also highlight some strategies for parameterized design and synthesis of this architecture. Formulations for multiobjective optimization and various search methods to find Pareto-optimized solutions are described in Section 3. Section 4 describes experimental results, compares various search methods, and presents postsynthesis validation of the presented strategy. In Section 5, discussion on wordlength search and multiobjective optimization is presented. Section 6 concludes the paper.

2. Image Registration

Medical image registration is the process of aligning two images that represent the same anatomy at different times, from different viewing angles, or using different imaging modalities. Image registration is an active area of research and over the last several decades numerous publications have outlined various methodologies to perform image registration and its applications. Maintz and Viergever [22] and Hill et al. [23] have presented a comprehensive summary of the range of the image registration domain. Several types of image registration are in routine use (see [22–25]); however, registration based on voxel intensities remains the most versatile, powerful, and inherently automatic way of achieving the alignment between two images. This approach, in general, attempts to find the transformation ($\hat{T}$) that optimally aligns a reference image (RI) with coordinates x, y,

and z and a floating image (FI) under an image similarity measure ($\mathbb{F}$):

$$\hat{T} = \arg\max_{T} \mathbb{F}(\mathrm{RI}(x,y,z), \mathrm{FI}(T(x,y,z))). \quad (1)$$

Many image similarity measures, such as the sum of squared differences and cross-correlation, have been used, but over the last decade mutual information (MI) has emerged as the preferred similarity measure. MI is an information theoretic measure and is calculated as

$$\mathrm{MI}(\mathrm{RI},\mathrm{FI}) = h(\mathrm{RI}) + h(\mathrm{FI}) - h(\mathrm{RI},\mathrm{FI}). \quad (2)$$

In this equation, $h(\mathrm{RI})$ and $h(\mathrm{FI})$ are the individual entropies and $h(\mathrm{RI},\mathrm{FI})$ is the mutual entropy of the images to be registered. These entropies are further calculated as:

$$\begin{aligned} h(\mathrm{RI}) &= -\sum p_{\mathrm{RI}}(x)\cdot \ln\left(p_{\mathrm{RI}}(x)\right), \\ h(\mathrm{FI}) &= -\sum p_{\mathrm{FI}}(x)\cdot \ln\left(p_{\mathrm{FI}}(x)\right), \\ h(\mathrm{RI},\mathrm{FI}) &= -\sum\sum p_{\mathrm{RI,FI}}(x)\cdot \ln\left(p_{\mathrm{RI,FI}}(x)\right). \end{aligned} \quad (3)$$

Here, the notations p_{RI}, p_{FI}, and $p_{\mathrm{RI,FI}}$ represent the individual probability distribution function (PDF) of RI, individual PDF of FI, and the mutual PDFs of RI and FI, respectively. These distributions are estimated from the individual and mutual histograms of the images to be registered. Additional details about computation of MI, its properties, and its application to image registration can be found in an article by Pluim et al. [25].

MI-based image registration has been shown to be robust and effective in multimodality image registration [24]. However, this form of registration typically requires thousands of iterations (MI evaluations), depending on image complexity and the degree of initial misalignment between images. Castro-Pareja et al. [4] have shown that calculation of MI for different candidate transformations is a factor limiting the performance of MI-based image registration. We have, therefore, developed an FPGA-based architecture for accelerated calculation of MI [6] that is capable of computing MI 40 times faster than software implementation. The transformation model (T in (1)) employed by this architecture is a locally rigid-body model consisting of three dimensional translations and rotations. Consequently, the analysis presented in this article pertains to locally rigid transformations. However, it must be noted that hierarchical rigid-body transformations can be used to represent deformable (nonrigid) transformation models as demonstrated in the volume subdivision-based approach reported by Walimbe and Shekhar [26].

2.1. FPGA-Based Implementation of Mutual Information Calculation

During the execution of image registration using this architecture, the optimization process is executed from a host workstation. The host provides a candidate transformation, while the FPGA-based implementation applies it to the images and performs the corresponding MI computation. The computed MI value is then further used by the host to update the candidate transformation and eventually find the optimal alignment between the RI and FI. Figure 1 shows the top-level block diagram of the aforementioned architecture. The important modules in this design are described in the following sections.

2.1.1. Voxel Counter

Calculation of MI requires processing (fetching the voxel from the image memory, performing coordinate transformation, and updating mutual histogram (MH)) each voxel in the RI. In addition, because the implemented algorithm processes the images on a subvolume basis, RI voxels within a 3D neighborhood corresponding to an individual subvolume must be processed sequentially. The host programs the FPGA-based MI calculator with subvolume start and end addresses, and the voxel counter computes the address corresponding to each voxel within that subvolume in z-y-x order.

2.1.2. Coordinate Transformation

The initial step in MI calculation involves applying a candidate transformation (T) to each voxel coordinate ($\vec{v}_r$) in the RI to find the corresponding voxel coordinates in the FI ($\vec{v}_f$). This is mathematically expressed as

$$\vec{v}_f = T\cdot\vec{v}_r. \quad (4)$$

The deformation model employed is a six-parameter rigid transformation model and is represented using a 4×4 matrix. The host calculates this matrix based on the current candidate transformation provided by the optimization routine and sends it to the MI calculator. A fixed-point representation is used to store the individual elements of this matrix. The coordinate transformation is accomplished by a simple matrix multiplication.

2.1.3. Partial Volume Interpolation

The coordinates mapped in the FI space ($\vec{v}_f$) do not normally coincide with a grid point (integer location), thus requiring interpolation. Nearest neighbor and trilinear interpolation schemes have been used most often for this purpose; however, partial volume (PV) interpolation, introduced by Maes et al. [24], has been shown to provide smooth changes in the histogram values with small changes in transformation. The reported architecture consequently implements PV interpolation as the choice of interpolation scheme. $\vec{v}_f$, in general, will have both fractional and integer components and will land within an FI neighborhood of size $2 \times 2 \times 2$. The interpolation weights required for the PV interpolation are calculated using the fractional components of $\vec{v}_f$. Fixed-point arithmetic is used to compute these interpolation weights. The corresponding floating voxel intensities are fetched by the image controller in parallel using the integer components of $\vec{v}_f$. The image controller also fetches the voxel intensity corresponding to $\vec{v}_r$. The MH then must be updated

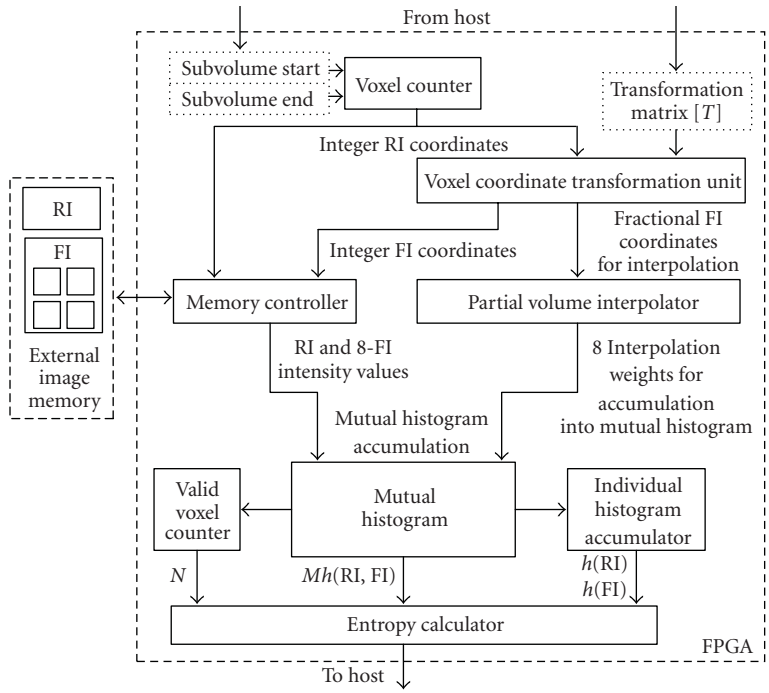

Figure 1: Top-level block diagram of FPGA-based architecture for MI calculation.

for each pair of reference and floating voxel intensities (eight in all) using the corresponding weights computed by the PV interpolator.

2.1.4. Image Memory Access

Images from different modalities (computed tomography (CT), magnetic resonance imaging (MRI), positron emission tomography (PET), etc.) have different native resolution, typical image dimensions, and dynamic range. Despite these variations, dimensions of most medical images are smaller than $512 \times 512 \times 512$ and are supported by our architecture. The dynamic range of these images is indicated by the number of bits used to represent the intensity (gray value) at every voxel. For MI-based registration, however, these images are typically converted to 7- or 8-bit representation as a part of image preprocessing. This is done to prevent dispersion of the MH and leads to improved quality of image registration. After this preprocessing step, all the gray values in the images are used for image registration.

The typical size of 3D medical images prevents the use of high-speed memory internal to the FPGA for their storage. Between the two images, the RI has more relaxed access requirements because it is accessed in a sequential manner (in *z-y-x* order). This kind of access benefits from burst accesses and memory caching techniques, allowing the use of modern dynamic random access memories (DRAMs) for image storage. For the architecture presented, both the RI and FI are stored in separate logical partitions of the same DRAM module. Because the access to the RI is sequential and predictable, the architecture uses internal memory to cache a block of RI voxels. Thus, during the processing of that block of RI voxels, the image controller has parallel access to both RI and FI voxels. The RI voxels are fetched from the internal FPGA memory, whereas the FI voxels are fetched directly from the external memory.

The FI, however, must be accessed randomly (depending on the current transformation T), and eight FI voxels (a $2 \times 2 \times 2$ neighborhood) must be fetched for every RI image voxel to be processed. To meet this memory access requirement, the reported architecture employs a memory addressing scheme similar to the cubic addressing technique reported in the context of volume rendering [4, 27] and image registration [4, 27]. A salient feature of this technique is that it allows simultaneous access to the entire $2 \times 2 \times 2$ voxel neighborhood. The reported architecture implements this technique by storing four copies of the FI and taking advantage of the burst mode accesses native to modern DRAMs. The image voxels are arranged sequentially such that performing a size-two burst fetches two adjacent 2×2 neighborhood planes, thus making the entire neighborhood available simultaneously. The image intensities of this neighborhood are then further used for updating the MH.

2.1.5. Updating the Mutual Histogram

For a given RI voxel (RV) and associated 3D neighborhood in the FI $(FV_0 : FV_7)$, there are eight intensity pairs $(RV, FV_0 : FV_7)$ and corresponding interpolation weights. Because the MH must be updated (read-modify-write) at these eight locations, this amounts to 16 accesses to MH memory for each RI voxel. This high memory access requirement is handled by using the high-speed, dual-ported memories internal to the FPGA to store the MH. The

operation of updating the MH is pipelined and, hence, read-after-write (RAW) hazards can arise if consecutive transactions attempt to update identical locations within the MH. The reported design addresses this issue by introducing preaccumulate buffers, which aggregate the weights from all conflicting transactions. Thus, all the transactions leading to an RAW hazard are converted into a single update to the MH, thereby eliminating any RAW hazards.

While the MH is being computed, the individual histogram accumulator unit computes the histograms for the RI and FI. These individual histograms are also stored using internal, dual-ported memories. The valid voxel countermodule keeps track of the number of valid voxels accumulated in the MH and calculates its reciprocal value. The reciprocal value of the number of valid voxels in the histogram is calculated by using successive subtraction operations. This operation takes N clock cycles (where N is the fractional wordlength of the reciprocal value) and must be performed only once per every MI calculation. The resulting value is then used by the entropy calculation unit for calculating the individual and joint probabilities and subsequently entropies as described in (3).

2.1.6. Entropy Calculation

The final step in MI calculation is to compute joint and individual entropies using the joint and individual probabilities, respectively. To calculate entropy, it is necessary to evaluate the function $f(p) = p \cdot \ln(p)$ for all the probabilities. As each probability P takes on values within $[0, 1]$, the corresponding range for the function $f(p)$ is $[-e^{-1}, 0]$. Thus, $f(p)$ has a finite dynamic range and is defined for all values of p. Several methods for calculating logarithmic functions in hardware have been reported [28], but of particular interest is the multiple lookup table (LUT)-based approach introduced by Castro-Pareja and Shekhar [5]. This approach minimizes the error in representing $f(p)$ for a given number and size of LUTs and, hence, is accurate and efficient. Following this approach, the reported design implements $f(p)$ using multiple LUT-based piecewise polynomial approximation.

2.2. Parameterized Architectural Design

Implementations of signal processing algorithms using microprocessor- or DSP-based approaches are characterized by a fixed datapath width. This width is determined by the hardwired datapath of the underlying processor architecture. Reconfigurable implementation based on FPGAs, in contrast, allows the size of datapath to be customized to achieve better tradeoffs among accuracy, area, and power. Moreover, this customization can also change at run time to accommodate varying design requirements. The use of such custom data representation for optimizing designs is one of the main strengths of reconfigurable computing [29]. It has been contended that the most efficient hardware implementation of an algorithm is the one that supports a variety of finite precision representations of different sizes for its internal variables [8]. In this spirit, many commercial and research efforts have employed parameterized design style for intellectual property (IP) cores [30–34]. This parameterization capability not only facilitates reuse of design cores but also allows them to be reconfigured to meet design requirements.

During the design of the aforementioned architecture, we adopted a similar design style that allows configuration of the wordlengths of the internal variables. Hardware design languages such as VHDL and Verilog natively support hierarchical parameterization of a design through use of *generics* and *parameters*, respectively. This design style takes advantage of these language features and is employed for the design of all the modules described earlier. We highlight the main features of this design style using illustrative examples. Consider a design module with two input variables that compute an output variable through arithmetic manipulation of the input variables. The wordlength of the input variables (denoted by IP1_WIDTH, IP2_WIDTH) and that of the output variable (denoted by OP_WIDTH) are the design parameters for this module. The module can then be parameterized for these design variables as illustrated in Figure 2(a).

In a pipelined implementation of an operation, a module may have multiple internal pipeline stages and corresponding intermediate variables. Wordlengths chosen for these intermediate variables can also impact the accuracy and hardware requirements of a design. In our implementation scheme, we do not employ any rounding or truncation for the intermediate variables, but deduce their wordlengths based on the wordlengths of the input operands and the arithmetic operation to be implemented. For example, multiplication of two 8-bit variables will, at the most, require a 16-bit-wide intermediate output variable. A parameterized implementation of this scenario is illustrated in Figure 2(c). Sometimes it is also necessary to instantiate a vendor-provided or a third-party IP core, such as a first in/first out (FIFO) module or an arithmetic unit, within a design module. In such cases, we simply pass the wordlength parameters down the design hierarchy to configure the IP core appropriately and thereby maintain the parameterized design style (see, e.g., Figure 2(b)).

When signals cross module boundaries, the output wordlength and format (position of the binary point) of the source module should match the input wordlength and format of the destination module. This is usually achieved through use of a rounding strategy and right- or left-shifting of the signals. Adopting "rounding toward the nearest" strategy to achieve wordlength matching is expected to introduce the smallest error but requires additional logic resources. In our design, we therefore implement truncation (or "rounding toward zero" strategy), while the signal shifting is achieved through zero padding. Both these operations are parameterized and take into account the wordlengths and the format at the module boundaries (see, e.g., Figure 2(c)). Thus, this parameterized design style enables the architecture to support multiple wordlength configurations for its internal variables.

```
--Declaration of a parameterized entity
entity Module1 is
 generic(
  IP1_WIDTH:INTEGER;
  IP2_WIDTH:INTEGER;
  OP_WIDTH:INTEGER);
 port(
  s1 : IN STD_LOGIC_VECTOR (IP1_WIDTH-1 DOWNTO 0);
  s2 : IN STD_LOGIC_VECTOR (IP2_WIDTH-1 DOWNTO 0);
  o1 : OUT STD_LOGIC_VECTOR (OP_WIDTH-1 DOWNTO 0));
end Module1;
```

(a)

```
--Instantiation of a vendor supplied
--IP-core, scfifo. The width of the
--FIFO is set to be equal to that of
--the signal to be buffered (o1).
fifo1 : scfifo
 generic map(
  LPM_NUMWORDS => (2**LOG2_DEPTH),
  LPM_WIDTH => OP_WIDTH,
  LPM_WIDTHU => LOG2_DEPTH)
 port map(
data => o1,...);
```

(b)

```
--Declaration of an intermediate variable with appropriate wordlength
signal i1 : STD_LOGIC_VECTOR (IP1_WIDTH+IP2_WIDTH-1 DOWNTO 0);
i1 <= s1 * s2; --Arithmetic operation (multiplication)

--Truncation of LSBs: Performed if (IP1_WIDTH+IP2_WIDTH) >= OP_WIDTH
o1 <= i1(IP1_WIDTH+IP2_WIDTH-1 DOWNTO IP1_WIDTH+IP2_WIDTH-OP_WIDTH);

--Signal-shifting: Performed if IP1_WIDTH+IP2_WIDTH) < OP_WIDTH
o1 <= i1 & CONV_STD_LOGIC_VECTOR(0,OP_WIDTH-(IP1_WIDTH+IP2_WIDTH));
```

(c)

Figure 2: Parameterized architectural design: (a) declaration of a parameterized entity; (b) an example instantiation of a vendor-supplied IP-core; (c) usage of parameterized internal variables and an example of truncation and signal shifting, performed at the module boundaries.

3. Multiobjective Optimization

The aforementioned architecture is designed to accelerate the calculation of MI for performing medical image registration. We have demonstrated this architecture to be capable of offering execution performance superior to that of a software implementation [6]. The accuracy of MI calculation (and, by extension, that of image registration) offered by this implementation, however, is a function of the wordlengths chosen for the internal variables of the design. Similarly, these wordlengths also control the hardware implementation cost of the design. For medical applications, the ability of an implementation to achieve the desired level of accuracy is of paramount importance. It is, therefore, necessary to understand the tradeoff between accuracy and hardware implementation cost for a design and to identify wordlength configurations that provide effective tradeoffs between these conflicting criteria. This multiobjective optimization allows a designer to systematically maximize accuracy for a given hardware cost limitation (e.g., imposed by a target device) or minimize hardware resources to meet the accuracy requirements of a medical application.

Section 3.1 provides a formal definition of this problem and Section 3.2 describes a framework developed for multiobjective optimization of FPGA-based medical image registration.

3.1. Problem Statement

Consider a system Q that is parameterized by N parameters n_i $(i = 1, 2, \ldots, N)$, where each parameter can take on a single value from a corresponding set of valid values (v_i). Let the design configuration space corresponding to this system be S, which is defined by a set consisting of all N-tuples generated by the Cartesian product of the sets v_i $\forall i$:

$$S = v_1 \times v_2 \times v_3 \times \cdots \times v_N. \tag{5}$$

The size of this design configuration space is then equal to the cardinality of the set S or, in other words, the product of the cardinalities of the sets v_i:

$$|S| = |v_1| \times |v_2| \times |v_3| \times \cdots \times |v_N|. \tag{6}$$

For most systems, not all configurations that belong to S may be valid or practical. We, therefore, define a subset $\Im$ $(\Im \subseteq S)$, such that it contains all the feasible system configurations. Now, consider m objective functions $(f_1, f_2, \ldots, f_m)$ defined for system Q, such that each function associates a real value for every feasible configuration $c \in \Im$.

The problem of multiobjective optimization is then to find a set of solutions that simultaneously optimizes the m objective functions according to an appropriate criterion. The most commonly adopted notion of optimality in multiobjective optimization is that of Pareto optimality. According to this notion, a solution c^* is *Pareto optimal* if there does not exist another solution $c \in \Im$ such that $f_i(c) \leq f_i(c^*)$, for all i, and $f_j(c) \leq f_j(c^*)$, for at least one j. The solution c^* is also called a *nondominated* solution because no other solution dominates (or is superior to) solution c^* as per the Pareto-optimality criteria. The set of Pareto-optimal solutions, therefore, includes all nondominated solutions.

Given a multiobjective optimization problem and a heuristic technique for this problem that attempts to derive Pareto-optimal or near Pareto-optimal solutions, we refer to solutions derived by the heuristic as "Pareto-optimized" solutions.

3.2. Multiobjective Optimization Framework

Figure 4 illustrates the framework that we have developed for multiobjective optimization of the aforementioned architecture. The framework has two basic components. The first is the search algorithm that explores the design space and generates feasible candidate solutions; the second is the objective function evaluation module that evaluates candidate solutions. The solutions and associated objective values are fed back to the search algorithm so that they can be used to refine the search. These two components are loosely coupled so that different search algorithms can be easily incorporated into the framework. Moreover, the objective function evaluation module is parallelized using a message passing interface (MPI) on a 32-processor cluster. With this parallel implementation, multiple solutions can be evaluated in parallel, thereby increasing search performance. These components are described in detail in the following sections.

3.2.1. Design Parameters

As described in Section 3.2, the architecture performs MI calculation using a fixed-point datapath. As a result, the accuracy of MI calculation depends on the precision (wordlength) offered by this datapath. The design parameters in this datapath define the design space and are identified and listed along with the corresponding design module (see Figure 1) in Table 1.

A fixed-point representation consists of an integer part and a fractional part. The numbers of bits assigned to these two parts are called the integer wordlength (IWL) and fractional wordlength (FWL), respectively. The individual numbers of bits allocated to these parts control the range and precision of the fixed-point representation. For this architecture, the IWL required for each design parameter can be deduced from the range information specific to the image registration application. For example, in order to support translations in the range of $[-64, 63]$ voxels, 7 bits of IWL (with 1 bit assigned as a sign bit) are required for the translation parameter. We used similar range information to choose the IWL for all the parameters, and these values are reported in Table 1. The precision required for each parameter, which is determined by its FWL, is not known a priori. We, therefore, determine this by performing multiobjective optimization using the FWL of each parameter as a design variable. In our experiments, we used the design range of $[1, 32]$ bits for FWLs of all the parameters. The optimization framework can support different wordlength ranges for different parameters, which can be used to account for additional design constraints, such as, for example, certain kinds of constraints imposed by third-party IP.

The entropy calculation module is implemented using a multiple LUT-based approach and also employs fixed-point arithmetic. However, this module has already been optimized for accuracy and hardware resources, as described previously [5]. The optimization strategy employed in this earlier work uses an analytical approach that is specific to entropy calculation and is distinct from the strategy presented in this work. This module, therefore, does not participate in the multiobjective optimization framework of this paper, and we simply use the optimized configuration identified earlier. This further demonstrates the flexibility of our optimization framework to accommodate arbitrary designer- or externally optimized modules.

3.2.2. Search Algorithms

An exhaustive search that explores the entire design space is guaranteed to find all Pareto-optimal solutions. However, this search can lead to unreasonable execution time, especially when the objective function evaluation is computationally intensive. For example, with four design variables, each taking one of 32 possible values, the design space consists of 32^4 solutions. If the objective function evaluation takes 1 minute per trial (which is quite realistic for multiple MI calculation using large images), the exhaustive search will take 2 years. Even with the 32-processor cluster that we employed

Table 1: Design variables for FPGA-based architecture. Integer wordlengths are determined based on application-specific range information, and fractional wordlengths are used as parameters in the multiobjective optimization framework.

Architectural module	Design variable	Integer wordlength (IWL) (bits)	Fractional wordlength (FWL) range (bits)
Voxel coordinate transformation	Translation vector	7	[1, 32]
	Rotation matrix	4	[1, 32]
Partial volume interpolation	Floating image address	9	[1, 32]
Mutual histogram accumulation	Mutual histogram bin	25	[1, 32]

Table 2: Number of solutions explored by search methods.

Search method	Number of solutions explored
Partial search	65 536
Random search	6000
EA-based search	6000

and assuming linear speedup, exhaustive search for a four-variable system will require about 3.5 weeks. This highlights the infeasibility of exhaustive search even for a system with relatively small number of design variables. Consequently, we have considered alternative search methods, as described below.

The first method is *partial search*, which explores only a portion of the entire design space. For every design variable, the number of possible values it can take is reduced by half by choosing every alternate value. A complete search is then performed in this reduced search space. This method, although not exhaustive, can effectively sample the breadth of the design space. The second method is *random search*, which involves randomly generating a fixed number of feasible solutions. For both of these methods, Pareto-optimized solutions are identified from the set of solutions explored.

The third method is performing a search using evolutionary techniques. EAs have been shown to be effective in efficiently exploring large search spaces [18, 19]. In particular, we have employed SPEA2 [20], which is quite effective in sampling from along an entire Pareto-optimal front and distributing the solutions generated relatively evenly over the optimal tradeoff surface. Moreover, SPEA2 incorporates a fine-grained fitness assignment strategy and an enhanced archive truncation method, which further assist in finding Pareto-optimal solutions. The flow of operations in this search algorithm is shown in Figure 4.

For the EA-based search algorithm, the representation of the system configuration is mapped onto a "chromosome" whose "genes" define the wordlength parameters of the system. Each gene, corresponding to the wordlength of a design variable i, is represented using an integer *allele* that can take values from the set v_i, described earlier. Thus, every gene is confined to wordlength values that are predefined and feasible for a given design variable. The genetic operators for cross-over and mutation are also designed to adhere to this constraint and always produce values from set v_i, for a gene i within a chromosome. This representation scheme is both symmetric and repair-free and, hence, is favored by the schema theory [35] and is computationally efficient, as described by Kianzad and Bhattacharyya [36].

3.2.3. Objective Function Models and their Fidelity

Search for Pareto-optimized configurations requires evaluating candidate solutions and determining Pareto-dominance relationships between them. This can be achieved by calculating objective functions for all the candidate solutions and by relative ordering of the solutions with respect to the values of their corresponding objective functions. We consider the error in MI calculation and the hardware implementation cost to be the conflicting objectives that must be minimized for our FPGA implementation problem. We model the FPGA implementation cost using two components: the first is the amount of logic resources (number of LUTs) required by the design and the second is the internal memory consumed by the design. We treat these as independent objectives in order to explore the synergistic effects between these complementary resources. Because of the size of the design space and limitations resulting from execution time, it is not practical to synthesize and evaluate each solution. We, therefore, employ models for calculating objective functions to evaluate the solutions. The quality of the Pareto-optimized solutions will then depend on the fidelity of these objective function models.

The error in MI calculation can be computed by comparing the MI value reported by the limited-precision FPGA implementation against that calculated by a double-precision software implementation. For this purpose, we have utilized a bit-true emulator of the hardware. This emulator was developed in C++ and uses fixed-point arithmetic to accurately represent the behavior of the limited-precision hardware. It supports multiple wordlengths for internal variables and is capable of accurately calculating the MI value corresponding to any feasible configuration. We have verified its equivalence with the hardware implementation for a range of configurations and image transformations. This emulator was used to compute the MI calculation error. The MI calculation error was averaged for three distinct image pairs (with different image modality combinations) and for 50 randomly generated image transformations. The same sets of image pairs and image transformations were used for evaluating all feasible configurations.

The memory required for a configuration is primarily needed for intermediate FIFOs, which are used to buffer

internal variables, and the MH memory. For example, a 64-word-deep FIFO used to buffer a signal with a wordlength of b will require $64 \times b$ bits of memory. In our architecture, the depth of the FIFOs and the dimensions of the MH are constant, whereas their corresponding widths are determined by the wordlength of the design parameters. Using these insights, we have developed an architecture-specific analytical expression that accurately represents the cumulative amount of memory required for all internal FIFOs and MH. We used this expression to calculate the memory requirement of a configuration.

For estimating the area requirements of a configuration, we adopt the area models reported by Constantinides et al. [11, 37]. These are high-level models of common functional units such as adders, multipliers, and delays. These models are derived from the knowledge of the internal architecture of these components. Area cost for interconnects and routing is not taken into account in this analysis. These models have been verified for the Xilinx Virtex series of FPGAs and are equally applicable to alternative FPGA families and for application-specific integrated circuit (ASIC) implementations. These models have also been previously used in the context of wordlength optimization [11, 37, 38].

We further evaluated the fidelity [39] of these area models using a representative module, PV interpolator, from the aforementioned architecture. This module receives the fractional components of the FI address and computes corresponding interpolation weights. We varied the FWL of the FI address from 1 to 32 bits and synthesized the module using the Altera Stratix II and Xilinx Virtex 5 as target devices. For a meaningful comparison, the settings for the analysis, synthesis, and optimization algorithms (e.g., settings to favor area or speed) for the design tools (Altera Quartus II and Xilinx ISE) were chosen to be comparable. After complete synthesis, routing, and placement, we recorded the area (number of LUTs) consumed by the synthesized design. This process was automated by using the Tcl scripting feature provided by the design tools and through the parameterized design style described earlier. We then compared the consumed area against that predicted by the adopted area models for all FWL configurations. The results of this experiment are presented in Figure 3. These results indicate that the area estimates (number of LUTs) predicted by the model are comparable to that obtained through physical synthesis for both the target devices. For quantitative evaluation, the fidelity of the area models was calculated as follows:

$$\text{Fidelity} = \frac{2}{N(N-1)}\left(\sum_{i=1}^{N-1}\sum_{j=i+1}^{N} F_{ij}\right), \tag{7}$$

where

$$F_{ij} = \begin{cases} 1, & \text{if } \operatorname{sign}(S_i - S_j) = \operatorname{sign}(M_i - M_j), \\ 0, & \text{otherwise.} \end{cases} \tag{8}$$

In this equation, the M_is represent the values predicted by the area models; the S_is represent the values obtained after physical synthesis. The fidelity of the area models when evaluated with respect to the synthesis results obtained for both Altera and Xilinx devices was 1, which corresponds to maximum ("perfect") fidelity.

An interesting observation is that in some cases the high-level area models underestimate by as much as 25% the number of LUTs required. This can be explained by the fact that these models were calibrated using previous generation devices [11, 37]. It must be, however, noted

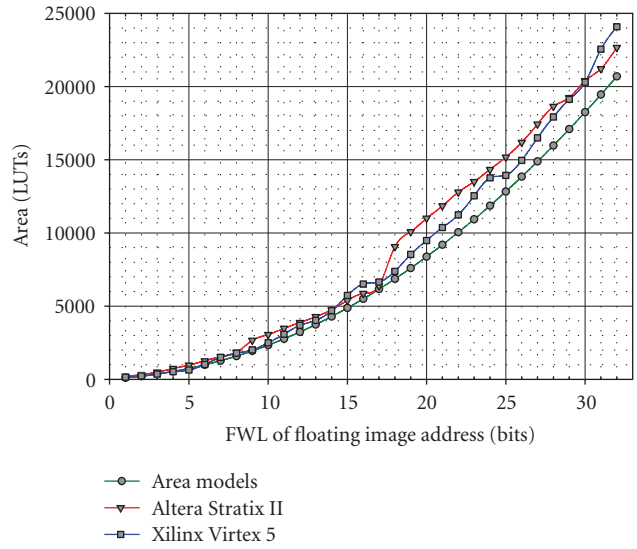

Figure 3: Comparison of the area values predicted by the adopted area models with those obtained after physical synthesis.

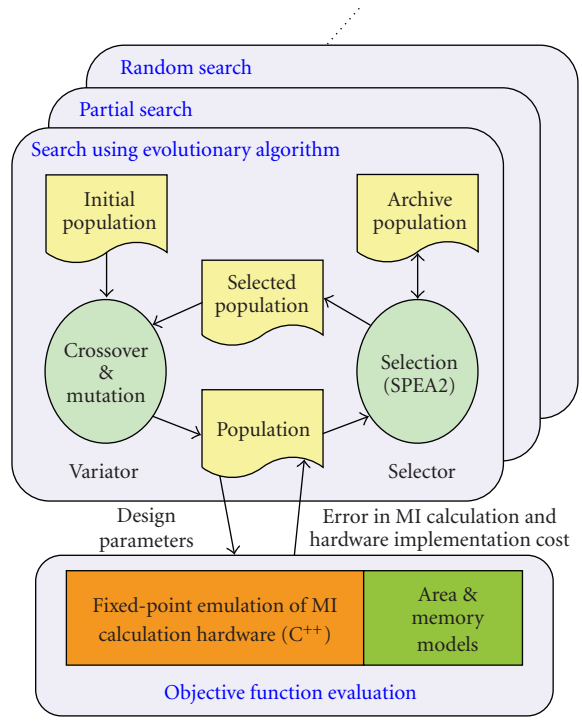

Figure 4: Framework for multiobjective optimization of FPGA-based image registration.

Table 3: Parameters used for EA-based search.

Parameter	Value
Population size	200
Number of generations	30
Cross-over probability	1.0
Mutation probability	0.06

that the Pareto-dominance relationship between the design configurations is maintained as long as the relative ordering (with respect to an objective function such as area) between two design configurations is preserved. Using more accurate area models will certainly improve the absolute prediction of area requirements corresponding to a given design configuration but, as such, will not affect the relative ordering of a set of design configurations. Designing accurate area models that take into account the latest devices, cross-vendor FPGA architectures, special-purpose computational units, and various synthesis optimizations is nevertheless important and will be a topic of a future investigation. The perfect fidelity we achieved for the current area models indicates that the relative ordering of FWL configurations with respect to their area requirements is consistent for the model and synthesized designs. These results further validate the applicability of using the aforementioned area models for multiobjective optimization.

4. Results

We performed multiobjective optimization of the aforementioned architecture using the search algorithms outlined in Section 3. To account for the effects of random number generation, the EA-based search and random search were repeated five times each, and the average behavior from these repeated trials is reported. The number of solutions explored by each search algorithm in a single run is reported in Table 2. The execution time of each search algorithm was roughly proportional to the number of solutions explored, and the objective function evaluation for each solution took approximately 1 minute using a single computing node. As expected, the partial search algorithm explored the largest number of solutions. The parameters used for the EA-based search are listed in Table 3. These parameters were identified experimentally. For example, using a population size of 100 yielded similar search results; however, the diversity of the solutions found in the objective space was relatively poor. Similarly, increasing maximum number generations beyond 30 did not yield a significant improvement in the quality of the search solutions. The cross-over and mutation operators were chosen to be one-point cross-over and flip mutator, respectively. For a fair comparison, the number of solutions explored by the random search algorithm was set to be equal to that explored by the EA-based algorithm.

The solution sets obtained by each search method were then further reduced to corresponding nondominated solution sets using the concept of Pareto optimality. As described earlier, the objectives considered for this evaluation were the MI calculation error and the memory and area requirements of the solutions. Figure 5 shows the Pareto-optimized solution set obtained for each search method. Qualitatively, the Pareto front identified by the EA-based search is denser and more widely distributed and demonstrates better diversity than other search methods. Figure 6 compares the Pareto fronts obtained by partial search and EA-based search by overlaying them and illustrates that the EA-based search can identify better Pareto-optimized solutions, which indicates the superior quality of solutions obtained by this search method. Moreover, it must be noted that the execution time required for the EA-based search was more than 10 times faster than that required for the partial search.

4.1. Metrics for Comparison of Pareto-Optimized Solution Sets

Quantitative comparison of the Pareto-optimized solution sets is essential in order to compare more precisely the effectiveness of various search methods. As with most real-world complex problems, the Pareto-optimal solution set is unknown for this application. We, therefore, employ the following two metrics to perform quantitative comparison between different solution sets. We use the ratio of nondominated individuals (RNIs) to judge the quality of a given solution set, and the diversity of a solution set is measured using the cover rate. These performance measures are similar to those reported by Zitzler and Thiele [40] and are described below.

The RNI is a metric that measures how close a solution set is to the Pareto-optimal solution set. Consider two solution sets ($P1$ and $P2$) that each contain only nondominated solutions. Let the union of these two sets be P_U. Furthermore, let P_{ND} be a set of all nondominated solutions in P_U ($P_{\text{ND}} \subseteq P_U$). The RNI for the solution set P_i is then calculated as

$$\text{RNI}_i = \frac{|P_i \bigcap P_{\text{ND}}|}{|P_{\text{ND}}|}, \tag{9}$$

where $|\cdot|$ is the cardinality of a set. The closer this ratio is to 100%, the more superior the solution set is and the closer it is to the Pareto-optimal front. We computed this metric for all the search algorithms previously described, and the results are presented in Figure 7. Our EA-based search offers better RNI and, hence, superior quality solutions to those achieved with either the partial or random search.

The cover rate estimates the spread and distribution (or diversity) of a solution set in the objective space. Consider the region between the minimum and maximum of an objective function as being divided into an arbitrary number of partitions. The cover rate is then calculated as the ratio of the number of partitions that is covered (i.e., there exists at least one solution with an objective value that falls within a given partition) by a solution set to the total number of partitions. The cover rate (C_k) of a solution set for an objective function (f_k) can then be calculated as

$$C_k = \frac{N_k}{N}, \tag{10}$$

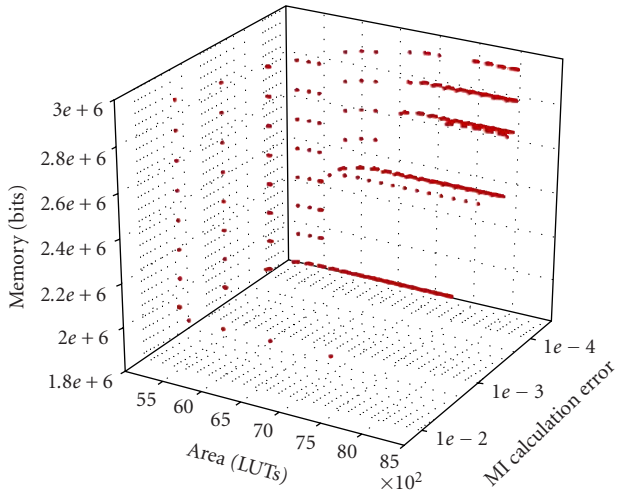

(a) Partial search

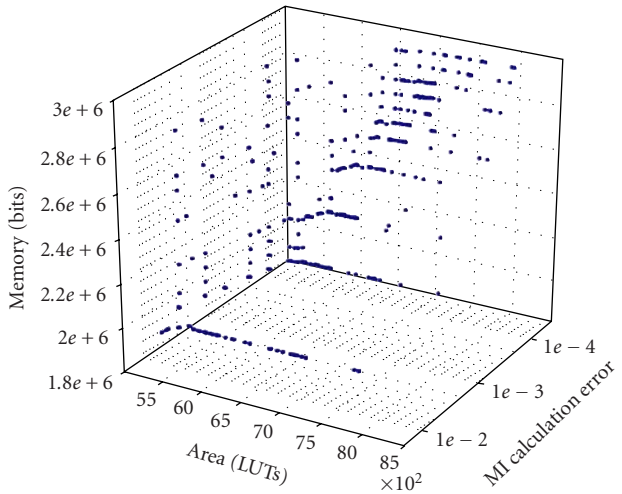

(b) EA-based search

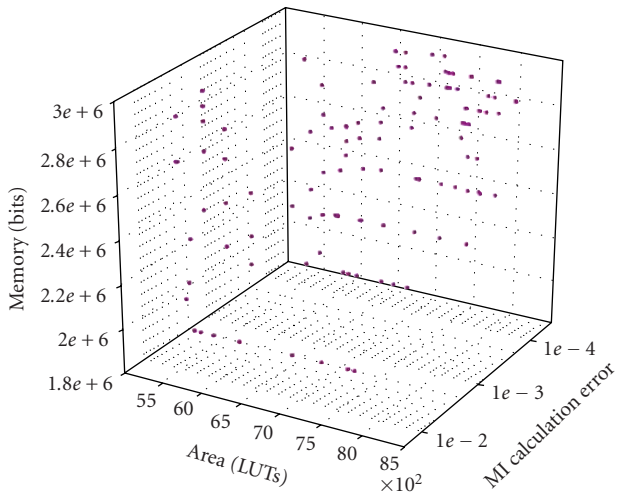

(c) Random search

FIGURE 5: Pareto-optimized solutions identified by various search methods.

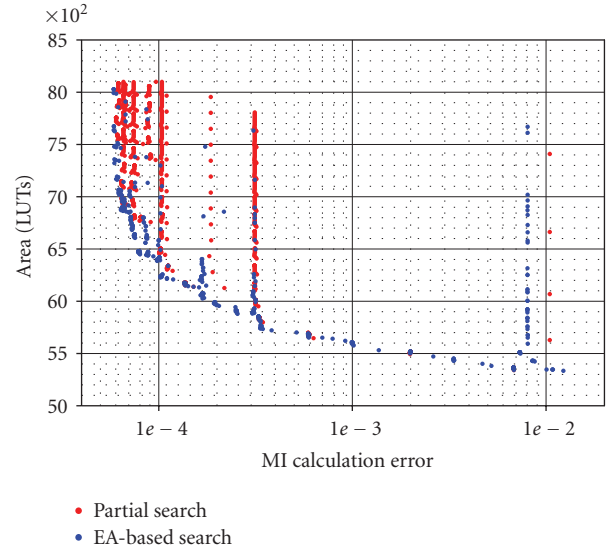

(a) Area versus MI calculation error

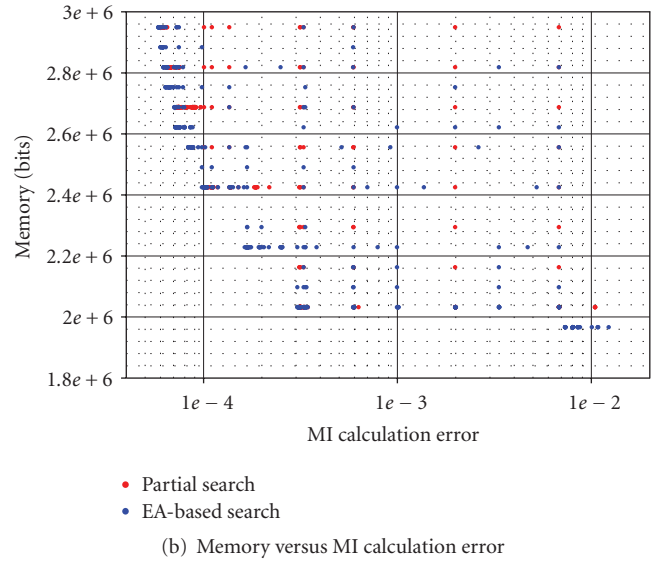

(b) Memory versus MI calculation error

FIGURE 6: Qualitative comparison of solutions found by partial search and EA-based search.

where N_k is the number of covered partitions and N is the total number of partitions. If there are multiple objective functions (e.g., m), then the net cover rate can be obtained by averaging the cover rates for each objective function as

$$C = \frac{1}{m}\sum_{k=1}^{m} C_k. \tag{11}$$

The maximum cover rate is 1 and the minimum value is 0. The closer the cover rate of a solution set is to 1, the better coverage and more even (more diverse) distribution it has. Because the Pareto-optimal front is unknown for our targeted application, the minimum and maximum values for each objective function were selected from the solutions identified by all the search methods. We used 20 partitions/decades for MI calculation error (represented

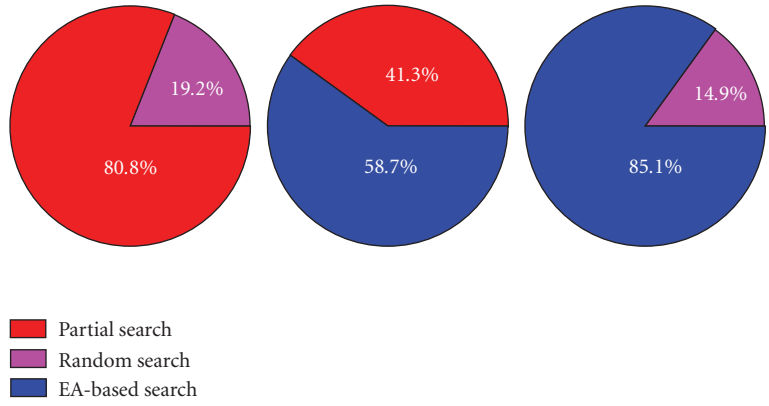

Figure 7: Comparison of search methods using the ratio of nondominated individuals (RNIs).

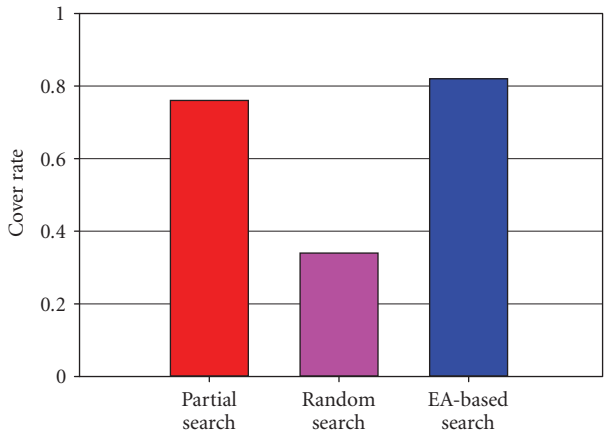

Figure 8: Comparison of search methods using cover rate.

using a logarithmic scale), 1 partition for every 50 LUTs for the area requirement, and 1 partition for every 50 Kbits of memory requirement. The cover rate for all the search algorithms described earlier was calculated using the method outlined above and the results are illustrated in Figure 8. The EA-based search offers a better cover rate, which translates to better range and diversity of solutions when compared with either partial or random searches. In summary, our EA-based search outperforms the random search and is capable of offering more diverse and superior quality solutions when compared with the partial search, using only 10% of the execution time.

4.2. Accuracy of Image Registration

An important performance measure for any image registration algorithm, especially in the context of medical imaging, is its accuracy. We did not choose registration accuracy as an objective function because of its dependence on data (image pairs), the degree of misalignment between images, and the behavior of the optimization algorithm that is used for image registration. These factors, along with its execution time, in our experience, may render registration accuracy as an unsuitable objective function, especially if there is nonmonotonic behavior with respect to the wordlength of design variables. Another important aspect is that the desired accuracy of registration depends on the application in which image registration is employed. For example, during an image-guided medical procedure high registration accuracy might be desired, whereas in a simple visualization task, slightly inaccurate image registration may be tolerated. Furthermore, in a multiresolution image registration approach slightly inaccurate (but, hardware resource-efficient) design configuration can be employed at the initial levels and a more accurate (but perhaps requiring more hardware resources) design configuration can be used at later levels. Thus, image registration accuracy is a constraint from an application perspective and, as such, is not used to guide the exploration of the design space. Instead, we used error in the MI calculation, which is relatively less application- and data-dependant, as an objective function.

Once the Pareto-optimized tradeoffs between MI calculation error and hardware resources are obtained through the presented approach, a system designer could evaluate the performance of these Pareto-optimized design configurations in the context of a specific target application. This can be done by using a set of sample image pairs acquired for that target application. To demonstrate the feasibility of this approach, we selected CT-CT registration as an example application. We randomly selected five clinical image pairs for this analysis and registered them using design configuration corresponding to each Pareto-optimized solution. These image pairs had the dimensions of 256 $\times$ 256 $\times$ 212–335 voxels and the resolution of 1.4–1.7 mm $\times$ 1.4–1.7 mm $\times$ 1.5 mm. This image registration was performed using the aforementioned bit-true simulator. The result of registration was then compared with that obtained using double-precision software implementation. Registration accuracy was calculated by comparing deformations at the vertices of a cuboid (with size equal to half the image dimensions) located at the center of the image. The results of this analysis, which establish the relationship between MI calculation error and the registration error specific to this application of CT-CT registration, are reported in Figure 9.

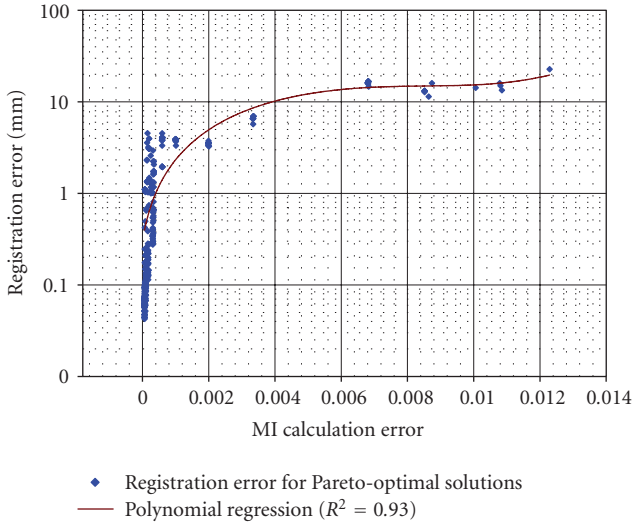

Figure 9: Relationship between MI calculation error and image registration error for an example application of CT-CT registration.

It must be noted that each point in this plot represents a valid design configuration. As expected, there is a good correlation between the MI calculation error and the accuracy of image registration. This demonstrates that optimized tradeoff curves between MI calculation error and hardware cost, as identified by our reported analysis, can be used to represent the relationships between registration accuracy and hardware cost with high fidelity. These relationships can then be used to identify a design configuration in order to achieve desired registration accuracy for this example application of CT-CT registration. Similar relationships specific to a target application (e.g., PET-CT registration) can be generated using the approach.

4.3. Postsynthesis Validation

We performed further validation of the presented multiobjective optimization strategy through physical design synthesis. We identified three solutions from the Pareto-optimized set obtained using the EA-based search and synthesized the aforementioned architecture with configurations corresponding to these solutions. These solutions were identified with no specific clinical application in mind, but such that the tradeoff between various objective functions (MI calculation error, area, and memory) can be readily appreciated. Figure 9 reports the registration accuracy (calculated using the bit-true emulator that we developed) for all the Pareto-optimized design configurations. The system designer will have access to all the Pareto-optimized design configurations along with their expected MI-calculation error and hardware resource requirements, and, as such, can select a design configuration to meet the requirements of a given application.

These three configurations, which offer gradual tradeoff between hardware resource requirement and error in MI calculation, are listed in the first column of Table 4. The wordlengths associated with each configuration correspond to the FWLs of the design variables identified in Table 1. The design was synthesized for these configurations and the resulting realizations were implemented using an Altera Stratix II EP2S180F1508C4 FPGA (Altera Corporation, San Jose, Calif, USA) on a PCI prototyping board (DN7000K10PCI) manufactured by the Dini Group (La Jolla, Calif, USA). We then evaluated the performance of the synthesized designs and compared it with that predicted by the objective function models. The results of this analysis are summarized in Table 4 and are described below.

The error in MI calculation was computed by comparing the MI value reported by the limited-precision FPGA implementation against that calculated by a double-precision software implementation. The MI calculation error was averaged for three distinct image pairs and for 50 randomly generated image transformations for each pair. These image pairs and the associated transformations were identical to those employed in the objective function calculation. In this case, the average MI calculation error obtained by all the design configurations was identical to that predicted by the objective function model. This is expected because of the bit-true nature of the simulator used to predict the MI calculation error. We repeated this calculation with a different set of three image pairs and 50 randomly generated new transformations associated with each image pair. The MI calculation error corresponding to this setup is reported in the second column of Table 4. The small difference when compared with the error predicted by the models is explained by the different sets of images and transformations used. The area and memory requirements corresponding to each configuration after synthesis are reported in columns three and four of Table 4, respectively. For comparison, we have also included the values predicted by the corresponding objective function models in parenthesis. It must be noted that for all three configurations, the relative ordering based on Pareto-dominance relationships with respect to each objective function is identical for both postsynthesis and model-predicted values.

We also evaluated the accuracy of image registration performed using the implementation corresponding to each design configuration. For this analysis, we considered the same five CT image pairs described above. As reported earlier, these image pairs had dimensions of $256 \times 256 \times 212$–$335$ voxels and the resolution of 1.4–$1.7\,\text{mm} \times 1.4$–$1.7\,\text{mm} \times 1.5\,\text{mm}$. The image registration results for one of those image pairs are illustrated in Figure 10. The result of registration between the remaining image pairs was also qualitatively similar. The registration error was calculated by comparing the obtained registration results with that obtained using double-precision software implementation. The mean and standard deviations of the registration error corresponding to each configuration are reported in Table 4. Good correlation is seen between the MI calculation error and the registration error, reinforcing the results presented in Section 4.2.

The performance of the resultant design configuration in terms of its raw clock rate is an important measure of the quality of a design. This clock rate directly affects the

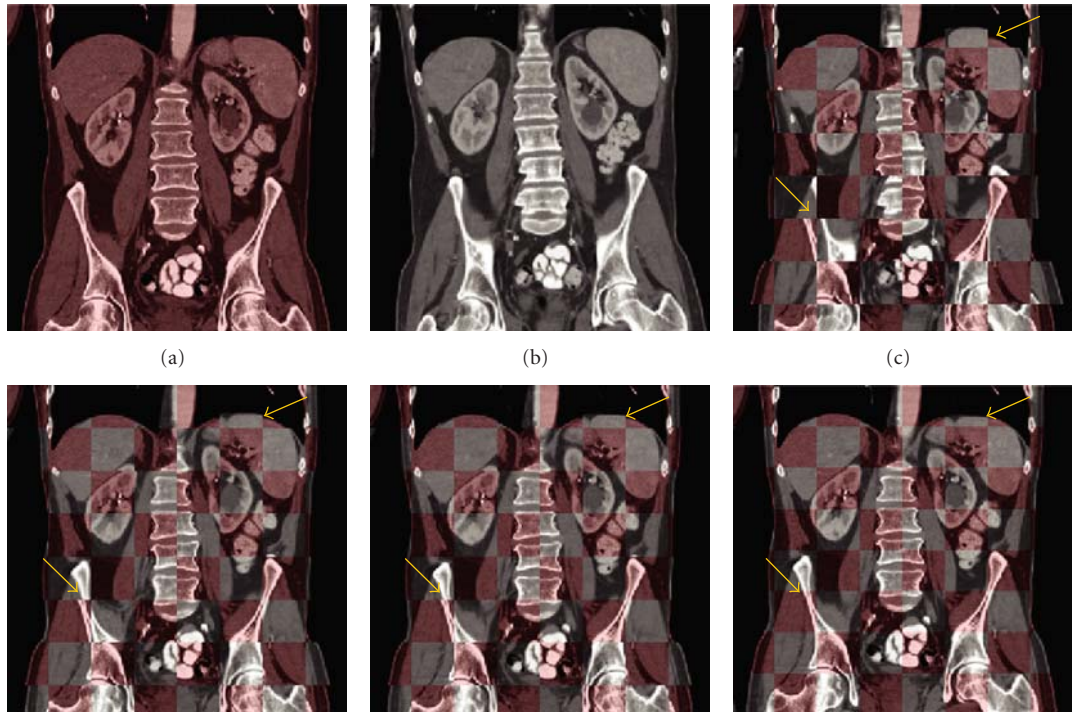

Figure 10: Results of image registration performed using the high-speed, reconfigurable implementation: (a) and (b) two distinct poses; (c) fusion of (a) and (b) using a checkerboard pattern. The misalignment between images is evident at the edges of the squares within the checkerboard pattern; (d)–(f) fusion images after registration using the identified design configurations. These configurations offer progressively reduced image registration error (3.82 mm, 1.57 mm, and 0.45 mm, resp.) and result in correspondingly improved image alignment. The arrows indicate representative regions with misalignment that are better aligned after registration.

Table 4: Validation of the objective function models using postsynthesis results. The wordlengths in a design configuration correspond to the FWLs of the design variables identified earlier (see Table 1).

Design configuration	Objective functions postsynthesis value (predicted value)			Registration error (mean ± standard deviations, mm)	Design speed (f_{max}) (MHz)
	MI calculation error	Area (no. of LUTs)	Memory (Mbits)		
{5, 6, 4, 9}	2.4×10^{-3} (2.1×10^{-3})	6527 (5899)	2.23 (2.23)	3.82 ± 1.24	211
{8, 9, 7, 12}	5.3×10^{-4} (5.2×10^{-4})	7612 (6754)	2.45 (2.45)	1.57 ± 0.69	197
{9, 12, 10, 17}	7.7×10^{-5} (7.8×10^{-5})	10356 (8073)	2.81 (2.81)	0.45 ± 0.16	184

maximum voxel throughput that can be achieved by the design and, consequently, has an impact on the execution speed of image registration. The speed of a design configuration depends on, among other factors, the wordlengths of the design parameters. For example, performing arithmetic and memory operations using parameters with wider wordlengths may incur additional latency. As a result, design configurations employing design parameters with wider wordlengths may be slightly slower, although more accurate, than design configurations with shorter wordlengths. To provide some insights about this phenomenon, we recorded the maximum clock rate achieved by each of the design configurations we identified for synthesis. This represents the maximum postsynthesis frequency at which the design can operate and is reported in the last column of Table 4. These results indicate that the Pareto-optimized designs are not unreasonably slow and that their performance is comparable to that achieved (200 MHz) for a user-optimized design reported earlier [6].

This postsynthesis validation further demonstrates the efficacy of the presented optimization approach for reconfigurable implementation of image registration. It also further demonstrates how the approach enables a designer to systematically choose an efficient system configuration to meet the registration accuracy requirements for a reconfigurable implementation.

5. Discussion

With the need for real-time performance in signal processing applications, an increasing trend is to accelerate computationally intensive algorithms using custom hardware implementation. A critical step in going to a custom hardware implementation is converting floating-point implementations to fixed-point realizations for performance reasons. This conversion process is an inherently multidimensional problem because several conflicting objectives, such as area and error, must be simultaneously minimized. By systematically deriving efficient tradeoff configurations, one can not only reduce the design time [10] but can also enable automated design synthesis [41, 42]. Moreover, these tradeoff configurations allow designers to identify optimized, high-quality designs for reconfigurable computing applications. Our work presented in this paper develops a framework for optimizing tradeoff relations between hardware cost and image processing accuracy in the context of FPGA-based medical image registration.

Earlier approaches to optimizing wordlengths used analytical approaches for range and error estimations [11–15]. Some of these have used the error propagation method (e.g., see [14]), whereas others have employed models of worst-case error [12, 15]. Although these approaches are faster and do not require simulation, formulating analytical models for complex objective functions, such as MI, is difficult. Statistical approaches have also been employed for optimizing wordlengths [43, 44]. These methods employ range and error monitoring for identifying appropriate wordlengths. These techniques do not require range or error models. However, they often need long execution times and are less accurate in determining effective wordlengths.

Some published methods search for optimum wordlengths using error or cost sensitivity information. These approaches are based on search algorithms such as "Local," "Preplanned," and "Max-1" search [16, 45]. However, for a given design scenario, these methods are limited to finding a single-feasible solution, as opposed to a multiobjective tradeoff curve. In contrast, the techniques that we have presented in this paper are capable of deriving efficient tradeoff curves across multiple objective functions.

Other heuristic techniques that take into account tradeoffs between hardware cost and implementation error and enable automatic conversion from floating-point to fixed-point representations are limited to software implementations only [42]. Also, some of the methods based on heuristics do not support different degrees of fractional precision for different internal variables [12]. In contrast, our framework allows multiple fractional precisions, supports a variety of search methods, and thereby captures more comprehensively the complexity of the underlying multiobjective optimization problem.

Other approaches to solve this multiobjective problem have employed weighted combinations of multiple objectives and have reduced the problem to mono-objective optimization [38]. This approach, however, is prone to finding suboptimal solutions when the search space is nonconvex [17]. Some methods have also attempted to model this problem as a sequence of multiple mono-objective optimizations [46]. The underlying assumption in this approximation, however, is that the design parameters are completely independent, which is rarely the case in complex systems. Modeling this problem as an integer linear programing formulation has also been shown to be effective [11]. But this approach is limited to cases in which the objective functions can be represented or approximated as linear functions of design variables.

EAs have been shown to be effective in solving various kinds of multiobjective optimization problems [18, 19] but have not been extensively applied to finding optimal wordlength configurations. One of the earlier attempts at using multiobjective EA formulation for wordlength optimization was reported by Istepanian and Whidborne [47]. This approach employed a simplistic model for hardware complexity and was limited to linear systems only. Leban and Tasic [48] also reported EA-based wordlength optimization of adaptive filters. However, this work was limited to mono-objective optimization only. More recently, Han et al. [49] reported EA-based multiobjective wordlength optimization for a filtering application. This work, however, considered only linear objective functions and lacked postsynthesis validation. In contrast, our work demonstrates the applicability of EA-based search for finding superior Pareto-optimized solutions in an efficient manner, even in the presence of a nonlinear objective function. Moreover, our optimization framework supports multiple search algorithms and objective function models and may be extended to a wide range of other signal processing applications. A preliminary version of the work presented in this article is published in [50]. This paper represents an enhanced and more thorough version of that work. New developments that we have incorporated into this paper include elaborating on the parameterized architectural design, evaluating the fidelity of the objective function models, and verifying the applicability of the proposed methodology through postsynthesis validation. In summary, this work has presented a framework that is capable of performing multiobjective wordlength optimization and identifying Pareto-optimized design configurations even in the context of nonlinear and complex objective functions. Through postsynthesis validation, this work has also demonstrated the feasibility of such a multiobjective optimization framework in the context of a representative image processing application, medical image registration.

6. Conclusion

One of the main strengths of reconfigurable computing over general-purpose processor-based implementations is its ability to utilize more streamlined representations for internal variables. This ability can often lead to superior performance and optimized fabric utilization in reconfigurable computing applications. Given this advantage, it is highly desirable to automate the derivation of optimized design configurations that can be switched among at run time. Toward that end, this paper has presented a framework for multiobjective wordlength optimization of finite-precision, reconfigurable

implementations. This framework considers multiple conflicting objectives, such as hardware resource consumption and implementation accuracy, and systematically explores tradeoff relationships among the targeted objectives. Our work has also further demonstrated the applicability of EA-based techniques for efficiently identifying Pareto-optimized tradeoff relations in the presence of complex and nonlinear objective functions. The evaluation that we have performed in the context of FPGA-based medical image registration demonstrates that such an analysis can be used to enhance automated hardware design processes and efficiently identifies a system configuration that meets given design constraints. Furthermore, the multiobjective optimization approach that we have presented is not application-specific and, with additional work, may be extended to a multitude of other signal processing applications.

Acknowledgments

This work was supported by the U.S. Department of Defense (TATRC) under Grant DAMD17-03-2-0001. The authors thank Dr. Nancy Knight for her help in editing and refining this manuscript. The authors also thank the journal's reviewers for their feedback and suggestions in improving this manuscript.

References

[1] C. R. Castro-Pareja, O. Dandekar, and R. Shekhar, "FPGA-based real-time anisotropic diffusion filtering of 3D ultrasound images," in *Real-Time Imaging IX*, vol. 5671 of *Proceedings of SPIE*, pp. 123–131, San Jose, Calif, USA, January 2005.

[2] O. Dandekar, C. R. Castro-Pareja, and R. Shekhar, "FPGA-based real-time 3D image preprocessing for image-guided medical interventions," *Journal of Real-Time Image Processing*, vol. 1, no. 4, pp. 285–301, 2007.

[3] S. Venugopal, C. R. Castro-Pareja, and O. Dandekar, "An FPGA-based 3D image processor with median and convolution filters for real-time applications," in *Real-Time Imaging IX*, vol. 5671 of *Proceedings of SPIE*, pp. 174–182, San Jose, Calif, USA, January 2005.

[4] C. R. Castro-Pareja, J. M. Jagadeesh, and R. Shekhar, "FAIR: a hardware architecture for real-time 3-D image registratio," *IEEE Transactions on Information Technology in Biomedicine*, vol. 7, no. 4, pp. 426–434, 2003.

[5] C. R. Castro-Pareja and R. Shekhar, "Hardware acceleration of mutual information-based 3D image registration," *Journal of Imaging Science and Technology*, vol. 49, no. 2, pp. 105–113, 2005.

[6] O. Dandekar and R. Shekhar, "FPGA-accelerated deformable image registration for improved target-delineation during CT-guided interventions," *IEEE Transactions on Biomedical Circuits and Systems*, vol. 1, no. 2, pp. 116–127, 2007.

[7] M. L. Silva and J. C. Ferreira, "Support for partial run-time reconfiguration of platform FPGAs," *Journal of Systems Architecture*, vol. 52, no. 12, pp. 709–726, 2006.

[8] G. A. Constantinides, P. Y. K. Cheung, and W. Luk, "The multiple wordlength paradigm," in *Proceedings of the 9th Annual IEEE Symposium on Field-Programmable Custom Computing Machines (FCCM '01)*, pp. 51–60, Rohnert Park, Calif, USA, April-May 2001.

[9] G. A. Constantinides and G. J. Woeginger, "The complexity of multiple wordlength assignment," *Applied Mathematics Letters*, vol. 15, no. 2, pp. 137–140, 2002.

[10] H. Keding, M. Willems, M. Coors, and H. Meyr, "FRIDGE: a fixed-point design and simulation environment," in *Proceedings of Design, Automation and Test in Europe (DATE '98)*, pp. 429–435, Paris, France, February 1998.

[11] G. A. Constantinides, P. Y. K. Cheung, and W. Luk, "Wordlength optimization for linear digital signal processing," *IEEE Transactions on Computer-Aided Design of Integrated Circuits and Systems*, vol. 22, no. 10, pp. 1432–1442, 2003.

[12] A. Nayak, M. Haldar, A. Choudhary, and P. A. B. P. Banerjee, "Precision and error analysis of MATLAB applications during automated hardware synthesis for FPGAs," in *Proceedings of Design, Automation and Test in Europe (DATE '01)*, pp. 722–728, Munich, Germany, March 2001.

[13] A. V. Oppenheim, R. W. Schafer, and J. R. Buck, *Discrete-Time Signal Processing*, Prentice Hall, Upper Saddle River, NJ, USA, 2nd edition, 1999.

[14] M. Stephenson, J. Babb, and S. Amarasinghe, "Bidwidth analysis with application to silicon compilation," in *Proceedings of the ACM SIGPLAN Conference on Programming Language Design and Implementation*, pp. 108–120, Vancouver, Canada, June 2000.

[15] S. A. Wadekar and A. C. Parker, "Accuracy sensitive wordlength selection for algorithm optimization," in *Proceedings of the IEEE International Conference on Computer Design (ICCD '98)*, pp. 54–61, Austin, Tex, USA, October 1998.

[16] H. Choi and W. P. Burleson, "Search-based wordlength optimization for VLSI/DSP synthesis," in *Proceedings of the 7th IEEE International Workshop on VLSI Signal Processing*, pp. 198–207, La Jolla, Calif, USA, October 1994.

[17] I. Das and J. E. Dennis, "A closer look at drawbacks of minimizing weighted sums of objectives for Pareto set generation in multicriteria optimization problems," *Structural and Multidisciplinary Optimization*, vol. 14, no. 1, pp. 63–69, 1997.

[18] M. S. Bright and T. Arslan, "Synthesis of low-power DSP systems using a genetic algorithm," *IEEE Transactions on Evolutionary Computation*, vol. 5, no. 1, pp. 27–40, 2001.

[19] C. L. Valenzuela and P. Y. Wang, "VLSI placement and area optimization using a genetic algorithm to breed normalized postfix expressions," *IEEE Transactions on Evolutionary Computation*, vol. 6, no. 4, pp. 390–401, 2002.

[20] E. Zitzler, M. Laumanns, and L. Thiele, "SPEA2: improving the strength Pareto evolutionary algorithm for multiobjective optimization," in *Proceedings of Evolutionary Methods for Design, Optimisation and Control with Applications to Industrial Problems (EUROGEN '01)*, pp. 95–100, Athens, Greece, September 2001.

[21] K. Deb, A. Pratap, S. Agarwal, and T. Meyarivan, "A fast and elitist multiobjective genetic algorithm: NSGA-II," *IEEE Transactions on Evolutionary Computation*, vol. 6, no. 2, pp. 182–197, 2002.

[22] J. B. A. Maintz and M. A. Viergever, "A survey of medical image registration," *Medical Image Analysis*, vol. 2, no. 1, pp. 1–36, 1998.

[23] D. L. G. Hill, P. G. Batchelor, M. Holden, and D. J. Hawkes, "Medical image registration," *Physics in Medicine & Biology*, vol. 46, no. 1, p. 1, 2001.

[24] F. Maes, A. Collignon, D. Vandermeulen, G. Marchal, and P. Suetens, "Multimodality image registration by maximization of mutual information," *IEEE Transactions on Medical Imaging*, vol. 16, no. 2, pp. 187–198, 1997.

[25] J. P. W. Pluim, J. B. A. Maintz, and M. A. Viergever, "Mutual-information-based registration of medical images: a survey," *IEEE Transactions on Medical Imaging*, vol. 22, no. 8, pp. 986–1004, 2003.

[26] V. Walimbe and R. Shekhar, "Automatic elastic image registration by interpolation of 3D rotations and translations from discrete rigid-body transformations," *Medical Image Analysis*, vol. 10, no. 6, pp. 899–914, 2006.

[27] M. Doggett and M. Meissner, "A memory addressing and access design for real time volume rendering," in *Proceedings of the IEEE International Symposium on Circuits and Systems (ISCAS '99)*, pp. 344–347, Orlando, Fla, USA, May-June 1999.

[28] D. M. Mandelbaum and S. G. Mandelbaum, "A fast, efficient parallel-acting method of generating functions defined by power series, including logarithm, exponential, and sine, cosine," *IEEE Transactions on Parallel and Distributed Systems*, vol. 7, no. 1, pp. 33–45, 1996.

[29] T. J. Todman, G. A. Constantinides, S. J. E. Wilton, O. Mencer, W. Luk, and P. Y. K. Cheung, "Reconfigurable computing: architectures and design methods," *IEE Proceedings: Computers and Digital Techniques*, vol. 152, no. 2, pp. 193–207, 2005.

[30] Altera Corp., "Altera IP Megacore Library," http://www.altera.com/literature/lit-ip.jsp.

[31] W. Luk, S. Guo, N. Shirazi, and N. Zhuang, "A framework for developing parametrised FPGA libraries," in *Proceedings of the 6th International Workshop on Field-Programmable Logic Smart Applications, New Paradigms and Compilers (FPL '96)*, pp. 24–33, Darmstadt, Germany, September 1996.

[32] W. Luk and S. McKeever, "Pebble: a language for parametrised and reconfigurable hardware design," in *Proceedings of the 8th International Workshop on Field-Programmable Logic Smart Applications, New Paradigms and Compilers (FPL '98)*, pp. 1–9, Tallinn, Estonia, August 1998.

[33] Xilinx Inc., "Xilinx Core Generator," http://www.xilinx.com/ise/products/coregen_overview.pdf.

[34] J. Zhao, W. Chen, and S. Wei, "Parameterized IP core design," in *Proceedings of the 4th International Conference on ASIC*, pp. 744–747, Shanghai, China, October 2001.

[35] T. Back, U. Hammel, and H.-P. Schwefel, "Evolutionary computation: comments on the history and current state," *IEEE Transactions on Evolutionary Computation*, vol. 1, no. 1, pp. 3–17, 1997.

[36] V. Kianzad and S. S. Bhattacharyya, "Efficient techniques for clustering and scheduling onto embedded multiprocessors," *IEEE Transactions on Parallel and Distributed Systems*, vol. 17, no. 7, pp. 667–680, 2006.

[37] G. A. Constantinides, P. Y. K. Cheung, and W. Luk, "Optimum wordlength allocation," in *Proceedings of 10th Annual IEEE Symposium on Field-Programmable Custom Computing Machines*, pp. 219–228, Napa, Calif, USA, April 2002.

[38] K. Han and B. L. Evans, "Optimum wordlength search using sensitivity information," *EURASIP Journal on Applied Signal Processing*, vol. 2006, Article ID 92849, 14 pages, 2006.

[39] N. K. Bambha and S. S. Bhattacharyya, "A joint power/performance optimization technique for multiprocessor systems using a period graph construct," in *Proceedings of International Symposium on System Synthesis (ISSS '00)*, pp. 91–97, Madrid, Spain, September 2000.

[40] E. Zitzler and L. Thiele, "Multiobjective evolutionary algorithms: a comparative case study and the strength Pareto approach," *IEEE Transactions on Evolutionary Computation*, vol. 3, no. 4, pp. 257–271, 1999.

[41] G. A. Constantinides, P. Y. K. Cheung, and W. Luk, "Optimum and heuristic synthesis of multiple word-length architectures," *IEEE Transactions on Very Large Scale Integration (VLSI) Systems*, vol. 13, no. 1, pp. 39–57, 2005.

[42] K.-I. Kum, J. Kang, and W. Sung, "AUTOSCALER for C: an optimizing floating-point to integer C program converter for fixed-point digital signal processors," *IEEE Transactions on Circuits and Systems II*, vol. 47, no. 9, pp. 840–848, 2000.

[43] S. Kim, K.-I. Kum, and W. Sung, "Fixed-point optimization utility for C and C++ based digital signal processing programs," *IEEE Transactions on Circuits and Systems II*, vol. 45, no. 11, pp. 1455–1464, 1998.

[44] K.-I. Kum and W. Sung, "Combined word-length optimization and high-level synthesis of digital signal processing systems," *IEEE Transactions on Computer-Aided Design of Integrated Circuits and Systems*, vol. 20, no. 8, pp. 921–930, 2001.

[45] M.-A. Cantin, Y. Savaria, and P. Lavoie, "A comparison of automatic word length optimization procedures," in *Proceedings of the IEEE International Symposium on Circuits and Systems*, pp. 612–615, Phoenix, Ariz, USA, May 2002.

[46] T. Givargis, F. Vahid, and J. Henkel, "System-level exploration for Pareto-optimal configurations in parameterized system-on-a-chip," *IEEE Transactions on Very Large Scale Integration (VLSI) Systems*, vol. 10, no. 4, pp. 416–422, 2002.

[47] R. S. H. Istepanian and J. F. Whidborne, "Multi-objective design of finite word-length controller structures," in *Proceedings of the Congress on Evolutionary Computation (CEC '99)*, pp. 1–68, Washington, DC, USA, August 1999.

[48] M. Leban and J. F. Tasic, "Word-length optimization of LMS adaptive FIR filters," in *Proceedings of the 10th Mediterranean Electrotechnical Conference (MALECON '00)*, pp. 774–777, Lemesos, Cyprus, May 2000.

[49] K. Han, A. G. Olson, and B. L. Evans, "Automatic floating-point to fixed-point transformations," in *Proceedings of the 40th Asilomar Conference on Signals, Systems, and Computers (ACSSC '06)*, pp. 79–83, Pacific Grove, Calif, USA, October 2006.

[50] O. Dandekar, W. Plishker, S. S. Bhattacharyya, and R. Shekhar, "Multiobjective optimization of FPGA-based medical image registration," in *Proceedings of the IEEE Symposium on Field-Programmable Custom Computing Machines (FCCM '08)*, pp. 183–192, Stanford, Calif, USA, April 2008.

AUGMENTED REALITY FOR LAPAROSCOPIC SURGERY USING A NOVEL IMAGING METHOD – INITIAL RESULTS FROM A PORCINE ANIMAL MODEL

R Shekhar PhD, C Godinez MD, S Kavic MD, E Sutton MD, V Bhat, O Dandekar, I George, A Park MD.
Department of Surgery, University of Maryland School of Medicine

Background: Intraoperative appreciation of visible anatomy along with awareness of underlying structures and vasculature is invaluable to the operating surgeon. The advent of minimally invasive techniques, with reduced tactile feedback and limited visual displays has only heightened the need for improved visualization of target anatomy and adjacent but visually imperceptible structures. Current laparoscopic images are rich in surface detail but provide no information on deeper features. We are developing a novel method of performing laparoscopic surgery using a 64-slice computed tomography (CT) scanner with continuous scanning capability. This study describes our work to date to produce an augmented reality (AR) image that instantaneously renders intraoperative CT images with the live images from the laparoscope.

Methods: Under an Institutional Animal Care and Use Committee (IACUC)-approved protocol, we conducted a series of CT-guided laparoscopic operations using a non-survival porcine model. A fully equipped laparoscopic surgical suite was assembled within the CT scan room. A multidisciplinary research team comprised of minimally invasive surgeons, radiologists, and biomedical engineers contributed to study design and conducted the experiments. We employ a 64-slice CT scanner with continuous scanning capability to image the surgical field approximately once per second. An infrared detection system tracked the position of a specially-equipped laparoscope in order to reconcile the laparoscopic view with the corresponding 3-D CT image. Laparoscopic operations performed included peritoneoscopy, cholecystectomy, hepatic wedge resection, and gastrorrhapy, with intraoperative CT scanning. Deformable image registration (alignment) techniques and low-dose reconstruction methods allow intraoperative CT scanning at 25 mAs, roughly 10 times lower than the standard diagnostic dose. Using commercially available software, we generate an AR image that merges recontructed intraoperative CT with images from the laparoscope.

Results and Conclusions: Through a series of six operative experiments, we have amassed a data set that includes rendered video and laparoscopic images, demonstrating the feasibility of merging optical surface information with ragiographically imaged deep anatomic features (Fig 2). Our method represents an accurate, instantaneous high refresh-rate approach to AR, which we have termed “live AR.” These initial experiments represent the first use of a new surgical visualization capability, with potential to significantly enhance operative performance.

Surgical Innovation
Volume 15 Number 1
March 2008 7-16

10.1177/1553350608316573
http://sri.sagepub.com
hosted at
http://online.sagepub.com

Novel, Web-Based, Information-Exploration Approach for Improving Operating Room Logistics and System Processes

Paul G. Nagy, PhD, Ramon Konewko, MS, Max Warnock, Wendy Bernstein, MD, Jacob Seagull, PhD, Yan Xiao, PhD, Ivan George, BS, Adrian Park, MD

Routine clinical information systems now have the ability to gather large amounts of data that surgical managers can access to create a seamless and proactive approach to streamlining operations and minimizing delays. The challenge lies in aggregating and displaying these data in an easily accessible format that provides useful, timely information on current operations. A Web-based, graphical dashboard is described in this study, which can be used to interpret clinical operational data, allow managers to see trends in data, and help identify inefficiencies that were not apparent with more traditional, paper-based approaches. The dashboard provides a visual decision support tool that assists managers in pinpointing areas for continuous quality improvement. The limitations of paper-based techniques, the development of the automated display system, and key performance indicators in analyzing aggregate delays, time, specialties, and teamwork are reviewed. Strengths, weaknesses, opportunities, and threats associated with implementing such a program in the perioperative environment are summarized.

Keywords: graphical dashboarding; business intelligence; scorecarding; information visualization; quality

Management of the modern perioperative environment is a challenging act of balance and orchestration that often tilts perilously close to chaos. Many unforeseen delays (including, but by no means limited to, patient transport; case cart preparation; consent forms; and slow turnover) can trigger a cascade of events that escalate throughout the day, resulting in frustration for physicians, staff, and patients. The cumulative effects of many small and interacting delays keep the operating room (OR) from running at peak efficiency and can, in some cases, contribute to more serious errors in management and care.

From the Departments of Diagnostic Imaging (PGN, MW), Anesthesia (WB, YX), Surgery (JS, IG, AP), University of Maryland School of Medicine; and Department of Surgery (RK), University of Maryland Medical Center, Baltimore, Maryland.

Address correspondence to: Paul G. Nagy, PhD, Department of Diagnostic Imaging, University of Maryland School of Medicine, 22 S Greene St, Baltimore, MD 21201; e-mail: pnagy@umm.edu.

Managers trying to address these delays in an ad hoc fashion find themselves playing "whack-a-mole" with serial problems; as soon as one glitch is resolved, another rears its head. The result is a reactive approach that focuses on immediate problems at the expense of the time and effort needed to identify root causes and long-term solutions that will prevent recurrences. The good news is that various routine clinical information systems now gather enormous volumes of data that surgical managers can access to create a seamless and proactive approach to streamlining operations and minimizing delays.

However, the process of leveraging these data in support of routine improvements presents its own challenges, particularly in rethinking traditional reporting and analysis techniques. In the past, paper spreadsheet–based reporting methodologies have been used in management meetings, an approach that is insufficient to handle or analyze even the broadest trends in the increasingly large volumes of

useful data collected. This traditional, tactical approach most often focuses on only the short-term history of operations and fails to identify the small, recurrent delays that may occur across services.

Transparency and a broad scope of accountability are widely recognized as hallmarks of high reliability and dedication to quality in health care organizations.[1] These values, along with an emphasis on verifiable metrics and automated means of collection and assessment, have figured in significant advances in operations research in the management of the surgical environment in the past 5 years.[2-6] These advances contribute to the fulfillment of important goals of surgical units, including patient safety, access to ORs, economic efficiency, waiting time, and staff satisfaction.[6] Moreover, they have provided novel information about what factors contribute to which specific quality goals. Simulation studies using operations research, for example, have indicated that although immediate quality improvements in patient safety, waiting time, and satisfaction on the day of surgery should be a primary focus, only longer term decisions on staffing will provide economic efficiencies.[6,7] Thus, in general, reduction in turnover time will not result in increased volume,[8] but access to historical data and application of operations research methods can point to staffing solutions that will optimize economic efficiency.[9]

Our goal, as part of a grant on the OR of the Future from the Telemedicine and Advanced Technology Research Center, was to accelerate the adoption of these advances by providing an automated, holistic view of operations that would enable the managers to discover patterns and causes of delays. We created a Web-based, graphical dashboard that could be used to interpret clinical operational data, could allow managers to see trends in data, and could help identify inefficiencies that were not apparent with more traditional approaches. This dashboard was designed to provide a visual decision support tool that would also assist managers in pinpointing problem areas in which the greatest benefits could be achieved by applying time and energy toward continuous quality improvement.

What is Business Intelligence?

The field of business intelligence, sometimes referred to as business analytics, is the utilization of data warehousing, data mining, modeling, and forecasting to aid in managerial decision support systems.[10,11] Business intelligence is defined as extracting useful information from the data generated by operational systems of an enterprise.[12] Many top corporate executives use business intelligence–generated electronic scorecarding and dashboarding methodologies to manage their operations with real time–decision making support. A 2007 Gartner Inc worldwide survey of 1400 chief information officers ranked business intelligence as the number 1 technology priority for remaining strategically competitive.[13] Business intelligence methodologies extend directly to consumers in certain markets. Financial Web sites provide individual investors with extensive research and graphical performance analysis of publicly traded companies.

Large academic medical centers, which often generate revenues in excess of US$200 million, are in the same financial league as the medium-to-large businesses in which dashboards are commonplace. Yet few medical centers have invested in the development and routine implementation of tools to analyze and improve the efficiency and effectiveness of perioperative management and operations. Many ORs continue to "fly blind" regarding concepts such as indexing and performance measurement.

Internal graphical dashboards have been proven in other environments to provide useful and productive platforms for continuous quality improvement. The Six Sigma quality methodology, for example, frequently uses dashboards for process management.[14] A dashboard can provide a consistent framework of defined metrics, known as key performance indicators, that aid in defining and redefining quality and goals, as well as offering quantifiable data on achievements.[15] Evidence of consistent improvements through a public dashboard is then used to help align the various parts of an organization to target enhanced performance.

The Potential of Information Visualization

Our project was designed to provide a visual knowledge exploration system to assist managers and senior leadership in understanding trends and patterns. The tools used in this system provide interactive views of data at various granularities and in a series of graphical or tabular formats. These tools can quickly and with minimal user effort impose various

types of analyses on the full data set or on interactively selected subsets of data.

The goal of a visual knowledge exploration system is to provide tools that facilitate interaction with information in an easy, transparent, and meaningful manner. A well-designed graph can tap into the pattern-recognition capabilities of the human visual system. In certain types of patterns, human vision can identify a unique (outlier) value within 200 milliseconds, regardless of whether few or many data points are present.[16,17] However, this ability is entirely dependent on the manner in which the pattern is displayed. Proper visual display is crucial to the use of large data sets for complex decision-making support. The optimal type of data display has been the focus of a substantial body of literature and reporting, and the definitive answer changes as rapidly as new technologies enter the information arena.[18-22] Some studies suggest the superiority of graphical formats (bar charts, pie charts, etc) over tabular presentation (data tables) for certain tasks, whereas the reverse is true for other tasks. More recent work indicates that a constellation of factors must be considered in determining the most advantageous data set display formats, including type of task, underlying structure of the data, and the knowledge level of the users.[23]

What Is the Problem with Paper-Based Reporting?

The benefits of graphical dashboarding can be appreciated more fully by looking at the limitations of traditional paper-based reporting in identifying and managing ongoing operations challenges. Understanding these limitations is important because in many institutions paper-based reporting is so engrained into routine practice that clinicians and perioperative managers may find it difficult to take the steps needed to adapt to other methodologies. Paper-based reporting management systems are limited in the following areas:

Time

Significant time is required to gather information from various sources and compile reports by hand. Decision making is a time-sensitive activity that requires actionable information. Decision making, a process that that should be based on fresh data, is adversely affected when time simply does not permit the preparation of all possible permutations of analyses that might be informative and useful.

Effort

The inherent limitations of paper restrict the number of questions than can be asked and tend to generalize rather than to drill down in areas of analyses. Expanding the scope of a paper report requires extra labor. Most often, the result is a trade-off between the time required to generate the report and the quality of effort required in preparing the results for analysis.

Hindsight

One of the most frustrating characteristics of paper-based reports is that they provide only answers to questions that were identified before the management meeting and discussion. New questions asked during the meeting must be tabled until the next meeting so that analysts can gather the new information required. These tabled questions prevent more purposeful discussions about the data and leave managers with limited information to support decision making in the short term.

Scope of Report

The amount of information that can be contained in a paper-based report is limited, as is the amount of information that can be reviewed within a reasonable amount of time. Selectivity becomes a necessity; yet, it is difficult to predict which questions managers will have during any given meeting. Attempts to broaden the scope of paper-based reports can be both time consuming and problematic; the larger the amount of data in a paper report, the more difficult it is to find any specific piece of information.

Granularity

Aggregate statistics do not allow the user to drill down to understand the underlying distributions to evaluate credibility. Mean statistics offered in most paper-based reports are unreliable when describing nonnormal distributions of data. A single chart or table on paper can show only one view, and it is difficult to present both overviews and detailed information in a single presentation. Showing trends can

obscure source data, where showing only source data can obscure trends. Including both or all in a paper-based report can be labor/time intensive to review and is impractical as a routine practice.

Multiple Versions of Truth

Different groups generating separate reports or even the same reports at different times can result in conflicting operation directives that can add to confusion in effective decision making. The human intervention inherent in paper-based reporting can also introduce bias that may lead to data analysis errors. Moreover, the passage of time between the collection or analysis of data and final reporting may mean that no direct links exist between current operational data and the paper-based report.

Dashboard Design

Organization of the Web Site

The Web site was designed to allow analysis from several perspectives. One of the principle mantras of information visualization and data discovery, identified by Shneiderman,[24] is the ability to overview first, zoom, filter, then details-on-demand. The ability to view data from multiple perspectives assists and increases confidence in decision making. The user accesses each category via a navigation bar of tabs at the top of the Web site. As the user navigates through the system, a trail (called a breadcrumb; Figure 1) is displayed to illustrate how the user navigated to that point and to allow easy backtracking.

To create a concise visualization environment, we created graphs that were clickable within a drill-down interface to provide fast and intuitive zooming and filtering of data. These graphs also provide detailed information about data points when the user hovers over a data marker with the mouse. One of the core requirements for a management dashboard is that it be Web based to allow secure access to all authorized users from any location at any time.

Standard data warehousing techniques were used extraction, transformation, and loading. The database was populated by parsing a text file in a comma-separated delimiter format provided by Cerner SurgiNet Surgical Information System (Kansas City, Missouri). The text file was converted to ANSI Structured Query Language commands as

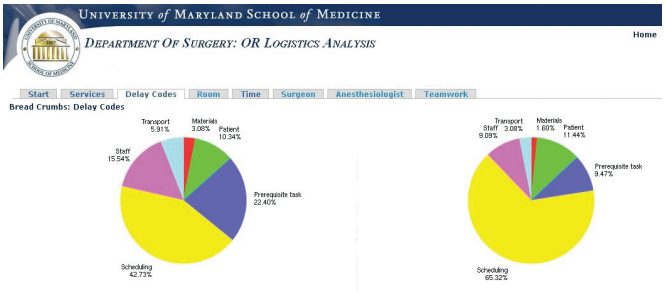

Figure 1. A, Pie chart analysis of number of occurrences of each delay type. B, Pie chart of the relative amount of delay caused by each delay type.

inserts using the MySQL database administration utility PhpMyAdmin. Data were anonymized for patient information because the focus of the system was operational efficiency, not identifying specific patient-associated incidents. In all, 6 months of operational data were uploaded into the system, incorporating performance statistics on 7807 cases on 8 MB of disk space on the server. These cases incorporated all of the operating rooms with both inpatient and outpatient admissions.

Identifying Key Performance Indicators

The American Association of Clinical Directors derived a common glossary of the exact meaning of times used for scheduling and monitoring surgical procedures.[25] Time stamps were extracted from the clinical database for scheduled start time, time at which the patient enters the operating room, the time at which surgery begins, surgery end time, time at which the patient leaves the room, and the turnover time of the room. As a hospital policy, when a case begins 15 or more minutes later than scheduled, the circulation nurse must specify a reason for the delay. These performance data are combined with data from the case such as the room, surgeon, anesthesiologist, case number of the day, and the service.

A total of 43 delay types were identified as reasons for delays. These were grouped into general root causes of materials, patient, prerequisite task(s), scheduling, staff, and transport. At the top of the delay analysis page, as shown in Figure 1, pie charts demonstrate the relative number of delays per root cause and their cumulative impact in time. Although some delays are not numerous, they might have a

large effect on the operations of an OR. The user clicks on the pie chart, selects a root cause, and presents with an analysis page of all the underlying delay causes for that root cause, broken down in the same way by relative number and impact. By selecting a delay cause, the system moves to show a breakdown by specialty, displaying the number of incidents and their average delay times. Selecting a service displays all the cases, and by selecting a case, the details for that case can be displayed. Within the span of 4 clicks, a user can drill down from all the cases in the database to the details of an individual case. The delay analysis tool is useful in understanding the cumulative cost of systemic delays and which specialties are most affected by them.

Temporal Analysis

The temporal perspective provides a daily tactical review of cases to determine over a specified period of time which ones were delayed and why. To present the utilization levels of the ORs in a given day, we used a polar chart showing cumulative room utilization as a function of the hour of the day (Figure 2). This is useful for look at the relationship between room utilization and staffing levels. The user can drill down to the specifics of a single case or can choose to look at data grouped by room or specialty. System delay types, such as transport issues, can affect multiple rooms and specialties across suites of ORs over different periods of time.

Service analysis focuses on key performance indicators within each specialty. Medical specialties within the OR have widely differing dynamics for case efficiency, utilization, turnover, and case length based on a number of factors, including but not limited to procedure complexity and patient acuity. For some types of data analysis involving services or subspecialties, bubble charts provided a useful way to organize data (Figure 3). The bubble chart plots each service by its average case length in the x axis and average delay duration in the y axis. The size of the bubble for each specialty is directly proportional to the number of cases performed. The more cases a service performs, the larger becomes the diameter of the bubble.

For each specialty analysis, the site provides histograms for case length and delay duration. Histographic analysis is useful in determining the distribution type, the spread of the distribution, and the existence of outliers that may distort statistical analysis.

Another display generated was a scatter graph of all cases plotted by their scheduled case lengths

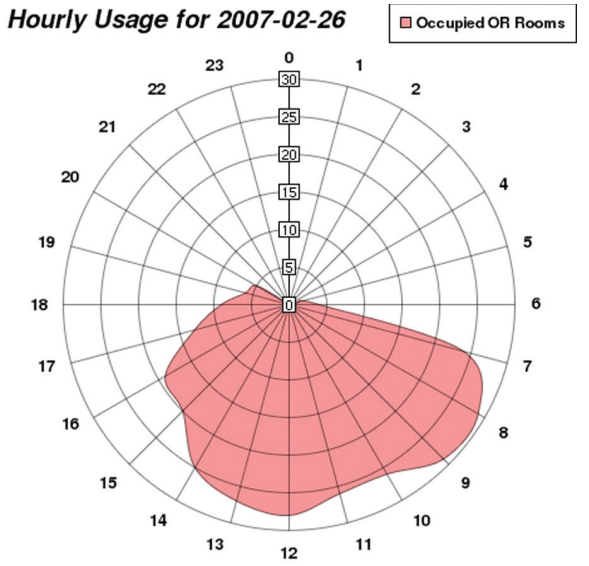

Figure 2. A polar chart of room occupation as a function of the hour of the day. OR indicates operating room.

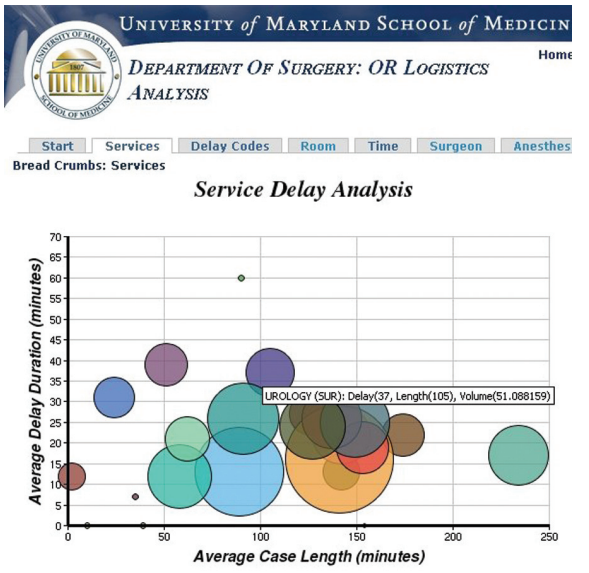

Figure 3. A bubble chart of the services within surgery plotted along their average case length versus their average delay duration. The size of each bubble is proportional to the number of cases performed by the service.

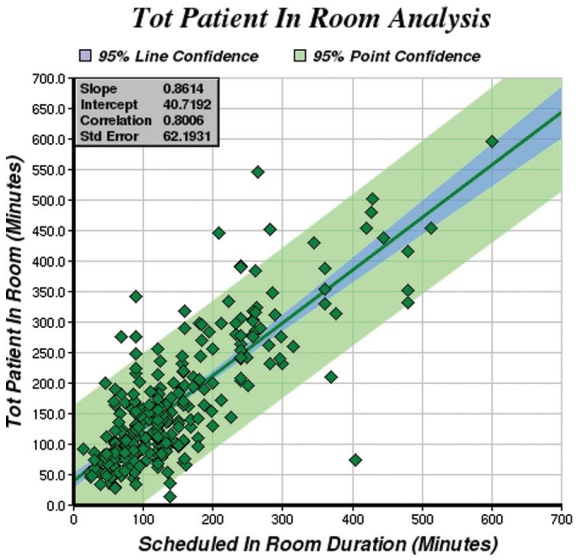

Figure 4. A scatter plot with confidence banding plotting the scheduled in room duration versus the actual patient time in the room.

compared with actual duration (Figure 4). Regression analysis shows potential correlations along with graphical bands illustrating confidence intervals for the line and the points. This index of predictability of scheduling is especially useful in identifying and drilling down on the outlier cases to understand their causes of variance. Each diamond represents an individual case, and by clicking on a diamond, the details of that case are displayed (Figure 5).

Teamwork Analysis

With a surgeon and principal anesthesiologist assigned to each case, we can display delay causes for those cases. As shown in the spider graph in Figure 6, delays are grouped by and aggregated by the blue bars. The farther were the bars, the greater were the number of occurrences for that root cause. The overlapping orange are the average delays by root cause for all physicians in that specialty, normalized by the number of procedures done by that physician.

Using this teamwork analysis, it is possible to identify specific teams that appear to work well together and those that are not routinely time efficient. Other factors, of course, must be considered in reviewing these data, and it would be difficult to determine root causes for efficiency or inefficiency in a specific case. However, this knowledge may provide strategic

Internal Case Number 7694

Or Group	GENERAL OR
Patient Type	Inpatient Admission
Delay Reason	No Delay
Scheduled Start Time	Thu May 03 10:30:00 -0400 2007
Patient In Room Time	Thu May 03 11:07:00 -0400 2007
Patient Out Room Time	Thu May 03 12:22:00 -0400 2007
Surgeon	[redacted]
Speciality	UROLOGY
Case Start Time	Thu May 03 11:26:00 -0400 2007
Or Room	G08
Anest	[redacted]
Sched Anest Type	General Mask
Surgery Start Time	Thu May 03 11:26:00 -0400 2007
Surgery Stop Tme	Thu May 03 12:08:00 -0400 2007
Nurse Unit	W5A Surg
Admit Time	Wed May 02 19:05:00 -0400 2007
Scheduled Or Room	
Anest Type	General Mask
Discharge Time	Fri May 04 12:51:00 -0400 2007
Exp Would Class	Contaminated
Patient Age	[redacted]
Wound Class	Contaminated
Sched Anest	-
Case Level	Elective
Case Minutes	42
Tot Patient In Room	75
Total Patient In Room Anes	0
Total Patient In Room Surgery	19
Total Setup Minutes	35
Total Surgery Minutes	42
Total Delay Duration	0
Turnover Minutes	67
Scheduled Case Duration	405
Case Number	2

Figure 5. A detailed report of a given case. OR indicates operating room.

information that could contribute to what business intelligence experts call a discovery cascade.

Results

Results of an initial rollout of the Web system were assessed through interviews with senior management. This included discussions with the chief medical officer, chief operations officer, chief nursing officer, chairs of surgery and anesthesiology, and several perioperative managers. In presenting this potentially disruptive tool to management, we performed a strengths, weaknesses, opportunities, and threats analysis (known in business intelligence parlance as a SWOT analysis) to classify their observations.

Strengths

Our Web-based approach was seen as a powerful tool that would aid management in identifying systemic, process-driven root causes for delays and other problems and that had the potential for positive

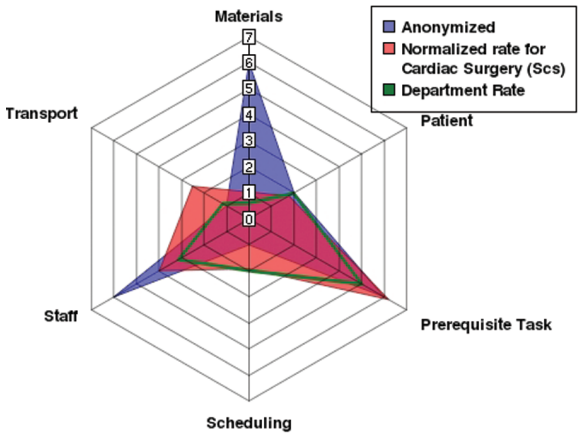

Figure 6. A spider graph of the number of delays broken down by delay type and plotted for the entire department and the section.

effects on the culture of the organization. Among the positive aspects they cited were: (1) this approach turns traditional paper-based data into knowledge and presents this knowledge in easy-to-digest chunks; (2) the dashboard is independent of any single vendor; (3) if used with a data repository, it has the potential ability to link data from different information systems; (4) it provides a systemic view that can calculate the total costs of root causes; (5) it provides a quick visual way to target improvement; (6) additional metrics can be added at the request of management with minimum programming effort; (7) visual displays made outliers and trends more easily identifiable and rendered distributions more easily understood than standard aggregate statistics.

Weaknesses

The reviewers identified 4 areas of weakness and potential improvement for the Web-based system.

Timeliness. Depending on the method of data extraction, data may not be live or near live. If data are provided via an upload, they will be only as recent as the last event. The dashboard optimally should have an Open Database Connectivity connection to a clinical data repository (CDR) or similar copy of the live production environment. The update schedule of the CDR will determine the timeliness of the dashboard.

Personnel resources. Skilled personnel are required to build and maintain a graphical dashboarding application. A surgical informaticist is a good choice as they have the clinical domain experience combined with the principles of management and information technology. This person needs to guide the development of metrics using clinical knowledge to extract meaningful and relevant data. This individual can also play a crucial role in bridging the cultures among health care providers, information technology specialists, and business process managers.[26]

Hardware resources. Hardware resources include access to server space with sufficient processing power and storage to handle a large database. The database storage space required is minimal; however, the central processing unit that drives the data mining must be powerful.

Management training. The introduction of analytics and acceptance of business intelligence practices within a group, particularly one that already has a long-engrained operations process, cannot be accomplished overnight.[11] An investment of time and effort is required and involves education of managers on the use of these tools and the ways in which they can be incorporated into decision making. In the process, the focus of the managers and the entire organization should change from trying to understand the latest event to looking at trends within the data to predict what will happen next and to identify ways to achieve the best possible results.

Opportunities

A dynamic surgical block utilization chart with easily available drilldown, as created in our project, allows surgical chiefs to continually monitor utilization. The drilldown permits them to see which days are being underutilized and by whom and points to immediate courses of action rather than waiting for end-of-year retrospective and analysis. When competition is fierce for OR time, this transparency can be extraordinarily valuable for surgical practices.

Another potential benefit can accrue from matching staffing with caseload to optimize OR efficiency.[27] Cases in overutilized time are 1.75 times more expensive than cases during normal staffing hours, the goal is to match caseload with staff.[28] The dashboard tool pulls in scheduling data from the clinical information system and can display the number of projected cases at 1-hour intervals. The dashboard can also use retrospective data on add-on

cases to estimate a caseload probability by the hour. To maximize efficiency, a user input can be created whereby a manager or charge nurse may enter data on staffing levels, helping to match caseload to staffing.

Along with the scheduling efficiency, OR senior staff and managers may want to match clinical proficiencies with cases. Displays can be created to show circulator/scrub combinations with surgical specialties and case types similar to the surgeon–anesthesia graphs presented. This gives opportunities to the managers to maximize good teams and to identify teams that need improvement.

Many opportunities are available for benchmarking between services and between organizations. The only limitation is the ability to capture data from an information system or network, to apply a meaningful analysis, and to provide an easily understood graphic for the appropriate audience.

Current Procedure Terminology (CPT) codes would be an important additional piece of information because case efficiency should be benchmarked against similar cases. For example, cardiac thoracic cases have long turnover times because of the degree of complexity involved in setup of equipment, drawing of drugs, patient preparation, etc. National benchmarking can be imported to compare against the organization's benchmarks reports for CPT and disease-related groups, morbidity and mortality, length of stay, and complications and can be presented in an easy-to-navigate and easy-to-understand visual.

Opportunities for assessing clinical outcomes include measures such as infection control, preoperative antibiotic compliance, unplanned returns to the OR, staff compliance on chart quality, timeliness, completeness, staff arrival time, etc. Financial reports can include direct costs, indirect costs, contribution margins per case/specialty, labor costs, supply costs per case, and metrics associated with defining and monitoring best practices.

Threats

In all, 2 potential threats to a system, such as the one we devised were identified by the interview group and by our own developers.

The first threat is in the area of data quality and integrity. The data retrieved for our clinical information system have 2 sources of origin. First, scheduling data are obtained. These include, but are not limited to, scheduled start date and time, duration, procedure, surgeon, and anesthesiologist. The schedulers at our institution reside both centrally in a surgical posting office and decentralized in physicians' offices (in the oral maxillofacial and organ transplant services). Because scheduling data do not directly enter the patient's medical record or roll directly into clinical documentation that must be reviewed and modified by a nurse, it is assumed that the risk for bias is minimal. Manipulation of case durations and scheduled start times is limited by system controls. The surgical posting office does have the ability to override system data (eg, for scheduled case duration, which is a by-product of historical averages), but this is not done without the approval from a supervisor.

Data from nursing documentation is under constant review by various clinicians to audit work. This process ensures data integrity and compliance and serves as a modest check and balance. Most of these data are objective, and although some bias may be present, this will most likely be minimal. The area of documentation that is most prone to bias is the "delay reason," because of its highly subjective nature and possible repercussions from management. Another factor for inaccurate delay reporting is the phenomenon of cascading delays (ie, when a delay early in the day causes delays in subsequent cases). By the time of the third or fourth delayed case, it is difficult to ascertain the cause other than to note that the previous case "ran over." During this series of delays, an entirely different cause of delay may happen in a specific case, but the reference point of a scheduled start time is lost, so that it is much more difficult to document a delay cause and duration. Of course, time stamps (in-room time minus scheduled start time) provide well documented and precise record of delay in minutes, but this does not qualify delay by reason type and provides no insights for root cause analysis.

The second threat to initiation of a system such as the one we developed lies in the general perceptions by staff and physicians. Many may feel that they are being spied upon or monitored, especially in areas in which no previous metrics existed. Others may find themselves out of their routine comfort zones. Underperforming staff who worry that they may be identified by the system may aggressively resist implementation of the new tools or work to undermine data integrity. Depending on the organization's structure, the open availability of data could result in punishment for individuals or a group rather than the intended promotion of positive departmental

and institutional change. Moreover, in environments in which competition for OR time is strong, surgical chiefs may be tempted to use data as a weapon to promote their own agendas.

The transparency of the data should alleviate some of these concerns. Team members should be able to see the data in which performance is being judged. In the past, data was obtained by someone walking around with a clipboard or in a back office recording data off charts, with limited or no ways to verify whether the data were true and accurate. With the drilldown features and different ways of organizing data for dashboard display, team members can easily view the raw data.

Conclusion

Strategic decisions made based on the management instinct have a lasting effect on the well-being of an organization. Management could benefit from the adoption of business intelligence tools that provide a quantifiable, validated alternative to instinct and ad hoc choices decision making.

Behavior and practice changes are central to achieving the objective of quality reports that drive efficiency. Too often, data are not integrated within the scope of daily practice. Acceptance of the importance of data must become a part of the culture of the organization. Graphical dashboards that present information down to the simplest, easiest-to-understand, and most accurate levels can compel this behavior change. Managers in the perioperative environment should seize the opportunity to integrate data into their organizations' cultures. Our research suggests that one promising approach is in Web-based tools that can be made for targeted audiences and adjusted by role, position, or location. The result can be total participation in quality improvement and constant feedback that provides long-term rewards in cost efficiencies, staff and physician satisfaction, and improved patient outcomes.

Acknowledgments

This project was supported by an OR of the Future grant from the Telemedicine and Advanced Technology Research Center. We would like to thank Dr Nancy Knight from the University of Maryland for her expert assistance in preparing this manuscript.

Reference

1. Weick KE, Sutcliffe KM. *Managing the Unexpected—Assuring High Performance in an Age of Complexity*. San Francisco, CA: Jossey-Bass; 2001.
2. Dexter F, Xiao Y, Dow AJ, Strader MM, Ho D, Wachtel RE. Coordination of appointments for anesthesia care outside of operating rooms using an enterprise-wide scheduling system. *Anesth Analg*. 2007;105:1701-1710.
3. Dexter F. Why calculating PACU staffing is so hard and why/how operations research specialists can help. *J Perianesth Nurs*. 2007;22:357-359.
4. Dexter F. Bed management displays to optimize patient flow from the OR to the PACU. *J Perianesth. Nurs*. 2007;22:218-219.
5. Dexter F. Operating room utilization: information management systems. *Curr Opin Anaesthesiol*. 2003;16:619-622.
6. Dexter F, Epstein RH, Traub RD, Xiao Y. Making management decisions on the day of surgery based on operating room efficiency and patient waiting times. *Anesthesiology*. 2004;101:1444-1453.
7. Macario A, Chow JL, Dexter F. A Markov computer simulation model of the economics of neuromuscular blockade in patients with acute respiratory distress syndrome. *BMC Med Inform Decis Mak*. 2006;6:15.
8. O'Sullivan CT, Dexter F, Lubarsky DA, Vigoda MM. Evidence-based management assessment of return on investment from anesthesia information management systems. *AANA J*. 2007;75:43-48.
9. O'Neill L, Dexter F. Tactical increases in operating room block time based on financial data and market growth estimates from data envelopment analysis. *Anesth Analg*. 2007;104:355-368.
10. Davenport TH. Competing on Analytics. *Harv Bus Rev*. January 2006;1-12.
11. Davenport TH, Harris JG. Competing On Analytics: The New Science of Winning. 1st ed. Boston, MA: Harvard Business School Press; 2007.
12. Chisholm M. The Twin Towers of BI Babel: Enterprise Architecture. BI Review, December 2007. http://www.bireview.com/issues/2007_42/10000440-1.html. Accessed January 10, 2008.
13. Beer S. Business Intelligence top priority of CIOs, February 2007. http://www.itwire.com.au/content/view/9906/53. Accessed January 10, 2008.
14. Pande PS, Neuman RP, Cavanagh RR. *The Six Sigma Way: Team Fieldbook*. New York, NY: McGrawHill; 2002.
15. Malik S. *Enterprise Dashboards: Design and Best Practices for IT*. Hoboken, NJ: John Wiley & Sons; 2005.
16. Treisman. Preattentive processing in vision. *Comput Vis Graph Image Process*. 1985;31:156-177.
17. Treisman A, Gormican S. Feature analysis in early vision: evidence from search asymmetries. *Psychol Rev*. 1988;95:15-48.

18. Washburne JN. An experimental study of various graphic, tabular, and textual methods of presenting quantitative material. *J Educ Psychol*. 1927;18:361-376.
19. Tufte ER. *The Visual Display of Quantitative Information*. Cheshire, CT: Graphics Press; 1983.
20. Cleveland WS, McGill R. Graphical perception and graphical methods for analyzing scientific data. *Science*. 1985;229:828-833.
21. Montazemi AR, Wang S. The effects of modes in information presentation on decision-making: a review and meta-analysis. *J Manage Inf Syst*. 1988;5:101-27.
22. Feldman-Stewart D, Brundae MD, Zotov V. Further insight into the perception of quantitative information: judgments of gist in treatment decisions. *Med Decis Making*. 2007;27:34-43.
23. Meyer J, Shamo MK, Gopher D. Information structure and the relative efficacy of tables and graphs. *Hum Factors*. 1999;41:570-587.
24. Shneiderman B. Inventing discovery tools: combining information visualization with data mining. *Inf Vis*. 2002; 1:5-12.
25. Procedural Times Glossary of the AACD. http://www.aacdhq.org/Glossary.htm. Accessed January 10, 2008.
26. Charters KG. Nursing informatics, outcomes, and quality improvement. *AACN Clin Issues*. 2002;14: 282-294.
27. Dexter F, Ledolter J, Wachtel RE. Tactical decision making for selective expansion of operating room resources incorporating financial criteria and uncertainty in subspecialties' future workloads. *Anesth Analg*. 2005;100: 1425-1432.
28. Strum DP, Vargas LG, May J. Surgical subspecialty block utilization and capacity planning: a minimal cost analysis model. *Anesthesiology*. 1999;90:1176-1185.

A Research Portfolio for Innovation in the Surgical Environment

Gerald R. MOSES,[a, 1] PhD, Adrian E. PARK,[b] MD,
[a] *University of Maryland Medical Center, Baltimore MD*
[b] *Department of Surgery, University of Maryland Medical Center*

Abstract. The University of Maryland Medical Center and School of Medicine have sponsored a program of research targeted at the enabling of technologies for enhanced training, clinical effectiveness and patient safety. The pillars of this research included scientific approaches related to Informatics, Smart Image, Simulation and Ergonomics and Human Factors. The evolving research effort opened the door to a revised concept of basic surgical sciences that underpin training and performance in the operative environment.

Keywords. Surgery, training, innovation, surgical basic sciences

Background

The phrase, operating room of the future (ORF), has been used to describe the development of medical technology and the improvement of function and safety of the perioperative environment. The research program in the Department of Surgery at the University of Maryland has extended the meaning of the ORF to the study of functions and interactions of people, processes and technology producing a safe and efficient operating suite.

The Research Portfolio

For five years, the University of Maryland Medical Center and School of Medicine have sponsored a program of research targeted at the enabling of technologies for enhanced training, clinical effectiveness and patient safety. Initially, under the rubric of "The Operating Room of the Future" various pillars of research were established that proposed to advance the state of medicine, notably surgery. The pillars included scientific approaches related to Informatics, Smart Image, and Simulation. The evolving research effort opened the door to a revised concept of basic surgical sciences that underpin training and performance in the operative environment.

Developments led to two important changes; the adoption of a new mantra, Innovation in the Surgical Environment, to replace the Operating Room of the Future; and the addition of another research pillar, that of Ergonomics and Human Factors.

[1] Corresponding Author: Gerald Moses, MASTRI Center, Division of General Surgery, University of Maryland Medical Center, 22 S. Greene Street, Baltimore, MD 21201; gmoses@smail.umaryland.edu

Progress has been achieved in each of the pillars of research, as reported at a recent annual conference that sought to apply lessons learned form the high-stakes environments of aviation and astronautics to the practice of surgery.

Research Pillars

The medical informatics pillar includes a Perioperative Scheduling Study, a study of workflow around performance indicators in the peri-operative environment and building a graphical dashboard to allow data mining and trend analysis of operating indicators. The surgical simulation pillar entails both physical and cognitive simulation for training with emphasis upon laparoscopic surgery. A third pillar is entitled "Smart Image" in which we are seeking to push the boundaries of real time deformable image registration with a goal of performing the 1st fully smart image guided laparoscopy. A recently added pillar of ergonomics and human factors addresses the impact of stress movements and position upon the surgeon performing minimally invasive or "open" procedures.

Informatics: Workflow and Operations Research for Quality (WORQ)

The Perioperative Scheduling Study is looking at how using post-operative destination information during the process of surgery scheduling can influence congestion in post-operative units such as intensive care units (ICUs) and intermediate care units (IMCs), which lead to overnight boarders in the post-anesthesia care unit (PACU). We have developed a mathematical congestion evaluation model for evaluating congestion in post-operative units, including ICUs, IMCs, and floor units. This model requires data about post-operative destinations and length-of-stay distributions for different types of surgeries. We have analyzed data about cardiac surgeries from two years and have analyzed UMMC financial records for all of the surgical cases for fiscal year 2007. We have developed an algorithm for predicting bed requirements based on the surgical schedule and have conducted a preliminary study comparing these predictions to other prediction methods for two units. The preliminary results show that the new bed requirements prediction method is more accurate.

Informatics: Operating Room Glitch Analysis (OGA)

The OGA project, focusing on institutional learning, is looking at the workflow around performance indicators in the peri-operative environment and building a graphical dashboard to allow data mining and trend analysis of operating indicators.

We have integrated into the data architecture a javascript based bubble chart that provides several interactive features to allow thorough data discovery. The bubble chart can play over time to see how the size of the bubbles change, which relates to the number of cases performed, as well as their x and y axis location. The x and y axis can represent delay duration, actual procedure time, scheduled procedure time, or turnover time. The bubble can also be tagged to provide a contrail to show performance over time. Figure 1 indicates an analysis of service delay as related to average length of surgical procedure.

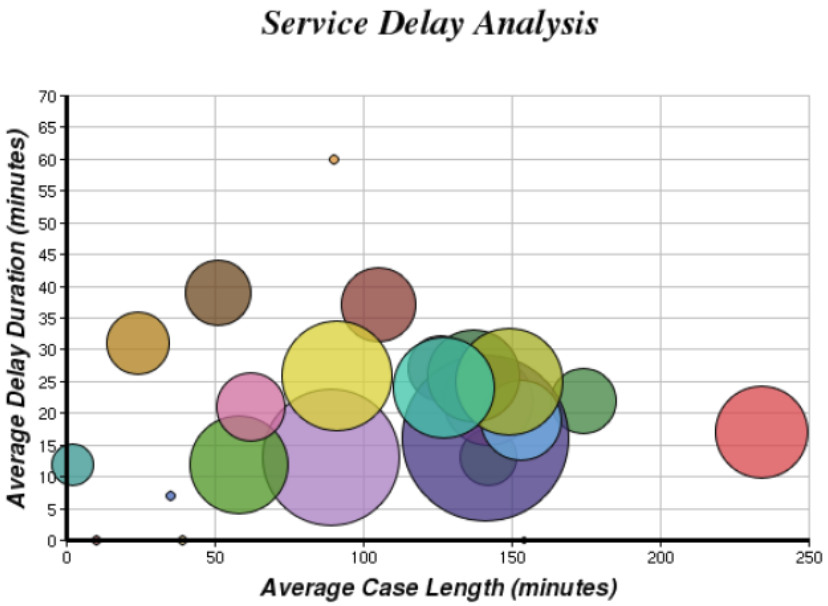

Figure 1. Service delay as related to average length of surgical procedure.

Informatics: Video Summarization of Key Events in Surgery

The technique of summarization is used when confronted with the task of gleaning succinct information from large amounts of data. For example, our national intelligence services use both machine and human analysis to prepare the daily Intelligence Summary for the President. A similar challenge is presented to those who train surgeons using a vast archive of surgical video. A key element in teaching is the extraction of the right video event to make the critical point to surgical trainees.

Recent decades have seen an increasing use of VR and simulation aids in surgical training. The typical approach is to use sensors to capture the kinematics of the tools, as well as force/torque measures. One thread of work directly analyzes these measurements to construct Markov Models that describe the state and transitions for a surgical procedure, and it is then shown that the transition probabilities between states are different at different levels of expertise.

An alternative approach is for an expert to look at the video of the surgical procedure (or training), identify key steps/events (either done well or incorrectly), and then judge the skill level of the performer. This approach can bring to bear the expert's knowledge and intuition of the complex interaction between tools, movements, organs, cutting planes etc. The drawback however is that it requires the review of a video that can be very time-consuming. We propose to address this problem by developing techniques to automatically identify key scenes/events in a video of laparoscopic surgeries.

Simulation

We are conducting multiple studies of the effects of physical box trainers, virtual reality (VR) trainers, and mixed modality training for acquiring laparoscopic surgery skills. These studies support the actions and operations of the Maryland Advanced Simulation Training, Research and Innovation (MASTRI) center. Additionally, we are developing a cognitive simulator and building knowledge representations based on ontology of focused human anatomy/physiology to emulate the surgical/clinical experience. The cognitive simulator, the Maryland Virtual Patient, has been developed by construction of a computational model of the cognitive agent, and by testing the goal- and plan-based reasoning component and its interaction with the interoceptive and language perception modules and verbal, mental and physical action simulation modules.

We have continued to work on the natural language substrate of the system, concentrating on enhancements required for processing dialog (not expository text). Further, we have implemented an enhanced microtheory of indirect speech acts, and continued working reference resolution algorithms.

The research work encompasses work targeted upon the acquisition of ontology and lexicon knowledge., and improvement of the DEKADE user interface. The current version of the cognitive simulation system includes multiple scenarios of physician-patient interface related to LERD/GERD patient conditions.

Smart Imaging

Surgical practice is considered among the most complex and difficult fields. That no two patients are exactly alike is one of the challenges that make it so. Anatomic and physiologic differences make each case unique. In surgery, these variations can complicate an operation; the discovery of unexpected anatomical variations often requires a surgeon to stray from standard, well-practiced techniques to attempt a novel approach to the procedure. With novelty comes a reduced margin of safety. This situation is exacerbated by a trend toward further physical separation between the patient and interventionalists (e.g., surgeons, endoscopists, radiologists) and a greater dependence on an image of the patient's (target) anatomy to effect therapy or establish a diagnosis.

"Smart image," as we have defined it, refers either to the process of extracting elements from an environment and imparting them to an image or to acquiring elements from within a scene and enhancing them. The result in either case is a more meaningful visualization of the operative field. Although many applications exist within this definition, Maryland's smart image team is working toward performing the first laparoscopic surgery guided completely by smart image.

Typically in laparoscopic procedures, diagnostic imaging—including x-rays, computerized tomography (CT), and magnetic resonance imaging (MRI) scans—can provide a preview of patient physiology. Often, however, these diagnostic images are in a static format that does not allow the care provider to interact meaningfully with the information the images contain. Current advances in smart imaging can be used to improve patient safety by providing the caregiver with a more interactive experience. A set of two-dimensional (2D) slices of a CT scan can be transformed into a three-

dimensional (3D) computer model so that surgeons can preview a realistic view of the patient's anatomy before an operation. This type of smart imaging provides an interactive "fly-through" view that allows the surgeon to explore the anatomy in detail.

With advances in computing power, these previews could be mapped more realistically to interactive simulators that would permit rehearsal of a surgical procedure that might include attempts at novel approaches before surgery begins. During real surgery, these smart diagnostic images could be integrated into the surgeon's actual view of the patient.

We are working toward matching the minimally invasive surgeon's video view of the surface anatomy with computer-generated models from Digital Imaging and Communications in Medicine (DICOM) data sets. Such imaging could provide the surgeon with real-time "x-ray vision" during the operation. Thus, the underlying structure, such as the position of a tumor beneath the surface of a larger anatomic structure or blood vessels within the liver, could be seen. Vessels could be contrast-enhanced in a single, high-resolution CT scan before the surgery. Then, during surgery, low-dose/low-resolution CT scans could be used to transform the high-resolution CT image to match the movement of the patient's anatomy during surgery. This would allow intraoperative visualization of anatomy that retains the enhanced contrast vessels, a unique ability that is not possible at present.

CT scans can provide enhanced intraoperative visualization of deep structures far superior to that of laparoscopes. However, the use of continuous CT exposes the patient and surgeon to a radiation level that remains a concern. Therefore, a major thrust of our work is to design, develop, and test several dose-reduction strategies and to incorporate these into our proposed continuous CT-guided surgical navigation system. Our preliminary work suggests that our strategies would allow us to lower the net radiation exposure to the patient to levels commonly viewed as safer in cardiac catheterization and interventional radiology procedures. In the long term, we also propose using telemanipulators to remove surgeons from the CT room and thereby shield them entirely from radiation exposure while they are performing the procedure.

Ergonomics and Human Factors

Recently, a fourth pillar was added to our research portfolio, that of Ergonomics and Human Factors. These are two related branches of study that examine the relationship between people and their work environment. Ergonomics often focuses on the physical environment and the human body, while human factors center more on the cognitive aspects of performance. The same ergonomics and human factors techniques credited with making industrial processes safer and more efficient can be applied to the analysis and improvement of OR operations. Tools, such as video analysis and motion tracking, can be used to analyze current practices, identify inefficiencies and dangers, develop solutions, and measure improvement. "Best practices" to maximize safety and efficiency can be developed based on empirical data.

Our discussion of workflow to this point has taken a macro or panoramic view; for example, how might we most effectively track and bring together the people and assets necessary to ensure that a patient's surgical experience is safe and efficient. Through human factors and ergonomics, we have the ability to focus on a more micro-level

analysis, such as measurements of surgeon/instruments interface and how the physical interface between the surgeon and the patient could be improved.

In the future, OR workspace layout would be optimized through ergonomic data and human factors analysis, and this optimization would lead to the establishment of "best practices" for an array of surgical operations. Proper layout would reduce risks of infection, speed operations, and reduce fatigue of surgeons and staff, all elements that could contribute to a reduction in adverse events and improved patient safety.

Future Vision of the Operating Room Environment

Well-trained care providers, who have reached a level of proficiency on realistically simulated patients, are supported by an array of smart technology enabling surgical procedures to be performed in an ever safer environment. Cases start on time with all team members informed of the goals and possible trouble spots of each operation. Contingency plans are in place for dealing with anticipated complications. The smart environment checks that all required equipment and people are present and cross-checks drugs and blood products brought into the room, ensuring patient compatibility in terms of allergies and blood type. Surgeons do not have to fight fatigue and discomfort during surgery, as the layout of the surgical workspace is ergonomically correct. Thus, the time and effort needed to perform surgery is minimized and improvement of both technique and outcomes is realized.

A New Set of Basic Surgical Sciences

The potential of surgical care in the future can be realized by incorporating into the training of surgeons a new set of basic surgical sciences, those of advanced imaging, informatics systems, simulation and ergonomics and human factors. These do not replace the well established scientific bases of anatomy, physiology, pathology and related areas of study. Rather they add a vital underpinning to the knowledge and expertise required of future practitioners.

References

[1] Shekhar, R., Dandekar, O., Kavic, S.,George, I., Mezrich, R., and Park, A. "Development of continuous CT-guided minimally invasive surgery," in Medical Imaging 2007 Visualization and Image-Guided Procedures, San Diego, CA, USA, 2007, pp65090D-8.

[2] Shetye, A. and R. Shekhar, "A statistical approach to high-quality CT reconstruction at low radiation doses for real-time guidance and navigation," in Medical Imaging 2007: Physics of Medical Imaging, San Diego, CA, USA, 2007, pp. 65105U-11.

[3] Lee G, Kavic SM, George IM, Park AE (2007) MIS surgical ergonomics: Future Trends, Annual conference of Medicine Meets Virtual Reality (MMVR), Long Beach, CA.

[4] Moses G.R., Seagull FJ, George I.M.and Park A.E. The MASTRI Center – Medical Simulation for Skill Acquisition. Proceedings of MODSIM World Conference 2007

Review Article

Surgical Innovation
Volume 14 Number 3
September 2007 153-167

10.1177/1553350607307956
http://sri.sagepub.com
hosted at
http://online.sagepub.com

Methodological Infrastructure in Surgical Ergonomics: A Review of Tasks, Models, and Measurement Systems

Gyusung Lee, PhD, Tommy Lee, MD, David Dexter, MD, Rosemary Klein, MA, and Adrian Park, MD

Though in its infancy, the discipline of surgical ergonomics is increasingly valued. Still, little has been written regarding this field's tasks, models, and measurement systems. These 3 critical experimental components are crucial in objectively and accurately assessing joint and postural control as exhibited by expert laparoscopic surgeons. Such assessments will establish characteristic patterns important for surgical training. In addition, risk factors associated with both minimally invasive surgical instruments and the operating room environment can be identified and minimized. Our review focuses on evidence-based experimental ergonomic studies undertaken in the field of laparoscopic surgery. Publications were located through PubMed and other database and library searches. This article describes tasks, models, and measurement systems and considers their specific applications and the types of data obtainable with the use of each. Advantages and limitations, especially those of measurement systems, are compared and discussed. Future trends and directions believed necessary for optimal investigation and results are also addressed.

Keywords: surgical ergonomics; methodology; measurement systems; laparoscopy; review

The rapid acceptance of laparoscopic surgery as a clinical alternative to traditional open surgery sometimes obscures the fact that minimally invasive surgery (MIS) is still relatively new. Newer still is our realization of the physical demands MIS can make on its practitioners, but those are precisely the issues that the very recent discipline of surgical ergonomics seeks to understand and address. Like all disciplines that start out at once self-contained yet also multidisciplinary, the field of MIS ergonomic research is fast becoming broadened through a variety of different approaches, so numerous that those outside the field as well as many inside the field may possess scant knowledge regarding the vast methodologic array of tasks, models, and assessments in use.

Ergonomics examines and seeks to minimize risk factors between human beings and the tasks and environments that occupy them. Its historical origins are traceable to two editions (1700 and 1713) of De Morbis Artificum Diatriba, or Diseases of Workers, in which the job hazards workers encountered were characterized by Bernardo Ramazzini, often termed occupational medicine's founder,[1] and also to the 1857 article, "An essay on ergonomy, or science of labour, based on the laws of natural science," by W.B. Jastrzebowski, who is credited with the first use of the term derived from coupling the Greek words for work ("ergon") and for natural law ("nomos").[2] Despite those and other early influences, the science of ergonomics is still regarded as a fairly recent discipline, one just shy of its 60th anniversary as a formal body of knowledge.[3]

The relative youthfulness of ergonomics belies the significance of the contributions it has made in many occupational fields, including the military, athletics, and medicine, in addition to other environments. Fatigue, stress, and equipment use as factors affecting task performance were of great interest to the military during World War II. Indeed, to study the strain that might be experienced by air personnel flying long-range missions, a simulated cockpit was

From the Department of Surgery, University of Maryland, Baltimore.

Address correspondence to: Adrian Park, MD, University of Maryland, Department of Surgery, 22 S Greene St, S4B14, Baltimore, MD 21201; e-mail: apark@smail.umaryland.edu.

built by Kenneth Craik, inaugural director of the Applied Psychology Research Unit (Cambridge).[4] Among the many sports benefiting from ergonomic applications is track and field. Proper shoe design and material composition can greatly reduce fatigue level and improve running performance.[5] "Dispersion of attentional resources"—a unique measure recently established within the anesthesia work domain for evaluating the workplace awkwardness that results from simultaneous task performance—is typical of knowledge ascertained through ergonomic clinical research.[6] Ergonomic theory, design, and applications play an important role in everyday life, as is evidenced by accumulating research on everything from the effect of computer keyboard designs on users with upper extremity musculoskeletal disorders[7] to the collection and analysis, using motion capture and pressure sensors, of posture parameters and sitting strategies to determine car seat design that is both comfortable and ergonomically sound.[8]

The study of ergonomics in the surgical arena has acquired increased importance with the advent and widespread acceptance of laparoscopic procedures. Overall, the case has been made that its advantages often make MIS the preferable alternative for patients. Specifically, it falls to surgical ergonomics to make the case through problem definition, research surveys and studies, and data acquisition and analysis that MIS is often a demanding alternative for its surgical practitioners. This phenomenon results primarily from the different nature of the minimally invasive surgical environment, which surfaces new issues for the surgeon whose access to information and ability to move are limited in particular ways.

Though literature reviews of ergonomics in minimally invasive surgery have been undertaken, they remain few in number. In explanation of a newly coined term—minimal-access surgery (MAS)-related surgeon morbidity syndromes—a lengthy review was undertaken covering a broad array of issues identified as problematic, such as instrument design, operative display systems, and access ports in addition to injury mechanisms resulting from procedural technique.[9] A limited review covered ergonomic laparoscopic research accomplished within 3 broad categories: physical, sensorial, and cognitive.[10] A more comprehensive review detailed the variety of MIS ergonomic studies on visualization, manipulation, posture, and workload (mental and physical), as well as on the operating environment overall.[11] The effects of visual and haptic perception, often reduced, on surgical performance are reviewed in an article that also investigates research on force.[12]

In this review we focus on the methodology specifically used within the MIS ergonomic discipline for collection and analysis of data. In doing so, we examine and discuss the tasks and models germane to studies within this field. Our intention is to reveal the depth and breadth of the research approaches used at this young stage of MIS ergonomics, particularly through review and discussion of tasks, models, and measurements, and to suggest how improvement and development of these essential factors will profoundly affect future research and outcomes.

Tasks and Models

Two crucial design components in surgical ergonomic research are tasks and models. As laparoscopy evolves into a well-accepted, established discipline, the tasks involved in MIS procedures have increasingly become more standardized, gaining acceptance from MIS professional and accrediting organizations.[13-17] The result is that these tasks, for example, Fundamentals of Laparoscopic Skills (FLS), are increasingly used in MIS ergonomic research. Additionally, tasks such as partial circle-cutting have been created specifically to facilitate surgical ergonomic research. The term "models" refers to physical forms—in MIS often animal, artificially made, or simulated—that are meant to provide a realistic approximation of operating room (OR) conditions and human anatomy.

Static Tasks

Static tasks involve no motion. An example of a static task is the opening and closing of an instrument against a spring-loaded clip at a set resistance[18,19] while the instrument is held in a fixed position.[20]

Simple Navigation Tasks

Although they do not simulate any particular operative procedure, these tasks involve joint movement and instrument manipulation, thus permitting measurement. Through a variety of navigational skill tasks, fairly simple outcome metrics, including time and error, can be derived. These types of tracking tasks include navigation around an electrified wire course[21] and simple touching of labeled points on a target.[22,23]

Computerized formats of these simple navigation tasks exist. For example, the Dundee Endoscopic Psychomotor Tester (DEPT) evaluates the user's ability to navigate a 5-mm probe with one hand through a series of holes on a target plate, culminating in touching a plate behind the target plate.[24,25] Its successor, the Advanced Dundee Endoscopic Psychomotor Tester (ADEPT), evaluates the subject using both hands simultaneously—using one of 2 standard laparoscopic instruments with one hand to execute the original task, while the other manipulates the target.[26] In addition to the metrics of execution time, number of errors, and successful task completion, ADEPT is capable of measuring flight trajectory by recording instrument positions in 3D space.

Manipulation Tasks

The most fundamental laparoscopic skills, such as object manipulation, suturing, and cutting, comprise this group of tasks, which require bimanual coordination. Most studies have used as their model some form of standard laparoscopic trainer box, as doing so makes research less reliant on proprietary, often expensive or inaccessible technology. For example, small object manipulation into a small aperture, instrument-to-instrument rope passing, and cable tying have been used as a representative series of tasks for assessing laparoscopic muscle activation.[27] Other groups testing similar skills have used tasks involving transfers, shape cutting, point touching, and needle handling.[28-30] Cutting partial circles has been used for assessing operative table height[31] and monitor height.[32] A more difficult task that required lifting and cutting of various threads from a foam board[33] was used to examine the effects of 2D- versus 3D-viewing technology on task performance.

The most commonly used manipulation tasks have been variations of suturing and tying. Such study tasks and models have ranged from tying of knots only,[34-40] to suture placement and tying on an artificial surface,[41-44] to suturing of porcine enterotomies.[45-50] As much as possible, objective metrics have been developed for these types of tasks. For example, Cuschieri and colleagues developed a knot quality score related to the knot breaking or slipping force and the strength of the suture material itself.[51] Suturing tasks with their specific marked targets are easily graded based on accuracy of suture placement and time to completion. Enterotomy closures have been graded based on leak pressure.

Traditional Training Boxes

The traditional training box comes in various forms, but its basic construct remains the same. It is a confined space roughly approximating the abdominal cavity into which ports may be placed to allow instrument access. Visualization is achieved through a camera, which can be a laparoscope or simple charge-coupled device (CCD) camera. A multitude of different tasks such as object transfer, circle cutting, and bowel suturing can be conducted within this environment.

Virtual Reality Models

Virtual reality (VR) simulators are becoming increasingly lifelike as they incorporate haptic feedback and actual laparoscopic instruments, among other elements. They also come advantageously incorporated with a sizable number of reproducible and standardized measures, as well as a wide range of possible exercises. The simulated tasks used so far have not been operative simulations per se but instead have been simulations of drills designed to develop laparoscopic skills. For example, a needle manipulation drill on a LapSim (Surgical Science, Gothenburg, Sweden) has recently been used to study the potential benefit of armrests.[52] MIST-VR (Medical Education Technologies, Inc., Sarasota, Florida), with its variety of simulated tasks, has been used to measure the effect of cognitive distraction[53] and physical workload,[54] and the clipping and cutting tasks simulated by the Xitact 500 LS (Xitact SA, Morges, Switzerland) have been used to assess instrument handle types.[55] Despite the possibilities and potentials offered, no single simulator has gained widespread use in ergonomic analysis. In addition, to be proposed as optimal models for use in ergonomic studies, VR simulators must improve overall in terms of the still generally unrealistic quality of their replicated visual and haptic feedback, variables that may result in subjects making movements that would not be made in real or more realistic circumstances.

Intraoperative Model

As an ergonomic research environment in which to conduct task and movement research, the OR is completely realistic and completely validated. The drawbacks to use of the OR for such research, however, are considerable. Difficulties in getting ergonomic

equipment into the OR environment have barely been overcome. Two formidable issues encountered are sterilization and cumbersome wiring. Another aspect that must be considered is that such research within the OR would have to be properly limited to the expert as the subject, thus excluding comparative data on trainees or those with less experience. These obstacles have not, however, prevented all intraoperative ergonomic research. Surgeon posture,[56] camera operator movement,[57] and hand movements[58] have all been recorded during laparoscopic cholecystectomies. Other ergonomic studies, unhindered by OR limitations, have investigated display system,[59] operative flow, and procedures.[60-62]

Discussion

Task and model complexity in MIS ergonomic studies vary depending on the goal of each experiment. The data measured from simple static or manipulation tasks are relatively easy to analyze and provide basic ergonomic or performance information. With data obtained from more complex tasks that provide more comprehensive information, such as body control strategies, the experiment must be very carefully designed and performed to minimize variability within and between subjects. For instance, laparoscopic suturing is a widely used task in surgical ergonomic research. Although this is an essential skill, the performance of which is unofficially acknowledged as the hallmark of a skilled laparoscopic surgeon, it seldom represents more than a small fraction of the time spent in a laparoscopic procedure. Maneuvers such as exposure, retraction, and dissection are far more frequently employed tasks requiring more extended time expenditure, yet they are not often the subject of ergonomic analysis. Tasks such as these must be deemed worthy of research consideration. Additionally, more models and tasks for surgical ergonomic studies should be standardized in the manner of the FLS.

Sophisticated measurement systems built from a variety of technologies determine what types of data are obtainable through evaluative use of tasks and models. Among the most widely used are motion analysis for capture of body movement patterns and electromyography (EMG) analysis for monitoring muscle activation, although force plate analysis for evaluation of postural stability is gaining in importance.

Motion Analysis

Human movement is the result of complex processes involving the brain, spinal cord, peripheral nerves, muscles, bones, and joints. Motion capture technology, which evolved continuously from basic photography to sophisticated computer-aided motion analysis systems, allows study of these complex processes through analysis of kinematic data that represent the relative movements of segments connected with rotating joints. Motion capture systems have been used in various fields of application, including gait analysis,[63,64] sports science and athletic training,[65,66] biomechanics and neuroscience research,[67-69] and film and animation production.[70,71] Surgical ergonomics in laparoscopy is a relatively new field employing motion analysis. A wide variety of movements, ranging from the maneuvering of surgical instruments to the upper and/or lower body movements of surgeons, are captured as kinematic data and analyzed to provide detailed information about what constitutes ergonomic safety for surgeons performing MIS tasks and procedures.

Technologies

Throughout the development of motion analysis systems, different technologies have been used for accurate, objective movement measurements. Having considered all motion capture technologies, including ultrasound tracking and electric/mechanical goniometers, we posit that the most representative technologies, as evidenced by research group use, are orientation, electromagnetic, optical, and video-based motion analysis systems (Table 1).

An orientation sensor system measures 3 angular movements—yaw, pitch, and roll. Electromagnetic tracking systems use Faraday's law to measure the orientation and location data of each sensor. With optical motion capture systems (Figure 1), light-emitting diode (LED) strobes surrounding a camera lens transmit light into a measurement space from within which retroreflective markers—placed to represent joint and segmental landmarks—reflect light back to the camera. Recent optical motion capture systems are capable of handling hundreds of markers and reconstructing body movements in real time. With these relatively new systems, movement at each joint can be calculated in 3 directions (flexion/extension,

Table 1. Motion Analysis Technologies in Surgical Ergonomics

Technology	User groups	Components
Orientation sensor	Berguer et al,[31] Smith et al,[32,54] Kondraske et al[73]	Solid-state 3-axis pitch, roll, and yaw sensor
Electromagnetic tracking	Huber et al,[33] Rasmus et al,[57] Dosis et al,[58,83] Ridgway et al,[75] Datta et al,[74] Mackay et al,[76] Bann et al,[77] Khan et al,[78] Moorthy et al,[79, 81] Hernandez et al,[80] Munz et al,[82] Aggarwal et al,[84] Smith et al[85]	Electromagnetic field generator and receivers
Optical tracking	Emam et al,[35,36,38,47-49] Person et al,[56] van Veelen et al,[59] Lee et al,[72, 88,89] Patil et al,[86] Gillette et al[87]	Computer-controlled video camera and retroreflective markers
Video analysis	van Veelen et al,[29, 40] Matern et al,[30, 90] Joice et al[45, 62]	Video recording and observation

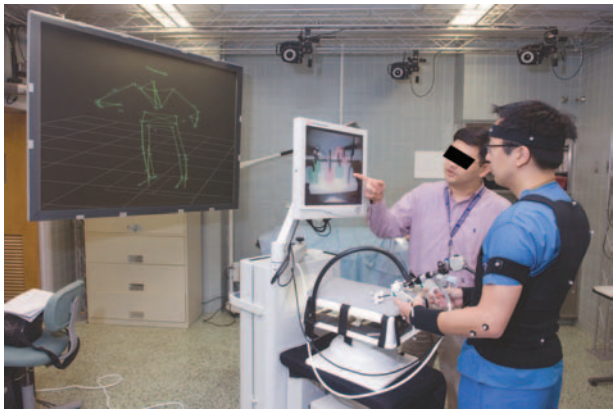

Figure 1. An optical motion analysis system with multiple cameras mounted on truss system tracks a set of reflective markers attached to the anatomical landmarks of a surgeon. The data is used to reconstruct the surgeon's body movement, which is then visualized as a stick diagram.

abduction/adduction, and internal/external rotation) and, for posture analysis specifically, the center of mass (CoM) can be calculated from combined kinematic and anthropometric data derived from subject measurement.[72]

The simplest system setup for video analysis involves a single camcorder or digital camera to monitor the subject's movement in 1 plane, for example, the sagittal plane. In surgical ergonomic studies, the endoscopic image has often been used to monitor performance accuracy and laparoscopic instrument movements. Video recordings captured by one or two cameras at different angles also provide approximate kinematic data analysis of surgeons' body movements.

Comparison of Motion Analysis Systems

By far the most economical motion analysis method in comparison with either electromagnetic or optical motion capture is the orientation sensor system. A significant limitation is that, although this system allows obtainment of absolute orientation information regarding each body segment to which an orientation sensor is attached, it does not record the locations of individual body segments; thus, full-joint kinematic analysis is very difficult.

The best overall accuracy and resolution is provided by an optical motion analysis system using digital cameras. With these systems, however, blocking problems are common, making optical motion tracking especially problematic for use in an actual OR, where obstacles located between markers and motion cameras may hinder or obscure detection of reflective markers. Another limitation associated with this system is that "ghost markers," or interfering noises, occur as a result of reflections from the metallic surfaces of surgical instruments or devices.

Electromagnetic tracking systems, although not plagued by the blocking issue, are bedeviled by data collection interference that, particularly in the OR theater, occurs as a result of other sources in the same field generating electromagnetic fields or as a result of metallic objects.[84] Moreover, their measurement volume is not spacious. Both issues result in measurement accuracy being significantly decreased when a sensor is not within transmitter range.

Video analysis is the simplest of such systems.[45,62] Although it has been used in ergonomic studies for accuracy assessment of task completion and movement tracking of laparoscopic instruments, the outcomes obtained by such video analysis are considered very subjective and qualitative. Thus, this system should not be used in a stand-alone manner, but only in conjunction with a quantitative motion capture system so that the two sets of data can be time synchronized for accurate assessment of body or surgical instrument motion.[35,58,83,86]

Table 2. Applications in Surgical Ergonomics Using Kinematic Data from Motion Analysis Systems

Assessments
Physical workload and fatigue[31,54]
Effect of operating room components:
Display systems[32,33,59]
Instrument handle design[38,40,44,49]
Instrument, task and scope location/orientation[36,47,48]
Operating table height[29,31]
Skill, dexterity, efficiency[35,44,73-80,82,85,88]
Others[45,62]

Motion Data Analysis

Kinematic data, the measurement outcome of motion analysis systems, are helpful in addressing a variety of surgical ergonomic issues. Table 2 shows important implications of motion analysis data. Berguer, Smith, and colleague used motion analysis in addition to EMG for measurement of upper arm elevation level to calculate physical effort/workload.[31,54] The effects on performance and body movements of changing variable elements in a variety of OR components—including display, instruments, and operating table—have been investigated. Attempts to determine what constitutes an optimal laparoscopic display system have been marked by obtaining and analyzing data, predominantly objective but also subjective (eg, self-reports), on head rotation, instrument tracking, and task accuracy in relation to a considerable array of display types, heights, and locations.[32,33,59] One study defined optimal table height as necessary for surgeons to achieve optimal task performance with minimal shoulder discomfort and workload. It suggested that the optimal table height could be easily found by having the instrument handle as held in the surgeon's hand and the surgeon's elbow at the same level.[31] Another study found optimal operating surface height to be between a factor 0.7 or 0.8 of elbow height.[29] Several studies have investigated how laparoscopic instrument handles, believed to be a primary cause contributing to unsafe ergonomics, can be redesigned to improve surgical performance and ergonomics.[38,40,44,49]

Cuschieri and colleagues have characterized joint movement in maximum movement, minimum movement, and range of motion (ROM), in addition to angular velocity. They have used these kinematic measures in their investigations on the effects of instrument, endoscope, and surgical task location and orientation. In doing so they have found appropriate intracorporeal and extracorporeal length ratios and alternative endoscope angles and been able to postulate on what constitutes proper orientation of task targets.[36,47,48]

Motion analysis data has also been used to describe skill and dexterity levels. Joint kinematic analysis can characterize surgical movement patterns used by expert surgeons,[35,44,88] compare different surgical techniques,[75,78] and assist in defining learning curves.[85] Darzi and colleagues defined motion efficiency by studying what was required for the hand to accomplish its objectives, specifically in terms of number of movements, length of travel path, and measurements of performance time. Those studies resulted in motion efficiency being defined as the least number of hand movements employed, a definition that has also been said to characterize the best kinematics and to provide the best quantifying measurement of surgical dexterity.[74-77]

Motion analysis additionally has been used in robot-assisted surgery and robotic camera control to assess the efficiency of these technologies.[73,79,80,82] In other studies, assessment of motion analysis system data has been applied to accuracy of surgical outcomes and to instrument tracking.[45,62]

Discussion

New developments and improvements in hardware, software, and research variables will extend the application of motion analysis in surgical ergonomics. Advancements in computers, digital video equipment, and digital technology allow multiple camcorders to be synchronized during motion capture, making possible 3D motion analysis. Although these advanced systems are capable of providing kinematic analysis in addition to digital imaging, they have not yet been used in surgical ergonomic research. The accuracy of research will be greatly improved by technologies in magnetic field generation and sensor detection that are being developed and incorporated to overcome noise interference and signal attenuation.

As motion analysis becomes a more common methodology in surgical ergonomics research, the demand will be that such systems provide more sophisticated data that will allow more refined, comprehensive assessment of issues ranging from fatigue to joint control strategies. Currently, traditional research variables, such as ROM, which characterizes the absolute difference between two extremes and is widely used to explain joint movement range, are too limited

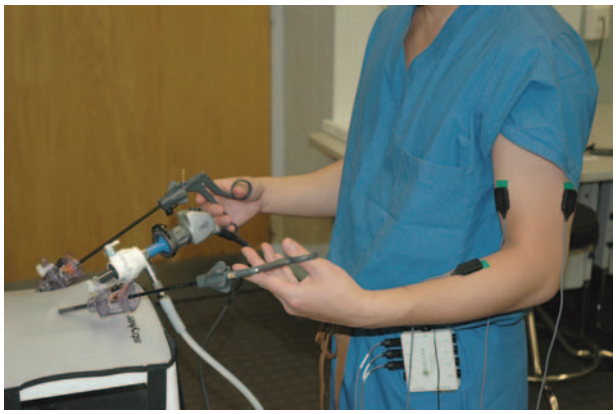

Figure 2. For EMG measurement, surface electrodes with built-in amplifiers are attached to target muscles.

to offer much information. One limitation of ROM, for instance, is that even a few extreme outliers may mislead and result in inaccurate interpretation.

Many kinematic variables used in surgical ergonomic studies, such as mean joint angle (MJA) or maximum angular velocity (MaxV), are calculated over a certain period of performance. Although these variables have been successfully used in surgical ergonomic analysis, the single values they provide cannot be used to explain details such as how or when joint angles change significantly or whether a specific pattern of joint movement exists. For more useful, comprehensive characterization of surgical joint movements, more research variables and analysis approaches will have to be developed to fill the gaps that traditional variables cannot explain. For example, Lee et al[88] used MJA and mean joint movement amplitude (MJMA), calculated from MJA and standard deviation, to study the joint movement range exhibited by very experienced and less experienced surgeons performing a pegboard transfer task. In another study, a pegboard transfer task was partitioned by subfunctions into several subtasks, and joint kinematics were investigated within those individual subtasks.[91]

As more sophisticated, comprehensive data sets emerge from motion analysis studies to give depth and definition to research, revisiting early surgical ergonomic study variables should become more commonplace. For example, motion efficiency has been defined by the number of hand movements used to complete a task. The relationship between motion efficiency and manual dexterity, however, is proving to be more complex than first thought (consider, for instance, that the instrument maneuverings by highly skilled surgeons might well strategically involve many hand movements) and certainly merits further consideration.

Electromyography

With laparoscopic procedures ever more prevalently used, MIS practitioners are reporting different patterns and types of fatigue and discomfort. The most common discomforts reported are located in the arms, neck, and upper back. EMG is one of the best objective tools for studying the mechanisms underlying the muscular discomfort or fatigue reported by laparoscopic surgeons, as EMG measures and evaluates the electrical activity of muscles in action and at rest. Ergonomists have long been acquainted with the many different ways EMG can be used to quantify physical workload and muscular discomfort.[92]

Technology

There are two types of electrodes used for EMG measurement: fine wire and surface. For evaluation with higher reliability of muscle fatigue and force, it has been proven that surface EMG is superior to fine-wire EMG.[93,94]

A fine-wire electrode made of thin and flexible metal is directly introduced into the target muscle to monitor the activation pattern of a single motor unit. Using a fine-wire electrode, it is possible to pick up an electrical signal without having attenuation caused by resistance of skin and tissues. The major limitations of the fine-wire electrode are its inability to measure the activity of a muscle as a whole and its invasive, often pain-causing nature.

Surface EMG is a simple, noninvasive way to evaluate the superficial muscles' activities (Figure 2). Though placement of the electrodes is relatively quick, painless, and sanitary, care must be taken to set them so as to minimize the effect of noise signals coming from more superficial or nearby muscles. Since skin and underlying tissues between the electrode and the target muscles serve as electrical resistance, the surface EMG provides only relative amplitude information, in contrast to the absolute values provided by fine-wire EMG. However, surface electrodes, owing to their considerable advantages, are dominant in surgical ergonomic studies for measurement of physical workload and upper body fatigue.

Electromyography Assessment Variables

EMG data provide fundamental information about amplitude (how much) and timing (when) of muscle activation. Analysis of EMG data allows characterization of the relationship between muscle activation and its outcomes (joint movement, force, or torque), as well as estimation of muscle fatigue level.

Currently, EMG data analysis is performed using one of two methods. The more basic measurement is a simple comparison of average or peak amplitudes of EMG signals over a certain period of time.[95] Such a basic comparison, although useful, cannot be used to compare activation amplitudes from different muscle groups used by an individual subject or the same muscle group used by a number of subjects. However, percentage of maximum voluntary contraction (%MVC) can be obtained by calculating the percentage ratio of measured EMG amplitude to a reference value, most commonly MVC. These normalized numbers can then be used for comparisons.

Frequency analysis is a third measurement used for muscle fatigue level assessment, a specific element of muscle activation. Muscle fatigue is perhaps the most significant ergonomic risk factor for surgeons, but use of amplitude and %MVC only indirectly infers its measurement.[96]

Electromyography Data Analysis

Amplitude analysis of EMG signals has been used in several studies in surgical ergonomics.[18,31,32,44,97] Berguer and colleagues compared EMG amplitudes to posit the optimal working angle for a laparoscopic instrument,[18] optimal ergonomic table height,[31] and proper monitor height.[32] Uchal et al[44] reported that no muscle activation differences occurred in a comparison of laparoscopic instrument handles, in-line vs pistol grip. Maithel et al[97] compared head-mounted and traditional video displays during simulated laparoscopic procedures and used EMG analysis to compare which display system caused more muscle fatigue.

Other studies used %MVC analysis.[19,21,28,29,41,98,99] Berguer and colleagues have shown that laparoscopic technique requires more physical effort than open surgical technique.[41,98] They also used the same analysis to compare different instrument grips.[19] Matern and colleagues have compared different monitor positions[99] and instrument handle designs.[21] Determination of optimal operating surface height has been another application.[29] Fatigue responses in several muscle groups have also been studied, with emphasis on effects of different monitor positions and levels of surgical experience.[28]

There are studies that have attempted to add other measurements to %MVC normalized EMG data. For example, Quick et al[27] have defined relative time of activation (RAT) as the percentage of time duration at which %MVC of each muscle group is 10% or higher. RATs were then calculated from individual muscle groups during different tasks, which proved useful to explain each muscle's activation timing during a specific task and to provide information for assessing muscle specific overuse. Jonsson has introduced the concept of amplitude probability distribution function (APDF) to evaluate the distribution of muscle contractions over a period of time. This approach identifies the percentage of time that muscle activity is below a preset proportion of MVC.[100,101] Jonsson also proposed the 10th percentile data that is commonly known as the static load level and has been used in surgical ergonomics to serve as a threshold in defining continuous work and minimal risk muscular load.[28]

Additionally, total physical workload as an assessment of fatigue has been obtained by calculating the time integral (that is, the area under the signal) of EMG over a specified period.[98] This approach, however, is appropriate only when each individual task is given a set time frame; it is not appropriate for evaluation of tasks unconstrained by time.

Discussion

Currently, the majority of EMG studies in surgical ergonomics investigate muscular workload during laparoscopic tasks through analysis of signal amplitude or %MVC. As muscular fatigue is a crucial variable in ergonomic risk analysis, it requires a more specific, accurate measurement tool. Frequency analysis, commonly considered the gold standard for studying muscular fatigue in biomechanic and neuroscience research,[102,103] has currently been used in only a few surgical ergonomic studies.[49,104] Frequency analysis should be used more intensively in our field.

Additionally, since the factor of muscle fatigue is so important, research tools must be developed that are capable of providing more detailed information in regard to issues that include: identification of muscular fatigue initiation, quantification of fatigue progress, and assessment of potential ergonomic risks of extreme fatigue. Also crucial is the need to

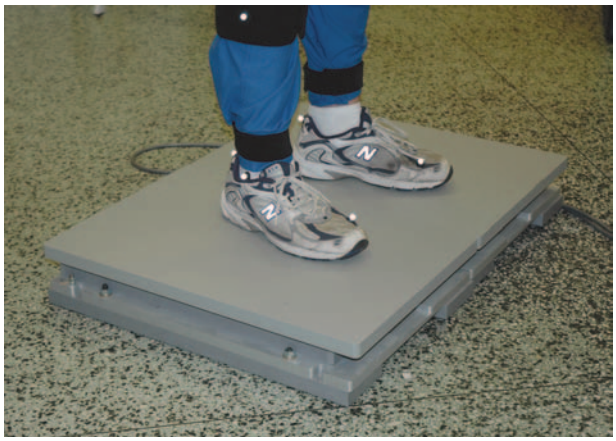

Figure 3. A surgeon performs a task with each foot on a single force plate. Data collected from each force plate is used for postural analysis.

determine risk levels within different muscle groups. This determination would be accomplished by establishing and considering those anatomical and geometric differences, such as type, size, length, strength, and frequency of use, that exist between and among muscles. If such detailed data could be generated and studied, ergonomics research could determine quantification and normalization through intermuscle comparisons, thereby acquiring vital knowledge about the vulnerability of individual muscles.

Force Plate Systems

Force plate—also called force platform—systems are a staple for scientific measurement of body posture within many motion analysis laboratories, yet they have seen limited use in surgical ergonomics (Figure 3).

Because the geometry of the human body consists of bigger and heavier masses at the upper body with supports at the lower body, posture during standing often has been portrayed as an inverted pendulum.[105] This is because even though quiet standing appears to be static, such posture actually relies on dynamics. The CoM is located at a short distance in front of the ankle joint, and therefore gravity alone can cause the body to topple forward. Our bodies are effectively engineered to keep us from falling face forward by two calf muscles—the soleus and the gastrocnemius—that actively compensate for gravity's effect and allow us to maintain proper static posture.[106]

Single or multiple force plate systems have been used to investigate both sway and balance control during quiet standing,[107,108] perturbed standing,[109] and functional standing or walking.[110,111]

Technology

A force plate provides valuable information about ground reaction force (GRF), which is equal in intensity and opposite in direction to that force exerted by the foot of the weight-bearing limb. The force plate usually has a rigid top plate made of a large piece of metal or glass. Force sensors at each of its 4 supporting corners produce an electric output proportional to the force applied to the upper surface and the contact point location.

Force sensors are either piezoelectric or strain gauge. Piezoelectric systems use quartz transducers to produce electricity that is proportional to the level of pressing. These systems require special cabling and charge amplifiers and generally have greater sensitivity and force measurement range than strain-gauge systems. However, piezoelectric systems may not be used for studies that involve prolonged standing, since the electrical charge attenuates over time. A strain-gauge system needs no special cables or amplifiers, and its electric signal does not decrease over time.

Use of a force platform makes obtainable the 3 components (vertical, lateral, and fore-aft) of force, the two coordinates of the center of pressure (CoP), and the rotational forces (moments) about the x, y, and z axis. The location of the CoP on a 2D surface has been widely used in postural analysis.

Force Plate Data

The importance of good posture for surgeons, as well as for other medical staff, is well documented.[112,113] Upper body postures, including head, arm, and trunk movements, have been analyzed in several studies[31-33,56,59,72,84] in attempts to define what constitutes optimal surgical posture, yet few studies in surgical ergonomics have used balancing information available from force plate systems alone.

Berguer et al[114] used force plate data to compare surgeons' postures during laparoscopic and open surgical procedures. Using a single force plate system and analyzing the locations and ROM of CoP in two directions (anterior-posterior and medial-lateral), the study concluded that during laparoscopic procedures, surgical posture was less dynamic, as was shown by significantly reduced ROM of CoP. Using primarily FLS tasks, Park and colleagues have studied changes in surgeons' postures during task performance.[72,87,89,115]

In the first study, they found that when CoP excursions were defined by outer boundaries, a significant increase in movements could be correlated to task difficulty.[87] Another study analyzed the postural control strategies used by surgeons of differing experience levels in the performance of 3 different FLS tasks. The more experienced surgeons used unique postural controls during each task, and their strategies differed from those used by less experienced surgeons.[89] To demonstrate that postural instability does not necessarily correlate to poor performance, another study used CoM as a measurement. A much-experienced surgeon with a wrist complication made compensatory arm movements to minimize wrist flexion and exhibited strategic movements that, although they appeared to signal postural instability, actually proved necessary to achieve successful task performance.[72] For a more systematic assessment, Lee and Park used principal component analysis (PCA) for construction of an ellipse that covered 95% of CoP excursions to characterize sway areas, directions, and shape.[115] In that same study, a new variable was termed and defined: postural stability demand (PSD), a calculation of the absolute distance between CoP and CoM. Through this rarely used measurement, it was discovered that during performance of each of 3 FLS tasks, less experienced surgeons exhibited high PSD, which implied higher postural instability.

Discussion

Maintaining good posture is absolutely necessary for top surgical performance. The balancing activity measured by force plate systems should be regarded as a necessity for postural analysis undertaken in surgical ergonomics.

Alone, the data obtained from force plates are useful. Ultimately, however, such data, if combined with motion analysis data, will allow calculations by which more detailed mechanical assessments may be acquired. Then, by applying biomechanical models (mathematical and/or analytical algorithms) to that more robust description, crucial information regarding the underlying etiology of the extreme muscular fatigue and physical complications often experienced by laparoscopic surgeons may be investigated.

Conclusions

We have intensively reviewed what we have identified as the primary research components—that is tasks, models, and measurement systems—that form the essential methodology of MIS ergonomics as this discipline moves through its initial maturation stages. In doing so, we have addressed elements including, but not limited to, background, technologies, applications, drawbacks, and advantages. In closing, we discuss limitations and possibilities we see inherent in these primary research components and proffer suggestions that if put into practice we believe will only augment the credible and useful findings already comprising surgical ergonomic research.

The quality and quantity of data collected are significantly dependent on tasks, models, and assessment systems. The research that has governed surgical ergonomics thus far has primarily addressed specifics through attempts to seek and obtain solutions that might be quickly applied to minimize the immediate effects of immediate problems. Current data collection, although useful, is limited in terms of what it can contribute to the formation of standard matrices.

For true effectiveness and validity, surgical ergonomic studies must expand in the near future to include more investigation and compilation of physical behavior characteristically engaged in by expert surgeons, including joint movement and postural control. Such research will promote extrapolation and description of characteristic patterns. Knowledge of such patterns is integral to the formation of standard matrices and will help to define what constitutes efficient, effective, and ergonomically safe physical behavior. Additionally, the creation and application of more objective training protocols promise to be important outcomes served by the development of such matrices.

Typically in a discipline's infancy, its studies address simple problems through simple constructs. For instance, it now appears that the range of acceptable movements or strategies employed by surgeons during task and procedure performance is far larger and more complex than envisioned in the early days of surgical ergonomic research. For specific illustration, early studies seemed to adequately explain that the fewer movements one used to complete a task (or the smaller the amount of overall motion involved in task execution) was indicative of what constitutes surgical maneuvering at its most effective and most efficient.

As our field becomes more established and sophisticated, however, it becomes more difficult to accept traditional concepts such as less or fewer are best. Discipline maturation requires that explanations

that gave meaning as research was conducted initially be subjected to scrutiny. Thus, the sanction accorded the concept of less or fewer movements is necessarily challenged by newer surgical ergonomic research that details the unique patterns of movements (sometimes many and sometimes few) creditable to each surgeon trying to successfully and competently achieve surgical goals while maintaining personal body comfort and stability.

Extended physical issues could well produce long-term effects resulting in surgeons abandoning what has long constituted their normal movement and replacing that with alternative compensatory movements in an effort to restore the originally enjoyed level of surgical movement. No matter how well-intentioned such compensatory movements might be, they may unintentionally cause secondary problems.

Secondary muscle strategies, for instance, employed as a result of compensatory movements, constitute unique patterns whose explorations should be undertaken in future surgical ergonomic studies. As a specific example, we offer that one muscle group experiencing extended fatigue might be expected to give over to another muscle group. The secondary group of muscles, taking over for the primary group, is not likely to have been trained, a situation that could well incur loss of performance accuracy.

Surgical ergonomics research is now addressing issues and seeking solutions that will result in levels of data acquisition that are still rare. Though our review indicates a paucity of data acquired within the OR, indications are that the challenges of safely and unobtrusively conducting ergonomic research in that environment will increasingly be undertaken. As VR models become more realistic and comprehensive, simulation in the laboratory environment will yield more sophisticated information. A broadening and deepening of the laparoscopic tasks studied (current research is too dependent on suturing) should also occur.

Measurements as well as assessment systems, often used across disciplines and in multiple combinations, but now only marginally considered within our discipline (as we have indicated has been the case with force plate/force platform systems), will with more prevalent use permit us to gather more detailed, robust data. And there is no doubt that the future surely holds in store for us the formation of large, cross-disciplinary databases in which the growing amount of surgical ergonomic research will be stored and referenced.

The ideal result of these efforts would be comprehensive characterization of surgical movement in relation to task or procedure. This result would then allow exact movements (with, presumably, their associated excellent clinical outcomes) to be patterned and then to be incorporated into the teaching of novice surgeons. Furthermore, and perhaps more urgently, such knowledge would facilitate better design not only of surgical instruments but also of the surgical workspace, which would lessen or eliminate the ergonomic ravages of MIS currently associated with laparoscopic surgical performance.

References

1. Franco G, Fusetti L. Bernadino Ramazzini's early observations of the link between musculoskeletal disorders and ergonomic factors. *Appl Ergon*. 2004;35:67-70.
2. Scheer SJ, Mital A. Ergonomics. *Arch Phys Med Rehabil*. 1997;78(Suppl 3):S36-S45.
3. Wilson JR. Fundamentals of ergonomic in theory and practice. *Appl Ergon*. 2000;31:557-567.
4. Craik K. Theory of the human operator in control systems. *Br J Psychol*. 1947;38:56-61.
5. Nigg BM, Stefanyshyn D, Cole G, Stergiou P, Miller J. The effect of material characteristics of shoe soles on muscle activation and energy aspects during running. *J Biomech*. 2003;36:569-575.
6. Seagull FJ, Ward R, Mills J, Goodrich C, Xiao Y. Measuring awkwardness of workplace layout: dispersion of attentional and psychomotor resources within the anesthesia workspace. *Proceedings of the Human Factors and Ergonomics Society 48th Annual Meeting*. 2004;48:1755-1758.
7. Tittiranonda P, Rempel D, Armstrong T, Burastero S. Effect of four computer keyboards in computer users with upper extremity musculoskeletal disorders. *Am J Ind Med*. 1999;35:647-661.
8. Andreoni G, Santambrogio GC, Rabuffetti M, Pedotti A. Method for the analysis of posture and interface pressure of car drivers. *Appl Ergon*. 2002;33:511-522.
9. Reyes DAG, Tang B, Cuschieri A. Minimal access surgery (MAS)-related surgeon morbidity syndromes. *Surg Endosc*. 2006;20:1-13.
10. Goossens RHM, van Veelen MA. Assessment of ergonomics in laparoscopic surgery. *Minim Invasive Ther Allied Technol*. 2001;10:175-179.
11. Berguer R. Surgery and ergonomics. *Arch Surg*. 1999; 134:1011-1016.
12. Xin H, Zelek JS, Carnahan H. Laparoscopic surgery, perceptual limitations and force: a review. On-line proceedings of the first Canadian student conference on biomedical computing. Available at: http://cscbc2006.cs.queensu.ca/assets/documents/Papers/paper144.pdf. Accessed May 30, 2007.

13. Derossis AM, Fried GM, Abrahamowicz M, Sigman HH, Barkun JS, Meakins JL. Development of a model for training and evaluation of laparoscopic skills. *Am J Surg*. 1998;175:482-487.
14. Derossis AM, Antoniuk M, Fried GM. Evaluation of laparoscopic skills: a 2-year follow-up during residency training. *Can J Surg*. 1999;42:293-296.
15. Feldman LS, Hagarty SE, Ghitulescu G, Stanbridge D, Fried GM. Relationship between objective assessment of technical skills and subjective in-training evaluations in surgical residents. *J Am Coll Surg*. 2004;198:105-110.
16. Peters JH, Fried GM, Swanstrom LL, et al; SAGES FLS Committee. Development and validation of a comprehensive program of education and assessment of the basic fundamentals of laparoscopic surgery. *Surgery*. 2004;135:21-27.
17. Korndorffer JR Jr, Dunne JB, Sierra R, Stefanidis D, Touchard CL, Scott DJ. Simulator training for laparoscopic suturing using performance goals translates to the operating room. *J Am Coll Surg*. 2005;201:23-29.
18. Berguer R, Forkey DL, Smith WD. The effect of laparoscopic instrument working angle on surgeons' upper extremity workload. *Surg Endosc*. 2001;15:1027-1029.
19. Berguer R, Gerber S, Kilpatrick G, Remler M, Beckley D. A comparison of forearm and thumb muscle electromyographic responses to the use of laparoscopic instruments with either a finger grasp or palm grasp. *Ergonomics*. 1999;42:1634-1645.
20. Matern U, Giebmeyer C, Bergmann R, Waller P, Faist M. Ergonomic aspects of four different types of laparoscopic instrument handles with respect to elbow angle. *Surg Endosc*. 2002;16:1528-1532.
21. Matern U, Kuttler G, Giebmeyer C, Waller P, Faist M. Ergonomic aspects of five different types of laparoscopic instrument handles under dynamic conditions with respect to specific laparoscopic tasks: an electromyographic-based study. *Surg Endosc*. 2004;18:1231-1241.
22. Ahmed S, Hanna GB, Cuschieri A. Optimal angle between instrument shaft and handle for laparoscopic bowel suturing. *Arch Surg*. 2004;139:89-92.
23. Mishra RK, Hanna GB, Brown SI, Cuschieri A. Optimum shadow-casting illumination for endoscopic task performance. *Arch Surg*. 2004;139:889-892.
24. Hanna GB, Cuschieri A. Influence of the optical axis-to-target view angle on endoscopic task performance. *Surg Endosc*. 1999;13:371-375.
25. Hanna GB, Drew T, Clinch P, et al. A microprocessor-controlled psychomotor tester for minimal access surgery. *Surg Endosc*. 1996;10:965-969.
26. Hanna GB, Drew T, Clinch P, Hunter B, Cuschieri A. Computer-controlled endoscopic performance assessment system. *Surg Endosc*. 1998;12:997-1000.
27. Quick NE, Gillette JC, Shapiro R, Adrales GL, Gerlach D, Park AE. The effect of using laparoscopic instruments on muscle activation patterns during minimally invasive surgical training procedures. *Surg Endosc*. 2003;17:462-465.
28. Uhrich ML, Underwood RA, Standeven JW, Soper NJ, Engsberg JR. Assessment of fatigue, monitor placement, and surgical experience during simulated laparoscopic surgery. *Surg Endosc*. 2002;16:635-639.
29. van Veelen MA, Kazemier G, Koopman J, Goossens RHM, Meijer DW. Assessment of the ergonomically optimal operating surface height for laparoscopic surgery. *J Laparoendosc Adv Surg Tech*. 2002;12:47-52.
30. Matern U, Eichenlaub M, Waller P, Rückauer KD. MIS instruments: an experimental comparison of various ergonomic handles and their design. *Surg Endosc*. 1999;13:756-762.
31. Berguer R, Smith WD, Davis S. An ergonomic study of the optimum operating table height for laparoscopic surgery. *Surg Endosc*. 2002;16:416-421.
32. Smith WD, Berguer R, Nguyen NT. Monitor height affects surgeons' stress level and performance on minimally invasive surgery tasks. *Stud Health Technol Inform*. 2005;498-501.
33. Huber JW, Taffinder N, Russell RCG, Darzi A. The effects of different viewing conditions on performance in simulated minimal access surgery. *Ergonomics*. 2003;46:999-1016.
34. Crosthwaite G, Chung T, Dunkley P, Shimi S, Cuschieri A. Comparison of direct vision and electronic two- and three-dimensional display systems on surgical task efficiency in endoscopic surgery. *Br J Surg*. 1995;82:849-851.
35. Emam TA, Hanna GB, Kimber C, Cuschieri A. Difference between experts and trainees in the motion pattern of the dominant upper limb during intracorporeal endoscopic knotting. *Dig Surg*. 2000;17:120-125.
36. Emam TA, Hanna GB, Kimber C, Dunkley P, Cuschieri A. Effect of intracorporeal-extracorporeal instrument length ratio on endoscopic task performance and surgeon movements. *Arch Surg*. 2000;135:62-65.
37. Patil PV, Hanna GB, Frank TG, Cuschieri A. Effect of fixation of shoulder and elbow joint movement on the precision of laparoscopic instrument manipulations. *Surg Endosc*. 2005;19:366-368.
38. Emam TA, Frank TG, Hanna GB, Stockham G, Cuschieri A. Rocker handle for endoscopic needle drivers. *Surg Endosc*. 1999;13:658-661.
39. Hanna GB, Shimi SM, Cuschieri A. Task performance in endoscopic surgery is influenced by location of the image display. *Ann Surg*. 1998;227:481-484.
40. van Veelen MA, Meijer DW, Uijttewaal I, Goossens RHM, Snijder CJ, Kazemier G. Improvement of the laparoscopic needle holder based on new ergonomic guidelines. *Surg Endosc*. 2003;17:699-703.
41. Berguer R, Chen J, Smith WD. A comparison of the physical effort required for laparoscopic and open surgical techniques. *Arch Surg*. 2003;138:967-970.

42. Berguer R, Smith WD, Chung YH. Performing laparoscopic surgery is significantly more stressful for the surgeon than open surgery. *Surg Endosc*. 2001;15:1204-1207.
43. Moorthy K, Munz Y, Undre S, Darzi A. Objective evaluation of the effect of noise on the performance of a complex laparoscopic task. *Surgery*. 2004;136:25-30.
44. Uchal M, Brogger J, Rukas R, Karlsen B, Bergamaschi R. In-line vs pistol-grip handles in a laparoscopic simulator: a randomized controlled crossover trial. *Surg Endosc*. 2002;16:1771-1773.
45. Joice P, Hanna GB, Cuschieri A. Ergonomic evaluation of laparoscopic bowel suturing. *Am J Surg*. 1998;176: 373-378.
46. Brown SI, Frank TG, Shallaly E, Cuschieri A. Comparison of conventional and gaze-down imaging in laparoscopic task performance. *Surg Endosc*. 2003;17:586-590.
47. Emam TA, Hanna G, Cuschieri A. Comparison of orthodox vs off-optical axis endoscopic manipulations. *Surg Endosc*. 2002;16:401-405.
48. Emam TA, Hanna G, Cuschieri A. Ergonomic principles of task alignment, visual display, and direction of execution of laparoscopic bowel suturing. *Surg Endosc*. 2002; 16:267-271.
49. Emam TA, Frank TG, Hanna GB, Cuschieri A. Influence of handle design on the surgeon's upper limb movements, muscle recruitment, and fatigue during endoscopic suturing. *Surg Endosc*. 2001;15:667-672.
50. Ahmed S, Hanna GB, Cuschieri A. Optimal angle between instrument shaft and handle for laparoscopic bowel suturing. *Arch Surg*. 2004;139:89-92.
51. Hanna GB, Frank TG, Cuschieri A. Objective assessment of endoscopic knot quality. *Am J Surg*. 1997;174: 410-412.
52. Galleano R, Carter F, Brown S, Frank T, Cuschieri A. Can armrests improve comfort and task performance in laparoscopic surgery? *Ann Surg*. 2006;243:329-333.
53. Goodell KH, Cao CGL, Schwaitzberg SD. Effects of cognitive distraction on performance of laparoscopic surgical tasks. *J Laparoendosc Adv Surg Tech*. 2000; 16:94-98.
54. Smith WD, Berguer R. A simple virtual instrument to monitor surgeons' workload while they perform minimally invasive surgery tasks. *Stud Health Technol Inform*. 2004;363-369.
55. Matern U, Koneczny S, Tedeus M, Dietz K, Buess G. Ergonomic testing of two different types of handles via virtual reality simulation. *Surg Endosc*. 2005;19:1147-1150.
56. Person JG, Hodgson AJ, Nagy AG. Automated high-frequency posture sampling for ergonomic assessment of laparoscopic surgery. *Surg Endosc*. 2001;15:997-1003.
57. Rasmus M, Riener R, Reiter S, Schneider A, Feussner H. In vivo kinematic measurement during laparoscopic cholecystectomy. *Surg Endosc*. 2004;18:1649-1656.
58. Dosis A, Aggarwal R, Bello F, et al. Synchronized video and motion analysis for the assessment of procedures in the operating theater. *Arch Surg*. 2005;140:293-299.
59. van Veelen MA, Jakimowicz JJ, Goossens RHM, Meijer DW, Bussmann JBJ. Evaluation of the usability of two types of image display systems during laparoscopy. *Surg Endosc*. 2002;16:674-678.
60. Tang B, Hanna GB, Joice P, Cuschieri A. Identification and categorization of technical errors by observational clinical human reliability assessment (OCHRA) during laparoscopic cholecystectomy. *Arch Surg*. 2004;139: 1215-1220.
61. Geryane MH, Hanna GB, Cuschieri A. Time-motion analysis of operation theater time use during laparoscopic cholecystectomy by surgical specialist residents. *Surg Endosc*. 2004;18:1597-1600.
62. Joice P, Hanna GB, Cuschieri A. Errors enacted during endoscopic surgery—a human reliability analysis. *Appl Ergon*. 1998;29:409-414.
63. Lee G, Pollo FE. Technology overview: the gait analysis laboratory. *J Clin Eng*. 2001;26:129-135.
64. Giannini S, Catani F, Benedetti MG, Leardini A. *Gait Analysis: Methodologies and Clinical Applications.* Amsterdam, Netherlands: IOS Press; 1994.
65. Simon GSC, Andrew JR. A three-dimensional examination of the planar nature of the golf swing. *J Sports Sci*. 2005; 23:227-234.
66. Prassas S, Kwon YH, Sands WA. Biomechanical research in artistic gymnastics: a review. *Sports Biomech*. 2006; 5:261-291.
67. Kerrigan DC, Lelas JL, Goggins J, Merriman GJ, Kaplan RJ, Felson DT. Effectiveness of a lateral-wedge insole on knee varus torque in patients with knee osteoarthritis. *Arch Phys Med Rehabil*. 2002;82:889-893.
68. Siegler S, Liu W. Inverse dynamics in human locomotion. In: Allard P, Cappozzo A, Lundberg A, Vaughan CL, eds. *Three-Dimensional Analysis of Human Locomotion*. New York, NY: John Wiley & Sons; 1997.
69. Lee G, Fradet L, Ketcham CJ, Dounskaia N. Efficient control of arm movements in advanced age. *Exp Br Res*. 2006;177;78-94.
70. Menache A. *Understanding Motion Capture for Computer Animation and Video Games.* San Francisco, CA: Morgan Kaufmann Publishers; 1999.
71. Katherine P, Christoph B. Motion capture assisted animation: texturing and synthesis. Computer Graphics. Proceedings of the 29th Annual Conference on Computer Graphics and Interactive Techniques, San Antonio, TX, 23-26 July 2002. New York, NY: ACM Press; 2002.
72. Lee G, Kavic SM, George IM, Park AE. Postural instability does not necessarily correlate to poor performance: case in point. *Surg Endosc*. 2006;21:471-474.
73. Kondraske GV, Hamilton EC, Scott DJ, et al. Surgeon workload and motion efficiency with robot and human laparoscopic camera control. *Surg Endosc*. 2002;16: 1523-1527.
74. Datta V, Chang A, Mackay S, Darzi A. The relationship between motion analysis and surgical technical assessment. *Am J Surg*. 2002;184:70-73.

75. Ridgway PF, Ziprin P, Datta VK, et al. Laboratory-based validation of a novel suture technique for wound closure. *Ann Plast Surg*. 2002;49:291-296.
76. Mackay S, Datta V, Mandalia M, Bassett P, Darzi A. Electromagnetic motion analysis in the assessment of surgical skill: relationship between time and movement. *ANZ J Surg*. 2002;72:632-634.
77. Bann SD, Khan MS, Darzi A. Measurement of surgical dexterity using motion analysis of simple bench tasks. *World J Surg*. 2003;27:390-394.
78. Khan MS, Bann SD, Darzi A, Butler PEM. Use of suturing as a measure of technical competence. *Ann Plast Surg*. 2003;50:304-309.
79. Moorthy K, Munz Y, Dosis A, et al. Dexterity enhancement with robotic surgery. *Surg Endosc*. 2004;18:790-795.
80. Hernandez JD, Bann SD, Munz Y, et al. Qualitative and quantitative analysis of the learning curve of a simulated surgical task on the da Vinci system. *Surg Endosc*. 2004; 18:372-378.
81. Moorthy K, Munz Y, Undre S, Darzi A. Objective evaluation of the effect of noise on the performance of a complex laparoscopic task. *Surgery*. 2004;136:25-30.
82. Munz Y, Moothy K, Dosis A, et al. The benefits of stereoscopic vision in robotic-assisted performance on bench models. *Surg Endosc*. 2004;18:611-616.
83. Dosis A, Bello F, Moorthy K, Munz Y, Gillies D, Darzi A. Real-time synchronization of kinematic and video data for the comprehensive assessment of surgical skills. *Stud Health Technol Inform*. 2004:82-88.
84. Aggarwal R, Dosis A, Bello F, Darzi A. Motion tracking systems for assessment of surgical skill [letter to editor]. *Surg Endosc*. 2007;21:339.
85. Smith SGT, Torkington J, Brown TJ, Taffinder NJ, Darzi A. Motion analysis. *Surg Endosc*. 2002;16:640-645.
86. Patil PV, Hanna GB, Cuschieri A. Effect of the angle between the optical axis of the endoscope and the instruments' plane on monitor image and surgical performance. *Surg Endosc*. 2004;18:111-114.
87. Gillette JC, Quick NE, Adrales GL, Shapiro R, Park AE. Changes in posture mechanics associated with different types of minimally invasive surgical training exercises. *Surg Endosc*. 2003;17:259-263.
88. Lee G, Weiner M, Kavic SM, George IM, Park AE. Joint kinematics vary with performance skills during laparoscopic exercise [fundamentals of laparoscopic surgery (FLS) task 1]. *Gastroenterology*. 2006;130(Suppl 2):A911.
89. Lee G, Weiner M, Kavic SM, George IM, Park AE. Pilot study—correlation between postural stability and performance time during fundamentals of laparoscopic surgery (FLS) tasks. *Br J Surg*. 2006;93(Suppl 1):206.
90. Matern U, Kuttler G, Giebmeyer C, Waller P, Faist M. Ergonomic aspects of five different types of laparoscopic instrument handles under dynamic conditions with respect to specific laparoscopic tasks: an electromyographic-based study. *Surg Endosc*. 2004;18;1231-1241.
91. Lee G, Dexter DJ, Lee TH, Park AE. Subtask analysis of joint angles is key to characterizing surgical movement. *Gastroenterology*. 2007;132(Suppl 1):A894.
92. Koneczny S, Matern U. Instruments for the evaluation of ergonomics in surgery. *Min Invas Ther & Allied Technol*. 2004;13:167-177.
93. Gopher D, Donchin E. Workload—an examination of the concept. In: Boff KR, Kaufman L, Thomas J, eds. *The Handbook of Perception and Human Performance, Vol 2: Cognitive Processes and Performance*. New York, NY: Wiley; 1986.
94. Lofland KR, Mumby PB, Cassisi JE, Palumbo NL, Camic PM. Assessment of lumbar EMG during static and dynamic activity in pain-free normals: implications for muscle scanning protocols. *Biofeedback Self Regul*. 1995;20:3-18.
95. Hagg G, Luttmann A, Jager M. Methodologies for evaluating electromyographic field data in ergonomics. *J Electromyogr Kinesiol*. 2000;10:301-312.
96. Newton RU, Murphy AJ, Humphries BJ, Wilson GJ, Kraemer WJ, Hakkinen K. Influence of load and stretch shortening cycle on the kinematics, kinetics and muscle activation that occurs during explosive upper-body movements. *Eur J Appl Physiol*. 1997;75:333-342.
97. Maithel SK, Villegas L, Stylopoulos N, Dawson S, Jones DB. Simulated laparoscopy using a head-mounted display vs traditional video monitor: an assessment of performance and muscle fatigue. *Surg Endosc*. 2005;19: 406-411.
98. Berguer R, Forkey DL, Smith WD. Ergonomic problems associated with laparoscopic surgery. *Surg Endosc*. 1999;13:466-468.
99. Matern U, Faist M, Kehl K, Giebmeyer C, Buess G. Monitor position in laparoscopic surgery. *Surg Endosc*. 2005;19:436-440.
100. Ankrum DR. On the confusion between static load level and static task. *Appl Ergon*. 2000;31:545-546.
101. Jonsson B. Quantitative electromyographic evaluation of muscular load during work. *Scand J Rehabil Med Suppl*. 1978;6:69-74.
102. Lyons MF, Rouse ME, Baxendale RH. Fatigue and EMG changes in the masseter and temporalis muscles during sustained contractions. *J Oral Rehabil*. 1993; 20:321-331.
103. Kupa EJ, Roy SH, Kandarian SC, De Luca CJ. Effects of muscle fiber type and size on EMG median frequency and conduction velocity. *J Appl Physiol*. 1995;79: 23-32.
104. Judkins TN, Oleynikov D, Narazaki K, Stergiou N. Robotic surgery and training: electromyographic correlates of robotic laparoscopic training. *Surg Endosc*. 2006;20:824-829.
105. Gage WH, Winter DA, Frank JS, Adkin AL. Kinematic and kinetic validity of the inverted pendulum model in quiet standing. *Gait Posture*. 2004;19:124-132.

106. Loram ID, Maganaris CN, Lakie M. Paradoxical muscle movement in human standing. *J Physiol*. 2004;556.3: 683-689.
107. Masani K, Popovic MR, Nakazawa K, Kouzaki M, Nozaki D. Importance of body sway velocity information in controlling ankle extensor activities during quiet stance. *J Neurophysiol*. 2003;90:3774-3782.
108. Winter DA, Patla AE, Prince F, Ishac M, Gielo-Perczak K. Stiffness control of balance in quiet standing. *J Neurophysiol*. 1998;80:1211-1221.
109. Rietdyk S, Patla AE, Winter DA, Ishac MG, Little CE. Balance recovery from medio-lateral perturbations of the upper body during standing. *J Biomech*. 1999;32: 1149-1158.
110. Halliday SE, Winter DA, Frank JS, Patla AE, Prince F. The initiation of gait in young, elderly, and Parkinson's disease subjects. *Gait Posture*. 1998;8:8-14.
111. Karst GM, Venema DM, Roehr TG, Tyler AE. Center of pressure measures during standing tasks in minimally impaired persons with multiple sclerosis. *J Neurol Phys Ther*. 2005;29:170-180.
112. Kant IJ, de Jong LC, van Rijssen-Moll M, Borm PJ. A survey of static and dynamic work postures of operating room staff. *Int Arch Occup Environ Health*. 1992;63:423-428.
113. van Veelen MA, Nederlof EAL, Goossens RHM, Schot CJ, Jakimowicz JJ. Ergonomic problems encountered by the medical team related to products used for minimally invasive surgery. *Surg Endosc*. 2003;17:1077-1081.
114. Berguer R, Rab GT, Abu-Ghaida H, Alarcon A, Chung J. A comparison of surgeons' posture during laparoscopic and open surgical procedures. *Surg Endosc*. 1997;11:139-142.
115. Lee G, Park AE. Development of a novel tool to more precisely analyze postural stability of laparoscopic surgeons. *Surg Endosc*. 2007;21(Suppl 1):S317.

Surg Endosc
DOI 10.1007/s00464-008-0141-4

Ergonomic risk associated with assisting in minimally invasive surgery

Gyusung Lee · Tommy Lee · David Dexter · Carlos Godinez · Nora Meenaghan · Robert Catania · Adrian Park

Received: 10 April 2008 / Accepted: 13 August 2008

Abstract
Background Given the physical risks associated with performing laparoscopic surgery, ergonomics to date has focused on the primary minimally invasive surgeon. Similar studies have not extended to other operating room staff. Simulation of the assistant's role as camera holder and retractor during a Nissen fundoplication allowed investigation of the ergonomic risks involved in these tasks.
Methods Seven subjects performed camera navigation and retraction tasks using a box trainer on an operating room table that simulated an adult patient in low lithotomy position. Each subject stood on force plates at the simulated patient's left side. A laparoscope was introduced through a port into the training box with four 2-cm circles as rear-panel targets located in relation to the assistant as distal superior, proximal superior, distal inferior, and proximal inferior target effects. The subjects held the camera with their left hand, pointing it at a target. The task was to match the target to a circle overlaid on the monitor. Simultaneously, a grasper in the right hand grasped and pulled a panel-attached band. A minute signal moved the subject to the next target. Each trial had three four-target repetitions (phase effect). The subjects performed two separate trials: one while holding the camera from the top and one while holding it from the bottom (grip effect). A $4 \times 3 \times 2$ (target × phase × grip) repeated-measures design provided statistics. Dividing the left force-plate vertical ground reaction forces (VGRF) by the total VGRF from both plates provided a weight-loading ratio (WLR).
Results The WLR significantly increased ($p < 0.005$) with proximal targets (2 by 80% and 4 by 79%). The WLR decreased 75%, 74%, and 71% over time. No difference existed between the grip strategies (grip effect, $p > 0.5$).
Conclusions A high-risk ergonomic situation is created by the assistant's left or caudal leg disproportionately bearing 70–80% of body weight over time. A distance increase between the camera head location and the camera holder increases ergonomic risk. The phase effect was interpreted as a compensatory rebalancing to reduce ergonomic risk. Ergonomic solutions minimizing ergonomic risks associated with laparoscopic assistance should be considered.

Keywords Camera assistant · Ergonomics · Force plate · Laparoscopic assistance · Postural analysis · Simulation

G. Lee · T. Lee · D. Dexter · C. Godinez · N. Meenaghan · R. Catania · A. Park (✉)
Division of General Surgery, Department of Surgery, School of Medicine, University of Maryland, 22 South Greene Street, Room S4B14, Baltimore, MD 21201, USA
e-mail: apark@smail.umaryland.edu

G. Lee
e-mail: glee@smail.umaryland.edu

T. Lee
e-mail: tlee@smail.umaryland.edu

D. Dexter
e-mail: ddexter@smail.umaryland.edu

C. Godinez
e-mail: cgodinez@smail.umaryland.edu

N. Meenaghan
e-mail: nmeenaghan@smail.umaryland.edu

R. Catania
e-mail: rcatania@smail.umaryland.edu

It is well known that maintaining correct posture is a very important ergonomic factor in minimizing physical risks associated with the performance of complex tasks [1–3].

Awkward working posture can cause increased stress for certain body parts, resulting in fatigue, musculoskeletal disorders, and nerve problems [4].

To maintain proper balance, the human body requires continuous active control. Because two-thirds of body mass ordinarily is in the top two-thirds of a person's height above ground level, the body has been described as an unstable balance system, and the standing posture often is referred to as an inverted pendulum [5]. For this reason, posture during quiet standing actually relies on dynamic control although the posture may appear to be static [6].

Many everyday tasks consist primarily of static posture while the upper body performs more dynamic motions (e.g. cashiers at registers, secretaries at computers, bus drivers). Ergonomic evaluations and assessments have been undertaken in various industrial workplaces to address the levels of postural stress/discomfort quantitatively for descriptions of optimal work postures [1, 7]. Increasing numbers of posture studies involving health care workers have been conducted, but their focus has been primarily on low back pain problems experienced by hospital nurses.

Ergonomic stress during dynamic tasks such as patient lifting and transferring is only part of a broader picture. Prolonged static posture has been associated also with ergonomic stress [8]. The physical stress associated with the fixed work posture of many surgeons and operating room staff can result in discomfort, fatigue, and musculoskeletal disorders.

Performing a laparoscopic surgical procedure places particularly high physical and cognitive demands on surgeons that differ substantively and dramatically from those experienced during open surgery. Knowledge of ergonomics related to primary laparoscopic surgeons has been well described in previous studies. Several minimally invasive surgery (MIS) components including long-shaft instruments, access ports, and endoscopic image display systems have been identified as contributing to ergonomically unfavorable postures assumed and maintained by laparoscopic surgeons during procedural performances [9–12].

Motion analysis and force plates have been among the tools used to examine surgeons' body movements, specifically the measurement and analysis of postural sway [13]. Upper body movements have been characterized by Person et al. [14], who demonstrated the feasibility of using an optoelectric measurement system for automated posture sampling in the study of surgical ergonomics.

Berguer et al. [15] compared surgeons' postures during laparoscopic and open surgical procedures by analyzing the locations and range of motion (ROM) of the center of pressure (COP) in two directions (anteroposterior and mediolateral). They concluded that during laparoscopic procedures, surgical posture is less dynamic, as shown by significantly reduced ROM of COP.

Gillette et al. [16] calculated the outer boundaries to quantify the amount of sway in COP excursions. They found that significant increases in movement could be correlated with task difficulty. Additionally, postural control strategies used by surgeons of differing experience levels have been analyzed during fundamentals of laparoscopic surgery task performance. These studies concluded that each task required unique postural control mechanisms and that a significant difference in sway control was evident among surgeons with different surgical skill levels [17, 18].

For a more systematic assessment of postural control, Lee and Park [19] characterized sway areas, directions, and shape by constructing an ellipse using principal component analysis that covered 95% of COP excursions. In that same study, postural stability demand (PSD) was calculated as the absolute distance between COP and the center of mass. This analysis showed that less experienced surgeons exhibited high PSD, which implied higher postural instability during performance of laparoscopic surgery task fundamentals.

Another postural study using center of mass sway analysis demonstrated that postural instability does not necessarily correlate with poor performance [20]. A highly experienced surgeon with a wrist condition made compensatory arm movements to minimize wrist flexion. This surgeon also exhibited strategic movements that although appearing to signal postural instability, actually proved to be necessary for achieving successful task performance.

The ergonomics associated with the operating surgeon's performance are understandably a priority. Although an active part of the entire operation, the laparoscopic assistant has not until currently been properly the subject of ergonomics studies.

Nissen fundoplication, a common procedure, involves both advanced and basic laparoscopic skills. The inexpensive, easily constructed box trainer we designed provides a simulation alternative to the animal models that to date have dominated studies of minimally invasive fundoplication task performance.

While performing a fundoplication, the surgeon stands centered between the patient's legs in alignment with the diaphragmatic hiatus. This position keeps the surgeon facing straight ahead in as neutral a posture as possible and one assumed to be ergonomically favorable. In contrast, the camera holder is positioned to accommodate the surgeon, which usually means standing to one side of the patient and thus not in optimal alignment with the working area. To accommodate, the camera holder is forced to rotate his or her upper body while simultaneously reaching across the operative field to hold the camera or retract tissues for the surgeon.

This study aimed to quantify ergonomic risks associated with the tasks performed during a fundoplication by the

camera assistant. The particular segment of the study reported involves postural balancing. We hypothesized that postural balancing is affected by the grip used to hold the camera and the location and relocation of the camera head in relation to different targets. We also investigated how fatigue influences postural balancing over time-framed (early, middle, late) phases of task performance.

Materials and methods

This institutional review board–approved study was performed in the Surgical Ergonomics Laboratory at the Maryland Advanced Simulation, Training, Research, and Innovation (MASTRI) Center at the University of Maryland. Seven right-handed subjects possessing different levels of MIS experience ranging from medical student to fellow from the Department of Surgery at the University of Maryland School of Medicine volunteered, signed an informed consent, and agreed to perform camera navigating and retracting tasks.

An adult patient in low lithotomy position was simulated by a training box on an operating room table. An extended arm board was attached to the table bearing the trainer box as a representation of the obstruction that would be caused by the patient's left leg. Additionally, to simulate the situation of the assistant working around the arm of the operating surgeon, we inserted two graspers through ports set on the right and left sides of the camera port and instructed each subject to work around these graspers. At the left side of the simulated patient, each subject stood on two force plates (Advanced Mechanical Technology Inc., Watertown, MA, USA), one leg on each (Figs. 1 and 2).

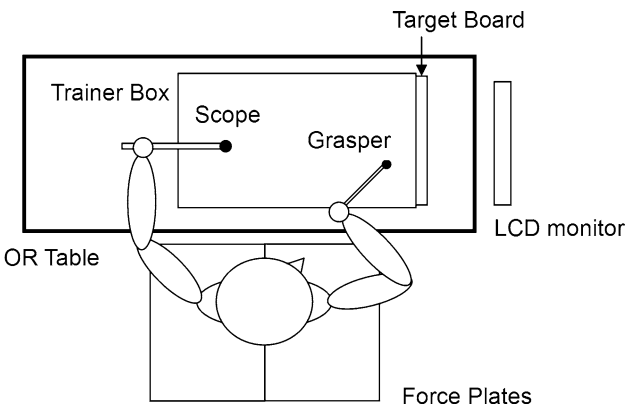

Fig. 1 Experimental setup for the simulation of the camera assistant's roles as a camera holder and retractor during a Nissen fundoplication. A trainer box placed on the operating room table simulates a patient in low lithotomy position. A board with targets, circles, and bands is attached to the side of the trainer box at the location of the simulated patient's head. While performing the tasks, the subject stands on two force plates

A 0° scope displayed endoscope images on a standard liquid crystal display (LCD) monitor positioned at eye level at the head of the bedside. A laparoscope was introduced into the training box, which also contained four 2-cm circles functioning as targets placed on the rear panel in the following relations to the assistant: distal superior, proximal superior, distal inferior, and proximal inferior (target effect). Four additional 2-cm circles approximately 10 cm apart were marked in a straight line between the superior and inferior targets. A rubber band was stapled to each of the outermost circles (A, C) for the purpose of retraction to the inner circles (B, D) (Fig. 3).

Each subject performed a 12-min trial that consisted of three 4-min phases (early-, middle-, and late-phase effect). In each phase of four dual-task modules, the subject performed camera-holding and -pointing tasks (moving from target 1 through target 4) together with grasping and retraction tasks (moving from A to B, C to D, A to B, and C to D). Each subject performed two trials, one while holding the camera from the top and one while holding it from the bottom (grip effect).

Specifically, the camera-holding and -pointing task required holding the camera with the left hand and pointing it at a target (Fig. 4). On the screen were two circles (diameters of 4.5 cm for the larger and 2.5 cm for the smaller) printed on a transparency attached to the monitor. The task for the subject was to maintain the target's accuracy constraints by confining it between the boundaries of both circles. The grasping and retraction task required holding a grasper in the right hand to grasp a rubber band at one location and retract it to another. Both tasks were always executed simultaneously.

Once both retraction and camera pointing were completed, the subject was asked to maintain accuracy constraints of both the grasping and camera-pointing tasks for a minute. While doing so, each subject was free to change or adjust his or her posture.

The amplitudes of the vertical ground reaction forces (VGRF) exerted by both the left and right legs onto each force plate were collected and recorded at 200 Hz. While each subject maintained static posture for each of the four tasks within each of the three phases, data permitting calculation of a weight-loading ratio (WLR) were obtained. To quantify the balancing taking place between the two legs, we derived the WLR by dividing the left force plate VGRF by the total VGRF from both plates.

$$WLR = \frac{\text{Left VGRF}}{\text{Left VGRF} + \text{Right VGRF}} \times 100$$

Thirty-nine 9.5-mm retroreflective sphere markers were attached to each participant according to Plug-in-Gait (ViconPeak, Lake Forest, CA, USA) marker placement designations. The markers were placed on bands around the

Fig. 2 Each subject while standing on two force plates performs the camera-pointing task with the left hand and the retraction task with a grasper in the right hand. Reflective markers and electromyographic electrodes are attached to the subject for motion and muscle activation analysis

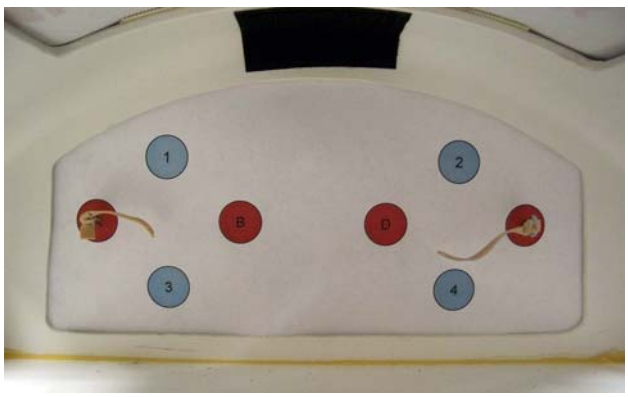

Fig. 3 Inside view of the trainer box showing the target board. Four circles numbered 1 to 4 are the targets for the camera-pointing task. Another four circles are labeled A to D. Circles A and D have rubber bands attached for the tissue retraction task

Fig. 4 Screen shot of the monitor showing a target confined between the two circles on the monitor

head, wrists, and knees; a custom-made vest and waist belt; bare arms; and the shoulder, thighs, and shanks of the participants' medical scrubs. Placement of elastic bands and a vest over the scrub suit of each participant permitted the markers to be attached securely to anatomic landmarks. A (ViconPeak, Lake Forest, CA, USA) motion capture system consisting of 12 high-speed, high-resolution, infrared digital cameras tracked the markers and reconstructed body segment movement in three-dimensional (3D) space. The location data of each marker were sampled at 100 Hz.

Statistical analysis

An overall 4 × 3 × 2 (target × phase × grip) analysis of variance (ANOVA) with repeated measures was applied to characterize the extent to which each laparoscopic assistant's body weight was distributed by each leg. Then the main effects of these three factors (target, phase, grip) and their interactions were analyzed. The significance level was set at a p value of 0.05.

Results

The data on the two grip strategies collected separately showed no statistical difference between them in terms of weight balancing ($p > 0.5$). Therefore, the data were consolidated for further analysis using 4 × 3 (target × phase) repeated-measures ANOVA. The significant

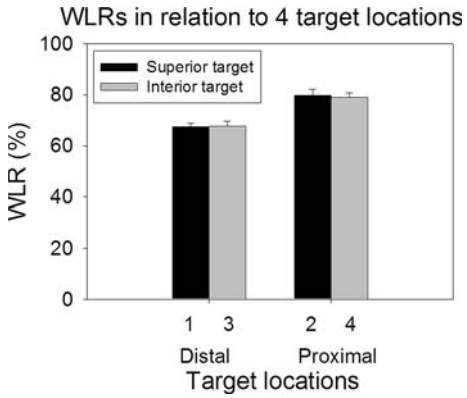

Fig. 5 Target effect as it relates to the weight-loading ratio (WLR), which significantly increased with proximal targets (i.e., 2, 4) by 11.8% compared with distal targets (i.e., 1, 3). No difference was found between targets on the same side (i.e., inferior, 3 and 4; superior, 1 and 2)

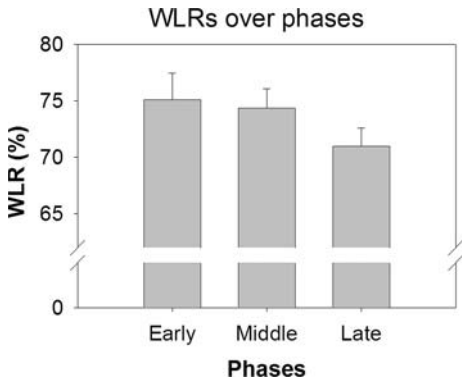

Fig. 6 Phase effect on weight-loading ratio (WLR), which decreased as each four-target phase of task performance was repeated

main result was that the WLR was found to be different among the four targets ($p < 0.005$), as shown in Fig. 5. Post hoc tests further showed that the WLR significantly increased with proximal targets (i.e., 2, 4) by 11.8% compared with distal targets (i.e., 1, 3). No difference was found between targets on the same side (inferior, 3 and 4; superior, 1 and 2). The findings also showed that WLR decreased as the four target camera navigation modules were repeated (phase effect, $p < 0.05$) (Fig. 6). The interaction effect between the target and phase factors was not significant ($p > 0.05$).

Discussion

This study investigated the ergonomic risks potentially experienced by laparoscopic assistants during a simulated laparoscopic Nissen fundoplication. Specifically, it analyzed the postural balancing that occurs as camera navigation and target retraction tasks are performed. Postural balancing analysis, achieved by what we termed WLR, using a force-plate system, demonstrated that the assistant's left leg disproportionately bore 70% to 80% of body weight over time, thus creating a high-risk ergonomic situation. It can reasonably be assumed that if the camera holder stood on the patient's right side, the data would be a mirror image of that presented in this discussion (i.e., more load on the right leg).

Additionally, after introduction of the camera through the one access port used in our study, we discovered an ergonomic risk traceable to the fulcrum effect. Specifically, when the camera was pointed toward the proximal target, the camera head actually moved toward the distal location. This is referred to as the target effect. The risk presented in this situation is that that the camera assistant must maintain continuous extension of the left arm while simultaneously leaning the entire body left.

When we considered the fatigue effect on postural balancing over phases, we found that WLR decreased as a phase was repeated (early, middle, late). This is referred to as the phase effect. We interpreted this WLR result as indicative of the camera assistant acting in a compensatory manner to combat the increased muscular fatigue that developed over time. Considering that this compensatory action resulted in a reduction of ergonomic stress at the joint of the left leg, we propose ergonomic solutions such as camera-handle attachments to minimize the time-accrued effects of the extended arm and unbalanced leaning posture. Another solution to minimize fatigue and maximize postural stability may be to train the camera assistant in a simulated situation, as done in our study, before actual operating room performance of a fundoplication, with specific instructions given on the need to rebalance weight as accurate camera pointing and retraction are repeatedly achieved.

To mitigate obstructions that potentially create positioning issues, compensatory action also is probable such as equipping the operating table with stirrups or having the assistant work around the arms of the operating surgeon. In this study, our attention to such obstructions was minimal.

Ergonomic studies in laparoscopic surgery have focused on understanding and improving the ergonomic risks and benefits involved in the primary surgeon's performances [21]. In a recent literature review, these evidence-based experimental ergonomic studies were discussed in detail, including examination of their methodological infrastructures (e.g., tasks, models, measurement systems) [13]. Additionally, the obtained data and specific applications covered in these ergonomic studies were summarized. In brief, the review investigated studies on the effects that operating room components such as display systems [22–24], instrument handle designs [25–28], operating table heights [29, 30], and instrument, scope, and task locations/

orientations [31–33] have on task performance in addition to the physical workload of primary surgeons.

The studies reviewed also quantitatively assessed levels of primary laparoscopic surgeons' skills, dexterity, and motion efficiency [27, 34, 35]. The majority of models and tasks used in the reviewed studies were designed to simulate the instrument maneuvering exercised and the surgical tasks performed by primary surgeons [29, 30, 36–39].

This review examining the current body of ergonomic research related to laparoscopic surgery showed the need to extend that analysis to support staff who have an active role in operating room procedures. The few existing studies on the task performance of camera assistants had goals quite different from ergonomic risk investigation. One study investigated the application of an electromagnetic motion tracking system for simple measurements of the movements of the camera and holding arm [40]. Another study compared motion efficiencies measured from human camera drivers and robot-assisted camera control [41].

In a series of studies focused on products rather than task performance, Van Veelen et al. [24] investigated the relation of display locations to assistants' neck movements and muscle activation during camera holding, although not comparatively [29]. In an observational survey study, Van Veelen made the statement that positioning of the camera may be associated with physical discomfort of the back [42].

The strength of the conclusions we reached about the hypotheses proposed in this study compel us to analyze further our data collection with the purpose of understanding the association of specific muscle groups to fatigue. We also have begun to develop a method for calculating the compressive joint reaction forces related to physical stress. An understanding of underlying stress and fatigue mechanisms, coupled with our current findings from WLR analysis, promises to allow for further identification and minimization of evident ergonomic risks in the execution of camera-pointing and retraction tasks performed by laparoscopic assistants.

Acknowledgments This study was supported by a grant from the U.S. Army Medical Research and Materiel Command (USAMRMC), and equipment was provided in part by U.S. Surgical. The authors acknowledge the thoughtful and careful assistance of Rosemary Klein in the editing of this article.

References

1. Bhatnager V, Drury CG, Schiro SG (1985) Posture, postural discomfort, and performance. Hum Factors 27:189–199
2. Liao MH, Drury CG (2000) Posture, discomfort, and performance in a VDT task. Ergonomics 43:345–359
3. Van Wely P (1970) Design and disease. Appl Ergon 1:262–269
4. Keyserling RM (1986) A computer-aided system to evaluate postural stress in the workplace. Am Ind Hyg Assoc J 47:641–649
5. Winter DA (1995) Human balance and posture control during standing and walking. J Biomech 3:193–214
6. Gage WH, Winter DA, Frank JS, Adkin AL (2004) Kinematic and kinemtic validity of the inverted pendulum model in quiet standing. Gait Posture 19:124–132
7. Corlett EN, Bishop RP (1976) A technique for assessing postural discomfort. Ergonomics 19:175–182
8. Kant IJ, de Jong LC, Van Rijssen-Moll M, Borm PJ (1992) A survey of static and dynamic work postures of operating room staff. Int Arch Occup Environ Health 63:423–428
9. Patkin M, Isabel L (1995) Ergonomics, engineering, and surgery of endosurgical dissection. J R Coll Surg Edinb 40:120–132
10. Reyes DAG, Tang B, Cuschieri A (2006) Minimal access surgery (MAS)-related surgeon morbidity syndromes. Surg Endosc 20:1–13
11. Berguer R, Forkey DL, Smith WD (1999) Ergonomic problems associated with laparoscopic surgery. Surg Endosc 13:466–468
12. Carswell CM, Duncan C, Seales WB (2005) Assessing mental workload during laparoscopic surgery. Surg Innov 12:80–90
13. Lee G, Lee T, Dexter D, Klein R, Park AE (2007) Methodological infrastructure in surgical ergonomics: a review of tasks, models, and measurement systems. Surg Innov 14:153–167
14. Person JG, Hodgson AJ, Nagy AG (2001) Automated high-frequency posture sampling for ergonomic assessment of laparoscopic surgery. Surg Endosc 15:997–1003
15. Berguer R, Rab GT, Abu-Ghaida H, Alarcon A, Chung J (1997) A comparison of surgeons' posture during laparoscopic and open surgical procedures. Surg Endosc 11:139–142
16. Gillette JC, Quick NE, Adrales GL, Shapiro R, Park AE (2003) Changes in posture mechanics associated with different types of minimally invasive surgical training exercises. Surg Endosc 17:259–263
17. Lee G, Kavic SM, George IM, Park AE (2006) Correlation between postural stability and performance time during fundamentals of laparoscopic surgery (FLS) tasks. Br J Surg 93(Suppl):S206
18. Savoie S, Tanguay S, Centomo H, Beauchamp G, Anidjar M, Prince F (2007) Postural control during laparoscopic surgical tasks. Am J Surg 193:498–501
19. Lee G, Park AE (2007) Development of a more robust tool for postural stability analysis of laparoscopic surgeons. Surg Endosc 22:1087–1092
20. Lee G, Kavic SM, George IM, Park AE (2007) Postural instability does not necessarily correlate to poor performance: case in point. Surg Endosc 21:471–474
21. Van Veelen MA, Jakimowicz JJ, Kazemier G (2004) Improved physical ergonomics of laparscopic surgery. Min Invas Ther Allied Technol 13:161–166
22. Smith WD, Berguer R, Nguyen NT (2005) Monitor height affects surgeons' stress level and performance on minimally invasive surgery tasks. Stud Health Technol Inform 111:498–501
23. Huber JW, Taffinder N, Russell RCG, Darzi A (2003) The effects of different viewing conditions on performance in simulated minimal access surgery. Ergonomics 46:999–1016
24. Van Veelen MA, Jakimowicz JJ, Goossens RHM, Meijer DW, Bussmann JBJ (2002) Evaluation of the usability of two types of image display systems during laparoscopy. Surg Endosc 16:674–678
25. Emam TA, Frank TG, Hanna GB, Stockham G, Cuschieri A (1999) Rocker handle for endoscopic needle drivers. Surg Endosc 13:658–661
26. Van Veelen MA, Meijer DW, Uijttewaal I, Goossens RHM, Snijder CJ, Kazemier G (2003) Improvement of the laparoscopic

needle holder based on new ergonomic guidelines. Surg Endosc 17:699–703
27. Uchal M, Brogger J, Rukas R, Karlsen B, Bergamaschi R (2002) In-line vs. pistol-grip handles in a laparoscopic simulator: a randomized controlled crossover trial. Surg Endosc 16:1771–1773
28. Emam TA, Frank TG, Hanna GB, Cuschieri A (2001) Influence of handle design on the surgeon's upper limb movements, muscle recruitement, and fatigue during endoscopic suturing. Surg Endosc 15:667–672
29. Van Veelen MA, Kazemier G, Koopman J, Goossens RHM, Meijer DW (2002) Assessment of the ergonomically optimal operating surface height for laparoscopic Surgery. J Laparoendosc Adv Surg Tech 12:47–52
30. Berguer R, Smith WD, Davis S (2002) An ergonomic study of the optimum operating table height for laparoscopic surgery. Surg Endosc 16:416–421
31. Emam TA, Hanna GB, Kimber C, Dunkley P, Cuschieri A (2000) Effect of intracorporeal–extracorporeal instrument length ratio on endoscopic task performance and surgeon movements. Arch Surg 135:62–65
32. Emam TA, Hanna G, Cuschieri A (2002) Comparison of orthodox vs off-optical axis endoscopic manipulations. Surg Endosc 16:401–405
33. Emam TA, Hanna G, Cuschieri A (2002) Ergonomic principles of task alignment, visual display, and direction of execution of laparoscopic bowel suturing. Surg Endosc 16:267–271
34. Emam TA, Hanna GB, Kimber C, Cuschieri A (2000) Difference between experts and trainees in the motion pattern of the dominant upper limb during intracorporeal endoscopic knotting. Dig Surg 17:120–125
35. Datta V, Chang A, Mackay S, Darzi A (2002) The relationship between motion analysis and surgical technical assessment. Am J Surg 184:70–73
36. Matern U, Kuttler G, Giebmeyer C, Waller P, Faist M (2004) Ergonomic aspects of five different types of laparoscopic instrument handles under dynamic conditions with respect to specific laparoscopic tasks: an electromyographic-based study. Surg Endosc 18:1231–1241
37. Hanna GB, Drew T, Clinch P, Hunter B, Shimi S, Dunkley MP, Cuschieri A (1996) A microprocessor-controlled psychomotor tester for minimal access surgery. Surg Endosc 10:965–969
38. Quick NE, Gillette JC, Shapiro R, Adrales GL, Gerlach D, Park AE (2003) The effect of using laparoscopic instruments on muscle activation patterns during minimally invasive surgical training procedures. Surg Endosc 17:462–465
39. Crosthwaite G, Chung T, Dunkley P, Shimi S, Cuschieri A (1995) Comparison of direct vision and electronic two- and three-dimensional display systems on surgical task efficiency in endoscopic surgery. Br J Surg 82:849–851
40. Riener R, Reiter S, Rasmus M, Wetzei D, Feussner H (2003) Acquisition of arm and instrument movements during laparoscopic interventions. Min Invas Ther Allied Technol 12:235–240
41. Kondraske GV, Hamilton EC, Scott DJ, Fischer CA, Tesfay ST, Taneja R, Brown RJ, Jones DB (2002) Surgeon workload and motion efficiency with robot and human laparoscopic camera control. Surg Endosc 16:1523–1527
42. Van Veelen MA, Nederlof EA, Goossens RH, Schot CJ, Jakimowicz JJ (2003) Ergonomic problems encountered by the medical team related to products used for minimally invasive surgery. Surg Endosc 17:1077–1081

Endoscopic Video Texture Mapping on Pre-built 3D Anatomical Objects without Camera Tracking

Xianwang Wang, *Student Member, IEEE,* Qing Zhang, *Student Member, IEEE,* Qiong Han, Ruigang Yang, *Member, IEEE,* Melody Carswell, *Member, IEEE,* and Brent Seales, *Member, IEEE*

***Abstract*—Traditional minimally invasive surgeries use a view port provided by an endoscope. We argue that a useful addition to typical endoscopic imagery would be global 3D view providing a wider field of view with explicit depth information for both the exterior and interior of target anatomy. One way to implement such a 3D view is to extract texture images from an endoscopic video sequence and map the textures onto pre-built 3D objects. This paper presents a novel method for registering endoscopic videos to a 3D surface model derived from MR/CT. Our approach differs from previous approaches, because no camera tracking information is required a priori. We takes advantage of the fact that nearby frames within a video sequence usually contain enough coherence to allow a 2D-2D registration, which is a much well-studied problem. The texturing process can be bootstrapped by an initial 2D-3D user-assisted registration of the first video frame followed by mostly-automatic texturing of subsequent frames. We perform experiments on phantom and real data, validate the algorithm against the ground truth, and compare it with the traditional tracking method in simulations. Experiments show that our method improves registration performance compared to the traditional tracking approach.**

***Index Terms*—MIS, Computer-augmented Reality, 3D Reconstruction, 3D to 2D Registration.**

I. Introduction

Minimally invasive surgery (MIS) has become a major component of modern surgical practice. Although certain risks exist, MIS causes less operative trauma for the patient than an equivalent open surgery. Many important MIS techniques are realized by a endoscopic camera, providing an interior portal into the patient's body through which a surgeon views both anatomical structures and surgical instruments. In addition to the constrained movement of the surgical instruments and difficult hand-eye coordination in endoscopic surgery, a surgeon is faced with perceptual challenges such as the apparent lack of 3D depth information and the narrow field of view (FOV) from the 2D camera. Given these visual limitations, endoscopic surgery often takes longer than its counterpart open surgery ([1], [2]). Seasoned surgeons might be able to adjust themselves to this challenging display environment; however, this accommodation to the endoscopic environment requires increased workload and lengthier training than open surgery ([3], [4], [5]).

One important goal of building a new display environment for endoscopic surgery is to provide enhanced intra-operative guidance cues for surgeons. These cues would, ideally, include depth information of both the exterior and interior of the objects and a wider FOV, which should ease the stress on surgeons associated with the traditional endoscopic camera view and help them achieve more precise and reliable surgical performance. A computer augmented environment ([6], [7]) is the key for building the next generation endoscopic surgical displays. Such an environment can be realized by combining 3D anatomical models, often built from pre-operative scans, and the realtime 2D endoscopic camera view.

One way to combine a 3D anatomical object and its corresponding 2D endoscopic view is to use general 3D-2D registration techniques, texturing the camera video sequence to the 3D surface object. The challenge is determining an accurate mapping between coordinates in the 2D and 3D data sets. There has been an increasing demand for rendering, visualizing, and analyzing the object's geometry and its surface texture in medical applications such as surgical planning, non-invasive diagnosis and treatment, and image-guided surgery. Traditionally, if geometry and texture are acquired at the same time with the same sensor ([8], [9]), then the alignment of images to the model can be achieved automatically and no further 3D-2D registration is needed. In most cases, however, specialized 3D scanners are used to acquire the precise geometry, and high quality digital cameras are used to capture detailed texture information. Thus, the images have to be registered with the 3D geometry to build correspondences between the geometry and texture information.

This texture-to-geometry registration problem has been handled by pose tracking of the camera ([10], [11]). With precise instrumentation and/or fiducial markers, satisfactory results have been obtained. However, there are certain applications in which neither of these requirements can be satisfied. In MIS, endoscopes that are introduced through a small port into a body cavity provide high-resolution video images of a limited view of the surgical site. Since the FOV of the endoscope is small, a major limitation is lack of enough fiducial marks between consecutive frames. Besides, the endoscope cannot be directly tracked in a surgical setting. Instead, a tracker is used and attached to the *outside* of the endoscope, as shown in Figure 12. The long offset between the tracker and endoscope magnifies the tracking error (see the analysis in Appendix). The error is about 5.5 pixels for images with the resolution 640×640 as computed in the example. Another approach for 3D-2D registration is to find a parameterization of a 3D surface model onto a 2D texture domain, while maintaining certain criteria, such as the minimization of distortions and

Xianwang Wang, Qing Zhang, Ruigang Yang, Qiong Han, Melody Carswell, and Brent Seales are with the Center of Visualization & Virtual Environment (CVVE), Department of Computer Science, Department of Psychology, University of Kentucky, Lexington, Kentucky, 40507 USA (email: xwang@cs.uky.edu, URL: http://www.vis.uky.edu/)

compliant with user-defined feature point locations (e.g., [12], [13], [14]). While these methods are satisfactory for a single image, applying the manual selection of feature points in every video frame is too tedious.

In this paper, we combine 2D tracking with parameterization-based texture mapping without camera tracking. The basic idea is to boot-strap the registration process using an interactive method (such as the one from [12]) and then to use vision-based 2D tracking to find 2D-2D sparse correspondences between images. Since the first frame has 3D-2D correspondences, each new frame, based on the overlapping area to the previous frame, can be "pasted" onto the 3D model automatically using a parameterization-based method. In this way, we convert the difficult 3D-to-2D registration problem into a well-studied and understood problem of 2D-to-2D matching. Our method is very general, and it can be used for images that can not be modeled by perspective projection. In addition, when the camera is indeed projective and the object is (almost) rigid, we introduce a projective correction term in the parameterization process so that accurate registration can be achieved over a wide range of viewpoint changes. Unlike projective texture mapping, this projective correction term is a soft constraint so our method is more robust against errors in the 3D model or even slightly deformed models. In both cases, we avoid the problem of camera calibration or external tracking.

In essence, our approach combines the strength of both visual tracking (automatic) and parameterization-based texture mapping (more flexible), leading to a new means to quickly and semi-automatically add textures to 3D models.

In the remainder of this paper, we review related work in computer augmented surgery and recent 3D-2D registration techniques before turning to a detailed description of the proposed video sequence texture mapping algorithm. We then demonstrate the application of our method on phantom and real data, and provide an evaluation of the method by formally comparing it to the traditional tracking method.

II. Related Work

The rich literature in computer augmented surgery includes methods providing better perception and guidance in both open and MIS surgeries. The use of preoperative images has become a standard in these surgeries. Among the pioneer work, [6] rendered registered stereo views from endoscopic cameras to a patient's exterior anatomy, to augment open surgeries. [15] presented a visualization system for robot assisted coronary artery bypass graft by registering a preoperative coronary tree model to realtime endoscopic images using manually picked landmarks. [7] projected a reconstructed mesh of the entire surgical field from stereo onto 3D preoperative images. [16] registered 3D surfaces reconstructed by laser range scanner to preoperative CT images and [17] pushed the idea one step further to track cortical surface deformation via serial laser range scans and non-rigid image registration. [18] approached real-time fusion of endoscopic views with dynamic 3D cardiac images on a phantom by trying to solve registration of deformable models. Most closely to our proposed method, [10] showed how to automatically register endoscopic brain images to 3D brain meshes, which will be further detailed when we discuss 2D and 3D registration methods, which are a key component in computer augmented surgery.

Several registration techniques of a 2D image and a 3D geometric model have been proposed so far. The first approach estimates the pose of a camera through corresponding pairs of 2D and 3D point features, fiducial landmarks. The accuracy of the pose estimation algorithm is determined by the accuracy of locating the 2D and 3D features, the accuracy of finding correspondences, and the number of features. It can be difficult to locate landmarks, since some landmarks maybe hidden. Often, many features are needed to estimate the pose, which are not always available in medical imaging. Instead of directly searching for 3D-2D point pairs, some registration techniques use reflectance images. These approaches first extract feature points [19] or edges [20] from reflectance images and texture images, then apply some constraints (e.g. epipolar constraints [20] and optical flow constraints [21]) to estimate pose information. These methods also suffer from the problem of location of features.

Some other registration techniques inspect larger image features such as contour lines within a 2D image and a projected image of 3D model. With the correspondences of 2D photometrical contours and projected 3D geometrical contours on the 2D image, the camera transformation can be estimated by minimizing the error, which can be defined as the sum of minimal distance between the 3D model and a projection ray ([22], [23]), or the sum of distances between points on a contour of an image and on a projected contour line of a 3D model ([24], [25]). However, if the number of correspondences is not sufficient, the contour-based approaches are likely to converge to the local minimums if an initial alignment error is large.

Once an initial mapping between 3D and 2D is established, a vision-based tracking technique is employed to improve the robustness of the registration. It first extracts features using algorithms such as the Kanade-Lucas-Tomasi (KLT) ([26], [27]) and the Scale Invariant Feature Transform (SIFT) ([28], [29]). The orientation and position of pose are estimated by feature correspondences. Then, the 3D-2D projective transform is applied for the projective texture mapping onto the geometry. Dey et al. [10] suggests this technique for the fusion of freehand endoscopic brain images to the surfaces. Methods relying solely on projective mapping require that the underlying object be rigid, which may not be true for the majority of organ images.

Minimizing the distortions (e.g. area, length or angle distortion), or stratifying user-defined positional constraints, parameterization avoids the process of determining the parameters of the cameras. Levy [12] suggests a method to satisfy the user-specified constraints in the least-squares sense. Desbrun et al. [13] use Lagrange multipliers to incorporate positional constraints into the formulation of parameterization, and [30] use Steiner vertices to satisfy the constraints. Matchmaker [14] automatically partitions a mesh into genus-0 patches, and satisfies the use-specified correspondences between the patches and one or two texture image(s). Cross-parameterization [31] and

inter-surface mapping [32] use similar approach of mapping between two surfaces, rather than between a surface and texture space, while Zhou et al. [33] suggest a similar approach between a surface and multiple texture images.

III. Methods

This paper presents a new technique to map the acquired endoscopic video (Figure 1a) onto the 3D object model. Figure 1 illustrates the novel texturing processing pipeline, which includes three stages: single view mapping, panorama construction, and incremental texturing mapping.

1) **single view mapping:** We adopt the Least Square Conformal Mapping (LSCM) algorithm [34], where a user can assign correspondences between a 3D model and a 2D texture map and the system optimizes a mapping that minimizes distortions. The model is parameterized (Figure 1c) over the first frame with a set of user-specified correspondences (Figure 1b), using linear system solver (Figure 1d).
2) **panorama construction:** In Figure 1e, the current frame taken from a different view point is stitched with the previous frames into a single large image that is continuous in geometry and shading. This is a 2D-2D registration process.
3) **incremental texture mapping:** This is the heart of our algorithm, as show in Figure 1f. The subsequent endoscopic images from video are mapped onto the geometry incrementally. Our algorithm takes advantage of the fact that nearby frames within a video sequence usually contain enough coherence to allow a 2D-2D registration. The system propagates the user constraints defined in the single viewing mapping to the panorama.

A. Single View Mapping

Parameterization of 3D surface over a plane is to establish a one-to-one mapping between the planar domain and the surface domain, while the metric distortion introduced by mapping has to be kept to the minimum. To obtain visually pleasing result, the feature correspondences have to be enforced between the texture and the 3D surface. Our algorithm combines the method of matching features [12] and the method of least square conformal maps [34]. As shown in the dashed red box in the figure 1, the single view mapping contains three components: 3D-2D feature correspondences, parameterization and linear system solver. To define the mapping procedure, we introduce the following notations:

We represent the model with a triangle mesh $\tau = \{\tau_1, \tau_2, ..., \tau_q\}$ with vertices $\mathbf{x}_1, \mathbf{x}_2, ..., \mathbf{x}_n$, where τ_i denotes a triangle in the model. Parameterizing a mesh is to construct a piecewise linear mapping between τ and a 2D texture U. such as:

$$\chi : \tau \rightarrow U$$
$$\mathbf{x}_i \rightarrow \mathbf{u}_i$$

where $\mathbf{x}_i = (x_i, y_i, z_i)^t$ denotes the 3D position of the node in the original mesh τ, $\mathbf{u}_i = (u_i, v_i)^t$ is the 2D position of the corresponding node in the 2D texture U.

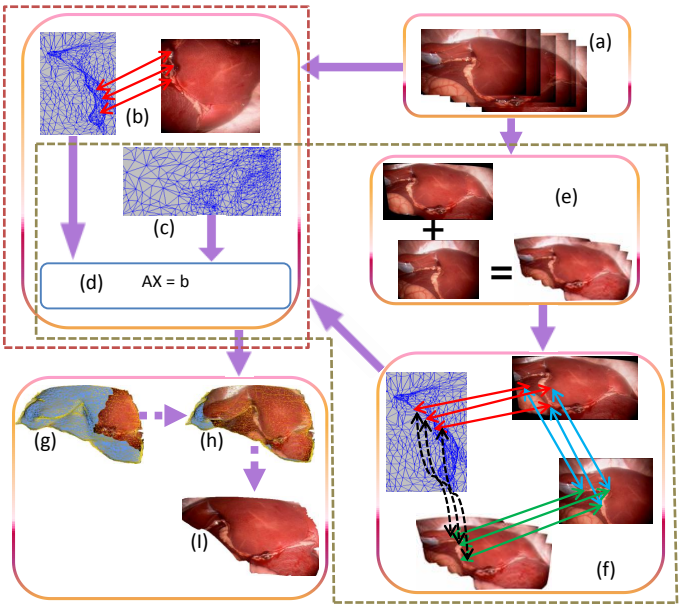

Fig. 1. The pipeline of our system for texturing endoscopic images to 3D surfaces. (a) images extracted from the endoscopic video. (b) 3D-2D feature correspondences; (c) parameterization; (d) linear system solver; (e) panorama construction; (f) incremental texturing mapping; (g) the result of the single view mapping; (h) the intermediate result of texture mapping; (i) The final result of texture mapping.

*1) **3D-2D Feature Correspondence**:* Although a planar parameterization of the mesh is widely used for texture mapping, it can not satisfy any special correspondence between the mesh and the texture ([34], [35]). The algorithm must handle user-defined feature correspondences, while maintaining a valid one-to-one mapping between the 3D mesh and 2D texture images or panoramas. The correspondences may be represented by providing each vertex $\mathbf{x}_i$ with its image $\mathbf{u}_i$ through mapping that satisfies [12]:

$$\psi(\mathbf{x}_i) = \lambda_1 \cdot \mathbf{u}_{i_1} + \lambda_2 \cdot \mathbf{u}_{i_2} + \lambda_3 \cdot \mathbf{u}_{i_3} \quad (1)$$

$$\chi(\mathbf{u}_i) = \lambda_1 \cdot \mathbf{x}_{i_1} + \lambda_2 \cdot \mathbf{x}_{i_2} + \lambda_3 \cdot \mathbf{x}_{i_3} \quad (2)$$

where $(\lambda_1, \lambda_2, \lambda_3)$ are the barycentric coordinates at $\mathbf{x}_i$ in the triangle $\{\mathbf{x}_{i_1}, \mathbf{x}_{i_2}, \mathbf{x}_{i_3}\}$, computed as follows:

$$\begin{pmatrix} \lambda_1 \\ \lambda_2 \\ \lambda_3 \end{pmatrix} = \frac{1}{A_{\tau_i}} * \begin{pmatrix} y_{i_2} - y_{i_3} & x_{i_3} - x_{i_2} & x_{i_2}y_{i_3} - x_{i_3}y_{i_2} \\ y_{i_3} - y_{i_1} & x_{i_1} - x_{i_3} & x_{i_3}y_{i_1} - x_{i_1}y_{i_3} \\ y_{i_1} - y_{i_2} & x_{i_2} - x_{i_1} & x_{i_1}y_{i_2} - x_{i_2}y_{i_1} \end{pmatrix} \begin{pmatrix} x \\ y \\ 1 \end{pmatrix} \quad (3)$$

where $A_{\tau_i} = (x_{i_1}y_{i_2} - x_{i_2}y_{i_1}) + (x_{i_2}y_{i_3} - x_{i_3}y_{i_2}) + (x_{i_3}y_{i_1} - x_{i_1}y_{i_3})$ denotes twice the area of the triangle.

Each 3D-2D feature correspondence is defined to $(\mathbf{x}_j, \mathbf{u}_j)$. $\mathbf{u}_j$ is the desired texture coordinates at $\mathbf{x}_j$. Thus, we can define the objective functions to minimize the mapping error at all the m constrained features points.

$$C(\mathbf{u}) = \sum_{j=1}^{m} \|\mathbf{u}_j - \psi(\mathbf{x}_j)\|^2 \quad (4)$$

Recalled from Equation 1 , the mapping at $\mathbf{x}_j$ is a linear combination of the values $\mathbf{u}_{i_k}$ at the vertices of the triangle that contains $\mathbf{x}$. Then, $C(\mathbf{u})$ can be defined as follows, by replacing the $\psi(\mathbf{x}_j)$.

$$C(\mathbf{u}) = \sum_{j=1}^{m}\{(u_j - \sum_{k=1}^{3}\lambda_k \cdot u_{j_k})^2 + (v_j - \sum_{k=1}^{3}\lambda_k \cdot v_{j_k})^2\} \quad (5)$$

*2) **Parameterization**:* Assigning texture coordinates to a 3D mesh can be regarded as a parameterization of the surface. Consider the triangle $\tau_i = \{\mathbf{x}_1, \mathbf{x}_2, \mathbf{x}_3\}$, with the texture coordinates $\{\mathbf{u}_1, \mathbf{u}_2, \mathbf{u}_3\}$ associated with its vertices. The gradient of τ_i can be expressed in the local orthonormal basis $(\mathbf{x}_1, \mathbf{X}, \mathbf{Y})$:

$$\begin{pmatrix} \partial u/\partial x & \partial v/\partial x \\ \partial u/\partial y & \partial v/\partial y \end{pmatrix} = \frac{1}{A_{\tau_i}} * \begin{pmatrix} y_2 - y_3 & y_3 - y_1 & y_1 - y_2 \\ x_3 - x_2 & x_1 - x_3 & x_2 - x_1 \end{pmatrix} \begin{pmatrix} u_1 & v_1 \\ u_2 & v_2 \\ u_3 & v_3 \end{pmatrix} \quad (6)$$

The basis can be computed as follows:

$$\mathbf{X} = \frac{\mathbf{x}_2 - \mathbf{x}_1}{\|\mathbf{x}_2 - \mathbf{x}_1\|}; \mathbf{Y} = \frac{\mathbf{X} \times (\mathbf{x}_3 - \mathbf{x}_1) \times \mathbf{X}}{\|\mathbf{X} \times (\mathbf{x}_3 - \mathbf{x}_1) \times \mathbf{X}\|}$$

We use the least square conformal mapping, which is a planar quasi-conformal parameterization method using a least-square approximation of the Cauchy-Riemann equation [34]. The Cauchy-Riemann equation says ψ is conformal on τ_i if and only if the following equation

$$\frac{\partial \psi}{\partial x} + i\frac{\partial \psi}{\partial y} = 0 \quad (7)$$

holds true on each triangle of τ_i. This conformal condition in general cannot be strictly satisfied, so the minimization of the violation of this condition was defined in the least square sense:

$$\begin{aligned} C(\tau) &= \sum_{\tau_i \in \tau} \int_{\tau_i} \left| \frac{\partial \psi}{\partial x} + i\frac{\partial \psi}{\partial y} \right|^2 dA \\ &= \sum_{\tau_i \in \tau} \left| \frac{\partial \psi}{\partial x} + i\frac{\partial \psi}{\partial y} \right|^2 A_{\tau_i} \end{aligned} \quad (8)$$

where the last equality follows since $\left|\frac{\partial \psi}{\partial x} + i\frac{\partial \psi}{\partial y}\right|$is a constant complex number. A_{τ_i} denotes the area of the triangle τ_i. Let $\mathbf{u}_j = u_j + iv_j$ and

$$\begin{cases} W_1 = (x_3 - x_2) + i(y_3 - y_2) \\ W_2 = (x_1 - x_3) + i(y_1 - y_3) \\ W_3 = (x_2 - x_1) + i(y_2 - y_1) \end{cases} \quad (9)$$

The Cauchy-Riemann equation 7 can be rewritten as follows using the complex number:

$$\frac{\partial \psi}{\partial x} + \frac{\partial \psi}{\partial y} = \frac{i}{A_{\tau_i}} \begin{pmatrix} W_1 \\ W_2 \\ W_3 \end{pmatrix}^T \begin{pmatrix} U_1 \\ U_2 \\ U_3 \end{pmatrix} = 0 \quad (10)$$

Thus, the objective function can be written in the quadratic form such as

$$\begin{aligned} C(\tau) &= \sum_{\tau_j \in \tau} C(\tau_j) \\ &= \sum_{\tau_j \in \tau} \frac{1}{|A_{\tau_j}|^2} \left| \begin{pmatrix} W_{j_1,\tau_j} \\ W_{j_2,\tau_j} \\ W_{j_3,\tau_j} \end{pmatrix}^T \begin{pmatrix} U_{j_1} \\ U_{j_2} \\ U_{j_3} \end{pmatrix} \right|^2 \end{aligned} \quad (11)$$

where j_1, j_2, j_3 are the vertices index of triangle τ_j.

*3) **Linear System Solver**:* The cost function $C(M)$ can be defined as the weigted sum of the equations 5 and 11. It can be therefore written as follows:

$$\begin{aligned} C(M) &= C(\mathbf{u}) + wC(\tau) \\ &= \sum_k (b_k - \sum_{i=1}^{2n} a_{k,i} \cdot x_i)^2 = \|A \cdot \mathbf{z} - \mathbf{b}\|^2 \end{aligned} \quad (12)$$

where the vector $\mathbf{z}$ is composed of all unknowns (u_i, v_i), defined by $z_i = u_i$ and $z_{i+1} = v_i$, w is the weight set to 10 in our experiments. We use the conjugate gradient method to solve the minimization problem of the least square in equation 12. Algorithm 1 summaries the techniques of the single view texture mapping we discussed above.

Algorithm 1: Single view mapping

1. initialize **A** = [], and **b** = 0.
2. for each feature correspondence between the surface and the texture
   (a) compute λ_1, λ_2, and λ_3 using Eq. 2.
   (b) add one row in the sparse matrix **A** and and set the value of λ_i in this row and **b** using Eq.5, based on the index of u and v.
3. for each triangle τ_i on the surface
   (a) Compute W_1, W_2, and W_3 using Eq. 6 and Eq. 9.
   (b) add two rows corresponding to the real and imaginary parts of W_i in the sparse matrix **A** and set the value of W_i in these two rows, based on the index of u and v.
4. compute the **z** (e.g, texture coordinates) using Eq. 12 by the conjugate gradient method.

B. Panorama Construction

The full scene cannot be always captured by a single view. It is common to take multiple images and compose them into panorama. There are two main techniques of panorama construction, feature-based approach [36], and image-based approach [37]. Feature-based approach has lower complexity of the matching problem than image-based approach, since it only uses a few salient image features, such as corners, while image-based approach attempts to match bitmaps. We use the feature-based approach similar to the one [36], which is insensitive to the ordering, orientation, scale, illumination of the images and image noise. We briefly outline the procedure here (see [36] for details).

1) Extract and match SIFT features between all pairs of the images.
2) Use RANSAC to select a set of inliers that are compatible with a similarity transformation between each pair of images
3) Verify the match and discard all feature matches which are not geometrically consistent with the transformation between the images.
4) Given the set of geometrically consistent matches between the images, apply bundle adjustment to solve for all the transformations jointly.

C. Video Sequence Mapping

We propose two approaches to achieve video sequence mapping, *extrapolation texture mapping* and *incremental texture mapping*. They transfer the 3D-2D feature correspondences that are defined in the single view mapping to new frames, using the 2D feature matching found during the panorama reconstruction stage.

To describe the mapping procedure conveniently, we introduce the following notations:

- T_n: the time of adding the frame n.
- F_n: the new frame needed to map over the 3D surface at T_n.
- P_n: the panorama constructed by P_{n-1} and F_n at T_n.
- $M_{F_n \leftrightarrow P_{n-1}}$: the set of matching feature points between P_{n-1} and F_n, $\{(\mathbf{u}_{P_{n-1},j}, \mathbf{u}_{F_n,j})$, where $\mathbf{u}_{P_{n-1},j}$ is one feature point in P_{n-1}, and $\mathbf{u}_{F_n,j}$ is the corresponding feature point in $F_n\}$.
- $M_{P_{n-1} \leftrightarrow P_n}$: the set of matching feature points between P_{n-1} and P_n, $\{(\mathbf{u}_{P_{n-1},j}, \mathbf{u}_{P_n,j})$, where $\mathbf{u}_{P_{n-1},j}$ is one feature point in P_{n-1}, and $\mathbf{u}_{P_n,j}$ is the corresponding feature point in $P_n\}$.

The problem of video sequence mapping that we need to solve is: given a 3D model with a well-mapped area where we have the 3D-2D correspondences between the model τ and the texture or panorama P_{n-1} , we need to map F_n onto the model.

Extrapolation Texture Mapping: Figure 2 shows the process of this approach. For the first frame at time T_0 in the video sequence, we can register it with the 3D model interactively or via a few fiducial marks. At time $T_n (n > 0)$, the new panorama P_n is constructed with P_{n-1} and F_n using the panorama construction algorithm we described above. Given the 3D-2D correspondences $\chi : \mathbf{x}_i \rightarrow \mathbf{u}_{P_{n-1},i}$ (Figure 2a) between P_{n-1} and the model τ and the 2D-2D correspondences $M_{P_{n-1} \leftrightarrow P_n} = \{(\mathbf{u}_{P_{n-1},j}, \mathbf{u}_{P_n,j}\})$ (Figure 2b) between P_{n-1} and P_n, we can transfer the correspondences to $\widetilde{\chi} : \mathbf{x}_i \rightarrow \mathbf{u}_{P_n,j}$ (Figure 2c) between the model and P_n, because the set $\{\mathbf{u}_{P_j}\}$ belongs to the set $\{\mathbf{u}_{P_i}\}$. Thus, we know the partially 3D-2D feature correspondences between P_n and the model. The objective function can be defined to minimize the mapping error at these transferred correspondences as follows:

$$\widetilde{C}(\mathbf{u}) = \sum_{j=1}^{\widetilde{m}} \|\mathbf{u}_{P_n,j} - \widetilde{\chi}(\mathbf{x}_j)\|^2 \qquad (13)$$

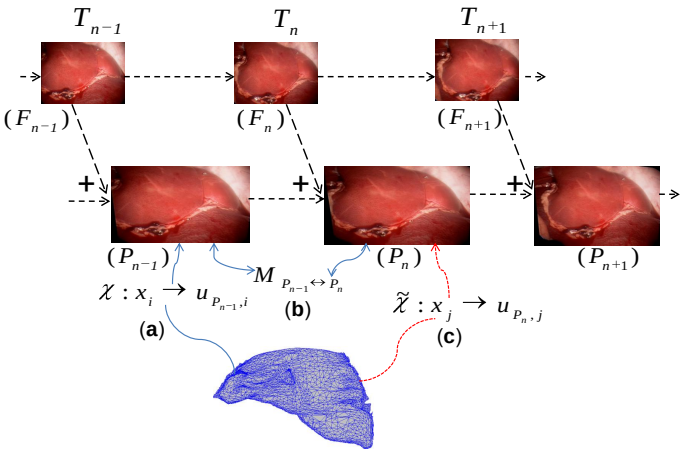

Fig. 2. Extrapolation texture mapping. (a) the 3D-2D correspondences between the model τ and P_{n-1}. (b) the 2D-2D correspondences between P_{n-1} and P_n. (c) the 3D-2D correspondences needed to find between the model τ and P_n.

Similar to the equation 5, $\widetilde{C}(\mathbf{u})$ can be rewritten:

$$\widetilde{C}(\mathbf{u}) = \sum_{j=1}^{\widetilde{m}} \{(u_{P_n,j} - \sum_{k=1}^{3} \lambda_k \cdot u_{i_k})^2 + (v_{P_n,j} - \sum_{k=1}^{3} \lambda_k \cdot v_{i_k})^2\} \qquad (14)$$

where, $\widetilde{m}$ is the number of the transferred correspondences between between the model and P_n. By weighted summing the terms from equations 14 and 11, the objective function $C(M)$ can be therefore written as follows:

$$\begin{aligned} C(M) &= \widetilde{C}(\mathbf{u}) + \varepsilon C(\tau) \\ &= \sum_{k} (b_k - \sum_{i=1}^{2n'} a_{k,i} \cdot x_i)^2 = \|A \cdot \mathbf{z} - \mathbf{b}\|^2 \end{aligned} \qquad (15)$$

ε is set to 10 in our experiments. The linear system solver in single-view mapping algorithm is employed to solve the problem above.

The advantage of extrapolation texture mapping is that it can deal with arbitrary images, as long as there is a large amount of overlap between P_{n-1} and F_n. Since there is no additional feature constraints added to the 3D model, the mapping can drift over an extended sequence. To address this limitation, we propose another method, incremental texture mapping.

Incremental Texture Mapping: We assume the images are captured by a perspective camera. For each frame of video sequence, we can find the projection matrix **P** between the model and this frame. Thus, we can use the projective constraint to improve the texturing mapping. Figure 3 shows the per-frame computation procedure.

First, the first frame at time T_0 in the video sequence is registered with the 3D model manually. At time $T_n (n > 0)$, we have the panoramic texture P_{n-1}, the frame F_n needed to register, and the mapping $\chi : \mathbf{x}_i \rightarrow \mathbf{u}_i$ at T_{n-1} (Figure 3a). First, the feature correspondences $M_{F_n \leftrightarrow P_{n-1}} = \{(\mathbf{u}_{P_{n-1},j}, \mathbf{u}_{F_n,j}\})$ between P_{n-1} and F_n are found using KLT algorithm (Figure 3b). For each feature point $\mathbf{u}_{F_n,j}$, we can find the mapping point $\mathbf{x}_{F_n,j}$ on 3D model, because $\chi : \mathbf{x}_i \rightarrow \mathbf{u}_i$ is known and $\mathbf{u}_{F_n,j}$ is in the set of $\{\mathbf{u}_i\}$. Thus, we have the correspondences

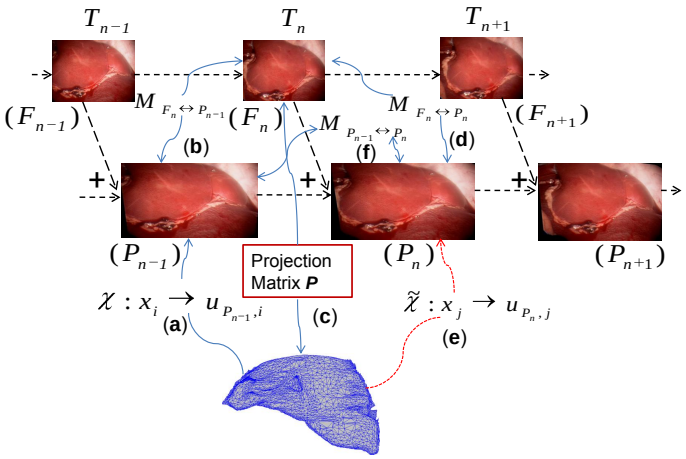

Fig. 3. incremental texture mapping. (a) the 3D-2D correspondences between the model τ and P_{n-1}. (b) the 2D-2D correspondences between P_{n-1} and F_n. (c) computation of the projection matrix $\mathbf{P}$ for frame F_n. (d) the 2D-2D correspondences between frame F_n and P_n. (e) the 3D-2D correspondences needed to find between the model τ and P_n. (f) the 2D-2D correspondences between P_{n-1} and P_n

$\{(\mathbf{x}_{F_n,j}, \mathbf{u}_{F_n,j})\}$ between F_n and the 3D model. Given these correspondences, we can compute a 3×4 projection matrix such that $\mathbf{u}_i = \mathbf{P}\mathbf{x}_i$ using the algorithm [38] for estimating $\mathbf{P}$ (Figure 3c). Similarly, we can find the $\hat{m}$ correspondences $M_{F_n \leftrightarrow P_n} = \{(\mathbf{u}_{P_n,j}, \mathbf{u}_{F_n,j})\}$ between P_n and F_n using KLT algorithm (Figure 3d). For each feature point $\mathbf{u}_{P_n,j}$ of P_n in $M_{F_n \leftrightarrow P_n}$, the 3D position $\mathbf{x}_{P_n,j}$ can be found by the intersection of inverse projection rays and the the 3D model. Then, the projective term can be defined as follows:

$$u_{P_n,j} = P\mathbf{x}_{P_n,j} \tag{16}$$

$$C(\mathbf{x}_{P_n}) = \sum_{j=1}^{\hat{m}} ||u_{P_n,j} - \tilde{\chi}(\mathbf{x}_{P_n,j})||^2 \tag{17}$$

Similar to the equation 5, the $C(\mathbf{x}_{P_n})$ can be rewritten:

$$C(\mathbf{x}_{P_n}) = \sum_{j=1}^{\hat{m}} \{(u_{P_n,j} - \sum_{k=1}^{3} \lambda_k \cdot u_{i_k})^2 + (v_{P_n,j} - \sum_{k=1}^{3} \lambda_k \cdot v_{i_k})^2\} \tag{18}$$

In addition, we can use the constraints that come from the extrapolation texture mapping (Figure 3e). The objective function $C(M)$ can be defined by weighted summing over equation 11, 15 and 18:

$$\begin{aligned} C(M) &= \widetilde{C}(\mathbf{u}) + \epsilon C(\tau) + \hat{\varepsilon} C(\mathbf{x}_{P_n}) \\ &= \sum_{k} (b_k - \sum_{i=1}^{2n} a_{k,i} \cdot x_i)^2 \end{aligned} \tag{19}$$

where ϵ is set to 10 and $\hat{\varepsilon}$ is set to 2 in our examples. Algorithm 2 summaries the techniques of the incremental texture mapping we discussed above.

Compared to extrapolation texture mapping, incremental texture mapping significantly improves the robustness of texture mapping, because it includes more constraints defined by perspective projection.

Algorithm 2 Incremental texture mapping

1. initialize $n =$ *number of frames* , i=1, and P_1 = F_1.
2. while $i \leq n$
   (1) case I (i == 1): perform single-view mapping for F_1.
   (2) case II ($1 < i \leq n$):
   a) construct panorama P_i using P_{i-1} and F_i.
   b) find correspondences $M_{F_i \leftrightarrow P_{i-1}}$ between P_{i-1} and F_i.
   c) compute the projection matrix $\mathbf{P}$ for the frame F_i.
   d) find correspondences $M_{F_i \leftrightarrow P_i}$ between P_i and F_i.
   e) compute 3d positions for feature points in $M_{F_i \leftrightarrow P_i}$.
   e) computer the $\mathbf{z}$ (e.g., texture coordinates) using the Eq. 19 by the conjugate gradient method.
   f) $i = i + 1$;
3. exit.

IV. Results

A. Visual Assessment

Based on the presented approaches above, we have implemented a flexible system for texture mapping. It is an interactive GUI, in which the user edits the correspondences between the model and the first frame. After that, the system can automatically register the subsequent frames from the video sequence or the user can add more correspondences to improve the accuracy. Three examples of varying complexity are used for demonstrating our system. Figure 4, Figure 5, and Figure 6 show the 3D model, the original frames extracted from the video sequence, the intermediate registration result, and a view of the final texture mapping results to the surface.

B. Error Analysis

A video image is a projection of the 3D scene onto a 2D imaging plane. This can be modeled using the pinhole camera.

$$\begin{pmatrix} u \\ v \\ 1 \end{pmatrix} \propto \begin{pmatrix} \lambda u \\ \lambda v \\ \lambda \end{pmatrix} = K_{int} \cdot M_{ext} \cdot \begin{pmatrix} x \\ y \\ z \\ 1 \end{pmatrix} \tag{20}$$

where $\mathbf{x} = (x, y, z, 1)^T$ denotes a world point in homogeneous coordinates, $\mathbf{u} = (u, v, 1)^T$ is a point on the 2D image, K_{int} denotes the 3×3 intrinsic matrix, representing the projection of 3D scene coordinates to the 2D image plane, M_{ext} represents the 3×4 extrinsic matrix, describing the position and orientation of the camera relative to the model, and λ is a scale factor for homogeneous coordinates. The extrinsic matrix has six degrees of freedom (DOF), corresponding to three translations t_x, t_y, and t_z along the x, y, and z axes, respectively, and also three rotations r_x, r_y, and r_z about the x, y, and z axes, respectively.

In the tracking system, the geometrical features such as points, or lines, are generally used to establish correspondences between the 2D video images and 3D models, and the correspondences are used to find the intrinsic and extrinsic parameters t_x, t_y, t_z, r_x, r_y and r_z. The video image noise and the soft tissue deformation in the model can lead to wrong correspondences. The wrong correspondences are the primary source of the registration error in the clinical application, since

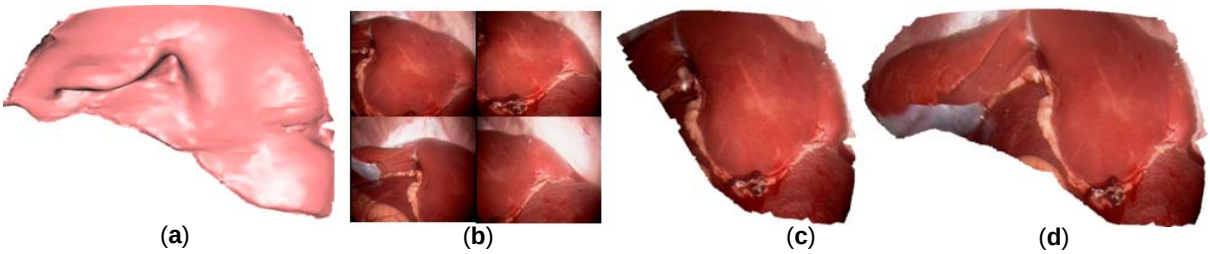

Fig. 4. Registration result of real data, pig liver. (a) liver model with 2446 vertices and 4498 triangles,; (b) 4 sample frames that extracted from the video sequence. (c) intermediate registration result with 20 frames, in which we use 20 3D-2D feature correspondences for the first frame; (d) final registration result with 60 frames.

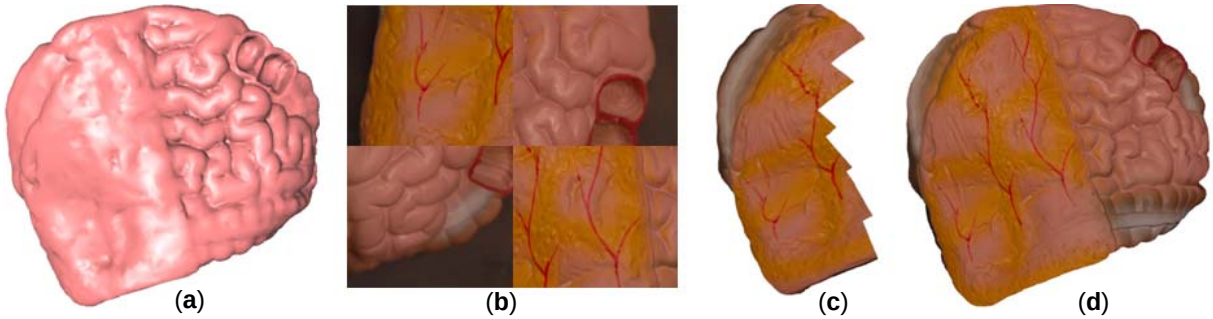

Fig. 5. Registration result of phantom data, front of human intestine model. (a) the front human intestine model with 9986 vertices and 20,000 triangles ; (b) 4 sample frames that extracted from the video sequence. (c) intermediate registration result with 16 frames, in which we use 16 3D-2D feature correspondences for the first frame; (d) final registration result with 40 frames.

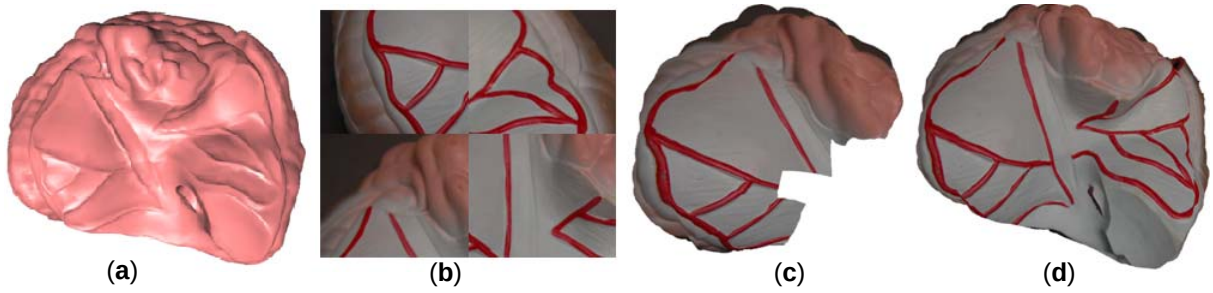

Fig. 6. Registration result of phantom data, back of human intestine model. (a) the back of human intestine model with 9986 vertices and 20,000 triangles ; (b) 4 sample frames that extracted from the video sequence. (c) intermediate registration result with 20 frames, in which we use 21 3D-2D feature correspondences for the first frame; (d) final registration result with 40 frames.

they result in the incorrect camera parameters and camera pose. These wrong pose parameters $t_x, \cdots, r_z$ produces an estimate $\hat{Q}$ of the true registration matrix $Q = K_{int} * M_{ext}$ for each frame.

To assess the robustness of our approach, we perform experiments on the simulation of the primary sources of registration error, image noise and soft tissue deformation. We compared our method with the traditional tracking method. The performance is analyzed with varying choices of the variance noise on the images and the different variational surface models. Both methods produce the estimation to the ground truth of texture coordinates, after the registration to all the video frames. To assess the accuracy of the integration of endoscopic images to the 3D model, we measured the error with the mean and standard deviation of the Euclidean distance in pixels between the ground truth and the estimated texture coordinates after registration.

1) Simulation of image noise: The test was performed to investigate how the performance of the algorithms varied with image noise. In the simulation, we use the mean kidney model in Figure 7 and 6 texture images, which have pre-calculated texture coordinates normalized to [0,1] as the ground truth. A zero mean Gaussian noise of different standard deviation values are added to the ground truth of the texture coordinate values of the mean kidney model. The texture coordinates are clipped to still lie within the range 0-1. This was repeated with noise of standard deviation 0.001, 0.008, 0.016, 0.024, 0.032, 0.048 and 0.064 texture coordinate values. For each frame, 30 2D-3D correspondences are randomly selected to estimate the registration matrix $\hat{Q}$, using the algorithm in [38]. The texture coordinate of each vertex is estimated by $\hat{x}_t = \hat{Q} * \mathbf{x}$. Similarly, we can have the estimated texture coordinate of each vertex $\hat{x}_i$ after applying incremental texture mapping on the simulated data with 30 3D-2D feature correspondences for the first frame. Thus, the mean and deviation of the mapping error

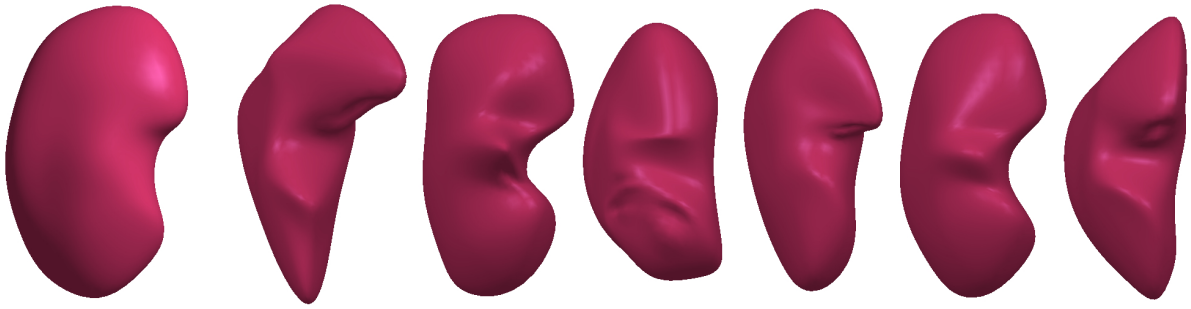

Fig. 7. The leftmost is the mean kidney in the trained shape statistics from 30 segmented kidneys; the rest six models are among the 49 sampled kidney models via Monte Carlo sampling, shown from a different angle.

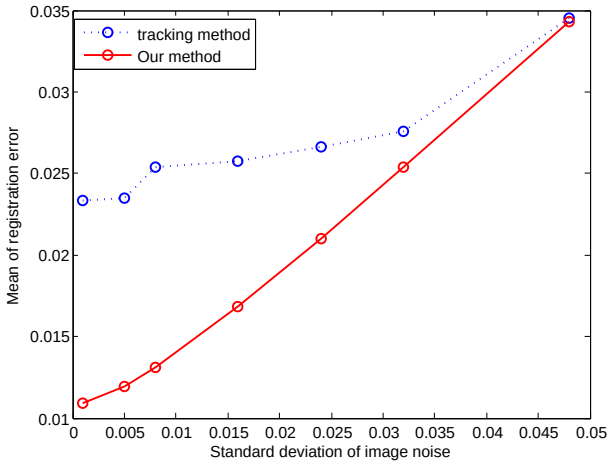

Fig. 8. Mean of registration error of our method against the traditional tracking method in the simulation of image noise. The Gaussian noise is added to the images with variance $\sigma = 0.001, 0.008, 0.016, 0.024, 0.032, 0.048,$ and 0.064. The red line indicates the results of our method.

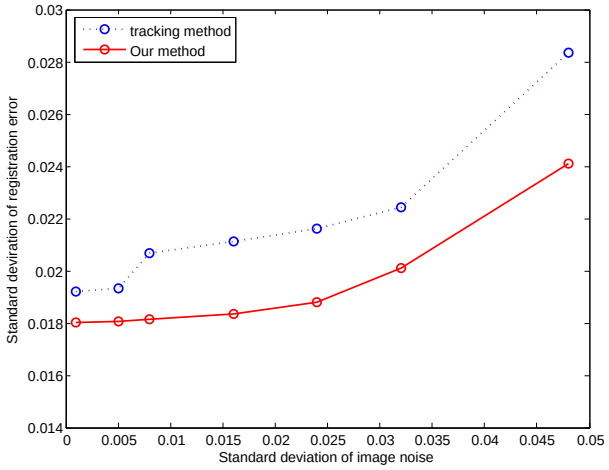

Fig. 9. Standard derivation of registration error of our method against the traditional tracking method in the simulation of image noise. The Gaussian noise is added to the images with variance $\sigma = 0.001, 0.008, 0.016, 0.024, 0.032, 0.048,$ and 0.064. The red line indicates the results of our method.

can be computed. Figure 8 and Figure 9 show the registration error comparison of our method against the tracking method for images with different variance noise.

The red line indicates the performance of our method, whereas the blue line shows the performance of the tracking method. The result shows the accuracy of our method is better than the tracking method, when noise is introduced to images. The reason is that the image noise with small standard deviation results in the wrong correspondences, which leads to the large variation in the estimation of the registration matrix Q. It can be seen that as the noise increases, our algorithm gets progressively less accurate, but it still works better than the tracking method, and does not fail completely. Furthermore, the standard deviation of noise for the captured endoscopic images is seldom higher than 0.024.

2) Simulation of soft tissue deformation: To simulate the tissue deformation, we generated 49 sample kidney models from 30 segmented human kidneys, each of which contains over ten thousand vertices and twenty thousand triangles. Each sampled model may be considered to be reasonable variation to the mean kidney model. Figure 7 shows some samples of these kidney models. We apply the tracking method and our algorithm to register these models to the 6 texture images, which texture coordinates are pre-calculated to the mean kidney model and other 49 kidney models as the ground truth. 30 3D-2D feature correspondences between the mean kidney model and each image are randomly selected for each image in the tracking method, while 30 3D-2D correspondences between the mean kidney model and he first image are manually selected in our method. For each model, the mean and standard deviation of the registration error are calculated, as discussed in the section above. The experiment results are shown in Figure 10 and Figure 11. The red line indicates the performance of our method, whereas, the blue line shows the performance of the tracking method. It shows that the robustness of our algorithm is not affected much by tissue deformation; on the other hand, the tracking method is very sensitive to deformation. It can be seen that our algorithm is more robust to the soft deformation in the models.

Limitation: As an incremental method, the error can still accumulate over a long sequence (a common problem in tracking). When the error becomes noticeable, one can easily add a few more control points and fix the drift problem. If a fully automatic process is desired (such as in a live surgical setting), fiducial points should be used. But unlike existing

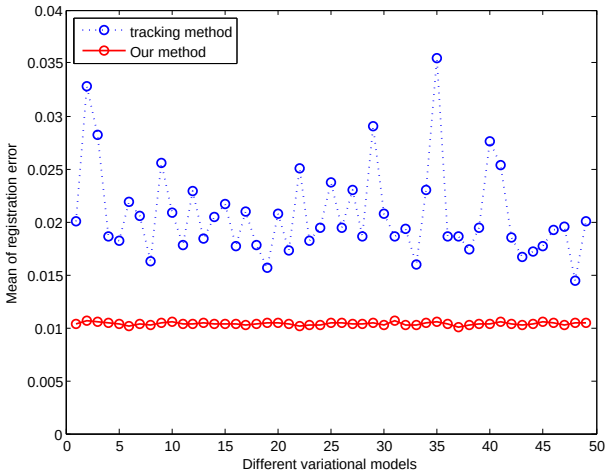

Fig. 10. Mean of registration error of our method against the traditional tracking method in the simulation of soft tissue deformation. 49 kidney models are variations of the mean kidney models. The red line indicates the results of our method.

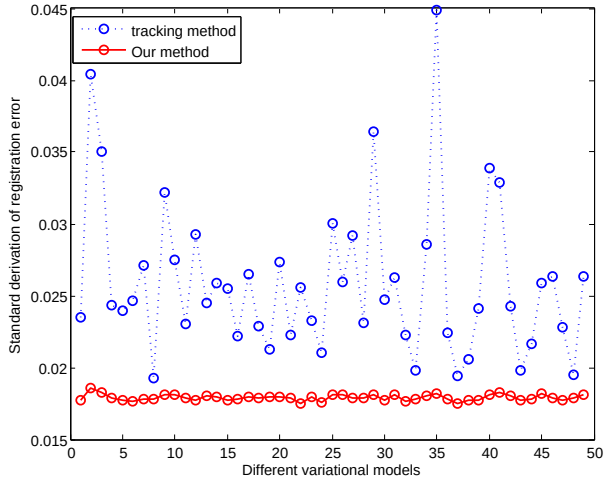

Fig. 11. Standard derivation of registration error of our method against the traditional tracking method in the simulation of soft tissue deformation. 49 kidney models are variations of the mean kidney models. The red line indicates the results of our method.

approaches that rely sole on fiducials, our method can be applied to dramatically reduce the number of fiducial marks required.

V. Conclusion

Our system provides a flexible, practical tool for texturing arbitrary models from video sequences. It allows the user to specify any arbitrary number of correspondences between the model and texture images. The algorithm then incrementally computes the texture coordinates of the vertices of the model through optimization, which satisfies the user-defined constraints. The texture mapping can achieve better accuracy with more selected correspondence feature points between the 3D object and the 2D texture. Our system has no hard constraints on the number of texture images and complexity of the models.

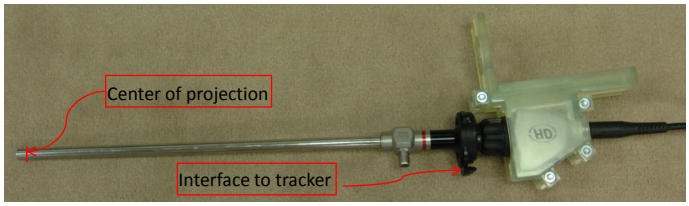

Fig. 12. The endoscope that is used in our experiment.

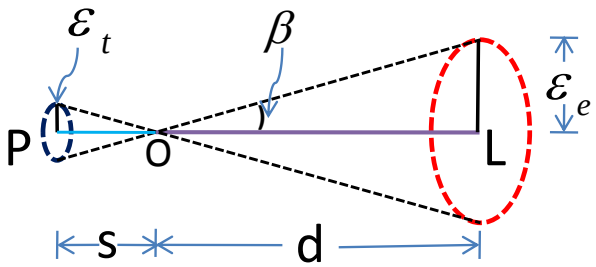

Fig. 13. A simplified example that demonstrates that the long offset between the endoscope and the tracker magnifies the tracking error. ε_t represents the tracking error of the tracker in images, corresponding to the minimal error β; ε_e denotes the magnified error of the endoscope in images; $s = |OP|$ is the length between the tip of the tracker and its virtual image plane; $d = |OL|$ is the length of the long offset.

Incremental texture mapping is achieved automatically or with a few user-define operations. We believe our approach is particular useful for image guided surgery, in which precise camera calibration and tracking are difficult.

Acknowledgements

Thanks to Adrian Park and his colleagues from the University of Maryland Medical Center for providing the 3D model and endoscopic videos used in this paper. This research was performed as part of a contract with the Maryland Advanced Simulation, Training, and Innovation Center at the University of Maryland Medical Center.

VI. Appendix

In a MIS setup, the imaging sensor on the endoscope cannot be directly tracked. A tracking device is usually attached to the other end of the scope, i.e. the end that is outside the body, as shown in Figure 12. The long offset between the endoscope and the tracker magnifies the tracking error. It can be seen from a simplified example in Figure 13, where the long offset OL is collinear with the principal ray OP of the tracker, the tracker and endoscope have the same minimal error β and the same image resolution. In general, the tracker can be defined as the mapping from the 3D world to a 2D image using pinhole camera model. When the tracker has an error ε_t in images, corresponding to the minimal error β, the error of the endoscope is $\varepsilon_e = \frac{d}{s} * \varepsilon_t$, where $s = |OP|$, the length between the tip of the tracker and its virtual image plane, and $d = |OL|$, the length of the long offset. When the tracker has the minimal error $0.1°$, $30°$ FOV, and $\frac{d}{s} = 10$, the endoscopic error may about 5.5 pixels for the images with the resolution 640×640. A detailed quantitative analysis are here.

As shown in Figure 14, the calibration process of endoscope includes two parts: the first one consists of the determination of intrinsic parameters of the endoscope K. The second one consists of computing and refining the transformation $M_{W\leftrightarrow C}$ between the endoscope and the tracker. The tracker can be represented with the matrix $P_{W\leftrightarrow O} = K[R|t]$, where $t = -R\tilde{C}$, and $\tilde{C}$ represents the coordinates of the tracker tip in the world coordinate. Similarly, we can represent the endoscope with $P_{C\leftrightarrow O} = K[R|t]M_{W\leftrightarrow C}$, where $[R|t]$ is the external matrix, and R is a 3×3 rotation matrix representing the orientation of the tracker. The assumption we make here is that the K and $M_{W\leftrightarrow C}$ are constants and no error is introduced by them after the calibration. We define $K[R'|t']$ is the noisy projection matrix of the tracker, corresponding to the correct projection matrix $K[R|t]$. In the same way, the noisy projection matrix of the camera is $K[R'|t']M_{W\leftrightarrow C}$ with the correct projection matrix $K[R|t]M_{W\leftrightarrow C}$. The error of the tracker for a pixel can be defined as $K([R'|t']/\alpha_1 - [R|t]/\alpha_2)\mathbf{x}$, and the error of the camera for a pixel is $K([R'|t']/\alpha_3 - [R|t]/\alpha_4)M_{W\leftrightarrow C}\mathbf{x}$, where $\mathbf{x}$ is a point in the world coordinate system, $\alpha_i (i = 1, \cdots, 4)$ are scales for pixels' homogeneous coordinates. To measure the error, we consider maximizing the following objective:

$$J(\mathbf{x}) = \frac{||P_t M_{W\leftrightarrow C}\mathbf{x}||^2}{||P_c\mathbf{x}||^2} \tag{21}$$

where $P_t = K([R'|t']/\alpha_1 - [R|t]/\alpha_2)$, and $P_c = K([R'|t']/\alpha_3 - [R|t]/\alpha_4)$. An important property of J is that it is invariant with respect to rescalings of $\mathbf{x}$. For this reason, we can transform the problem of maximizing J into the following constrained optimization problem,

$$\begin{array}{ll} \min\limits_{\mathbf{x}} & -\frac{1}{2}\mathbf{x}^T M_{W\leftrightarrow C}^T P_t^T P_t M_{W\leftrightarrow C}\mathbf{x} \\ s.t. & \mathbf{x}^T P_c^T P_c \mathbf{x} = 1 \end{array} \tag{22}$$

corresponding to the lagrangian,

$$\ell_P = -\frac{1}{2}\mathbf{x}^T M_{W\leftrightarrow C}^T P_t^T P_t M_{W\leftrightarrow C}\mathbf{x} + \frac{1}{2}\lambda(\mathbf{x}^T P_c^T P_c \mathbf{x} - 1) \tag{23}$$

By applying the KKT conditions, we get the following equation needs to hold at the solution,

$$M_{W\leftrightarrow C}^T P_t^T P_t M_{W\leftrightarrow C}\mathbf{x} = \lambda P_c^T P_c \mathbf{x} \tag{24}$$

This is a generalized eigenvalue problem. Plugging the solution back into the objective J, we find,

$$\begin{aligned} J(\mathbf{x}) &= \frac{||P_t M_{W\leftrightarrow C}\mathbf{x}||^2}{||P_c\mathbf{x}||^2} = \frac{\mathbf{x}^T M_{W\leftrightarrow C}^T P_t^T P_t M_{W\leftrightarrow C}\mathbf{x}}{\mathbf{x}^T P_c^T P_c \mathbf{x}} \\ &= \lambda\frac{\mathbf{x}^T P_c^T P_c \mathbf{x}}{\mathbf{x}^T P_c^T P_c \mathbf{x}} = \lambda \end{aligned} \tag{25}$$

from which, it immediately follows that the maximum of magnification of the endoscope error with respect to the tracker error is $\sqrt{\lambda_{max}}$. The analysis above shows how the long offset between the tracker and the endoscope affects the tracking method.

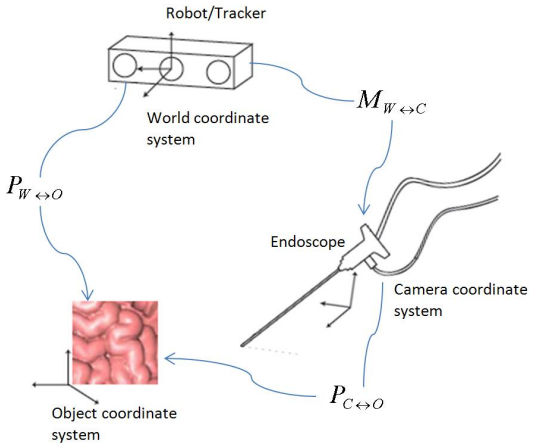

Fig. 14. Diagram to illustrate the calibration process of endoscope. $M_{W\leftrightarrow C}$ represents the transformation between the endoscope and the tracker; $P_{W\leftrightarrow O}$ denotes the tracker model; $P_{C\leftrightarrow O}$ stands for the endoscope model.

REFERENCES

[1] A. Park, M. Marcaccio, M. Sternbach, D. Witzke, and P. Fitzgerald, "Laparoscopic vs open splenectomy," vol. 134, no. 11, pp. 1263–1269, 1999.

[2] M. M. Reza, J. A. Blasco, E. Andradas, R. Cantero, and J. Mayol, "Systematic review of laparoscopic versus open surgery for colorectal cancer," vol. 93, no. 8, pp. 921–928, 2006.

[3] R. Berguer, W. Smith, and Y. Chung, "Performing laparoscopic surgery is significantly more stressful for the surgeon than open surgery," vol. 15, no. 10, pp. 1204–1207, 2001.

[4] M. I. Klein, M. A. Riley, J. S. Warm, and G. Matthews, "Perceived mental workload in an endocopic surgery simulator," in *the Human Factors and Ergonomics Society 49th Annual Meeting*, 2005, pp. 1014–1018.

[5] K. Subramonian, S. DeSylva, P. Bishai, P. Thompson, and G. Muir, "Acquiring surgical skills: a comparative study of open versus laparoscopic surgery," vol. 45, no. 3, pp. 346–351, 2004.

[6] H. Fuchs, M. A. Livingston, R. Raskar, D. Colucci, K. Keller, , A. State1, J. R. Crawford, P. Rademacher, S. H. Drake, and A. A. Meyer, "Augmented reality visualization for laparoscopic surgery," in *MICCAI '98: Proceedings of the First International Conference on Medical Image Computing and Computer-Assisted Intervention*, 1998, pp. 934–943.

[7] P. Paul, O. Fleig, and P. Jannin, "Augmented virtuality based on stereoscopic reconstruction in multimodal image-guided neurosurgery: Methods and performance evaluation," vol. 24, no. 11, pp. 1500–1511, 2005.

[8] K. Pulli, M. Cohen, T. Duchamp, H. Hoppe, L. Shapiro, and W. Stuetzle, "View-based rendering: Visualizing real objects from scanned range and color data," in *Eurographics Rendering Workshop*. Springer Wien, June 97, pp. 23–34.

[9] Y. Sako and K. Fujimura, "Shape similarity by homotropic deformation," *The Visual Computer*, vol. 16, no. 1, pp. 47–61, 2000.

[10] D. Dey, D. G. Gobbi, P. J. Slomka, K. J. M. Surry, and T. M. Peters, "Automatic fusion of freehand endoscopic brain images to three-dimensional surfaces: Creating stereoscopic panoramas," pp. 23–30, 2002.

[11] M. J. Clarkson, D. Rueckert, D. L. Hill, and D. J. Hawkes, "Registration of multiple video images to preoperative ct for image-guided surgery," in *SPIE Medical Imaging*, 1999, pp. 14–23.

[12] B. Levy, "Constrained texture mapping for polygonal meshes," in *Proceedings of SIGGRAPH*, 2001, pp. 417–424.

[13] M. Desbrun, M. Meyer, and P. Alliez, "Intrinsic parameterizations of surface meshes," in *Proceedings of Eurographics*, 2002.

[14] V. Kraevoy, A. Sheffer, and C. Gotsman, "Matchmaker: Constructing constrained texture maps," in *Proceedings of SIGGRAPH*, 2003, pp. 326–333.

[15] F. Mourgues, T. Vieville, V. Falk, and E. Coste-Maniere, "Interactive guidance by image overlay in robot assisted coronary artery bypass," in *Proceedings of Medical Image Computing and Computer-Assisted Intervention (MICCAI)*, 2003, pp. 173–181.

[16] M. I. Miga, T. K. Sinha, D. M. Cash, R. L. Galloway, and R. J. Weil, "Cortical surface registration for image-guided neurosurgery using laser-range scanning," vol. 22, no. 8, pp. 973–985, 2003.
[17] T. K. Sinha, B. M. Dawant, V. Duay, D. M. Cash, R. J. Weil, R. C. Thompson, K. D. Weaver, and M. I. Miga, "A method to track cortical surface deformations using a laser range scanner," vol. 24, no. 6, pp. 767–781, 2005.
[18] S. Szpala, M. Wierzbicki, G. Guiraudon, and T. M. Peters, "Real-time fusion of endoscopic views with dynamic 3-d cardiac images: A phantom study," vol. 24, no. 9, pp. 1207–1215, 2005.
[19] M. D. Elstrom and P. W. Smith, "Stereo-based registration of multi-sensor imagery for enhanced visualization of remote environments," in *Proceedings of the IEEE International Conference on Robotics & Automation*, 1999, pp. 1948–1953.
[20] R. Kurazume, K. Nishino, Z. Zhang, and K. Ikeuchi, "Simultaneous 2d images and 3d geometric model registration for texture mapping utilizing reflectance attribute," in *Proceedings of the 5th Asian Conference on Computer Vision*, 2002, pp. 23–25.
[21] K. Umeda, G. Godin, and M. Rioux, "Registration of range and color images using gradient constraints and range intensity images," in *Proceedings of the 17th International Conference on Pattern Recognition*, 2004, pp. 12–15.
[22] L. Brunie, S. Lavallee, and R. Szeliski, "Using force fields derived from 3d distance maps for inferring the attitude of a 3d rigid object," in *Proceedings of the Second European Conference on Computer Vision*, 1992, pp. 670–675.
[23] S. Lavallee and R. Szeliski, "Recovering the position and orientation of free-form objects from image contours using 3d distance maps," pp. 378–390, 1995.
[24] K. Matsushita and T. Kaneko, "Efficient and handy texture mapping on 3d surfaces," in *Computer Graphics Forum 18*, 1999, pp. 349–358.
[25] P. J. Neugebauer and K. Klein, "Texturing 3d models of real world objects from multiple unregistered photographic views," in *Computer Graphics Forum 18*, 1999, pp. 245–256.
[26] B. D. Lucas and T. Kanade, "An iterative image registration technique with an application to stereo vision," in *Proceedings of the 7th International Joint Conference on Artificial Intelligence*, 1981, pp. 674–679.
[27] C. Tomasi and T. Kanade, "Detection and tracking of point features," Carnegie Mellon University, Tech. Rep. CMU-CS-91-132, April 1991.
[28] D. G. Lowe, "Distinctive image features from scale-invariant keypoints," in *International Journal of Computer Vision*, vol. 20, 2003, pp. 91–110.
[29] D. Lowe, "Object recognition from local scale-invariant features," in *Proc. of the International Conference on Computer Vision ICCV*, 1999, pp. 1150–1157.
[30] I. Eckstein, V. Surazhsky, and C. Gotsman, "Texture mapping with hard constraints," in *Computer Graphics Forum*, vol. 20, no. 3, 2001, pp. 95–104.
[31] V. Kraevoy and A. Sheffer, "Cross-parameterization and compatible remeshing of 3d models," in *Proceedings of SIGGRAPH*, 2004, pp. 861–869.
[32] J. Schreiner, A. Asirvatham, E. Praun, and H. Hoppe, "Inter-surface mapping," in *Proceedings of SIGGRAPH*, 2004, pp. 870–877.
[33] K. Zhou, X. Wang, Y. Tong, M. Desbrun, B. Guo, and H.-Y. Shum, "Texturemontage," in *Proceedings of SIGGRAPH*, 2005, pp. 1148–1155.
[34] B. Levy, S. Petitjean, N. Ray, and J. Maillot, "Least squares conformal maps for automatic texture atlas generation," in *In Proceedings of SIGGRAPH*, 2002, pp. 362–371.
[35] A. Khodakovsky, N. Litke, and P. Schroder, "Globally smooth parameterizations with low distortion," in *Proceedings of SIGGRAPH*, vol. 1, 2003, pp. 350–357.
[36] M. Brown and D. G. Lowe, "Recognising panoramas," in *Proceedings of the Ninth IEEE International Conference on Computer Vision*, 2003, pp. 1218–1225.
[37] R. Szeliski and H.-Y. Shum, "Creating full view panoramic image mosaics and environment maps," in *In Proceedings of SIGGRAPH*, 1997, pp. 251–258.
[38] R. Hartley and A. Zisserman, *Multiple View Geometry in Computer Vision*, 2nd ed. Cambridge University Press, ISBN: 0521540518, 2004.

Submitted to ISBI 2009

MODEL BASED ESTIMATION AND VISUALIZATION OF GLOBAL OBJECT DEFORMATIONS FOR LAPAROSCOPIC RENAL CRYOABLATION

Qiong Han, Melody Carswell, Williams B. Seales

Center for Visualization and Virtual Environments
University of Kentucky

Stephen E. Strup M.D.

Division of Urology
Department of Surgery
University of Kentucky

ABSTRACT

The incorporation of pre-operative images into minimally invasive surgeries (MIS) can provide surgeons a global field of view and important visual cues that were not available, such as a tumor mostly hidden inside a target object. This paper focuses on using a geometric deformation model to guide the registration of a pre-built 3D model from pre-operative images to a small set of reconstructed 3D surface landmarks from a laparoscopic video sequence. Intra-operative tissue deformations of the target object are used to estimate deformations of important substructures, such as a tumor or a group of vessels, of the target object. Evaluation results of the registration and the deformation estimation show that our method performs well on the type of soft tissue deformations in our driving application.

***Index Terms*—** Deformable Model, Geometric Deformation Model, Intra-operative Navigation, Minimally Invasive Surgery

1. INTRODUCTION

Minimally invasive surgery (MIS) has the advantage of inducing less trauma to patients. However, the narrow field of view provided by an endoscopic or laparoscopic camera is one of the limiting factors of this technique. Recent research work has focused on incorporating preoperative images into MIS to provide more information intra-operatively.

[1] proposed to reconstruct a dense 3D surface from intra-operative data by Markov Random Field (MRF) based Bayesian belief propagation for smoothly fusing multiple depth cues, which requires repeatable tracking of a large number of feature points. In [2], a statistical deformation model was built from simulated deformations of a finite element model of prostates. As an extension to [2], Hu et al. included material properties in their simulated deformations and used a pre-learned statistical motion model to predict a displacement field over an entire prostate volume based on surface landmarks on the prostate [3].

This paper proposes a method to estimate and visualize intra-operative tissue deformations of a target anatomical object. Our method only requires a small number of reconstructed surface landmarks on the object, and it does not require modeling material properties. The estimated deformations of the target object are applied to substructures of the target object, such as a tumor mostly or entirely hidden within the surface of the target object. One of our driving applications is laparoscopic renal cryoablation on small tumors. A 3D visualization of the renal tumor during a laparoscopic cryoablation can greatly increase the positioning accuracy of the ablation site, compared with the current ultra-sound guided procedure.

In our method, a specific geometric deformation model is built for each target kidney to guide the registration of the pre-built kidney model to a small set of reconstructed 3D surface points from a laparoscopic video sequence. Once the model itself is registered, its deformations are applied to the tumor model. The tumor can then be visualized intra-operatively. If pre-planned needle insertion path is available, they can also be transformed into the camera view to better guide the ablation procedure.

Next section details our proposed method by its three main components: the geometric deformation model, the registration of the 3D model, and the implied deformations for the substructure(s). Section 3 describes the evaluation of the proposed method. Section 4 concludes this paper with discussions.

2. METHOD

In order to incorporate the pre-operative scans efficiently for a specific patient, we adopt a deformable model framework. The main components of our method are shown as follows:

1. Building a 3D model from the pre-operative scan image;
2. Building a geometric deformation model for the 3D model, controlled by a small number of parameters;
3. Identifying a small set of surface feature points of anatomical significance on the target object from the laparoscopic video sequence, tracking the feature points,

and reconstructing 3D landmarks from these tracked feature points;

4. Registering the pre-built 3D model to the reconstructed 3D landmarks using the geometric deformation model;

5. Applying the deformation of the registered 3D model to its internal or adjacent substructures, such as a tumor.

The 3D model is built from segmented pre-operative CT images. At this moment, the image segmentation is manually contoured by experts, and then a 3D deformable model is fitted into the segmentation using the binary fitting method described in [4]. The *discrete m-rep* [5] is chosen as the shape model because of its unique property of modeling both the surface and the interior volume of an object.

For the 3D reconstruction from a laparoscopic video sequence, a small set of anatomical points are identified by surgeons intra-operatively from the video sequence and are tracked throughout the procedure. Artificial markers can be used to increase the accuracy of the feature tracking. This set of tracked points are then fed into a structure from motion (SFM) toolkit to reconstruct their corresponding 3D surface landmarks. Although this step is not the main focus of this paper, the accuracy of the 3D reconstruction is crucial to the following steps. Ongoing research is being conducted to improve the reconstruction accuracy of the landmarks.

This paper focuses on components 2, 4, and 5 described above. Based on the assumption that a kidney goes through moderate global shape deformations before the needle insertion for a cryoablation, a geometric deformation model is defined to describe the global deformations, including bending and twisting. The modes of deformations, controlled by 3 parameters, are used as a shape prior model to guide the registration of the pre-built model to the reconstructed set of landmarks.

The advantage of our method is that only a small set of landmarks is needed, so it is feasible to use artificial markers to ensure robust tracking of the corresponding feature points and thus to ensure accurate reconstruction of the landmarks. The rest of this section details components 2, 4, and 5.

2.1. Definition of a geometric deformation model

A discrete m-rep $\mathbf{M}$ consists of a quad-mesh of basic components called medial atoms $\mathbf{m}_i, i = 1, 2, ..., n_m$. Each internal atom $\mathbf{m}_i$ has a hub position $\mathbf{p}_i$, two spokes $\mathbf{S}_i^{+1,-1}$ with length r_i and directions $\mathbf{U}_i^{+1,-1}$. Atoms at the edge of the quad-mesh also has a third spoke $\mathbf{S}^0$ with length of ηr and direction $\mathbf{U}^0$. More details of the m-rep can be found in [5].

To define a geometric deformation model for an m-rep $\mathbf{M}$, two axis directions for $\mathbf{M}$ are defined to form a reference frame. Assume the set of hub positions and spoke end points of all medial atoms in $\mathbf{M}$ is $\mathbf{S} = \{\mathbf{s}_j, j = 1, 2, ..., n_S\}$. Principal component analysis (PCA) is applied to the points in $\mathbf{S}$, and the first two principal directions, $\mathbf{A}_1$ and $\mathbf{A}_2$ corresponding to the biggest two eigenvalues of the covariance matrix, are defined as the axis directions of the local frame. The "origin" $\mathbf{O}$ of the frame is set at the arithmetic mean of points in $\mathbf{S}$. 3 geometric deformations are defined for each $\mathbf{M}$ based on the reference frame. These 3 deformations are chosen by experienced urologists with a comprehensive understanding of the deformations of kidneys:

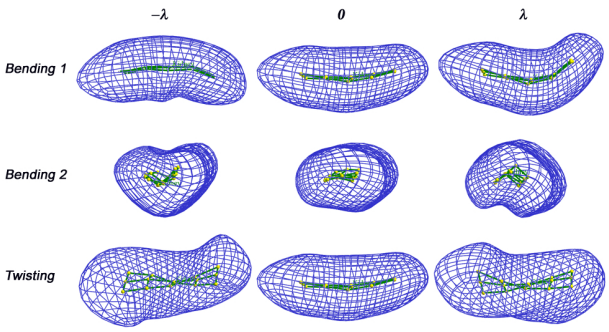

Fig. 1. Demonstration of the 3 modes of deformations of bending and twisting: each row shows one mode from $-\lambda$, 0, to λ, from left to right.

- $\mathbf{B}_1$ relative to $\mathbf{A}_1$: for each atom $\mathbf{m}_i$, let the distance from its hub position to axis $\mathbf{A}_1$ be $d_{i,1}$, atom $\mathbf{m}_i$ is rotated around $\mathbf{A}_1$ by a degree of $\alpha_1 d_{i,1}^2$;

- $\mathbf{B}_2$ relative to $\mathbf{A}_2$: for each atom $\mathbf{m}_i$, let the distance from its hub position and axis $\mathbf{A}_2$ be $d_{i,2}$, atom $\mathbf{m}_i$ is rotated around $\mathbf{A}_2$ by a degree of $\alpha_2 d_{i,2}^2$;

- **Tw**: project the hub position of each medial atom $\mathbf{m}_i$ into the reference frame spanned by $\mathbf{A}_1, \mathbf{A}_2$. Assume the projected point is (x_i', y_i'), so $\mathbf{m}_i$ is rotated around the axis $\mathbf{A}_1$ by a degree of $\beta x_i'$.

where $\alpha_1, \alpha_2, \beta$ are normally distributed random variables controlling the amount of bending relative to $\mathbf{A}_1$, bending relative to $\mathbf{A}_2$, and twisting **Tw**, respectively. These three deformations are demonstrated in figure 1 for one kidney model.

The means of α_1, α_2, and β, are all set 0, and the variances of them are 0.3, 0.15, and 0.2, respectively. These values are empirically determined to ensure the combined deformation applied to $\mathbf{M}$ does not yield any illegal shapes with local shape defects, such as folding. 100 sets of $(\alpha_1, \alpha_2, \beta)$ are sampled from the 3 zero-mean normal distributions. The combined deformation $\mathbf{D} = \mathbf{TwB}_2\mathbf{B}_1$ is applied to $\mathbf{M}$ to get $\mathbf{M}' = \mathbf{D} \circ (\mathbf{M})$. Principal geodesic analysis (PGA) [6] is applied to the 100 deformed m-reps to form a deformation prior model, given as a Frechét mean $\overline{\mathbf{M}}$, the first few principal geodesic directions ν_i representing more than 99% of the total shape variations, and the corresponding variances λ_i to

the principal geodesic directions. In practice, the first 3 principal geodesic directions and variances $\nu_i, \lambda_i, i = 1, 2, 3$ are used to describe the deformation model: $\{\overline{\mathbf{M}}|\lambda_i, \nu_i\}$.

2.2. Model registration

The mean model $\overline{\mathbf{M}}$ is registered (fitted) to a set of reconstructed landmarks $\mathbf{L} = \{\mathbf{l}_i \, i = 1, 2, ..., n_l\}$. For each $\mathbf{l}_i$, there is a corresponding point $\mathbf{k}_i$ on the implied surface of $\overline{\mathbf{M}}$. The fitting is implemented by minimizing an objective function:

$$\mathbf{M}' = \arg\min_{\mathbf{M}'} F(\mathbf{M}'(\{c_j, j = 1, 2, 3\}))$$

where $\mathbf{M}'$ is constructed by $\overline{\mathbf{M}}$ and a tangent vector $\sum_{j=1}^{3} c_j \nu_j$ via the exponential map [6], where c_j is the set of parameters controlling the deformations. $F(\mathbf{M}')$ has three components, $F(\mathbf{M}') = t_1 F_{fit}(\mathbf{M}') + t_2 F_{regularization}(\mathbf{M}') + (1 - t_1 - t_2) F_{leg}(\mathbf{M}')$, with t_1, t_2, and $t_1 + t_2 \in (0, 1)$ as two tuning parameters:

- $F_{fit} = \Sigma_{i=1}^{n_l} (\frac{dis(\mathbf{k}_i(\mathbf{M}'), \mathbf{l}_i)}{r_{mean}})^2$ measuring the fitting quality of the model to the set of landmarks, where dis is the Euclidean distance between a landmark $\mathbf{l}_i$ and its corresponding surface point $\mathbf{k}_i$ on the implied surface of $\mathbf{M}'$, and where r_{mean} is the geometric mean of the radii of all medial atoms in $\mathbf{M}'$ and is used to convert F_{fit} to be unitless, commensurate to the other 2 components of the objective function;
- $F_{maha} = \Sigma_{i=1}^{4} (\frac{c_j}{\lambda_j})^2$ is the squared Mahalanobis distance of the current model $\mathbf{M}'$ to the mean model $\overline{\mathbf{M}}$, penalizing large deformations of $\mathbf{M}'$;
- $F_{leg} = \Sigma_{i=1}^{n_m} f_{leg}(\mathbf{m}'_i)$, where $\mathbf{m}'_i$ is a medial atom in $\mathbf{M}'$, and where f_{leg} is the illegality penalty term defined by equation (12) in [4].

The overall objective function is optimized over principal geodesic components c_j in the deformation model, while big deformations and shape illegalities are penalized. To initialize the optimization, $\{c_j\}$ are all set 0, and $\overline{\mathbf{M}}$ is aligned to the set of landmarks $\mathbf{L}$ by a rigid transformation plus scaling. The objective function is optimized via conjugate gradient method. With only 3 parameters, the optimal solution converges fast, normally within 30-40 iterations.

2.3. Deformation application to important substructures

The models before and after the registration are used to imply a deformation field for the interior and the adjacent exterior volume of the target object. An m-rep parameterizes the interior and adjacent exterior volume. When the original m-rep is built from a segmented pre-operative image, its substructures, such as a tumor, are also built. The implied deformation field is applied to the tumor volume, voxel by voxel. Because of the enforced legality of the deformed $\mathbf{M}'$ by the illegality penalty term f_{leg} in the objective function, the volumetric legalities of both of the models, before and after the registration, are guaranteed. Therefore, the implied deformation field is guaranteed to be legal, without any local folding. Next section evaluates the proposed method and shows the results.

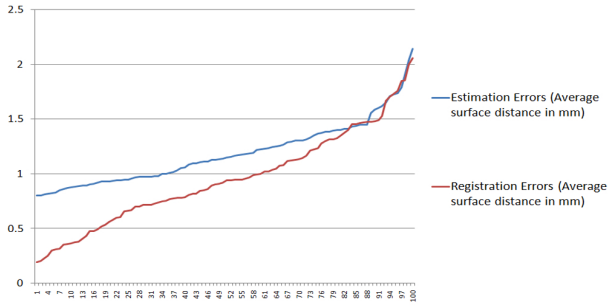

Fig. 2. Sorted evaluation results of registered kidney models or estimated tumor models in terms of average surface distances (ASD) between the registered or estimated models and their corresponding ground truth surface meshes. For almost all testing cases, the ASDs for the implied deformations to tumors are bigger than the ASDs for the registered kidney models.

3. RESULTS

In order to evaluate the proposed method, a set of kidney models with synthetic deformations is generated. Synthetic data provide the ground truth to measure the registration and estimation errors.

Learned PGA shape statistics from 50 kidney models are sampled by the Monte Carlo sampling scheme [7] to generate 100 testing kidney m-rep models $\{\mathbf{M}_i, i = 1, 2, .., 100\}$. A reference frame represented by $\mathbf{A}_{i,1}$ and $\mathbf{A}_{i,2}$ centered at $\mathbf{O}_i$ is calculated for each kidney m-rep $\mathbf{M}_i$. $\mathbf{M}_i$ is then transformed to align its reference frame to standard axes (y, z) centered at the origin. Each kidney volume, implied by the m-rep $\mathbf{M}_i$, is warped by a diffeomorphic deformation that is defined independently from the m-rep. We used a same set of deformations, including bending and twisting, to keep the synthesized deformations close to the real kidney deformations. Each diffeomorphic deformation $\mathbf{T}$ is defined as follows:

$$x' = x \quad (1)$$
$$y' = y\cos(\beta x) - z\sin(\beta x) + \alpha_2 x^2 \quad (2)$$
$$z' = y\sin(\beta x) + z\cos(\beta x) + \alpha_1 x^2 \quad (3)$$

where α_1, α_2 and β are 3 random variables controlling the deformation.

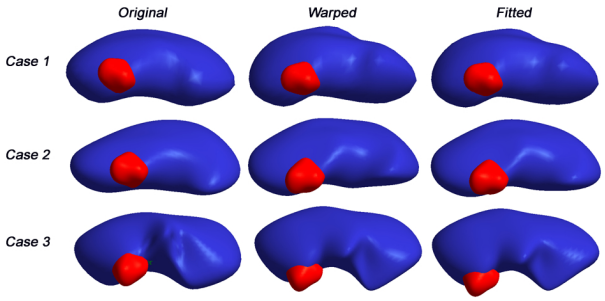

Fig. 3. 3 testing kidney m-reps, from left to right: the original kidney m-rep $\mathbf{M}_i$ (in blue), the ground truth surface mesh of the kidney and tumor (in red) reconstructed from warped object volume, and the fitted (registered) m-rep $\mathbf{M}_i'$ with the deformation applied to its attached tumor model.

Because the Jacobian determinant of $\mathbf{T}$ is 1, $\mathbf{T}$ is indeed a diffeomorphic deformation. A tumor m-rep $\mathbf{M}_{tumor}$ is attached to each testing kidney m-rep $\mathbf{M}_i$. A randomized $\mathbf{T}_i$ is applied to warp the volumes of $\mathbf{M}_i$ and $\mathbf{M}_{tumor}$. Surface meshes $\mathbf{S}'_{kidney,i}$ and $\mathbf{S}'_{tumor,i}$ are reconstructed from the warped kidney and tumor volumes as the ground truth, respectively.

A set of 6 landmarks $\mathbf{L}_i$ are automatically identified on each deformed kidney surface $\mathbf{S}'_{kidney,i}$. Using the proposed method, each model $\mathbf{M}_i$ is fitted to the set of landmarks $\mathbf{L}_i$ to form a registered kidney model $\mathbf{M}_i'$. The registration error is measured by the average surface distance between the implied surface mesh of $\mathbf{M}_i'$ and the ground truth surface $\mathbf{S}'_{kidney,i}$. The deformation between $\mathbf{M}_i$ and $\mathbf{M}_i'$ is then applied to the tumor $\mathbf{M}_{tumor}$ to form an estimated tumor model $\mathbf{M}'_{i,tumor}$. The estimation error is measured by the average surface distance between the implied surface mesh of $\mathbf{M}'_{i,tumor}$ and the ground truth surface $\mathbf{S}'_{tumor,i}$. The evaluation results of the registration and estimation are shown in figure 2.

The average surface distance is within the range of $1.35 - 2.17mm$, which is comparable to the reports results in [3]. Three testing kidneys are shown in figure 3.

4. DISCUSSION

The evaluation results show that our proposed registration and deformation estimation method performs well against simulated kidney models with moderate deformations. We are working on evaluating the proposed method on captured laparoscopic video sequences. Compared with previously proposed methods, our method uses a geometric deformation model. Our method is based on the reconstruction of a small set of 3D landmarks to estimate moderate soft tissue deformations. Given the small number of landmarks, it is feasible to use robust markers to significantly improve the quality of tracking, so we expect to have robust reconstructions in future experiments. Another direct application of our method is surgical planning. For example, with the renal tumor accurately located, pre-planned needle insertion paths can be adapted to the tissue deformations in real time.

One limitation of our method is that it is not designed to directly estimate large deformations. Although the current setup is suitable for our driving applications, such as renal cryoablation, in which the kidney can be controlled to have moderate deformations, a means to extend our method to handle large tissue deformations is to extend the geometric deformation model to a statistical deformation model that could be learned from sufficient amount of training data.

5. ACKNOWLEDGEMENTS

6. REFERENCES

[1] Benny P. Lo, Marco Visentini Scarzanella, Danail Stoyanov, and Guang-Zhong Yang, "Belief propagation for depth cue fusion in minimally invasive surgery," in *MICCAI*, 2008, pp. 104–112.

[2] Ashraf Mohamed, Christos Davatzikos, and Russell Taylor, "A combined statistical and biomechanical model for estimation of intra-operative prostate deformation," in *MICCAI*, 2002, pp. 452–460.

[3] Yipeng Hu, Dominic Morgan, Hashim Uddin Ahmed, Doug Pends, Mahua Sahu, Clare Allen, Mark Emberton, David Hawkes, and Dean Barratt, "A statistical motion model based on biomechanical simulations for data fusion during image-guided prostate interventions," in *MICCAI*, 2008, pp. 737–744.

[4] Qiong Han, Derek Merck, Josh Levy, Christina Villarruel, James N. Damon, Edward L. Chaney, and Stephen M. Pizer, "Geometrically proper models in statistical training," in *IPMI2007, LNCS 4584*. IPMI, 2007, pp. 751–762, Springer-Verlag.

[5] S. M. Pizer, T. Fletcher, Y. Fridman, D. S. Fritsch, A. G. Gash, J. M. Glotzer, S. Joshi, A. Thall, G. Tracton, P. Yushkevich, and E. L. Chaney, "Deformable m-reps for 3d medical image segmentation," *International Journal of Computer Vision - Special UNC-MIDAG issue*, vol. 55, no. 2, pp. 85–106, 2003.

[6] P. Thomas Fletcher, Conglin Lu, Stephen M. Pizer, and Sarang Joshi, "Principal geodesic analysis for the nonlinear study of shape," *Transactions on Medical Imaging (TMI)*, vol. 23, no. 8, pp. 995–1005, 2004.

[7] N. Metropolis and S. Ulam, "The monte carlo method," *Journal of the American Statistical Association*, vol. 44, no. 247, pp. 335–341, 1949.

Cognitive Simulation in Virtual Patients

Sergei Nirenburg, Marjorie McShane, Stephen Beale

University of Maryland, Baltimore County
{sergei,marge,sbeale,tomohara}@umbc.edu

Bruce Jarrell, George Fantry

University of Maryland School of Medicine
bjarrell@som.umaryland.edu
gfantry@medicine.umaryland.edu

The Maryland Virtual Patient (MVP) project aims to create an environment where a physician user can manage a complex virtual patient who is suffering from one or more diseases. Once developed, this environment will allow for multiple capabilities, including trial-and-error learning, tutored learning, and assistance with problem solving in treating real patients. Last year we presented our progress by demonstrating virtual patients suffering from complex esophageal diseases that progressed over time. These patients behaved in a clinically appropriate fashion and reacted in realistic ways to interventions. The physician could use drop-down menus to select queries, tests and interventions, as well as observe the responses and subsequent disease progression. Simulation was supported by an intelligent agent in the MVP whose main component is a model of normal and abnormal physiology. During the past year, we have developed three additional components of the intelligent agent: a) two types of perception: perception of stimuli originating inside of the body (interoception) and the perception of natural language communication (language perception), b) a model of cognitive decision-making and c) a model of verbal and simulated physical action.

Perception: The physiological component of the agent communicates with the cognitive component as simulated interoception to produce symptom perception by the cognitive agent. Language perception allows the cognitive agent to understand the meaning of inputs it obtains from the physician user.

Cognitive Decision-Making: This module of the system uses several types of input and knowledge to model agent decision making, including: interoception; input from the physician; the resident knowledge possessed by the agent; and the agent's personality traits.

Simulated Action: In the current simulation, the action can be verbal (for example, a response to the physician's question), or simulated physical (for example, taking medication or presenting at the physician's office). Our objective is to model these actions in a way that would be natural for people.

The variables used in building this model of an intelligent virtual patient include:

- Life goals, such as the desire to be healthy
- Character traits, such as
  - Attitude toward visits to the physician
  - Courage to be treated
  - Trust in the physician's skill
  - Suggestibility with respect to the physician's recommendations
- Physiological traits, such as

  - Tolerance to pain
  - Tolerance to symptoms
  - Tolerance to external stressors
- Intellectual traits, such as
  - Memory/forgetfulness of symptoms and events
  - Knowledge about the disease
  - Knowledge about the tests and interventions
  - Retention of knowledge gleaned in conversation with the physician.

Language Processing Capabilities.

When free-text input is received from the physician, it is interpreted and assigned a formal text meaning representation. During this process, both the meaning and intention of the input are determined. Indirect speech acts, such as implied questions not stated in a question format, are handled appropriately. Physician input that is currently interpreted by the MVP agent includes:

1. a request for physiological data (test results), perception of symptoms, and memory of health events
2. a request for permission to carry out a test or intervention
3. a request to perform an intervention
4. a request to return to see the physician at a later date
5. a response to an MVP question
6. unsolicited knowledge provided to the MVP by the physician

Natural language output is provided to the physician after processing by the MVP agent. All responses are based upon evaluations of the physiological state of the MVP in concert with the perception of symptoms and cognitive functions. Potential MVP agent output includes:

1. providing requested data
2. requesting additional information
3. inquiring about other treatment options available at a given time
4. agreeing to or refusing to submit to the physician's suggestion for a test or intervention
5. storing new knowledge in the MVP memory
6. presenting to the physician in response to an intolerable state of health (as defined by the MVP) for a first or subsequent visit
7. presenting to the physician at a later date in response to the physician's request

We will demonstrate this process by communicating in natural language with two simulated patients. The first patient is a knowledgeable individual who: a) foresees additional information the physician might desire, such as the frequency of a symptom when asked if he experiences that symptom, and b) desires a lot of additional information about what the user proposes to do. In addition, the first patient learns from the encounter, so that the next time the physician suggests an intervention which the patient already knows about, the patient agrees without further questioning because he remembers the results of the original decision-making process. The second patient: a) is a trusting individual who essentially agrees to all suggestions with no

questions asked and b) responds to all questions quite literally, not providing any additional explanatory information.

In summary, we will display several accomplishments:

1. The MVP retains its previous physiological complexity while gaining the ability to communicate in natural language and to incorporate interoception, cognitive traits and behavioral traits in its own health care decision-making
2. The MVP has personality traits that give it curiosity, free-will and other human characteristics when responding to the physician
3. The MVP can learn from explanations and actions by the physician and use that knowledge in future decisions about health care
4. The MVP interaction involves a conversation that is becoming very realistic.

Surgical Ergonomics in Minimally Invasive Surgery

Gyusung Lee, PhD

Surgical Ergonomics Laboratory
Maryland Advanced Simulation, Training, Research, and Innovation (MASTRI) Center

Division of General Surgery
University of Maryland School of Medicine
Baltimore, Maryland

Why Do We Need Ergonomics in MIS?

- Patients benefit while surgeons suffer
  - Patients: Less traumatic alternative to open surgery
  - Surgeons: Ergonomic problems are not inevitable
- Recent on-line survey study (Park *et al*., ACS 2008)
  - ~90% physical discomfort or complications
  - Complication report rate is correlated
    - with number of cases per year
    - not with age or practicing years
- Examples (Kano et al, 1993, 1995; Cuschieri, 1995 ; Berguer et al, 1999)
  - Increased upper extremity fatigue
  - Carpal tunnel syndrome & neuropraxia
  - Problems in neck, lower back, and lower extremities
- Surgeons deserve ergonomically friendly environment

2

Research Goals

Surgical Ergonomics Laboratory at the MASTRI Center

- **B**etter ergonomics
  - To identify the ergonomic risk factors associated with laparoscopy and find solutions (physical and cognitive ergonomics)
- **B**etter environment
  - To evaluate ergonomic impact and efficacy of new technolog**ies** and development
    - New laparoscopic instruments and training station
- **B**etter training
  - To create standard matrices of expert surgical movements from **analysis** of the characteristics of surgical movements
  - To develop more effective training protocol based on the standard matrices

3

What Makes Us Unique?

- Integration of state-of-the-art experiment systems
  - 12-camera Vicon™ motion analysis system
  - 2 AMTI™ force plates
  - 16-channel Delsys™ EMG system
  - Custom data analysis programs
- Systematic biomechanical approaches
  - Postural sway area analysis
  - Postural Stability Demand (PSD)
  - Biomechanical knee model

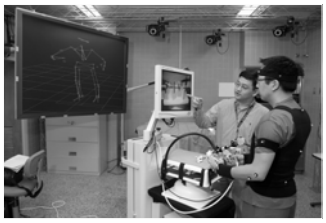

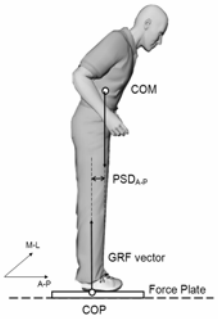

4

Past Projects

- Compensatory and strategic movement analysis during FLS tasks
  - Postural instability represented by increased postural sway does not necessarily correlate to poor surgical performance
- Postural sway analysis during FLS tasks
  - More experienced MIS surgeons used task-specific and skill-related postural control
- Surgical movement analysis
  - Experienced surgeons showed unique sets of joint movements
- Assessment of optimal OR table height
  - Different OR Table heights were required for laparoscopic instruments **of** different designs (pistol grip and in-line grip)
- Assessment of surgical assistant during simulated surgery
  - Due to the leaning posture and extended arm position, the supporting leg of the surgical assistant disproportionately bore 70-80% of whole body weight
- Online ergonomic survey study
  - Comprehensive survey study performed with 317 **practicing** MIS surgeons

5

Ongoing Projects

- Postural analysis of laparoscopic surgeons in OR theater
  - Force plate data collection during surgical cases
- Ergonomic assessment of one-handed vs. two-handed surgical technique during VR cholecystectomy
  - Determining which technique is more ergonomically sound and which is best used in training
- Assessment of ergonomics related to NOTES
  - Comprehensive comparison between traditional laparoscopy, flexible endoscopy, and innovative NOTES platform
- Longitudinal study of clinical fellowship program
  - Comparing surgical skill levels of research versus clinical fellows
- Ergonomic assessment of new laparoscopic instruments

6

What are our long-term goals?

- Expanding our research boundary to unexplored or less explored territories
  - New approaches
    - Development of analysis metrics for data collected over long-period of time (e.g. muscle workload)
    - Biomechanical models to better understand etiologies of physical symptoms
  - New research areas
    - Ergonomics in Flexible Endoscopy
    - Ergonomics in NOTES
    - Ergonomics associated with OR staff (other than surgeons)

7

What are our long-term goals? (cont.)

- Delivery of research outcomes for the real world
  - Application of research for better surgical training
    - Self-mentoring surgical training system with augmented reality
      - Collaboration of surgical ergonomics group with smart image group
  - Collaborations with industrial partners
    - Surgical instrument designs and testing
    - Intra-operative instrument tracking
  - Outreach
    - Presentations at national/international conferences & published manuscripts
    - Recommendations and guidelines, professional societies, grand rounds

8

Accomplishments

- 4 Peer-reviewed publications
  - **Lee G**, Kavic SM, George IM, Park AE (2007) Postural instability does not necessarily correlate to poor performance: Case in point, Surg Endosc. 21:471-474
  - **Lee G**, Lee T, Dexter D, Klein R, Park AE (2007) Methodological infrastructure in surgical ergonomics, a review of task, model, measurement systems. Surg Innov. 14(3):153-167
  - **Lee G**, Park AE (2007) Development of a more robust tool for postural stability analysis of laparoscopic surgeons. Surg Endosc. 22(4):1087-1092
  - **Lee G**, Lee TH. Dexter DJ, Godinez C, Meenaghan N, Catania R and Park AE (2008) Ergonomic risk of assisting in minimally invasive surgery, Surgical Endoscopy, Epub ahead of print
- Grant support
  - 2008 NOSCAR Olympus Medical Systems Research Award
  - Title: Quantitative ergonomic assessment of NOTES techniques

- 16 Conference abstracts
- **Lee G**, Weiner M, Kavic SM, George IM, Shapiro R, Park AE (2006) Postural instability does not necessarily correlate to poor performance, Surg Endosc 20 (Suppl 1): S345
- **Lee G**, Weiner M, Kavic SM, George IM, Park AE (2006) Pilot study – Correlation between postural stability and performance time during fundamentals of laparoscopic surgery (FLS) tasks, Br J Surg. 93 (Suppl 1): 206
- **Lee G**, Weiner M, Kavic SM, George IM, Park AE (2006) Joint kinematics vary with performance skills during laparoscopic exercise [Fundamentals of Laparoscopic Surgery (FLS) task 1], Gastroenterology. 130 (Suppl 4): A911
- **Lee G**, Kavic SM, Shapiro R, George IM, Park AE (2006) Analysis of systematic changes in posture and joint kinematics demonstrated by minimally invasive surgeons. Program No. 452.10, 2006 Neuroscience Meeting Planner, Atlanta, GA: Society for Neuroscience.
- **Lee G,** Kavic SM, George IM, Park AE (2007) MIS surgical ergonomics: Future Trends, Annual conference of MMVR, Long Beach, CA
- **Lee G** and Park AE (2007) Development of a novel tool to more precisely analyze postural stability of laparoscopic surgeons. Surg Endosc. 21 (Suppl 1): S317
- **Lee G**, Dexter DJ, Lee TH, Roth JS, Turner P, Kavic SM, Park AE (2007) Assessment of table height change with laparoscopic instrument change, Surg Endosc. 21 (Suppl 1): S421
- **Lee G**, Dexter DJ, Lee TH, Park AE (2007) Subtask analysis of joint angles is key to characterizing surgical movement. Gastroenterology. 132 (Suppl 1): A894
- **Lee G**, Lee TH, Klein R, Dexter DJ and Park AE (2008) Perfect partners: Surgical ergonomics and minimally invasive training, Annual conference of MMVR
- **Lee G**, Lee TH. Dexter DJ, Godinez C, Meenaghan N, Catania R and Park AE (2008) Ergonomic risk of assisting in minimally invasive surgery. Surg Endosc. 22 (suppl 1) :S160
- Park AE, Meenaghan N, Lee TH, Seagull FJ, **Lee G** (2008) Patients benefit while surgeons suffer: an impending epidemic, ACS 2008
- **Lee G**, Lee TH, Dexter DJ, Godinez C, Meenaghan N, Park AE (2008) Joint kinetic data augments traditional biomechanical approach to assess the ergonomics of laparoscopic camera assistants, Annual conference of MMVR
- **Lee G**, Meenaghan N, Lee TH, Dexter DJ, Godinez C, Seagull FJ, Park A (2008) A pain in the neck! The relationship of video monitors to surgeons's stress, Annual conference of SAGES 2009, Pheonix, AZ
- **Lee G**, Lee TH, Dexter DJ, Park AE (2008) Traditional biomechanical approach augmented by joint kinetic data in ergonomic risk assessment of laparoscopic assistants, Annual conference of SAGES 2009, Pheonix, AZ
- Seagull FJ, Lee TH, Sutton E, Godinez C, **Lee G**, Park AE (2008) A validated subjective rating of display quality: The Maryland Visual Comfort Scale, Annual conference of SAGES 2009, Pheonix, AZ
- **Lee G**, Seagull FJ, Park A (2008) The ergonomic limitations of robotic surgery, Annual conference of Minimally Invasive Robotic Association, Quebec, Canada

Acknowledgements

- Adrian Park, MD
- Stephen Kavic, MD
- Tommy H. Lee, MD
- Robert Catania, MD
- Elizabeth Franco, MD
- Carlos Godinez, MD
- Erica Sutton, MD
- David Dexter, MD
- Nora Meenaghan, MD
- Yassar Youseff, MD
- Gerald Moses, PhD
- F. Jacob Seagull, PhD
- Brent Seales, PhD
- Melody Carswell, PhD
- Tsegay Baraki, MSc
- Rosemary Klein, MA
- Ivan M. George
- Ethan Hagan, BS

10